Universidade do Minho
Escola de Engenharia

Jéssica Alexandra Henriques Correia

Development of (bio)molecules' cocktails (including (bio)polymers and (bio)surfactants) to promote additional oil recovery

janeiro de 2024

Development of (bio)molecules' cocktails(including (bio)polymers and (bio)surfactants) to promote additional oil recovery

Jéssica Correia

UMinho | 2024

Universidade do Minho
Escola de Engenharia

Jéssica Alexandra Henriques Correia

Development of (bio)molecules' cocktails (including (bio)polymers and (bio)surfactants) to promote additional oil recovery

Tese de Doutoramento
Doutoramento em Engenharia Química e Biológica

Trabalho efetuado sob a orientação do
Professor Doutor José António Couto Teixeira
e do
Doutor Eduardo José Gudiña Pérez

janeiro de 2024

Agradecimentos

Esta tese é o fruto tangível de um trabalho que, apesar de ser assinado individualmente, resulta do esforço e dedicação de várias pessoas a quem quero expressar o meu agradecimento.

Começo por expressar a minha gratidão aos meus orientadores, que foram essenciais para a realização desta tese. Ao Professor José António Teixeira, pela sua mentoria, apoio e infindável positivismo. Ao Eduardo Gudiña, pelo acompanhamento constante que me deu, pela motivação e paciência.

Agradeço à instituição de acolhimento, Centro de Engenharia Biológica da Universidade do Minho, por providenciar as condições indispensáveis à realização do meu trabalho científico e à PARTEX SERVICES PORTUGAL pela atribuição da bolsa de doutoramento (UMINHO/BD/2/2019) e pelo financiamento disponibilizado.

Agradeço também aos meus colegas do laboratório de fermentações pelo companheirismo durante os longos dias que passámos juntos, pelas discussões científicas e por todas as risadas que passaram pelo meio.

E por último, talvez às pessoas mais importantes em todo este processo, agradeço do fundo do meu coração: aos meus pais, por me darem apoio incondicional e a oportunidade de realizar este percurso; aos meus irmãos, Vânia e Pedro, pela motivação constante, compreensão e amizade; ao meu namorado, Heber Almeida, que me seguiu nesta aventura e me deu forças para chegar ao fim; e aos meus amigos, os que ficaram noutras terras e os que fiz na bela cidade de Braga.

STATEMENT OF INTEGRITY

I hereby declare having conducted this academic work with integrity. I confirm that I have not used plagiarism or any form of undue use of information or falsification of results along the process leading to its elaboration.

I further declare that I have fully acknowledged the Code of Ethical Conduct of the University of Minho.

Resumo

Desenvolvimento de cocktails de (bio)moléculas (incluindo (bio)polímeros e (bio)surfactantes) para promover a recuperação adicional de óleo

À medida que a população mundial aumenta, também aumentam as necessidades energéticas e a procura por combustíveis fósseis, devido ao atraso na implementação de fontes de energia mais amigas do ambiente. Além disso, as reservas de petróleo existentes estão a atingir o seu limite, tornando inviável a sua exploração do ponto de vista económico, sendo crucial melhorar os processos existentes que exploram a produção de petróleo. Tecnologias como a Recuperação Avançada de Petróleo com recurso a Microrganismos (MEOR, na sigla em inglês) utilizam biopolímeros e biosurfactantes produzidos por microrganismos para melhorar a produção de petróleo. Estas biomoléculas têm efeitos semelhantes à injeção dos compostos químicos, com a vantagem de serem menos prejudiciais para o meio ambiente.

Vários microrganismos produtores de biopolímeros e biosurfactantes foram estudados para sua aplicação em MEOR. Utilizando resíduos agroindustriais (água de maceração do milho e águas ruças), foi possível melhorar a produção de biosurfactantes (ramnolípidos) pela estirpe *Burkholderia thailandensis* E264 (em matraz e biorreator a escala laboratorial), assim como do biopolímero γ–PGA e biosurfactante pela estirpe *Bacillus velezensis* P#02, quando comparado com a produção em meio sintético. Para os biopolímeros estudados (de *B. velezensis* P#02, de *Rhizobium viscosum* CECT 908 e xantano), viscosidades mais elevadas e um módulo elástico mais prevalente foram as principais características que aumentaram a recuperação de petróleo em ensaios a escala laboratorial; comprovado pelos fatores de recuperação obtidos com o biopolímero produzido por *R. viscosum* CECT 908 em ensaios em colunas de areia usando óleos com diferentes viscosidades. Além disso, em estudos de simulação, foi possível observar o efeito favorável de um fluxo mais uniforme, tendo as simulações em que os biopolímeros foram injetados apresentado melhores recuperações de petróleo do que a injeção de água. Para os biosurfactantes, mecanismos que envolvem a redução da tensão superficial, emulsificação e alterações na molhabilidade do substrato estão associados à recuperação de petróleo. Ainda, em ensaios em colunas de areia onde se injetaram biopolímeros e biosurfactantes, demonstrou–se que estes podem atuar sinergicamente. Os resultados obtidos nesta tese fornecem dados importantes para o desenvolvimento de tecnologias alternativas que podem melhorar a recuperação de petróleo.

Palavras–chave: Biopolímeros, Biosurfactantes, Otimização de bioprocessos, Recuperação Avançada de Petróleo com recurso a microrganismos, Resíduos agroindustriais.

Abstract

Development of (bio)molecules' cocktails (including (bio)polymers and (bio)surfactants) to promote additional oil recovery

As world population rises, so does the energy demand and the need for fossil fuels, due to the delay in the implementation of more environmentally friendly energy sources. Furthermore, the existing crude oil reserves are being depleted and reaching their economic limit of exploitation. As such, it is crucial to improve the existing processes that explore the production of crude oil to recover the residual oil that remains trapped in the reservoirs and promote the exploration of unconventional crude oil reservoirs. Technologies such as Microbial Enhanced Oil Recovery (MEOR) use biopolymers and biosurfactants produced by microorganisms to improve oil production. These biomolecules have similar effects to their chemical counterparts, with the advantage of being less dangerous to the environment.

Several biopolymer– and biosurfactant–producing microorganisms were studied for their potential application in MEOR. Using agro–industrial residues (corn steep liquor and olive oil mill wastewater), it was possible to improve biosurfactant (rhamnolipids) production by *Burkholderia thailandensis* E264 (in flasks and bioreactor at laboratory scale), and both the biopolymer γ–PGA and biosurfactant production by *Bacillus velezensis* P#02, when compared with their production in synthetic media. For the studied biopolymers (from *B. velezensis* P#02, from *Rhizobium viscosum* CECT 908 and xanthan gum), it was found that higher apparent viscosities and a more prevalent elastic modulus were the main characteristics that increased oil production. That was demonstrated by the recovery factors obtained with the biopolymer from *R. viscosum* CECT 908 in sand–pack column assays using oils with different viscosities. Furthermore, in simulation studies, it was possible to see the favorable effect of a more uniform displacement front in oil recovery operations. The simulations where biopolymers were injected showed better recoveries than water injection. For biosurfactants, mechanisms involving surface tension reduction, emulsification and wettability alterations were all associated with oil recovery improvement. Additionally, in sand–pack column assays where biopolymers and biosurfactants were injected, it was shown that they can act synergistically in recovering oil. Overall, the results obtained in this thesis provide important insights for developing environmentally friendly technologies that can improve oil recovery.

Keywords: Agro–industrial residues, Biopolymers, Bioprocess optimization, Biosurfactants, Microbial Enhanced Oil Recovery

Contents

Agradecimentos ... iii
Resumo ... v
Abstract ... vi
List of abbreviations and variables ... xi
List of figures ... xiii
List of tables ... xvii
Scientific outputs ... xxii
Thesis outline ... xxiii
CHAPTER 1. The role of biosurfactants and biopolymers in Microbial Enhanced Oil Recovery ... 1
Abstract ... 2
1.1 Energy demand and fossil fuels ... 3
1.2 Microbial Enhanced Oil Recovery ... 5
1.3 Surfactant flooding in oil recovery ... 7
1.4 Biosurfactants: a green alternative to chemical surfactants to increase oil recovery ... 9
1.4.1 Biosurfactant MEOR: laboratory studies ... 13
1.4.2 Biosurfactant MEOR: field assays ... 26
1.5 Polymer flooding in oil recovery ... 28
1.6 Biopolymers: a sustainable alternative to chemical polymers in oil recovery ... 31
1.6.1 Biopolymer MEOR: laboratory studies ... 33
1.6.2 Biopolymer MEOR: field assays ... 40
1.7 Aim of the thesis ... 41
1.8 References ... 43
CHAPTER 2. Screening of biopolymer–producing microorganisms with potential application in Microbial Enhanced Oil Recovery ... 56
Abstract ... 57
2.1 Introduction ... 58
2.2 Materials and methods ... 59
2.2.1 Strains and culture conditions ... 59
2.2.2 Biopolymer recovery and quantification ... 61
2.2.3 Apparent viscosity measurements ... 61
2.3 Results ... 61

2.4 Discussion 63
2.5 References 65
CHAPTER 3. Screening biopolymer and biosurfactant production for application in Microbial Enhanced Oil Recovery 68
Abstract 69
3.1 Introduction 70
3.2 Materials and methods 71
3.2.1 Strains and culture conditions 71
3.2.2 Production of biomolecules in flasks 72
3.2.3 Production of biomolecules in bioreactor 73
3.2.4 Biopolymer recovery 74
3.2.5 Biosurfactant recovery 74
3.2.6 Analytical techniques 75
3.3 Results 76
3.3.1 Optimization of biopolymer production 76
3.3.2 Optimization of biosurfactant production by *B. subtilis* isolates 79
3.4 Discussion 82
3.5 References 85
CHAPTER 4. Application of biomolecules for Microbial Enhanced Oil Recovery 89
Abstract 90
4.1 Introduction 91
4.2 Materials and methods 92
4.2.1 Rhamnolipid production 92
4.2.2 Biopolymer production 93
4.2.3 Rheological properties and stability 94
4.2.4 Surface tension measurement 94
4.2.5 Oil recovery assays using sand–pack columns 94
4.3 Results 96
4.3.1 Rheological properties of the biopolymers 96
4.3.2 Oil recovery assays using biopolymers 102
4.3.3 Oil recovery assays using combinations of biopolymers and biosurfactants 104
4.4 Discussion 106

4.5 References 110
CHAPTER 5. Cost–effective rhamnolipid production by *Burkholderia thailandensis* E264 using agro–industrial residues 114
Abstract 115
5.1 Introduction 116
5.2 Materials and methods 117
5.2.1 Strain and culture conditions 117
5.2.2 Rhamnolipid production in flasks 118
5.2.3 Optimizing a glycerol and CSL–based medium for rhamnolipid production 119
5.2.4 Rhamnolipid production in bioreactor 119
5.2.5 Rhamnolipid recovery 120
5.2.6 Analytical techniques 120
5.2.7 Rhamnolipid characterization 122
5.2.8 Oil recovery assays 122
5.3 Results 124
5.3.1 Rhamnolipid production by *B. thailandensis* E264 in flasks 124
5.3.2 Optimization of rhamnolipid production in CSL medium supplemented with glycerol 127
5.3.3 Rhamnolipid production by *B. thailandensis* E264 in bioreactor 129
5.3.4 Rhamnolipid chemical characterization 131
5.3.5 Critical micelle concentration of rhamnolipids produced by *B. thailandensis* E264 133
5.3.6 Emulsification activity of the rhamnolipids produced by *B. thailandensis* E264 134
5.3.7 Effect of rhamnolipids produced by *B. thailandensis* E264 on the contact angle of water in an oil surface 136
5.3.8 Oil recovery assays 138
5.4 Discussion 142
5.5 References 148
CHAPTER 6. Biosurfactant and biopolymer co–production by *Bacillus velezensis* P#02 from agro–industrial wastes 153
Abstract 154
6.1 Introduction 155
6.2 Materials and methods 156
6.2.1 Strains and culture conditions 156

6.2.2 Biosurfactant production 157
6.2.3 Biopolymer production 157
6.2.4 Optimizing a synthetic medium for biosurfactant and biopolymer production 159
6.2.5 Identification of the isolate P#02 160
6.2.6 Analytical methods 161
6.2.7 Biopolymer characterization 162
6.2.8 Oil recovery in sand–pack columns 163
6.3 Results 163
6.3.1 Screening biosurfactant production by *Bacillus* sp. isolates 163
6.3.2 Screening biopolymer production by *Bacillus* sp. isolates 164
6.3.3 Optimization of biopolymer production by *Bacillus* sp. isolates 165
6.3.4 Identification of the isolate P#02 168
6.3.5 Optimizing a synthetic medium for biosurfactant and biopolymer production 169
6.3.6 Characterization of the biosurfactant produced by *Bacillus velezensis* P#02 172
6.3.7 Characterization of the biopolymer produced by *Bacillus velezensis* P#02 175
6.3.8 Evaluating the performance of the produced biomolecules in oil recovery assays using sand–pack columns 178
6.4 Discussion 180
6.5 References 183
CHAPTER 7. Reservoir simulation studies using biomolecules of interest for MEOR applications 188
Abstract 189
7.1 Introduction 190
7.2 Model description 191
7.3 Oil recovery simulations 193
7.3.2 Water flooding followed by MEOR 195
7.3.3 Biopolymer flooding 197
7.4 Discussion 199
7.5 References 200
CHAPTER 8. Conclusions and future perspectives 202
8.1 General conclusions 203
8.2 Future perspectives 205

List of abbreviations and variables

List of abbreviations

3–OH–FA	3–Hydroxy fatty acid
3–OH–FAME	3–Hydroxy fatty acid methyl ester
ANOVA	Analysis of variance
AOR	Additional oil recovery
API	American Petroleum Institute
BLASTn	Nucleotide–nucleotide blast
BP	Biopolymer
bpd	Barrels per day
BS	Biosurfactant
CCRD	Central composite rotational design
CFS	Cell–free supernatant
CFU	Colony forming units
CMC	Critical micelle concentration
COPAM	Companhia Portuguesa de Amidos
CSL	Corn steep liquor
CTAB	Hexadecyl–trimethylammonium bromide
DNS	Dinotrosalicylic acid
E_{24}	Emulsifying activity after 24h
EOR	Enhanced oil recovery
EPS	Extracellular polymeric substances
ESI	Electrospin ionization
FAS II	Fatty–acid *de novo* synthesis
FTIR	Fourier transform infrared spectroscopy
G	Shear (dynamic) modulus
G'	Storage (elastic) modulus
G''	Viscous (loss) modulus
GC–MS	Gas chromatography–mass spectrometry
η	(Apparent) Viscosity
HLB	Hydrophilic–lipophilic balance
HPAM	Hydrolyzed–polyacrylamide
HPLC	High–performance liquid chromatography
IFT	Interfacial tension
LB	Luria–Bertani
MELs	Mannosylerythritol lipids
MEOR	Microbial enhanced oil recovery
MIC	Microbiologically influenced corrosion
MRS	de Man, Rogosa, Sharpe
MS	Mass spectrometry
NCBI	National Center for Biotechnology Information
NMR	Nuclear magnetic resonance
OMP	Olive mill pomace
OMW	Olive–mill wastewater
OOIP	Original oil in place
PBD	Plackett–Burman experimental design
PBS	Phosphate–buffered saline solution
PV	Pore volume
RAR	Refinarias de Açúcar Reunidas
RF	Resistance factor
RL	Rhamnolipid
RL–MEA	Nonionic rhamnolipid monoethanol amide
RRF	Residual resistance factor
SID	Surface–induced dissociation
SRB	Sulfate–reducing bacteria
ST	Surface tension
TCA	Tricarboxylic acid
TLC	Thin–layer chromatography
uHPLC	Ultra–high–performance liquid chromatography
US$	United States Dollar
UV	Ultraviolet
vvm	Volume of air per unit volume per minute
WF	Water flooding
γ–PGA	Poly–γ–glutamic acid

List of variables

μ	Viscosity of fluid
k	Relative permeability of fluid
M	Mobility ratio
N_{CA}	Capillary number
θ	Contact angle
σ	Interfacial tension
S_{oi}	Initial oil saturation
S_{or}	Residual oil saturation
S_{orbf}	Oil recovered after biomolecules flooding
S_{orwf}	Oil recovered after water flooding
V	Linear velocity
ΔP	Pressure drop
λ	Mobility of fluid

List of figures

Figure 1.1 – Schematic representation of the Microbial Enhanced Oil Recovery (MEOR) process. Adapted from: Niu et al. (2020). 6
Figure 1.2 – Oil recovery mechanisms by surfactant activity: transition of (A) oil–wet mineral to (B) water–wet mineral and oil front deformation due to reduced interfacial tension. Adapted from: Lee et al. (2020). 9
Figure 1.3 – Laboratory sand–pack column biosurfactant flooding assays (Chapter 4). 14
Figure 1.4 – Oil recovery mechanism by polymer flooding: comparison between water flooding, where the injected fluid forms "fingers", which decreases the sweep efficiency, and polymer flooding, that standardizes the flow–front and increases the sweep efficiency. Adapted from: Pinho de Aguiar et al. (2021). 29
Figure 1.5 – Log–log plot for rheology of a shear–thinning fluid. Adapted from: Firozjaii & Saghafi (2020). 29
Figure 1.6 – Oil recovery mechanism by polymer flooding: adsorption of anionic polymers on reservoir rock surface by several types of interactions (hydrogen bonding, hydrophobic interaction, ion binding, electrostatic interaction, and Van der Waals forces). Adapted from: Rellegadla et al. (2017). 30
Figure 1.7 – Selective plugging mechanism during MEOR operations. Adapted from: Lee et al. (2020). 33
Figure 1.8 – Schematic overview of the main objectives of the thesis. 42
Figure 2.1 – Crude pullulan (g/L) produced over time by *Aureobasidium pullulans* CCY 27–1–94 grown in Ap1, Ap2 and Ap3 media (200 mL) in 500 mL flasks at 30°C and 150 rpm. 62
Figure 2.2 – Crude levan (g/L) produced after 120h by different *Bacillus subtilis* isolates (PX191, PX551, PX552, PX571 and PX572) grown in Bs1 medium (200 mL) in 500 mL flasks at 37°C and 150 rpm. 62
Figure 2.3 – Apparent viscosity (mPa s) values over time of culture broth samples of *Leuconostoc mesenteroides* A4 grown in different culture media (20 mL) in 100 mL flasks at 30°C and different agitation speeds. 63
Figure 3.1 – Apparent viscosity values of culture broth samples obtained from cultures of *Leuconostoc mesenteroides* A4 grown for 24h in a modified Lm4 medium containing different concentrations of sugarcane molasses (100–200 g/L) or different concentrations of CSL (1–20% (v/v)). 77

Figure 3.2 – Apparent viscosity values (mPa s) over time of *Rhizobium viscosum* CECT 908 grown in bioreactor with Rv1 medium at different operational conditions. 78
Figure 3.3 – Surface tension values (mN/m) over time of *Bacillus subtilis* #311 grown in batch mode in bioreactor with 10% (v/v) CSL medium. 80
Figure 3.4 – Surface tension values (mN/m), reducing sugars concentration (g/L) and cell dry weight (g/L) over time of *Bacillus subtilis* #311 grown in fed–batch mode in bioreactor with 10% (v/v) CSL medium. 81
Figure 4.1 – Steady flow curves for the solutions of biopolymer produced by *Rhizobium viscosum* CECT 908 in Rv2 medium (1 – 5 g/L), *Leuconostoc mesenteroides* A4 in Lm3 or Lm4 media (60 g/L) and commercial xanthan gum (1 – 5 g/L). Top: shear stress (Pa) as a function of shear rate (s^{-1}). Bottom: apparent viscosity (Pa) as a function of shear rate (s^{-1}). 97
Figure 4.2 – Dynamic viscoelastic properties of the solutions of biopolymer produced by *Rhizobium viscosum* CECT 908 in Rv2 medium (3 – 5 g/L), *Leuconostoc mesenteroides* A4 in Lm3 or Lm4 media (60 g/L) and commercial xanthan gum (2.5 – 5 g/L). Top: storage modulus (G') and loss modulus (G'') as a function of strain at a constant frequency (1 Hz). Bottom: G' and G'' as a function of frequency (Hz), at a constant strain (1% for xanthan gum and *R. viscosum* CECT 908; 5% for *L. mesenteroides* A4). .. 99
Figure 4.3 – Apparent viscosity values (mPa s) of aqueous solutions of the purified biopolymer (2.7 g/L) produced by *Rhizobium viscosum* CECT 908 grown in Rv2 medium, measured at different temperatures. 100
Figure 4.4 – Apparent viscosity values (mPa s) of aqueous solutions of the purified biopolymer (2 g/L) produced by *Rhizobium viscosum* CECT 908 grown in Rv2 medium with the addition of different NaCl concentrations. 100
Figure 5.1 – Surface tension values (mN/m), glycerol concentration (g/L) and bacterial growth (CFU/mL) over time of *Burkholderia thailandensis* E264 grown in standard (S) medium in flasks at 30°C and 180 rpm. 124
Figure 5.2 – Top: surface tension values (mN/m) and bacterial growth (CFU/mL); Bottom: carbon source and lactic acid concentrations (g/L), and bacterial growth (CFU/mL) over time of *Burkholderia thailandensis* E264 grown in flasks in CSL and CSL+OMW media at 30°C and 180 rpm. 126
Figure 5.3 – Response surface plot showing the interactive effect of glycerol (mL/L) and CSL (% (v/v)) concentrations on surface tension reduction. 129
Figure 5.4 – Surface tension values (mN/m) over time of *Burkholderia thailandensis* E264 grown in bioreactor with S, CSL and CSL+OMW media at different operational conditions. 130

Figure 5.5 – Top: surface tension values (mN/m) and bacterial growth (CFU/mL). Bottom: carbon source and lactic acid concentrations (g/L), and bacterial growth (CFU/mL) over time of *Burkholderia thailandensis* E264 grown in bioreactor with CSL+OMW medium at 30°C, 350 rpm and 0.3 vvm.... 130
Figure 5.6 – FTIR spectra of rhamnolipids produced by *Burkholderia thailandensis* E264 in standard, CSL and CSL+OMW media. 132
Figure 5.7 – Surface tension values (mN/m) of rhamnolipids produced by *Burkholderia thailandensis* E264 in standard, CSL, CSL+Glycerol and CSL+OMW media (both in flask and bioreactor), dissolved in 10 mM Tris–HCl buffer (pH 7.4) at different concentrations. 135
Figure 5.8 – Example of the decreasing contact angle of the rhamnolipids (5 x CMC) produced by *Burkholderia thailandensis* E264 in CSL medium on an oil–coated glass surface, showing a wettability alteration from oil/neutral–wet (at 0 min) to water–wet (at 5 min). 137
Figure 6.1 – Surface tension values (mN/m) of biosurfactants produced by *Bacillus velezensis* P#02 in CSLG and CSLG+Glut(10) media under static conditions and at 180 rpm, dissolved in PBS buffer at different concentrations. 173
Figure 6.2 – uHPLC spectra at 290 nm for the hydrolyzed and non–hydrolyzed biopolymer from *Bacillus velezensis* P#02, and the L–glutamic acid standard (5 g/L)..... 175
Figure 6.3 – NMR spectrum of γ–PGA produced by *Bacillus velezensis* P#02 in CSLG+Glut(10) medium. 176
Figure 6.4 – SID–Orbitrap MS spectrum of γ–PGA produced by *Bacillus velezensis* P#02 in CSLG+Glut(10) medium. 177
Figure 6.5 – Steady flow curves (apparent viscosity (Pa s) and shear stress (Pa) as a function of shear rate (s^{-1})) for the crude γ–PGA (25 g/L) produced by *Bacillus velezensis* P#02 in CSLG+Glut(10) medium. 178
Figure 6.6 – Dynamic viscoelastic properties of the crude γ–PGA (25 g/L) produced by *Bacillus velezensis* P#02 in CSLG+Glut(10) medium. Left: storage modulus (G') and loss modulus (G'') as a function of strain, at a constant frequency (1 Hz). Right: G' and G'' as a function of frequency (Hz), at a constant strain (1%). 178
Figure 7.1 – Reservoir model depicting the position of the injector wells (blue, INJ) and the producer wells (orange, PROD). 193
Figure 7.2 – Left: oil and water flow rate (m^3/day) through time. Right: oil recovery factor and water cut (%) through time, for water flooding simulations..... 194

Figure 7.3 – Oil saturation within the reservoir model after 12 months (top left), 34 months (top right), 10 years (bottom left) and 20 years (bottom right) of water flooding operations..... 194
Figure 7.4 – Top: oil recovery factor (%) through time. Bottom: water cut (%) through time for water flooding (WF) or water flooding followed by biopolymer flooding simulations using xanthan gum, the biopolymer from *Rhizobium. viscosum* CECT 908 and γ–PGA from *Bacillus velezensis* P#02 at different concentrations (1.0, 2.5 and 5.0 g/L)..... 196
Figure 7.5 – Left: oil and water flow rate (m^3/day) through time. Right: oil recovery factor and water cut (%) through time for biopolymer flooding simulations, using the biopolymer from *Rhizobium viscosum* CECT 908 at 5 g/L..... 198
Figure 7.6 – Oil saturation within the reservoir model after 1 (top left), 10 (top right), 20 (bottom left) and 30 years (bottom right) of biopolymer flooding operations, using the biopolymer from *Rhizobium viscosum* CECT 908 at 5 g/L..... 198

List of tables

Table 1.1 – Properties of the most relevant biosurfactants studied for application in oil recovery. 10
Table 1.2 – Summary of different laboratory–scale MEOR *ex situ* assays performed using biosurfactants produced by different microorganisms. 16
Table 1.3 – Summary of different laboratory–scale MEOR *in situ* assays performed using different biosurfactant–producing microorganisms. 20
Table 1.4 – Summary of different laboratory–scale MEOR *ex situ* assays performed using biopolymers produced by different microorganisms. 34
Table 1.5 – Summary of different laboratory–scale MEOR *in situ* assays performed using different biopolymer–producing microorganisms. 36
Table 2.1 – Description of the culture media and growth conditions for the microorganisms used in biopolymer production assays. 60
Table 3.1 – Description of the culture media for the microorganisms used in the optimization of biomolecules production. 72
Table 3.2 – Quantification of the crude biopolymers produced by *Aureobasidium pullulans* CCY 27–1–94 (pullulan) and *Leuconostoc mesenteroides* A4 (dextran) in different media and growth conditions; and viscosity of solutions prepared with different concentrations of the biopolymer produced in each condition. 76
Table 3.3 – Surface tension values (mN/m) obtained with the different *Bacillus subtilis* isolates grown in 10% (v/v) CSL medium for 48h at 37°C and 150 rpm. 79
Table 4.1 – Surface tension (mN/m) and apparent viscosity (mPa s) values of solutions containing biopolymer (BP) produced by *Rhizobium viscosum* CECT 908 in Rv2 medium (purified BP (1 g/L) and the diluted culture broth) and purified rhamnolipids (RL) (25 and 100 mg/L) produced by *Pseudomonas aeruginosa* PX112 in Pa1 medium. 101
Table 4.2 – Results obtained in *ex situ* MEOR sand–pack column assays with a heavy oil mixture ($\eta_{40°C}$ = 247 mPa s at 1.4 s^{-1}) using the crude biopolymer (BP) produced by *Leuconostoc mesenteroides* A4 in Lm3 and Lm4 media, and the BP produced by *Rhizobium viscosum* CECT 908 in Rv2 medium (diluted culture broth or purified BP) 102
Table 4.3 – Results obtained in *ex situ* MEOR sand–pack column assays with the oil from the Potiguar oilfield ($\eta_{40°C}$ = 110 mPa s at 1.4 s^{-1}) using xanthan gum (1 g/L), the biopolymer produced by *Leuconostoc mesenteroides* A4 in Lm3 medium (crude biopolymer and cell–free supernatant (CFS)) and

the biopolymer from *Rhizobium viscosum* CECT 908 in Rv2 medium (diluted culture broth or purified biopolymer). 103
Table 4.4 – Results obtained in *ex situ* MEOR sand–pack column assays with the oil from the Potiguar oilfield ($\eta_{40°C}$ = 110 mPa s at 1.4 s^{-1}) using commercial rhamnolipids (RL–90) and the cell–free supernatant (CFS) from *Pseudomonas aeruginosa* PX112 grown in CSLM medium, incubated for 48h and followed by xanthan gum (1 g/L) injection. 104
Table 4.5 – Results obtained in *ex situ* MEOR sand–pack column assays with a heavy oil mixture ($\eta_{40°C}$ = 247 mPa s at 1.4 s^{-1}) or the oil from the Potiguar oilfield ($\eta_{40°C}$ = 110 mPa s at 1.4 s^{-1}) using a solution containing both the purified biopolymer (BP) or the diluted culture broth from *Rhizobium viscosum* CECT 908 and the purified RLs from *Pseudomonas aeruginosa* PX112 (100 mg/L). 105
Table 5.1 – Characterization of corn steep liquor (CSL) and olive mill wastewater (OMW) used in this work. 118
Table 5.2 – Experimental level and ranges for the independent variables used in the CCRD. 119
Table 5.3 – Surface tension values (mN/m) obtained with *Burkholderia thailandensis* E264 grown in CSL (5–20% (v/v)) and CSL supplemented with OMW (5–25% (v/v)) at 30°C and 180 rpm. 125
Table 5.4 – Experimental CCRD matrix with the independent variables and surface tension (ST) reduction response, observed (measured in the cell–free supernatant diluted 2.5 times) and predicted by the first–order regression model. 128
Table 5.5 – Analysis of variance (ANOVA) for the surface tension reduction. 128
Table 5.6 – Rhamnolipid congeners produced by *Burkholderia thailandensis* E264 and their relative abundance in the different culture media. 133
Table 5.7 – The composition of 3–OH–FAMEs of rhamnolipids determined by GC–MS. The results represent the mean ± standard deviation of the analysis performed in triplicate. 133
Table 5.8 – Rhamnolipid (RL) titers obtained with *Burkholderia thailandensis* E264 in standard (S), CSL, CSL+Glycerol and CSL+OMW (both in flask and bioreactor) media; Critical micelle concentration (CMC) and minimum surface tension values (ST_{min}) of rhamnolipid solutions prepared in 10 mM Tris–HCl buffer (pH 7.4). 134
Table 5.9 – Emulsification indexes (E_{24}) obtained with purified rhamnolipids produced by *Burkholderia thailandensis* E264 in standard (S), CSL and CSL+OMW media at different concentrations. 136
Table 5.10 – Contact angle (°) measurements on an oil–coated glass surface for cell–free supernatants obtained from cultures of *Burkholderia thailandensis* E264 grown in different culture media (S, CSL and

CSL+OMW), rhamnolipid solutions (2 x critical micelle concentration (CMC) and 5 x CMC) and commercial rhamnolipids (RL–90 at 3 g/L, 2 x CMC and 5 x CMC). 137
Table 5.11 – Results obtained in MEOR sand–pack column assays performed with the Light Arabian crude oil ($\eta_{40°C}$ = 8 mPa s at 1.4 s^{-1}) using the cell–free supernatant obtained with *Burkholderia. thailandensis* E264 in CSL medium, incubated for 24h or 48h. 138
Table 5.12 – Results obtained in MEOR sand–pack column assays performed with the heavy crude oil mixture ($\eta_{40°C}$ = 247 mPa s at 1.4 s^{-1}) using the cell–free supernatant obtained with *Burkholderia thailandensis* E264 in CSL medium, followed by the culture broth obtained with *Rhizobium* viscosum CECT 908 in Rv2 medium. 139
Table 5.13 – Results obtained in MEOR sand–pack column assays performed with the crude oil from the Potiguar oilfield ($\eta_{40°C}$ = 110 mPa s at 1.4 s^{-1}) using commercial rhamnolipids (RL–90, 250 mg/L) and the cell–free supernatant (CFS) obtained with *Burkholderia thailandensis* E264 in CSL and CSL+OMW media, incubated for 24h and followed by xanthan gum (1 g/L) injection..... 140
Table 5.14 – Results obtained in MEOR sand–pack column assays performed with the crude oil from the Potiguar oilfield ($\eta_{40°C}$ = 110 mPa s at 1.4 s^{-1}) using commercial rhamnolipids (RL–90, 2 g/L) and the cell–free supernatant (CFS) obtained with *Burkholderia thailandensis* E264 in CSL and CSL+OMW media, incubated for 48h and followed by xanthan gum (1 g/L) injection. 140
Table 5.15 – Results obtained in oil recovery assays performed with the cell–free supernatant (CFS) from cultures of *Burkholderia thailandensis* E264 grown in standard (S), CSL and CSL+OMW media, and commercial rhamnolipids (RL–90) dissolved in the same uninoculated culture media at a concentration of 200 mg/L. 141
Table 6.1 – Experimental level and ranges for the independent variables used in the Plackett–Burman design (PBD). 160
Table 6.2 – Experimental level and ranges for the independent variables used in the central composite rotational design (CCRD)..... 160
Table 6.3 – Surface tension values (mN/m) obtained with the isolates P#01, P#02, P#03 and P#04 grown in LB medium at 37°C and 150 rpm. 164
Table 6.4 – Surface tension values (mN/m) of the cell–free supernatant (CFS) and apparent viscosity values (mPa s) of the crude biopolymer produced by the isolates P#02 and P#04 grown in different media at 37°C and 0 – 150 rpm for 48h. 164

Table 6.5 – Surface tension values (mN/m) of the cell–free supernatant (CFS) and apparent viscosity values (mPa s) of the crude biopolymer produced by the isolates P#02 and P#04 grown in different media at 30 – 50°C and 0 – 150 rpm for 48h. 165
Table 6.6 – Surface tension values (mN/m) of the cell–free supernatant (CFS) and apparent viscosity values (mPa s) of the crude biopolymer produced by the isolates P#02 and P#04 grown in different media with CSL (1 – 10% (v/v)) at 37°C and static conditions for 48h. 167
Table 6.7 – Surface tension values (mN/m) of the cell–free supernatant (CFS) and apparent viscosity values (mPa s) of crude biopolymer solutions obtained with the isolate P#02 grown in different media at 37°C and 0 – 150 rpm for 48h. 168
Table 6.8 – Plackett–Burman design (PBD) matrix with the independent variables and apparent viscosity ($\eta_{40°C}$) and ST reduction (measured in the cell–free supernatant diluted 10 times). 169
Table 6.9 – Regression analysis of the results obtained with the PBD for the apparent viscosity. 170
Table 6.10 – Regression analysis of the results obtained with the PBD for the ST reduction. 170
Table 6.11 – Central composite rotational design (CCRD) matrix with the independent variables and apparent viscosity ($\eta_{40°C}$) and ST reduction (measured in the cell–free supernatant diluted 10 times). 171
Table 6.12 – Biosurfactant titers obtained with *Bacillus velezensis* P#02 grown in CSLG and CSLG+Glut(10) media. Critical micelle concentration (CMC) and minimum surface tension values (ST_{min}) of biosurfactant solutions prepared in PBS. 172
Table 6.13 – Emulsification indexes (E_{24}) obtained with purified biosurfactants produced by *Bacillus velezensis* P#02 in CSLG and CSLG+Glu(10) media under static conditions and at 180 rpm, at different concentrations. 174
Table 6.14 – Contact angle (°) measurements on an oil–coated glass surface for biosurfactant solutions (2 x CMC and 5 x CMC) produced by *Bacillus velezensis* P#02 grown in CSLG and CSLG+Glu(10) media under static conditions and at 180 rpm. 174
Table 6.15 – Results obtained in MEOR sand–pack column assays performed with the crude oil from the Potiguar oilfield using the cell–free supernatant (CFS) obtained from cultures of *Bacillus velezensis* P#02 grown in synthetic (*ex situ* assay) and CSLG (*in situ* assay) media, followed by the injection of a xanthan gum solution (1 g/L) 179
Table 6.16 – Results obtained in MEOR sand–pack column assays performed with the crude oil from the Potiguar oilfield using the cell–free supernatant (CFS), crude biopolymer (BP) and CSF + crude (BP) obtained from *Bacillus velezensis* P#02 in CSLG+Glu(10) medium. 180

Table 7.1 – Reservoir properties for chemical EOR implementation. Adapted from (Chen et al., 2018) and (Xue et al., 2023)..... 191
Table 7.2 – Initial reservoir model properties..... 192
Table 7.3 – Oil recovery parameters for water flooding (WF) or WF followed by biopolymer flooding simulations using xanthan gum, the biopolymer from *Rhizobium. viscosum* CECT 908 and γ–PGA from *Bacillus velezensis* P#02 at different concentrations (1.0, 2.5 and 5.0 g/L). 197

Scientific outputs

Book chapters

Correia, J., Rodrigues, L. R., Teixeira, J. A., & Gudiña, E. J. (2021). Application of Biosurfactants for Microbial Enhanced Oil Recovery (MEOR). *In* Hemen Sarma, Majeti Narasimha Vara Prasad (eds.) *Biosurfactants for a Sustainable Future: Production and Applications in the Environment and Biomedicine* (Chapter 5, pp. 99–118). John Wiley & Sons Ltd. Wiley. https://doi.org/10.1002/9781119671022.ch5

Gudiña, E. J., Correia, J., & Teixeira, J.A. (2023). Application of biosurfactant in petroleum. *In* Pankaj Kumar, Ramesh Chandra Dubey (eds.). *Multifunctional Microbial Biosurfactants* (Chapter 18). Springer Nature Switzerland. https://doi.org/10.1007/978–3–031–31230–4_18

Scientific papers

Correia, J., Gudiña, E.J., Lazar, Z., Janek, T. & Teixeira, J.A. (2022). Cost–effective rhamnolipid production by *Burkholderia thailandensis* E264 using agro–industrial residues. Appl Microbiol Biotechnol, 106, 7477–7489. https://doi.org/10.1007/s00253–022–12225–1

Poster presentations

Correia, Jéssica, Gudiña, E.J., Rodrigues, L.R., & Teixeira, J.A. (2020). *Improved rhamnolipid biosurfactant production by Burkholderia thailandensis E264 using agro–industrial wastes*. [Poster presentation]. 1st International Conference on Biobased Surfactants, Gent, Belgium, 15–16 December 2020.

Correia, Jéssica, Gudiña, E.J., & Teixeira, J.A. (2022). *Improved rhamnolipid biosurfactant production by Burkholderia thailandensis E264 using agro–industrial wastes*. [Poster presentation]. BioIberoAmerica 2022 – 3rd IberoAmerican Congress on Biotechnology, Braga, Portugal, 7–9 April 2022.

Thesis outline

This thesis is organized into eight different chapters that compose a logical structure to understand the proposed research aims:

Chapter 1 gives an overview of the different approaches for Microbial Enhanced Oil Recovery (MEOR), focusing on the use of biosurfactants and biopolymers as an alternative to synthetic surfactants and polymers. The mechanisms of action for these molecules are analyzed, and their latest applications, both in laboratory studies and field trials, are summarized. Moreover, the main challenges and proposed solutions for applying biosurfactants and biopolymers in MEOR are discussed.

In Chapter 2, different biopolymer–producing microorganisms are screened for potential application in MEOR. The viscosity of the culture medium after microbial growth and the amount of crude biopolymer produced are the criteria for selecting the most interesting microorganisms.

In Chapter 3, biopolymer production with the microorganisms selected in the previous stage is optimized by adjusting the culture medium composition and growth conditions (temperature and agitation speed). Here, agro–industrial wastes and by–products are evaluated as alternative low–cost substrates for biopolymer production in some of the strains tested. In addition, potential scale–up strategies are proposed for biopolymer production by *Rhizobium viscosum* CECT 908 or biosurfactant production by *Bacillus subtilis* strains.

Chapter 4 focuses on the potential of these biopolymers for application in MEOR through sand–pack column assays. The rheological characteristics of these biopolymers are also presented to determine their viscosifying potential and their resistance to flow changes and stability under different environmental conditions. Moreover, the effect of using both biopolymers and biosurfactants in MEOR is evaluated.

Chapter 5 presents a detailed evaluation of biosurfactant (rhamnolipid) production by *Burkholderia thailandensis* E264. Rhamnolipid production is optimized using low–cost media comprising only agro–industrial wastes and by–products, both in flasks and in bioreactor. The surface–active properties and the chemical characterization of the rhamnolipids produced in the different media are then evaluated. Finally, these rhamnolipids are evaluated for application in oil recovery (sand–pack column assays) and bioremediation.

Chapter 6 shows a similar detailed evaluation of a different microorganism, *Bacillus velezensis* P#02 (isolated by our group from a Brazilian oil reservoir), that produces both a biosurfactant and a biopolymer.

The culture medium and growth conditions are optimized to promote biopolymer production using low–cost substrates. Then, the properties of the biopolymer (including the chemical composition) and the biosurfactant produced are evaluated, as well as different strategies for oil recovery purposes.

In Chapter 7, the biomolecules produced and evaluated throughout this work are used in simulation studies to determine their potential application in MEOR field trials for a reservoir with specific characteristics.

Chapter 8 summarizes the main conclusions, limitations, and future perspectives of the current research.

CHAPTER 1.

The role of biosurfactants and biopolymers in Microbial Enhanced Oil Recovery

This chapter is based on the following book chapters:

Gudiña, E. J., Correia, J., & Teixeira, J.A. (2023). Application of biosurfactant in petroleum. *In* Pankaj Kumar, Ramesh Chandra Dubey (eds.). *Multifunctional Microbial Biosurfactants* (Chapter 18). Springer Nature Switzerland. https://doi.org/10.1007/978–3–031–31230–4_18.

Correia, J., Rodrigues, L. R., Teixeira, J. A., & Gudiña, E. J. (2021). Application of Biosurfactants for Microbial Enhanced Oil Recovery (MEOR). *In* Hemen Sarma, Majeti Narasimha Vara Prasad (eds.) *Biosurfactants for a Sustainable Future: Production and Applications in the Environment and Biomedicine* (Chapter 5, pp. 99–118). John Wiley & Sons Ltd. Wiley. https://doi.org/10.1002/9781119671022.ch5

Abstract

Despite the significant efforts to expand the use of renewable energy sources, our society is still highly dependent on crude oil. Due to the progressive exhaustion of light crude oil reserves, oil companies are forced to develop innovative strategies to recover the entrapped oil remaining in the reservoirs. These technologies, known as Chemical Enhanced Oil Recovery, use chemical compounds to increase oil production. Surfactants and polymers are two of the most studied compounds for this application, either alone or combined. When injected into the oil wells, surfactants' primary mechanism of action is to reduce the high capillary forces that entrap the oil into the rock pores, while polymers increase the injected fluid's viscosity and the sweep efficiency. Biosurfactants, surface–active compounds synthesized by microorganisms, and biopolymers, viscoelastic extracellular polymeric substances, are promising alternatives to the chemical surfactants and polymers for application in oil recovery, as demonstrated by numerous studies performed in recent years. Biosurfactants usually exhibit excellent surface activity and are stable at extreme conditions, are environmentally friendly and can be produced using agro–industrial by–products. Biopolymers usually exhibit better viscoelastic properties when compared to chemical polymers, can sustain their structure and properties under high temperature and high salinity reservoir conditions, and are biodegradable.

1.1 Energy demand and fossil fuels

World population is expected to surpass 9000 million by 2040. At the same time, economic growth is projected to continue in the upcoming decades, mainly due to the development of emerging economies, which will increase energy demand (Z. Li et al., 2022; Sakthipriya et al., 2021). According to the International Energy Agency, crude oil demand increased in 2021 (achieving 96 million barrels per day (bpd)), after the severe decline observed in 2020 due to the Covid−19 pandemic, and it is expected to continue increasing up to 105 million bpd by 2026 (IEA, 2022). Despite the increasing concerns regarding climate change and global warming, and the development and implementation of renewable energies, fossil fuels will remain the main energy source in the short and medium term, as renewable energies can only partially replace crude oil consumption (Datta et al., 2020; Mahmoud et al., 2021).

To fulfil the increasing energy demand in the upcoming years, it is necessary to have an efficient exploitation of the existing crude oil reserves. The estimated proven oil reserves worldwide (conventional oil that can be recovered from oil reservoirs using existing technologies) is 1.67×10^{12} barrels, and, in the last years, the discovery of significant new oil reserves has not been reported (Sakthipriya et al., 2021). Furthermore, most of the already known oil reservoirs are approaching or will achieve their economic limit of exploitation in the near future (Nikolova & Gutierrez, 2020). Consequently, the development of technologies that allow the recovery of most of the oil present in the reservoirs is necessary, as well as the exploitation of unconventional crude oil reserves (oils that cannot be produced using conventional recovery technologies) (Hoseini−Moghadam et al., 2021; Xia et al., 2021; Zhang et al., 2020).

Oil recovery operations involve three phases. During primary recovery, the natural stored energy of the reservoir, resulting mainly from the expansion of fluids (gas, oil, and water), drives crude oil to the extraction wells. As the reservoir pressure decreases, it is necessary to use pumps to assist in oil recovery. Primary recovery is the least expensive phase of oil recovery, as it does not require special infrastructures. It can produce between 5 and 20% of the original oil in place (OOIP), depending on the properties of the reservoir and crude oil (Gudiña et al., 2012). When primary recovery becomes inefficient, it is necessary to inject water or gases to maintain the reservoir pressure and displace the remaining oil to the surface (secondary recovery). It is estimated that 50% of the oil produced worldwide is recovered through water flooding. This phase does not require great investment in new infrastructures (preexisting oil production wells can be used as injection wells). These techniques can extract up to 60% of the OOIP (Saravanan et al., 2020). When secondary recovery becomes uneconomical, between 30 and 60% of the OOIP remains

entrapped in the oil reservoir, it will be necessary to apply tertiary oil recovery techniques, known as Enhanced Oil Recovery (EOR). The application of these techniques is also necessary to recover unconventional oil reserves (e.g. extra–heavy crude oils, bitumen, oil sands, oil shale). EOR techniques can be divided into gas injection, chemical flooding, and thermal recovery (Niu et al., 2020).

Gases (natural gas, flue gas, CO_2, N_2) are used in tertiary oil recovery, not to repressurize the oil reservoir as in secondary oil recovery, but to reduce the oil density and viscosity, and to reduce the IFT between the displacing (injected water) and displaced fluid (crude oil). Among the different gases, CO_2 is the most widely used (Saravanan et al., 2020).

Regarding the thermal processes, the objective is to increase the reservoir temperature, in order to reduce the viscosity of crude oil and consequently improve its mobility through the porous network. This can be achieved through the injection of hot water or steam (cyclic or continuous steam injection) into the reservoir; another approach is *in situ* combustion of crude oil (Zhang et al., 2020).

The chemical processes consist of the addition of chemical compounds to the injected water to increase oil recovery. The compounds used include polymers, surfactants, acids, and solvents. Polymers are added to the injected water in order to increase its viscosity and reduce its mobility, improving the water–oil mobility ratio. This results in a more uniform oil displacement front and a more efficient displacement of the entrapped oil. Furthermore, polymers block the high–permeability channels of the oil reservoir, reducing its permeability and directing the injected water to oil–rich channels (Couto et al., 2019). Surfactants are amphiphilic compounds, containing both hydrophilic and hydrophobic moieties. Due to their structure, surfactants accumulate at the interface between the crude oil and water, reducing the interfacial tension (IFT) and promoting the displacement of the entrapped oil by the injected water. Furthermore, surfactants emulsify crude oil, allowing the mobilization of oil droplets by the injected water. Additionally, the adsorption of surfactants to the reservoir rock alters its wettability, changing the distribution of oil and water in the rock/fluid system (Pereira et al., 2013). Surfactants are commonly used in EOR in combination with salts or alkalis, which improve their activity by providing the appropriate environment to reduce the IFT. Furthermore, alkalis react with acidic components of crude oil to form surface–active compounds *in situ*, which contribute to decrease the IFT, reducing the amount of surfactant required to mobilize the entrapped oil. Surfactants can also be used in combination with polymers (surfactant–polymer flooding or alkali–surfactant–polymer flooding) to achieve high oil recoveries through the synergistic effect of combining different oil recovery mechanisms in a single treatment (Negin et al., 2017). Acids and solvents alter the porosity and permeability of oil reservoirs as

they can dissolve the reservoir rocks, releasing part of the entrapped oil. They can also act as emulsifiers and reduce crude oil viscosity (Tackie–Otoo et al., 2020).

The main disadvantage of chemical EOR is the negative environmental impact, as most of the polymers and surfactants used exhibit low biodegradability and are toxic to microorganisms, plants, and aquatic ecosystems. Regarding the thermal techniques, they consume high amounts of energy (Gudiña et al., 2012; Niu et al., 2020). Consequently, in order to ensure secure global energy supplies and minimize the environmental impact, it is necessary to develop alternative technologies to conventional EOR.

1.2 Microbial Enhanced Oil Recovery

Microbial Enhanced Oil Recovery (MEOR) is a cost–effective and environmentally friendly alternative to conventional EOR. The idea of using microorganisms to increase the productivity of oil reservoirs was first proposed almost 100 years ago. The basis of this technology is the use of microorganisms to produce metabolites and promote activities that contribute to increase the oil recovery (Beckman, 1926). MEOR can be applied *in situ* or *ex situ*. In *ex situ* approaches, selected microorganisms are used to produce metabolites (mainly biosurfactants and biopolymers) out of the reservoir. Subsequently, those metabolites (whole cultures, cell–free supernatants (CFS), or partially purified metabolites) are injected into the oil reservoir as an alternative to the chemical surfactants and polymers used in conventional EOR. In the *in situ* approaches, selected microorganisms are injected into the oil reservoir together with appropriate nutrients to allow their growth. If appropriate microorganisms are present in the oil reservoir, only nutrients are injected. In this approach, the injected or indigenous microorganisms can produce biosurfactants, biopolymers, biomass, acids, and gases directly into the oil reservoir (Figure 1.1). Furthermore, they can alter the properties of crude oil (e.g. by degrading the heavy oil fractions) to improve its mobility through the porous reservoir rock (Nikolova & Gutierrez, 2020).

MEOR is a cost–effective technology as agro–industrial residues and byproducts can be used as inexpensive substrates for microbial growth. Additionally, its application does not require the construction of new facilities, as the existing ones can be used to inject metabolites, nutrients, or microorganisms into the oil reservoir. It is also more environmentally friendly than conventional EOR because biosurfactants and biopolymers exhibit higher biodegradability and lower toxicity when compared with their chemical counterparts (Gudiña et al., 2012).

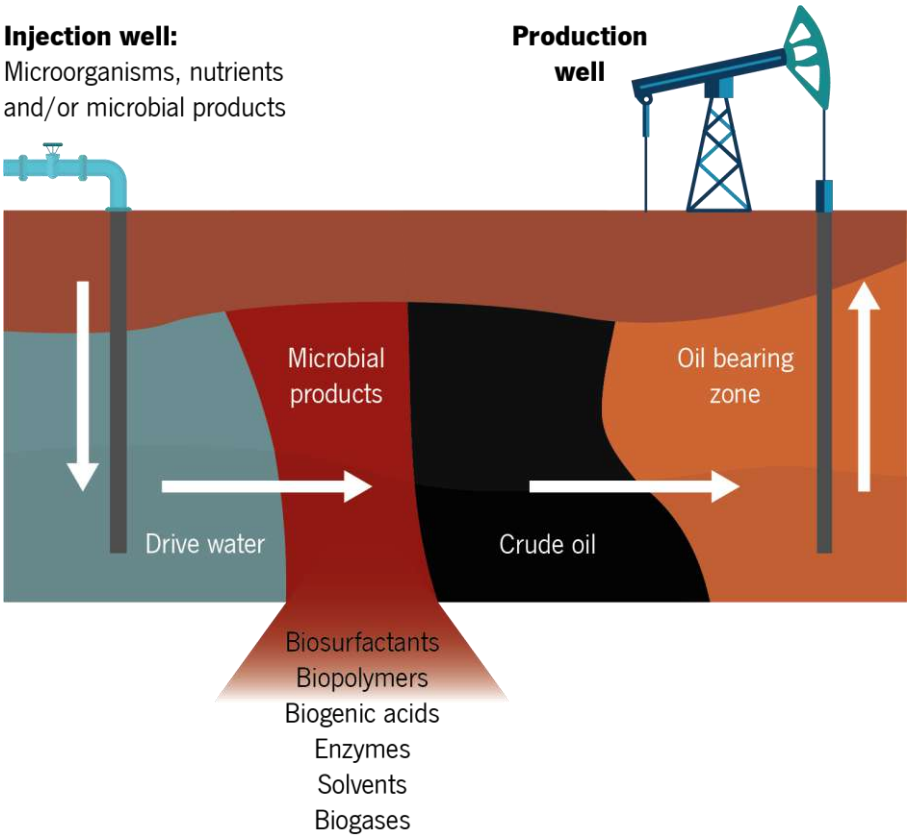

Figure 1.1 – Schematic representation of the Microbial Enhanced Oil Recovery (MEOR) process. Adapted from: Niu et al. (2020).

In situ MEOR is the simplest approach from an economic and technical point of view, as it just consists of the injection of nutrients (and eventually microorganisms) into the oil reservoir; after that, the oil production operations are stopped for several weeks to allow the production of metabolites; finally, the oil production operations are resumed. One of the advantages of *in situ* MEOR is that the metabolic activities can continue for long times without the need of further interventions. In addition, several beneficial activities can occur at the same time, which is advantageous to improve oil recovery (Ke, Sun, et al., 2018; Saravanan et al., 2020). However, this approach exhibits several limitations. One of the main drawbacks is the difficulty of finding microorganisms able to grow and produce the desired metabolites or activities in the oil reservoir. Although oil reservoirs harbor different microbial communities, they represent harsh environments that usually exhibit extreme conditions (Saravanan et al., 2020).

The most relevant factor for the application of *in situ* MEOR is the oil reservoir temperature, due to its significant effect on microbial growth and the production of metabolites. This parameter limits the reservoirs where this technology can be applied to those with temperatures below 90°C (Safdel et al., 2017). Accordingly, thermophilic microorganisms seem to be more appropriate for application in the *in*

situ MEOR (Elumalai et al., 2019; Tao et al., 2020). Furthermore, oil reservoirs are characterized by the lack of oxygen, which limits the useful microorganisms to anaerobic or facultative anaerobic ones. Another parameter that must be taken into consideration is the effect of high pressure on microbial growth and metabolite production. Additionally, injected and formation water can contain different ions (Na^+, K^+, Ca^{2+}, Mg^{2+}, Cl^-, HCO_3^-, SO_4^{2-}) with salinities that can achieve 250 g/L (Nikolova & Gutierrez, 2020).

Another drawback of *in situ* MEOR is that indigenous or injected microorganisms can be responsible for detrimental activities in the oil reservoir. Sulfate–reducing bacteria (SRB), manganese–oxidizing bacteria, or iron bacteria, which are common inhabitants of oil reservoirs, are responsible for the process known as microbiologically influenced corrosion (MIC), where the interaction of microorganisms with oil production and transportation infrastructures results in their corrosion and integrity reduction. This results in huge economic losses for the oil companies. Moreover, the production of H_2S by SRB results in the devaluation of crude oil (Elumalai et al., 2019). These detrimental microorganisms can be activated by the injection of nutrients into the oil reservoir.

Finally, *in situ* processes require more time as compared to *ex situ* ones, and the oil recovery operations must be stopped for several weeks. Besides, the development of accurate models to predict and follow the activity of microorganisms once injected into the oil reservoir is difficult. Although the *ex–situ* approach is less favorable from an economic point of view, it allows better control of the process, and the operational times are shorter when compared with the *in situ* processes.

1.3 Surfactant flooding in oil recovery

Surfactant flooding is one of the most popular and effective EOR techniques. Two forces define the displacement efficiency of crude oil into the reservoir in oil recovery operations, namely viscous and capillary forces. Viscous forces have a positive effect in oil recovery, as they contribute to oil mobilization. In contrast, capillary forces have a negative effect, as they are responsible for trapping crude oil within rock pores. The capillary number (N_{CA}) is a dimensionless number that establishes the relationship between viscous and capillary forces, as expressed by Equation (1.1):

$$N_{CA} = \frac{Viscous\ forces}{Capillary\ forces} = \frac{V \times \mu}{\sigma \times cos\theta} \tag{1.1}$$

where V and μ are the linear velocity (m/s) and the viscosity (mPa s) of the injected fluid, respectively; σ is the IFT between the injected and the displaced fluid (mN/m); and θ is the contact angle between the

reservoir rock and the wetting phase (Datta et al., 2020; L. Li et al., 2021; Negin et al., 2017; Zulkifli et al., 2019).

As N_{CA} increases, the ratio of viscous to capillary forces increases and the oil displacement efficiency also increases. For mature water–flooded reservoirs, N_{CA} values as low as 10^{-6}–10^{-7} have been reported, which results in high residual oil saturations. In order to substantially improve the mobilization of entrapped oil, N_{CA} needs to be increased by several orders of magnitude, up to 10^{-3}–10^{-1} (Tackie–Otoo et al., 2020). N_{CA} can be increased by increasing the viscous forces, *i.e.* increasing the flow rate and/or increasing the viscosity of the injected fluid (through the addition of (bio)polymers to the injected water), and by reducing the capillary forces, *i.e.* reducing the IFT and changing the wettability of the reservoir rock from oil–wet to water–wet (Negin et al., 2017).

The mechanism of action of surfactants in oil mobilization is the reduction of the capillary forces. The IFT between crude oil and water is around 10–40 mN/m. However, in the presence of surfactants, that value can be reduced to 10^{-2}–10^{-3}mN/m. This leads to a reduction of the capillary pressure and allows the deformation and mobilization of the oil droplets trapped into the rock pores (Figure 1.2). Furthermore, surfactants reduce the contact angle between the reservoir rock and the wetting phase, from values between 105 – 180° (oil–wet) to values below 75° (water–wet) (Hajibagheri et al., 2017; L. Li et al., 2021; Yun et al., 2020; Zulkifli et al., 2019). An oil–wet substrate means that oil has more affinity for the substrate than water, which makes oil extraction more difficult. However, in a water–wet condition, the affinity of crude oil for the reservoir rock is reduced, and it is more easily recovered (Ahmadi & Shadizadeh, 2018; Dong et al., 2022; Hoseini–Moghadam et al., 2021; Nasiri & Biria, 2020; Zulkifli et al., 2019) (Figure 1.2). Finally, surfactants can emulsify the entrapped oil, allowing its mobilization by the aqueous phase (Dong et al., 2022; Hoseini–Moghadam et al., 2021; Onaizi et al., 2021).

The selection of the most appropriate surfactant(s) for application in EOR requires previous studies considering the properties of the oil reservoir: rock composition; composition and pH of formation water (as they affect the charge of rock surfaces); temperature (the adsorption of nonionic surfactants onto rock surfaces increases as the temperature increases), etc. Surfactant loss due to adsorption to the reservoir rock reduces its effectiveness and causes economic losses (Z. Li et al., 2022). Examples of chemical surfactants commonly used in EOR include sulfate, sulfonate, carboxylate, ammonium bromide, and poly(ethylene/propylene) glycol derivatives (Negin et al., 2017).

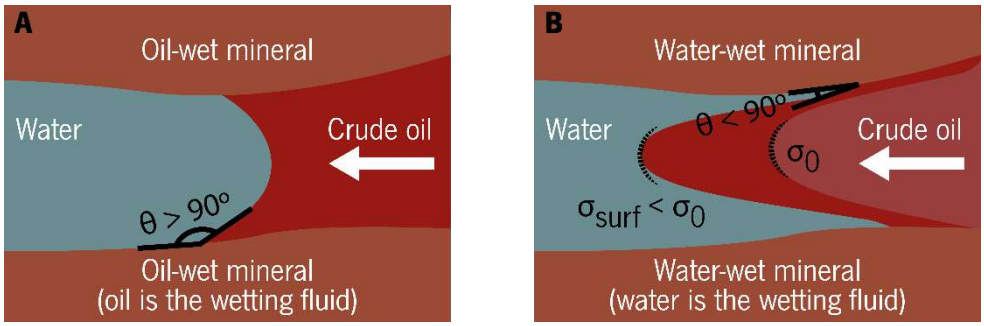

Figure 1.2 – Oil recovery mechanisms by surfactant activity: transition of (A) oil–wet mineral to (B) water–wet mineral and oil front deformation due to reduced interfacial tension. Adapted from: Lee et al. (2020).

1.4 Biosurfactants: a green alternative to chemical surfactants to increase oil recovery

Microbial biosurfactants have attracted considerable attention as alternatives to the chemical surfactants used in EOR (Niu et al., 2020; Saravanan et al., 2020). They comprise a diverse group of surface–active compounds produced by bacteria, yeasts and filamentous fungi, usually classified into two main classes: low molecular weight and high molecular weight biosurfactants (Gudiña, Pereira, et al., 2015). Low molecular weight biosurfactants are able to reduce the surface and IF tension, and usually exhibit emulsifying activity. They are characterized by an amphipathic structure, comprising hydrophilic and hydrophobic domains in the same molecule, which provides them their characteristic surface activity. The most representative groups are glycolipids (*e.g.* rhamnolipids, sophorolipids, threalose lipids, mannosylerythritol lipids (MELs)) and lipopeptides (*e.g.* surfactin, lichenysin, fengycin, pumilacidin) (Akanji et al., 2021; Al–Ghailani et al., 2021; Ali et al., 2019; Haloi et al., 2021; Qi Liu et al., 2021; Mahmoud et al., 2021). On the contrary, the high molecular weight biosurfactants (usually known as bioemulsifiers) exhibit remarkable emulsifying activity, but do not reduce the surface/IF tension. They consist of macromolecules, usually polysaccharides, proteins, lipoproteins, lipopolysaccharides, or glycolipoproteins. Examples are emulsan and alasan, produced by *Acinetobacter* sp. (Hongyan et al., 2017; Tao et al., 2020). Table 1.1 summarizes the main properties of the most relevant biosurfactants studied for application in oil recovery.

Table 1.1 – Properties of the most relevant biosurfactants studied for application in oil recovery.

Biosurfactant	Microorganism	CMC (mg/L)	ST (mN/m)	IFT (mN/m)	E_{24} (%)	Contact angle	Reference
Surfactin	*Bacillus amyloliquefaciens* SAS–1	–	22.9	–	78	–	R. Sharma et al. (2018b)
	Bacillus licheniformis AnBa7*	8	29.9	–	65	–	Mahmoud et al. (2021)
	Bacillus subtilis AB2.0	16	24.7	3.8	45	–	Alvarez et al. (2020)
	Bacillus subtilis AnPL–1*	30	28.5	2.29	71	–	F. Zhao et al. (2021)
	Bacillus subtilis BR–15	–	20.2	–	74	–	R. Sharma et al. (2018b)
	Bacillus subtilis BSFX026	36	28.0	–	60	60°→ 18°	Hu et al. (2021)
	Bacillus subtilis SL	154	25.6	0.95	67	–	Wu et al. (2022)
	Bacillus subtilis W19	100	28.0	2.0	–	83°→ 60°	Al–Ghailani et al. (2021)
	Bacillus subtilis WD3*	40	25.7	0.38	72	–	Aboelkhair et al. (2022a)
	Bacillus subtilis 22.2	250	–	0.056	–	71°→ 35°	Hadia et al. (2019)
	Bacillus tequilensis MK729017*	90	30.0	0.32	66	90°→ 26°	Datta et al. (2020)
	Bacillus velezensis H2O–1*	39	24.8	0.8	–	–	Guimarães et al. (2021)
Fengycin	*Brevibacillus borstelensis* YZ–2*	60	30.1	1.32	70	98°→ 10°	Dong et al. (2022)
Lichenysin A	*Bacillus licheniformis* Ali5	21	26.2	0.26	66	50°→ 17°	Ali et al. (2019)
Pumilacidin	*Bacillus safensis* CCMA–560	96	56.0	11.3	–	–	de Araujo et al. (2019)
Lipopeptide	*Bacillus halotolerans* XT–2*	46	25.5	1.55	85	–	X. T. Wang et al. ((2022)
	Luteimonas huabeiensis HB–2*	32	26.7	3.4	90	–	Ke, Sun, et al. (2018)
	Bacillus licheniformis DS1*	157	–	12.0	94	–	Purwasena et al. (2019)
	Bacillus licheniformis L20	–	42.0	–	62	91°→ 31°	Qi Liu et al. (2021)
	Bacillus licheniformis WD2*	60	27.1	1.27	50	–	Aboelkhair et al (2022b)
Rhamnolipid	*Achromobacter* sp. TMB1	90	27.0	0.9	–	75°→ 31°	Haloi et al. (2021)

	Pseudomonas aeruginosa HAK01	120	28.1	2.50	67	106°→7°	Khademolhosseini et al. (2019)
	Pseudomonas aeruginosa PBS	–	23.7	–	60	–	R. Sharma et al. (2018a)
	Pseudomonas sp. TMB2	120	28.0	0.8	78	75°→ 42°	Haloi et al. (2020)
	Burkholderia thailandensis E264	58	28.9		56	94°→ 41°	Correia et al. (2022) – Work presented on Chapter 5
Sophorolipid	*Meyerozyma* spp. MF138126	120	14.0	0.5	–	–	Akanji et al. (2021)
Threalose lipid	*Rhodococcus erythropolis* MN7*	13	40.8	–	55	–	Mahmoud et al. (2021)
Fatty acid	*Halomonas meridiana* BK–AB4	350	54.0	0.18	76	–	Sari et al. (2020)
Glycolipid + lipopeptide	*Pseudomonas mendocina* IFE11	125	31.0	–	68	–	Paul et al. (2022)

* Indigenous microorganism. –: not reported. CMC: critical micelle concentration. ST: minimum surface tension value. IFT: minimum interfacial tension value. E_{24}: emulsifying activity after 24 h.

Lipopeptide biosurfactants (mainly surfactin) are the most widely studied biosurfactants for application in oil recovery, followed by rhamnolipids (Table 1.1). In the case of lipopeptide biosurfactants, they comprise a cyclic peptide of 7 or 10 amino acids linked to a β–hydroxy or β–amino fatty acid of variable length (12–16 carbons) (Amani, 2015; Cui, Sun, et al., 2017; El–Sheshtawy et al., 2016; A. E. Elshafie et al., 2015; P. Gao et al., 2016). The producer microorganisms are mainly *Bacillus* spp., with special relevance for *Bacillus subtilis* and *Bacillus licheniformis*. In glycolipids, the hydrophilic domain consists of a carbohydrate (one or two molecules of rhamnose in rhamnolipids; the disaccharides sophorose and trehalose in sophorolipids and trehalolipids, respectively; and 1/4–*O*–β–D–mannopyranosyl–erythritol in MELs), whereas the hydrophobic domain consists of one, two, or three (hydroxy) fatty acids, of variable length (8–22 carbons) and saturation degree, or mycolic acids in the case of trehalolipids. Their main producers include *Pseudomonas* spp. (predominantly *Pseudomonas aeruginosa*), *Starmerella bombicola*, *Rhodococcus* spp. and *Pseudozyma* spp.

Generally, the biosurfactants presented in Table 1.1 exhibit a remarkable surface activity, as most of them reduce the surface tension (ST) to values below 30 mN/m and show considerable emulsifying activity (between 45 and 94%). Although in some cases the IFT values obtained are higher when compared with those reported for chemical surfactants (between 9×10^{-4} and 3 mN/m), it has to be taken into consideration that ultra–low IFT values are only achieved in the presence of salts or alkalis (Bera et al., 2014; Chen et al., 2013; Kumar & Mandal, 2016; Yun et al., 2020; J. Zhao et al., 2015). One advantage of biosurfactants when compared with chemical surfactants is their lower critical micelle concentration (CMC) values. Whereas for chemical surfactants the CMC values are usually between 100 and 3000 mg/L, in the case of biosurfactants they are usually between 10 and 200 mg/L (Table 1.1).

Although this parameter has been less studied, surfactin, fengycin, lichenysin and rhamnolipids have the capacity of changing the wettability of reservoir rocks to a water–wet or a more water–wet state (contact angle ≤ 75°), which contributes to improve oil recovery, as explained above. As it can be seen in Table 1.1, contact angles as low as 10° or 7° have been reported in the presence of fengycin and rhamnolipids (Dong et al., 2022; Khademolhosseini et al., 2019).

One important factor for the application of biosurfactants in oil recovery is their performance and stability at the oil reservoir conditions, usually characterized by high temperatures, pressures and salinities. Several lipopeptide biosurfactants maintained their surface–active properties at temperatures between 80 and 121°C and salinities between 100 and 200 g/L (Aboelkhair et al., 2022a; Datta et al., 2020; Guimarães et al., 2021; Qi Liu et al., 2021; Mahmoud et al., 2021; X. T. Wang et al., 2022; Wu

et al., 2022; F. Zhao et al., 2021), and even at pressures as high as 100 – 270 bar (Guimarães et al., 2021; Sakthipriya et al., 2021). Also, glycolipid biosurfactants remained stable at temperatures as high as 121°C, salinities between 40 and 200 g/L (Mahmoud et al., 2021; Sakthipriya et al., 2021), and pressures up to 80 bar (Khademolhosseini et al., 2019; Sakthipriya et al., 2021). In some cases, it has been reported a better performance for biosurfactants at high temperatures and high pressures. The IFT of heavy crude oil/brine systems in the presence of sophorolipids produced by *Meyerozyma* spp. MF138126 decreased from 4.3 mN/m at 1 bar to 0.25 mN/m at 45 bar, and from 10 mN/m at 25°C to 0.5 mN/m at 65°C (Akanji et al., 2021).

Another advantage of biosurfactants is their lower toxicity and higher biodegradability when compared with synthetic surfactants (Das & Kumar, 2019; Qiang Liu et al., 2015; Purwasena et al., 2019; Shreve & Makula, 2019; Varjani & Upasani, 2016). Biosurfactants produced by *Pseudomonas mendocina* IFE11 did not exhibit detrimental effects in phytotoxicity assays performed using *Vigna radiata* at concentrations up to 500 mg/L, and exhibited lower toxicity against animal cells when compared with the synthetic surfactant Tween 80 (Paul et al., 2022). Neither biosurfactants produced by *Bacillus safensis* J2 displayed phytotoxicity against wheat seeds (Das & Kumar, 2019). Aboelkhair et al. (2022b) performed a study of environmental and human health risk assessment regarding the use of *B. subtilis* WD3 and *B. licheniformis* WD2 to produce biosurfactants for application in oil recovery, using data available in the literature. They concluded that, in both cases, a low risk to human health and the environment is expected (Aboelkhair et al., 2022b).

Consequently, according to their properties, biosurfactants can be considered potential alternatives to synthetic surfactants for application in oil recovery.

1.4.1 Biosurfactant MEOR: laboratory studies

In order to study the performance and the mechanisms of action of (bio)surfactants and biosurfactant–producing microorganisms in oil recovery, different lab–scale models can be used to simulate the oil recovery operations, as reviewed by Rellegadla and co–workers (2019). One of the main advantages of using these models is that several assays can be performed simultaneously. The most common models are sand–pack columns (Figure 1.3) and cores. Sand–pack columns are cylindrical devices, usually made of glass, acrylic or stainless steel, of different volumes, which are filled with sand of different composition and size. Cores are cylindrical rock samples of variable size, usually collected from oil reservoirs or artificially constructed, which are placed into stainless steel containers (core

holders). Both models are provided with inlet and outlet tubes to allow the injection and recovery of the different fluids. The utilization of these models usually occurs in five consecutive steps:

- The models are first saturated with water or formation brine to determine parameters such as pore volume (PV), porosity, or permeability, and to establish the flow paths.
- Crude oil is then injected into the models. The volume required to saturate the model with oil corresponds to the OOIP.
- Subsequently, the models are flooded with water or formation brine until no oil is observed in the effluent, simulating the secondary water flooding process. The oil that remains in the model is set as the residual oil after water flooding, which is the target of the tertiary oil recovery methods studied.
- After that, the models are flooded with a solution of the selected (bio)surfactant (*ex situ* approach) or with selected microorganisms together with appropriate nutrients to allow their growth and the production of biosurfactants (*in situ* approach). In the last case, the system is closed after injection of the microorganisms and incubated at the reservoir conditions (temperature, pressure) for a variable shut–in time.
- Finally, another round of water flooding is conducted and the additional oil recovered (AOR) is quantified.

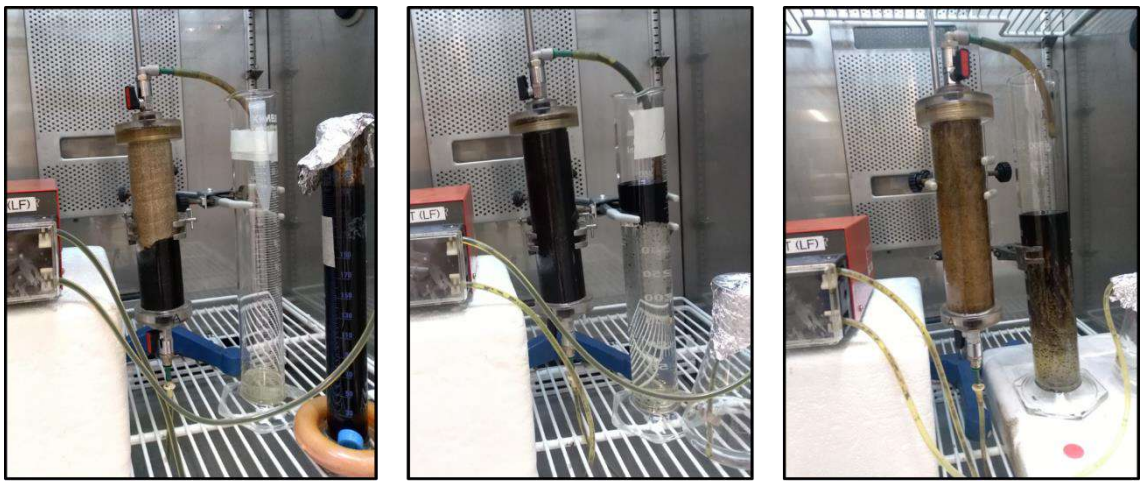

Figure 1.3 – Laboratory sand–pack column biosurfactant flooding assays (Chapter 4).

These studies are usually performed at controlled temperatures, and different flow rates can be used. They can be performed under anaerobic conditions (e.g. through the injection of N_2), under oxygen–limiting conditions, or under aerobic conditions (e.g. through the injection of air). Moreover, they can be performed at atmospheric pressure or under pressurized conditions (to simulate the oil reservoir conditions).

Table 1.2 summarizes some of the laboratory–scale biosurfactant MEOR assays performed using the *ex situ* strategy. According to these studies, biosurfactants produced by different microorganisms resulted in AORs between 3 and 69%. However, the results obtained in the different assays are often not comparable due to the heterogeneity of the experimental conditions used (crude oil properties, biosurfactant concentration and purity, type of model and substrate chosen, temperature, pressure, and flow conditions), generating a huge variability of results and, thus, limiting a clear perception of their value in real contexts. Furthermore, few studies compared the performance of biosurfactants and chemical surfactants. As an example, in sand–pack column assays, surfactin (AOR 15%) and rhamnolipids (AOR 15%) offered better results in oil recovery when compared with the chemical surfactants SDS (AOR 8.8%) and CTAB (AOR 7.0%) at the same concentration (200 mg/L) (Sakthipriya et al., 2021).

Table 1.3 gathers some of the lab–scale biosurfactant MEOR assays performed using the *in situ* approach. AORs between 1 and 37% were reported and the shut–in time ranged from 4 to 50 days. These experiments were performed at temperatures between 30 and 96°C, and pressures between 1 and 100 bar. In all the cases, microbial growth and biosurfactant production were observed, meaning that these microorganisms could be used in *in situ* biosurfactant flooding assays in oil reservoirs with those conditions of pressure and temperature. A relationship between the shut–in time and the AOR values obtained was not observed, due to the different conditions used in the different assays. For instance, the highest and one of the lowest AOR values reported (37% and 4%) were obtained with similar shut–in times (14 and 15 days) (Arora et al., 2019; F. Zhao, Li, et al., 2018). Neither a relationship between the environmental conditions and AOR was observed (Table 1.3).

Table 1.2 – Summary of different laboratory–scale MEOR *ex situ* assays performed using biosurfactants produced by different microorganisms.

Microorganism	Biosurfactant	Substrate (permeability)	Porosity (%)	Oil API gravity (°)	Oil viscosity (mPa s)	Temperature (°C)	Pressure (bar)	Flow rate (mL/min)	BS volume (PV)	Treatment – shut–in time	AOR (%)	Reference
Bacillus subtilis WD3 [1]	Lipopeptide	Sandstone core (206 mD)	21	41	2	60	1	0.25	4.0	CFS	39	Aboelkhair et al. (2022b)
Bacillus subtilis R1 [1]	Lipopeptide	Sand (100 mesh)	–	–	–	30	1	1.00	–	CFS	33	Jha et al. (2016)
Bacillus subtilis	Lipopeptide	Reservoir sandstone core (1824 mD)	16	–	598	65	1	0.05	0.5	BS – 3 days	10	Song et al. (2015)
Bacillus licheniformis WD2 [1]	Lipopeptide	Sandstone core (133 mD)	16	41	2	60	1	0.25	4.0	CFS	31	Aboelkhair et al. (2022b)
Bacillus licheniformis ATCC 14580 [1]	Lipopeptide	Sand (100 mesh)	21	–	–	35	1	2.50	0.6	Crude BS–1 day	11 [2]	El–Sheshtawy et al. (2015)
Bacillus licheniformis DS1 [1]	Lipopeptide	Berea sandstone	13	–	–	50	10	0.20	2.8	BS–12h	5 [2]	Purwasena et al. (2019)
Bacillus amyloliquefaciens [1]	Lipopeptide	Sandstone core (282 mD)	24	–	–	27–120	30	5	4.0	Culture broth	19–28	Okoro et al (2022)
Bacillus nealsonni [1]	Lipopeptide	Sandstone core (282 mD)	24	–	–	27–120	30	5	4.0	Culture broth	18–32	Okoro et al (2022)
Bacillus halotolerans XT–2 [1]	Lipopeptide	Artificial core	16	–	130	42	1	1.00	0.6	BS (200 mg/L)	13	X. T. Wang et al. (2022)
Bacillus subtilis RI4914 [1]	Surfactin	Sand	27	20	–	–	1	–	5.0	CFS	69	Fernandes et al. (2016)
Bacillus subtilis BR–15	Surfactin	Sand	18	–	5	–	1	–	0.6	CFS–2 days	66	R. Sharma et al. (2018b)
Bacillus subtilis RI4914 [1]	Surfactin	Sand	27	20	–	–	1	–	5.0	Partially purified BS (2 g/L)	40	Fernandes et al. (2016)
Bacillus subtilis WD3	Surfactin	Sandstone core (187–205 mD)	20	41	2	64	1	0.25–0.75	4.0	CFS	25–39	Aboelkhair et al. (2022a)

Bacillus subtilis PTCC 1365	Surfactin	Fractured and non–fractured glass micromodels (6020–7797 mD)	36	33	29	37	–	0.008	1.0	3	3–30	Soudmand–asli et al. (2007)
Bacillus subtilis YB7	Surfactin	Silica sand (159 mD)	33	26	23	80	1	5.00	0.5	BS (500 mg/L)	19	Sakthipriya et al. (2021)
Bacillus subtilis YB7	Surfactin	Silica sand (159 mD)	33	26	23	80	1	5.00	0.5	BS (200 mg/L)	15	Sakthipriya et al. (2021)
Bacillus subtilis BS–37 (mutant strain)	Surfactin	Sand (20–30 mesh)	–	–	–	60	1	1.00	3.0	BS (30 mg/L)	11 [2]	Qiang Liu et al. (2015)
Bacillus subtilis 22.2	Surfactin	Berea sandstone (153 mD)	22	42	1	25	45	0.05	3.0	BS (1 g/L)	9	Hadia et al. (2019)
Bacillus subtilis 22.3	Surfactin	Berea sandstone (153 mD)	21	27	2	25	24	0.05	3.0	BS (1 g/L)	3	Hadia et al. (2019)
Bacillus licheniformis L20	Surfactin	Core	42	–	–	80	200	0.50	5.1	CFS	20	Qi Liu et al. (2021)
Bacillus licheniformis ATCC 10716	Surfactin	Sand	21	–	–	35	–	2.50	0.6	CFS–1 day	11 [2]	El–Sheshtawy et al. (2016)
Bacillus amyloliquefaciens SAS–1	Surfactin	Sand	19	–	5	–	1	–	0.6	CFS–2 days	57	R. Sharma et al. (2018b)
Bacillus safensis J2 [1]	Surfactin	Sand (45 mesh)	–	–	–	–	1	–	–	BS	5 [2]	Das & Kumar (2019)
Candida tropicalis MTCC230 (adaptive strain)	Surfactin	Sand	15	–	–	–	1	2.50	0.6	CFS–1 day	40	Ashish (2018)
Bacillus licheniformis W16 [1]	Lichenysin A	Berea sandstone (250–260 mD)	18–22	37	2	60	1	0.40	5.0	CFS	26	Joshi, Al–Wahaibi, Al–Bahry, Elshafie, Al–Bemani, Al–Bahri, et al. (2016)
Bacillus licheniformis Ali5	Lichenysin A	Sand (100 mesh)	22	35	–	–	1	3.00	0.6	CFS–1 day	25 [2]	Ali et al. (2019)

Bacillus safensis CCMA–560	Pumilacidin	Berea sandstone (118 mD)	21	–	11	–	68	–	2.7	Alternate injection: BS (125 mg/L) and brine (30 g NaCl/L)	13	de Araujo et al. (2019)
Brevibacillus borstelensis YZ–2 [1]	Fengycin	Core (42 mD)	–	–	8	30	69	0.20	1.0	BS (120 mg/L)–2h	9	Dong et al. (2022)
Clostridium sp. N–4 [1]	Glycoprotein	Sand	28	18	1348	96	1	–	3.0	CFS	17 [2]	Arora et al. (2019)
Pseudomonas mendocina IFE11	Lipopeptide + glycolipid	Sand	–	–	–	–	1	–	1.3	CFS	44	Paul et al. (2022)
Ochrobactrum pseudintermedium C1 + *Bacillus cereus* K1	Glycoprotein and Glycolipid	Sand (60–100 mesh)	21	32	7	70	–	–	1.0	Crude BS	47	Bhattacharya et al. (2019)
Ochrobactrum pseudintermedium C1 + *Bacillus cereus* K1	Glycoprotein and Glycolipid	Sand (60–100 mesh)	21	32	10	40	–	–	1.0	Crude BS	41	Bhattacharya et al. (2019)
Pseudomonas aeruginosa PBS [1]	Rhamnolipid	Sand	17	–	–	–	1	–	0.7	CFS–1 day	56	R. Sharma et al. (2018a)
Pseudomonas aeruginosa HAK01	Rhamnolipid	Glass micromodel	–	20	242	25	1	0.05	0.4	BS (120 mg/L)	27 [2]	Khademolhosseini et al. (2019)
Pseudomonas aeruginosa CPCL	Rhamnolipid	Silica sand (154 mD)	33	26	23	80	1	5.00	0.5	BS (200 mg/L)	15	Sakthipriya et al. (2021)
Pseudomonas aeruginosa CPCL	Rhamnolipid	Silica sand (154 mD)	33	26	23	80	1	5.00	0.5	BS (500 mg/L)	14	Sakthipriya et al. (2021)
Pseudomonas aeruginosa	Rhamnolipid	Clay + sand (65–100 mesh)	21	22	–	30	1	0.70	–	BS (254 mg/L)	12	Câmara et al. (2019)
Pseudomonas aeruginosa Pa4	Rhamnolipid	Sand (60–100 mesh)	–	–	–	34	1	–	–	BS (100 mg/L)	10	Alvarez Yela et al. (2016)
Pseudomonas aeruginosa NCIM 5514	Rhamnolipid	Berea sandstone	19	36	623	70	1	0.12	0.5	Partially purified BS	9	Varjani & Upasani (2016)
Pseudomonas aeruginosa HATH	Rhamnolipid	Glass micromodel	42	34	–	80	1	0.50	2.0	BS (120 mg/L)	7	Amani (2015)
Pseudomonas aeruginosa WJ–1 [1]	Rhamnolipid	Sand	27	33	67	35	1	–	0.5	CFS–10 days	3 [2]	Cui, Sun, et al. (2017)

Pseudomonas putida PP021 [1]	Rhamnolipid	Sand	21	24	4	25	–	–	6.0	BS (100 mg/L)–3 days	48	Biktasheva et al (2022)
Pseudomonas putida PP021 [1]	Rhamnolipid	Reservoir rock	–	24	4	38	–	0.30	6.0	BS (100 mg/L)	20–22	Biktasheva et al. (2022)
Pseudomonas sp. TMB2	Rhamnolipid	Core rock plug	21	35	18	70	41		6.0	BS (120 mg/L)	17	Haloi et al. (2020)
Pseudoxanthomonas sp. G3	Rhamnolipid	Sand (50 mesh)	22	22–28	59	50	1	–	0.6	Crude BS–1 day	22 [2]	Astuti et al. (2019)
Acinetobacter junii BD [1]	Rhamnolipid	Glass micromodel	–	–	–	35	1	0.48	–	CFS	13	Dong et al. (2016)
Ochrobactrum anthropi HM–1	Rhamnolipid	Sand	–	–	–	–	1	–	–	CFS	45 [2]	Ibrahim (2018)
Citrobacter freundii HM–2	Rhamnolipid	Sand	–	–	–	–	1	–	–	CFS	42 [2]	Ibrahim (2018)
–	Rhamnolipid	Berea sandstone core (176 mD)	20	30	20	52	138	0.50	3.0	BS (5000 mg/L)	23	Al–Ghamdi et al. (2022)
Candida bombicola ATCC 22214	Sophorolipid	Berea sandstone core (250–350 mD)	20	37	–	60	1	0.40	5.0	CFS	27	A. E. Elshafie et al. (2015)
Candida albicans IMRU 3669	Sophorolipid	Sand	21	–	–	35	–	2.50	0.6	CFS–1 day	3 [2]	El–Sheshtawy et al. (2016)
Halomonas meridiana BK–AB4	Fatty acid	Berea sandstone core (200–250 mD)	27	45	–	65	–	–	–	BS–60h	24	Sari et al. (2020)
Escherichia coli W3110/pCA24N OmpA$^+$	Transmembrane protein (OmpA)	Sand (60–100 mesh)	–	–	–	34	1	–	–	OmpA (15.8 mg/L)	12	Alvarez Yela et al. (2016)
Geobacillus toebii R–32639 [1]	–	Cement + sand (50 mesh)	20–35	–	2	60	7	0.60	–	Bioproduct and brine–7 days	5 [2]	Fulazzaky & Astuti (2015)

All the recovery assays were performed using crude oil, except those described in Qiang Liu et al. (2015), Ashish (2018), Câmara et al. (2019), de Araujo et al. (2019) and Haloi et al. (2020), where a mixture of crude oil and kerosene (1:9 ratio), four stroke engine oil, diesel, or a mixture of crude oil, n–hexane (50%, w/w) and light paraffin oil respectively, were used.

[1] Indigenous microorganism. [2] Additional oil recovery (AOR) values are the corrected values obtained after subtracting the AOR obtained in the control assays.

–: Not reported. AOR: Additional oil recovery. BS: Biosurfactant. CFS: Cell–free supernatant. PV: Pore volume.

Table 1.3 – Summary of different laboratory–scale MEOR *in situ* assays performed using different biosurfactant–producing microorganisms.

Microorganism	Biosurfactant	Substrate (permeability)	Porosity (%)	API gravity (°)	Oil Viscosity (mPa s)	Temperature (°C)	Pressure (bar)	Flow rate (mL/min)	Culture volume (PV)	Shut–in time (days)	AOR (%)	Reference
Bacillus sp. W5 [1]	Lipopeptide	Heterogeneous core (235 mDa)	20	–	45	60	1	–	0.4	7	10 [2]	Qi et al. (2018)
Bacillus subtilis M15–10–1 [1]	Lipopeptide	–	–	36	18	40	1	–	0.2	7	9	P. Gao et al. (2016)
Bacillus halotolerans XT–2 [1]	Lipopeptide	Artificial core	16	–	130	42	1	1.000	0.6	20	25	X. T. Wang et al. (2022)
Luteimonas huabeiensis HB–2 [1]	Lipopeptide	Artificial core	29	24	359	40	79	–	0.5	14	22 [2]	Ke, Sun, et al. (2018)
Bacillus subtilis AnPL–1 [1]	Surfactin	Sandstone core (390 mD)	21	40	9	39	100		0.5	15	10	F. Zhao et al. (2021)
Bacillus subtilis SL	Surfactin	Core (14 mD)	–	31	17	55	30	0.200	0.5	4	6	Wu et al. (2022)
Fusant: *Bacillus mojavensis* JF–2 – *Pseudomonas stutzeri* DQ–1	Surfactin	Artificial core (373 mD)	25	–	–	39	1	1.000	1.0	10	4	X. Liang et al. (2017)
Bacillus licheniformis [1]	–	Reservoir sandstone core (7.5 mD)	16	37	22	50	1	0.200	0.3	7	22 [2]	Daryasafar et al. (2016)
Bacillus amyloliquefaciens 702 [1]	–	Artificial core (373 mD)	20	28	6	39	1	0.500	0.5	10	1 [3]	F. Zhao et al. (2017)
Clostridium sp. N–4 [1]	Glycoprotein	Sand	31	18	1348	96	1	–	1.3	14	37	Arora et al. (2019)
Pseudomonas sp. SWP–4	Rhamnolipid	Quartz sand (40–60 mesh)	30	18	220000	30	1	5.000	–	1	24	Lan et al. (2015)

Pseudomonas sp. WJ6	Rhamnolipid	Berea sandstone core (240 mD)	24	–	3500	35	1	–	0.5	50	12	Xia et al. (2021)
Pseudomonas aeruginosa WJ–1 [1]	Rhamnolipid	Sand	27	33	67	35	1	–	0.5	10	5	Cui, Sun, et al. (2017)
Pseudomonas aeruginosa DQ3 [1]	Rhamnolipid	Artificial core (331 mD)	15	28	10	42	1	0.200	0.3	15	4	F. Zhao, Li, et al. (2018)
Acinetobacter junii BD [1]	Rhamnolipid	Glass micromodel	–	–	–	35	1	0.008	–	1.5	10 [2]	Dong et al. (2016)
Pseudomonas aeruginosa L6–1 [1]	–	Oilfield sand	18	28	6	35	1	0.500	0.5	7	15	Cui, Zheng, et al. (2017)
Pseudomonas aeruginosa 709 [1]	–	Artificial core (359 mD)	19	28	6	39	1	0.500	0.5	10	7 [3]	F. Zhao et al. (2017)
Chelatococcus daeguensis HB–4 [1]	–	Mixed silica sands (80–200 mesh)	–	–	500	38	79	–	0.5	14	36 [2]	Ke et al. (2019)
Clostridium spp. [1]	–	Core	18	–	–	65	89	0.100	–	10	19	N. Sharma et al. (2020)
Methanogenic bacteria consortium [1]	–	–	27	–	1824	50	1	–	1.0	100	15	Xia et al. (2016)
Geobacillus toebii R–32639 [1]	–	Cement + sand (50 mesh)	20.0–35.0	–	2	60	7	0.600	–	7	11	Fulazzaky & Astuti (2015)

All the recovery assays were performed using crude oil. Additional oil recovery (AOR) values are the corrected values obtained after subtracting the AOR obtained in the control assays, unlesss stated otherwise.

[1] Indigenous microorganism. [2] AOR values were obtained without subtracting the AOR in the control assays. [3] AOR value is calculated as the volume of displaced oil after MEOR divided by the volume of original oil in place.

–: Not reported. BS: Biosurfactant. PV: Pore volume.

Again, comparison of the existing data is difficult due to the variability of the experimental conditions. Furthermore, in the *in situ* assays it becomes difficult to determine which factors lead to the mobilization of the residual oil since several mechanisms can occur simultaneously to biosurfactant production (Gudiña et al., 2013). For example, the bacterial consortium evaluated by Xia and co–workers (2016) was found to produce methane besides biosurfactants, which can increase oil recovery by increasing the pressure inside the model (Xia et al., 2016). *Geobacillus toebii* R–32639 produced biosurfactants and gases simultaneously, was able to degrade heavy oil fractions, and increased oil recovery by selective plugging (Fulazzaky & Astuti, 2015). *Pseudomonas* sp. WJ6, besides producing biosurfactants (rhamnolipids and lipopeptides), degrades asphaltenes and heavy crude oil under anaerobic conditions. In core–flooding experiments performed with this strain, besides a slight reduction in the ST (from 41 to 34 mN/m), the crude oil viscosity was reduced by 50% due to the degradation of heavy oil fractions (Xia et al., 2021). Other studies presented in Table 1.3 (P. Gao et al., 2016; Ke, Sun, et al., 2018; Ke et al., 2019; Lan et al., 2015) also reported the ability of the microorganisms used (*Luteimonas*, *Bacillus*, *Pseudomonas*, and *Chelatococcus* species) to degrade different crude oil fractions, which contributed to the reduction of the recovered oil's viscosity at the end of the assays.

Another important issue to take into consideration when applying *in situ* MEOR using exogenous strains is that the introduced microorganisms must be able to co–exist with the native bacterial communities present in the oil reservoir. Gao and co–workers (2016) evaluated the interactions between *B. subtilis* M15–10–1 and the indigenous microbial population from the oil reservoir. The results obtained demonstrated that the exogenous strain was able to grow in the presence of the indigenous microbes and, at the same time, stimulated the growth of native hydrocarbon–degrading bacteria. On the other hand, the introduction of exogenous strains or their (bio)products into the oil wells may inhibit certain detrimental native microorganisms, such as SRB, which hinder the oil recovery process (P. Gao et al., 2016). El–Sheshtawy and co–workers (2015) demonstrated that the lipopeptide biosurfactant produced by *B. licheniformis* ATCC14580 at a concentration of 1% inhibited the growth of SRB (El–Sheshtawy et al., 2015).

The effectiveness of biosurfactants in MEOR is highly dependent on the type of microorganism, the strategy (*in situ* or *ex situ*), and the experimental conditions used. Regarding the strategy used, some studies suggest that *in situ* oil recovery may yield better results (Arora et al., 2019; Cui, Sun, et al., 2017; Fulazzaky & Astuti, 2015), while others report the opposite (Dong et al., 2016). In sand–pack column assays performed with the rhamnolipid–producing strain *P. aeruginosa* WJ–1, a higher AOR was obtained

in the *in situ* assays (5.3%) compared to the *ex situ* ones (2.5%). According to the authors, this could be explained by the production of a higher amount of biosurfactant by the bacteria *in situ* (2.66 g rhamnolipid/L) when compared with the concentration injected in the *ex situ* assays (0.23 g rhamnolipid/L). Consequently, lower IFT values were achieved in the first case (1.7 mN/m *in situ* versus 5.5 mN/m *ex situ*). Furthermore, the diameter of the emulsified oil droplets was lower in the *in situ* assays (20–50 μm versus 40–80 μm *ex situ*), which facilitated the displacement of the entrapped oil (Cui, Sun, et al., 2017). In a similar way, a higher AOR was obtained with *G. toebii* R–32639 in the *in situ* assays (11.2%) when compared with the *ex situ* assays (5.4%), both of them performed at the same experimental conditions. This result was found to be the consequence of several oil recovery mechanisms occurring at the same time in the *in situ* assays (Fulazzaky & Astuti, 2015). Wang and co–workers (2022) compared the application of *Bacillus halotolerans* XT–2 in oil recovery in *in stu* and *ex situ* experiments using the same core system and operational conditions. AOR was higher in *in situ* assays (25%) than in *ex situ* assays (13%). *Ex situ* assays were performed through the injection of a solution containing 200 mg biosurfactant/L, whereas in *in situ* assays *B. halotolerans* XT–2 produced 345 mg biosurfactant/L under oxygen–limited conditions during the 20 days of incubation. As a result, the IFT value achieved in *in situ* experiments (0.89 mN/m) was lower than in *ex situ* assays (1.17 mN/m). Furthermore, in *in situ* assays, the viscosity of the crude oil was reduced from 112 to 66 mPa s, due to the degradation of long–chain *n*–alkanes (C_{22}–C_{34}), asphaltenes and paraffins by *B. halotolerans* XT–2, whereas in the *ex situ* experiments, only a slight decrease in crude oil viscosity (up to 102 mPa s) was observed (X. T. Wang et al., 2022). On the other hand, lower AOR values were obtained in the *in situ* assays using *Acinetobacter junni* BD when compared with the *ex situ* assays, which can be due to a low biosurfactant production in the *in situ* assays performed under reservoir conditions (Dong et al., 2016).

As in the case of chemical surfactants, the adsorption of biosurfactants to the rock surface is detrimental to oil recovery. The adsorption of rhamnolipids (anionic biosurfactants) produced by *Achromobacter* sp. TMB1 to sand surface decreased as the temperature increased (from 30 to 60°C), decreased as salinity decreased (from 15,000 to 1000 mg/L), and decreased as the pH increased (from 2 to 12) (Haloi et al., 2021). Accordingly, optimal conditions for rhamnolipid injection in oil recovery can be determined, considering this data, in order to minimize their adsorption to the reservoir rock, which results in a decrease in rhamnolipid concentration and reduces the efficiency of the process.

In order to reduce the adsorption of rhamnolipids to the rock surface, Li and co–workers (2022) synthesized derivatives of rhamnolipids through amidation to obtain nonionic rhamnolipid monoethanol

amide (RL–MEA). This modification, which neutralizes the negative charge of the carboxylic groups of rhamnolipids, did not have a negative effect on their surface activity. RL–MEA reduced the ST to similar values when compared with rhamnolipids (around 29 mN/m), exhibited lower CMC values than rhamnolipids, both in water (41 mg/L versus 75 mg/L) and 200 mM NaCl (30 mg/L versus 47 mg/L), and displayed better oil washing efficiency than rhamnolipids at low concentrations (100–500 mg/L). Furthermore, RL–MEA were more efficient in changing the wettability of crude oil–conditioned glass slides (reduced the contact angle to 46°) than rhamnolipids (contact angle 63°) at the same concentration (500 mg/L). Finally, the adsorption loss of RL–MEA on quartz sand was reduced by 20% when compared with rhamnolipids in assays performed at 60°C and 200 mM NaCl (Z. Li et al., 2022).

Although the formation of stable emulsions between the displacing fluid and crude oil is advantageous to recover the entrapped oil, it represents a problem in downstream processing. Rhamnolipids (1 g/L) proved to form stable oil/water nano–emulsions both with light (13 mPa s) and heavy (394 mPa s) crude oil, with 0% phase separation after 30 days (Onaizi et al., 2021). Interestingly, these stable nano–emulsions are easily destabilized at low pH values, which can be easily performed in downstream processing by the addition of sulfuric acid, allowing the separation of crude oil and water (Onaizi et al., 2021).

The oil industry has taken advantage of the synergistic effect of combining polymers and surfactants in oil recovery. In a similar way, biosurfactants can be used in combination with (bio)polymers to improve oil displacement efficiency. Qi and co–workers (2018) studied the compatibility between the biosurfactant–producing strain *Bacillus* sp. W5 and a weak gel (a mixture of a polymer and a delayed cross–linker) for application in oil recovery. It was demonstrated that *Bacillus* sp. W5 did not change the rheological properties of the weak gel, and the weak gel did not affect the bacterial growth or biosurfactant properties. Instead, it was found that oil recovery increased from 9.8 – 14.7% with the individual treatments, up to 23.6% when the weak gel and *Bacillus* sp. W5 were injected into the core simultaneously, demonstrating the potential of using biosurfactants and polymers together in MEOR (Qi et al., 2018). In a similar way, combining the biosurfactant–containing CFS from cultures of *B. subtilis* RI4914 with a partially purified biopolymer produced by the same strain increased oil recovery by 20% when compared with the effect of the CFS alone. AOR values obtained with the CFS were also higher than those obtained with solutions of the partially purified biosurfactant, probably due to the presence of compounds such as 2,3–butanediol, which acts synergistically with the biosurfactant in reducing the IFT (Fernandes et al., 2016). Al–Ghailani and co–workers (2021) studied the effect of combining the

biosurfactant surfactin (produced by *B. subtilis* W19) with the biopolymer schizophyllan (produced by *Schizophyllum commune* ATCC38548) and the alkali Na_2CO_3 in oil recovery. Na_2CO_3 had a positive effect in the surface–active properties of surfactin: surfactin (100 mg/L) alone reduced the IFT between the aqueous phase and crude oil to values around 1 mN/m, whereas in combination with Na_2CO_3 (9 g/L), the IFT was reduced up to 0.025 mN/m. The rheological properties of the biopolymer were not affected by the biosurfactant or the alkali, and the biopolymer did not affect the surface–active properties of the biosurfactant–alkali system. In core–flooding assays performed using Berea cores (oil viscosity 23 mPa s), the injection of 0.5 pore volumes (PV) of a formulation containing surfactin (400 mg/L), Na_2CO_3 (11 g/L) and schizophyllan (600 mg/L) resulted in an AOR of 32%, whereas in the absence of the biopolymer it was reduced to 17% (Al–Ghailani et al., 2021).

Another alternative to improve oil recovery rates is the use of engineered microorganisms better adapted to the oil reservoir conditions or with improved biosurfactant production yields. In that sense, protoplasts fusion technology is an interesting tool that allows combining the desired properties from different microorganisms. For example, the ability of *Bacillus mojavensis* JF–2 to produce a lipopeptide biosurfactant was combined with the ability of *Pseudomonas stutzeri* DQ1 to grow under anaerobic conditions. The resulting fusant produced a biosurfactant similar to that of the parental strain, under anaerobic conditions and temperatures up to 50°C. *In situ* oil recovery assays confirmed the applicability of this engineered strain in MEOR, with AOR values up to 4.2% (X. Liang et al., 2017). Alvarez Yela and co–workers (2016) compared the performance of rhamnolipids (produced by *P. aeruginosa* Pa4) and the transmembrane protein OmpA (produced by an engineered *Escherichia coli* strain) in oil recovery. The highest AOR (12%) was obtained with OmpA, which confirms the potential of using a protein with biosurfactant–like properties in MEOR (Alvarez Yela et al., 2016). Mutant strains (*B. subtilis* BS–37 and *Candida tropicalis* MTCC230), with the ability of producing higher amounts of biosurfactant when compared with the respective parental strains, were also evaluated for application in *ex situ* MEOR (Ashish, 2018; Qiang Liu et al., 2015). The results obtained demonstrated the feasibility of using the biosurfactants produced by these microorganisms in MEOR (Table 1.2).

Most of the studies presented in Table 1.2 and Table 1.3 were conducted at temperatures up to 60°C; however, most oil reservoirs exhibit higher temperatures. There is still a lack of information regarding microorganisms capable of growing and producing biosurfactants at temperatures usually found in oil reservoirs. Recently, a hyper–thermophilic *Clostridium* sp. strain, which can grow and produce biosurfactants at 96°C, was evaluated for application in MEOR (Arora et al., 2019). The glycoprotein

biosurfactant produced by this strain was stable at a wide range of temperatures (37 – 101°C), pH values (5 – 10), and salinities (up to 13%), being a great candidate for MEOR applications. Furthermore, sand–pack column studies conducted at 96°C yielded significant recovery rates in both *in situ* (37% AOR) and *ex situ* (17% AOR) assays. Two *Bacillus* strains isolated from the Gulf of Guinea oilfield were also evaluated for MEOR application under high temperature conditions (Okoro et al., 2022). From these, *Bacillus amyloliquefaciens* grew at temperatures up to 100°C and *Bacillus nealsonii* continued to show growth above 110°C. Oil recovery was tested with the culture broth of each of these microorganisms at different temperatures (27 – 120°C). Results show that at higher temperatures, AOR was higher for both strains, achieving a maximum of 27% for *B. amyloliquefaciens* and 32% for *B. nealsonii* at 120°C. Even though these assays were performed *ex situ*, the ability of the two strains to grow at very high temperatures opens the possibility of being used for *in situ* operations.

Another limitation for the application of biosurfactants in MEOR is the high cost of the substrates used to grow the producing microorganisms, which results in high production costs. Whereas the price of synthetic surfactants can be around 1–3 US$/kg, the price of sophorolipids (the cheapest and most widely available biosurfactant) is around 35 US$/kg (Roelants et al., 2019). Consequently, several studies evaluated the use of alternative carbon and nitrogen sources for their production (e.g. sugarcane and date molasses, vegetable oils, waste cooking oils, starch, cornmeal, paraffin, corn steep powder), in order to reduce their production costs (Das & Kumar, 2019; P. Gao et al., 2016; Ibrahim, 2018; Joshi, Al–Wahaibi, Al–Bahry, Elshafie, Al–Bemani, Al–Bahri, et al., 2016; Ke, Sun, et al., 2018; Ke et al., 2019; Lan et al., 2015; X. Liang et al., 2017). In other cases, the composition of the culture medium or the operational conditions were optimized to increase their productivity (Amani, 2015; Khademolhosseini et al., 2019). For instance, Gao and colleagues (2016) used corn steep powder as carbon source instead of glucose to grow *B. subtilis* M15–10–1 in the *in situ* MEOR assays, due to the high emulsifying activity obtained with this substrate (P. Gao et al., 2016). Sugarcane bagasse was used as the sole carbon source for the production of surfactin by *B. safensis* J2 for application in *ex situ* oil recovery assays. The produced biosurfactant was stable at different environmental conditions (30–90°C, pH 7–12, salinities up to 8%) and resulted in 4.5% AOR (Das & Kumar, 2019).

1.4.2 Biosurfactant MEOR: field assays

Field trials often rely on *in situ* biosurfactant–mediated oil recovery, with several successful assays reported in different types of fields, the most recent ones occurring mainly in China. In Shengli oilfield, a

number of recent trials were implemented where different nutrient solutions were injected to stimulate the growth of indigenous bacteria. It was found that, after treatment, *Pseudomonas* and *Bacillus* were among the dominant genera across the four blocks studied (Du et al., 2019; Xingbiao et al., 2015). Another trial reported in the Xinjiang field also relied on the injection of nutrients to enhance oil recovery. Again, *Pseudomonas* was the dominant group during the trial, suggesting that biosurfactants were the primary oil recovery mechanism (Saikia et al., 2012; Sarma et al., 2019). Additionally, bacteria from the genus *Acinetobacter*, which have been reported as biosurfactant and bioemulsifier producers, were also enriched in the production wells after nutrient injection (Chai et al., 2015). In Chunfeng oilfield, the recovery of ultra–heavy oil was enhanced through *in situ* MEOR. A selection of indigenous bacteria (*B. subtilis* XJZ2–1, *Pseudomonas* sp. XJZ3–1 and *Dietz coli* Z4M8–2) and one exogenous microbe (*B. subtilis* SLG5B10–17), together with nutrients and an activator solution, were injected into a production well over seven days, followed by a shut–in period of 166 days. After 13 months, oil production increased from 0.4 to 4.7 tons/day, with a peak production of 17 tons/day and a water cut of 34%. Furthermore, the results obtained showed a longer effective oil recovery period in the wells where MEOR was applied when compared with the adjacent wells treated with steam (X. Wang et al., 2016).

More recently, a large–scale pilot test was performed in Baolige oilfield, which involved 78 injection wells and 169 production wells. Indigenous *B. licheniformis* LC and *Rhodococcus* sp. JH were selected in laboratory assays to be used in the field trial, due to the high surface activity of their biosurfactants. After four injection cycles, applied over 43 months, additional oil production reached a total of 2.1×10^5 tons. However, it was found that in 15% of the extraction wells, oil production did not increase significantly. This was attributed to the fact that some of the wells were located within formations with poor homogeneity or with poor connectivity in the underground network, which negatively affected the bacterial flow through the well (Ke, Lu, et al., 2018). In the same field, a smaller trial was initiated shortly after, this time involving only two injection wells and eight production wells. The biosurfactant–producing bacterium *Luteimonas huabeiensis* HB–2, which was found to reduce oil–water IFT and decrease oil viscosity in lab–scale assays, was used in this trial. The field test was carried out through two bacterial injection cycles, both followed by a period of water flooding. By the end of the two cycles 2300 tons of additional oil were recovered, an enhancement that was attributed mainly to a reduction in oil viscosity (Ke, Sun, et al., 2018).

In the Jilin oilfield, Xia and collaborators (2021) performed field assays (reservoir temperature 35°C) using *Pseudomonas* sp. WJ6. During the 9 months after the injection of the microorganism with the

appropriate nutrients and a shut–in time of 21 days, oil production increased more than 11 times. Furthermore, as in the laboratory assays, the viscosity of the crude oil produced was reduced between 50 and 65% (Xia et al., 2021).

These figures demonstrate the potential of *in situ* biosurfactant production to improve oil recovery. However, besides biosurfactants, both exogenous and indigenous microorganisms also produce other metabolites (biopolymers, gases, acids, and solvents) and biomass, which can contribute to the observed increase in oil production.

1.5 Polymer flooding in oil recovery

Polymer flooding is another promising EOR strategy, with potential increases in oil recovery around 7–15% after water flooding is exhausted (Xue et al., 2023). The efficiency of oil recovery highly correlates to the volumetric sweep efficiency, which is determined by the mobility ratio (M) between the oil and water phases:

$$M = \frac{k_w \times \mu_0}{k_o \times \mu_w} \tag{1.2}$$

where k_w is the relative permeability of water in the water flooded zone, k_o is the relative permeability of oil in the oil–saturated zone, μ_o is the viscosity of the oil, and μ_w is the viscosity of water. A higher mobility ratio means that the water moves through the same channels past the oil phase and reaches the production well faster, leaving unswept oil trapped in the reservoir. Increasing the viscosity of the injected water leads to a more uniform displacement front and ultimately leads to an increased oil recovery (Equation 1.1 and Equation 1.2). Polymers have the ability to increase the viscosity of the injected water or displacement fluid, decreasing its mobility and improving sweep efficiency (Rellegadla et al., 2017) (Figure 1.4).

For application in oil recovery, the polymer solution must be able to generate viscosity at a minimum concentration. High polymer concentrations may lead to injectivity problems by increasing the pressure at the wellbore; while high molecular weight polymers, that can provide high viscosities at low concentrations, may increase the inaccessible pore volume since the polymer molecule can be larger than the pore size, as it will be explained bellow (Firozjaii & Saghafi, 2020). Thus, it is important to find an equilibrium between these two parameters that will generate the best results. Additionally, the polymers selected for EOR application must meet a number of requirements, including stability under

reservoir conditions (salinity, pressure and temperature) and high shear rates. They usually exhibit a shear–thinning or pseudoplastic behavior (Figure 1.5), exhibiting lower viscosities near the wellbore region, where shear rates are high due to the high flow rate necessary to facilitate polymer injection, and higher viscosities inside the well, as shear rates decrease, thus favoring oil displacement (Gudiña, Teixeira, et al., 2015).

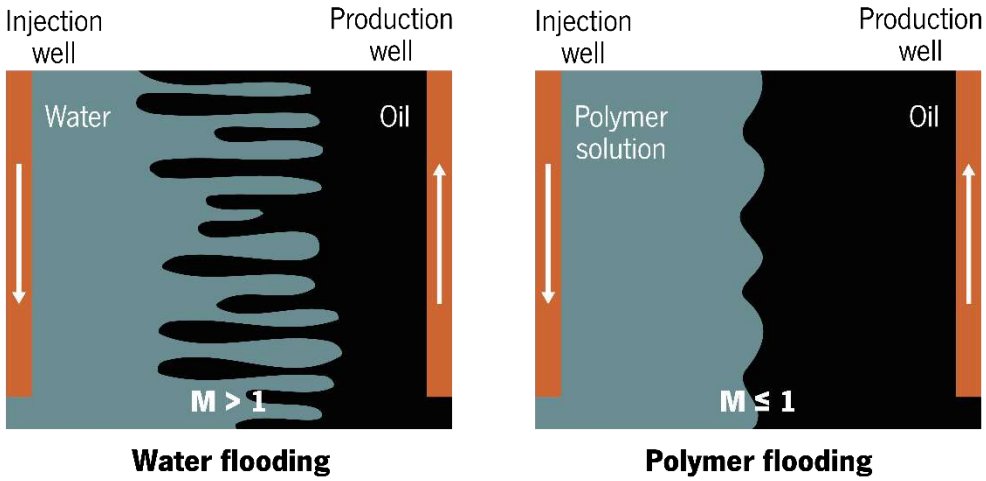

Figure 1.4 – Oil recovery mechanism by polymer flooding: comparison between water flooding, where the injected fluid forms "fingers", which decreases the sweep efficiency, and polymer flooding, that standardizes the flow–front and increases the sweep efficiency. Adapted from: Pinho de Aguiar et al. (2021).

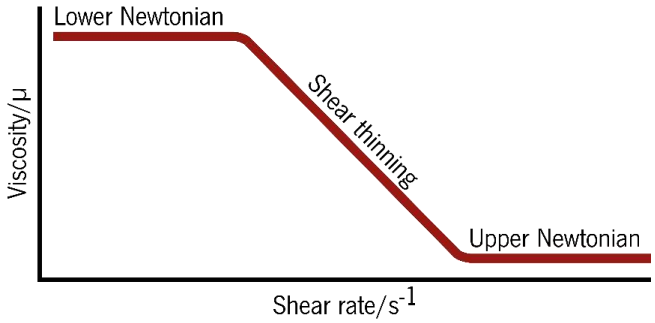

Figure 1.5 – Log–log plot for rheology of a shear–thinning fluid. Adapted from: Firozjaii & Saghafi (2020).

Furthermore, it is important to study the viscoelastic properties of the polymer solutions, as they influence sweep efficiency. Here, it becomes important to define the shear (or dynamic) modulus (G) that represents a material's stiffness and can be calculated as a measured contribution of the elastic and viscous components: the elastic (or storage) modulus (G'), which is a measure of resistance to the deformation, representing the energy stored by the material when subjected to shear stress; and the viscous (or loss) modulus (G''), that represents the energy loss (Lapasin & Pricl, 1999). The prevalence

of the elastic over the viscous modulus is usually favored in polymer flooding. Polymer solutions with a higher elastic modulus create a more stable flow front inside the reservoir pores that is able to displace the residual oil more efficiently (Veerabhadrappa et al., 2013). Additionally, the polymer exerts a pull force on oil droplets that are pushed out of dead–end pores, thus decreasing the residual oil saturation (Sheng, 2014).

Another oil recovery mechanism associated with polymer flooding is the reduction of rock permeability. Permeability reduction is caused by polymer adsorption (Figure 1.6), which is assumed to be an irreversible process that ultimately reduces the flow velocity of the injected water, even during subsequent water flooding processes (Sheng, 2014).

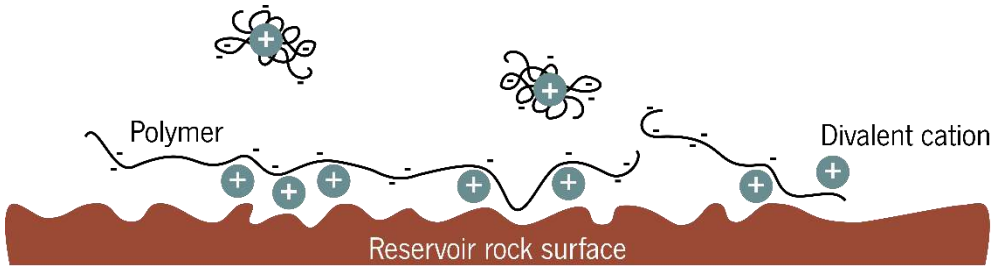

Figure 1.6 – Oil recovery mechanism by polymer flooding: adsorption of anionic polymers on reservoir rock surface by several types of interactions (hydrogen bonding, hydrophobic interaction, ion binding, electrostatic interaction, and Van der Waals forces). Adapted from: Rellegadla et al. (2017).

The effectiveness of this process depends on the type of polymer, the amount of polymer retained in the rock and the molecular weight (size) of the polymer in relation to the rock pores (Muhammed et al., 2020). Resistance factor (RF) and residual resistance factor (RRF) are used to characterize the polymer mobility relative to the process of permeability reduction. The RF denotes the mobility ratio of the fluid (water to polymer) as a function of permeability reduction and viscosity enhancement caused by the polymer (Equation 1.3) (Muhammed et al., 2020; C. Wang et al., 2018):

$$RF = \frac{\lambda_w}{\lambda_p} = \frac{\left(\frac{k}{\mu}\right)water}{\left(\frac{k}{\mu}\right)polymer} = \frac{\Delta P_{polymer}}{\Delta P_{water}} \quad (1.3)$$

where λ is the mobility of water (w) and polymer (p), k and μ represent the effective permeability and viscosity of water and polymer solution, and ΔP corresponds to the differential pressure between the inlet and outlet of a well (pressure drop) occurring during flooding operations. A higher RF means that a higher pressure is necessary to inject a polymer and maintain its flow through to the system in comparison to water (mobility reduction by polymer flooding). RRF, on the other hand, describes the ratio of water

permeability before and after polymer flooding, indicating the percentage of reduced rock permeability due to the adsorbed polymer (Equation 1.4) (Muhammed et al., 2020; C. Wang et al., 2018).

$$RRF = \frac{\left(\frac{k}{\mu}\right)before\ polymer\ flood}{\left(\frac{k}{\mu}\right)after\ polymer\ flood} = \frac{\Delta P_{water\ after\ polymer\ flood}}{\Delta P_{water\ before\ polymer\ flood}} \quad (1.4)$$

Usually, the greater the values of RF and RRF, the higher the potential to improve sweep efficiency and obtain higher oil recovery rates through polymer flood. However, if these values are too high, more polymer will be adsorbed into the rock pores and can cause injectivity problems associated with the blockage of pore throats at the well bore region (Muhammed et al., 2020).

A common example of chemical polymers used for EOR applications are hydrolyzed polyacrylamides (HPAMs) and their derivatives, that are extensively available, have low production costs and a high degree of customization (molecular weight, hydrolysis degree, etc.). However, these synthetic polymers are sensitive to reservoir conditions, namely salinity and temperature, which greatly decrease their thickening potential (Pu et al., 2018).

1.6 Biopolymers: a sustainable alternative to chemical polymers in oil recovery

Because commonly used synthetic polymers are susceptible to reservoir conditions, current research has been focusing on the use of biopolymers. Biopolymers are usually salt– and thermo–tolerant, rendering them a high thickening capability and stability under reservoir conditions. Their specific properties will depend on the source and their molecular structure (Pu et al., 2018).

Microbial biopolymers, commonly referred to as extracellular polymeric substances (EPS), consist of an assembly of monomers like nucleic acids (polynucleotides), amino acids (polypeptides) and carbohydrates (polysaccharides) (Lee et al., 2020). Several microorganisms, including species of the genera *Alcaligenes* (C. Gao, 2015; L. Xu et al., 2014), *Athelia* (Xia et al., 2018), *Aureobasidium* (A. Elshafie et al., 2017), *Kosakonia* (Ge et al., 2021), *Leuconostoc* (Soudmand–asli et al., 2007), *Pseudomonas* (H. Li et al., 2022; F. Zhao, Guo, et al., 2018), *Rhizobium* (Couto et al., 2019), *Schizophyllum* (Joshi, Al–Wahaibi, Al–Bahry, Elshafie, Al–Bemani, Al–Hashmi, et al., 2016), *Sclerotium* (K. Liang et al., 2019), *Sphingomonas* (Y. Li et al., 2017; K. Liang et al., 2019) and *Xanthomonas* (Ramos de Souza et al., 2022) produce exopolysaccharide biopolymers that can be repurposed for application in MEOR, since they typically form viscous hydrogels when in solution (Lee et al., 2020). Some polypeptides

produced by *Bacillus* spp. have also been studied for MEOR applications (Azarhava et al., 2020, 2021; Fan et al., 2020; Suthar et al., 2009), although these are not as common.

Among these, xanthan gum, produced by *Xanthomonas campestris*, is the most extensively studied biopolymer, due to its ability to increase the flood water viscosity at low concentrations, and its high resistance to shear stress, temperature and salinity (Pu et al., 2018). The double helix structure of xanthan gum gives it, and other biopolymers with similar structure, a high tolerance to temperature, being able to withstand temperatures up to 70°C. Furthermore, the presence of charge–free chains creates a shielding effect that enables xanthan gum to tolerate high salinity conditions without folding (Firozjaii & Saghafi, 2020). This is true for numerous biopolymers studied so far, that are able to retain their viscosity in solution at temperatures up to 90°C while withstanding salinities up to 200 g/L (Couto et al., 2019; C. Gao, 2015, 2016; Ge et al., 2021; Jang et al., 2015; Y. Li et al., 2017; K. Liang et al., 2019). Some biopolymers can be stable at even higher temperatures due to their rigid structures. Schizophyllan, for example, maintained its viscosity at temperatures as high as 135°C and was even shown to remain stable after ageing for over seven months at 120°C (Quadri et al., 2015). Sphingan can maintain around 75% of its original viscosity at temperatures as high as 120°C (Ji et al., 2020); the biopolymer produced by *Athelia* sp. can tolerate temperatures up to 145°C (Xia et al., 2018); and poly–γ–glutamic acid (γ–PGA) produced by *B. licheniformis* LMG 7559 can tolerate temperatures up to 275°C, showing only a 12% weight loss at this temperature (Azarhava et al., 2020).

These compounds also contribute to increase oil recovery through selective plugging (Figure 1.7), where the biopolymers redirect the injected water to oil–rich channels by plugging the high permeability regions in the rock (Rellegadla et al., 2017). This happens either because the biopolymers naturally adhere to the rock or indigenous bacteria feed on the biopolymers and stick to the rock surface. In turn, these bacteria may produce biosurfactants *in situ* that lower the IFT and further increase residual oil displacement (Rellegadla et al., 2017). Furthermore, biopolymers can be produced by bacterial cells inside the reservoir to form biofilms, which, in addition to contributing to selective plugging, have been shown to alter rock wettability (Karimi et al., 2012). Other biopolymers, like γ–PGA, can also change the wettability of the rock to a less oil–wet state. γ–PGA decreased the contact angle of a carbonate rock surface down to 37.5–44° due to the interactions between the negatively charged carboxyl groups of the γ–PGA molecules and the positive charges of the carbonate rock (Azarhava et al., 2021).

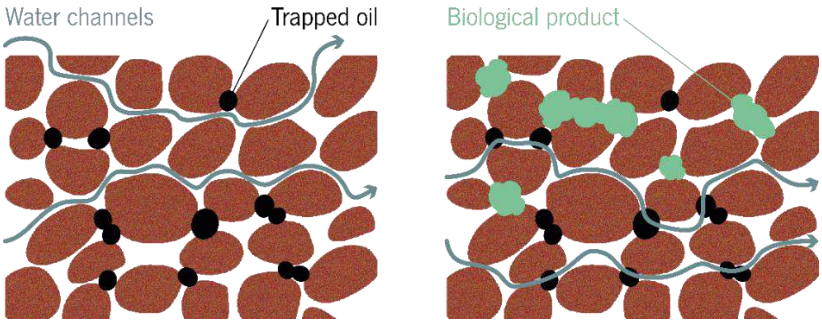

Figure 1.7 – Selective plugging mechanism during MEOR operations. Adapted from: Lee et al. (2020).

Thus, biopolymers can be considered viable alternatives to chemical polymers to be used in oil recovery. Nonetheless, the use of these bioproducts still presents some challenges: higher biological degradation that may force the use of biocides for MEOR applications; higher oxidative decomposition; poor filterability due to accumulation of biomaterial at the well bore region; and higher production costs, among others (Firozjaii & Saghafi, 2020; Pu et al., 2018).

1.6.1 Biopolymer MEOR: laboratory studies

Similarly to the application of biosurfactants in MEOR, biopolymers can be produced *ex situ* and injected into the oil well together with the flood water, or be produced *in situ* by stimulating injected or indigenous microbes. Table 1.4 summarizes some of the laboratory–scale *ex situ* assays performed using biopolymers produced by different microorganisms, which resulted in AORs between 9 and 36%. Even though most of the studies found for biopolymer MEOR were performed *ex situ*, some show the applicability of biopolymer–producing microorganisms in *in situ* strategies, as shown in Table 1.5. The AORs reported for these studies vary from 4 to 28%, with shut–in times from 3 to 20 days. Moreover, one of the *in situ* studies presented in Table 1.5 highlights the importance of nutrient injection together with the bacterial culture starter. Injection of nutrients or injection of the microbial culture (*B. licheniformis* DM–1) results in AORs of 6.9% and 3.8%, respectively, while the injection of both simultaneously increases the AOR to 19% (Fan et al., 2020). Thus, the oil recovery obtained is attributed to the growth of microorganisms and the resulting production of biopolymer that happens because the microbial cells have the necessary nutrients available.

Table 1.4 – Summary of different laboratory–scale MEOR *ex situ* assays performed using biopolymers produced by different microorganisms.

Microorganism	Biopolymer	Substrate (permeability)	Porosity (%)	Oil API gravity (°)	Oil viscosity (mPa s)	Temperature (°C)	Pressure (bar)	Flow rate (mL/min)	BP volume (PV)	Treatment – solution viscosity	AOR (%)	Reference
Xanthomonas campestris	Xanthan gum[1]	Sand (1490 mD)	39	–	458	50	–	0.5000	–	BP (1.75 g/L)	28	L. Xu et al. (2014)
Xanthomonas campestris	Xanthan gum[1]	Sand (207 mD)	34	–	458	50	–	0.5000	–	BP (1.75 g/L)	27	L. Xu et al. (2014)
Xanthomonas campestris IBSBF 2103	Xanthan gum	Carbonate rock core (1000 mD)	48	–	2	65	41	0.8000	3.0	BP (7 g/L) – 402 mPa s	27[2]	Ramos de Souza et al. (2022)
Xanthomonas campestris	Xanthan gum[1]	Glass beads (379 mD)	37	–	450	25	–	4.0000	3.0	BP (30 g/L) – 27.8 mPa s	21	Jang et al. (2015)
Xanthomonas campestris	Xanthan gum[1]	Sand (3767 mD)	40	–	300	65	–	3.0000	1.6	BP – 30 mPa s	15	Ji et al. (2020)
Xanthomonas campestris	Xanthan gum[1]	Sand (1816 mD)	44	–	274	75		0.5000	–	BP	14	Y. Li et al. (2017)
Xanthomonas campestris	Xanthan gum[1]	Artificial core	21	–	6	85	–	1.0000	1.0	BP – 19 mPa s	11	K. Liang et al. (2019)
Xanthomonas campestris	Xanthan gum[1]	Sand (1559 mD)	44	–	274	90		0.5000	–	BP	9	Y. Li et al. (2017)
Pseudomonas sp.	Xanthan gum	Glass micromodel (2000 mD)	43	–	32	40	1	0.0004	1.0	BP (1.69 g/L) – 71.2 mPa s	21	H. Li et al. (2022)
Alcaligenes sp.	Welan gum[1]	Sand (1372 mD)	38	–	458	50	–	0.5000	–	BP (1.75 g/L)	36	L. Xu et al. (2014)
Alcaligenes sp.	Welan gum[1]	Sand (178 mD)	34	–	458	50	–	0.5000	–	BP (1.75 g/L)	35	L. Xu et al. (2014)
Shingomonas sp. WG	Shingan	Sand (3600 mD)	36	–	300	65	–	3.0000	1.6	Culture broth – 30 mPa s	23	Ji et al. (2020)
Shingomonas sp. WG	Shingan	Sand (3709 mD)	34	–	300	65	–	3.0000	1.6	BP – 30 mPa s	15	Ji et al. (2020)
Shingomonas sp. WG	Shingan	Sand (3000 mD)	–	–	300	60	–	1.0000	–	BP (0.35 g/L)	17	Ji et al. (2022)
Sclerotium sp.	Scleroglucan[1]	Artificial core	21	–	6	85	–	1.0000	1.0	BP – 19 mPa s	13	K. Liang et al. (2019)
Schizophyllum commune	Schizophyllan[1]	Sandstone core (1900 mD)	24	26	35	55	–	–	4.0	BP (1 g/L) – 65 mPa s	10[2]	C. Gao (2016)
Schizophyllum commune	Schizophyllan[1]	Synthetic carbonate core (126 mD)	17	38	5	120	345	0.2000	0.5	BP	10[2]	Quadri et al. (2015)
Schizophyllum commune ATCC38548	Schizophyllan	Berea sandstone core	–	–	–	45	69	0.4000	6.0	BP broth	28	Joshi, Al–Wahaibi, Al–Bahry, Elshafie, Al–Bemani,

												Al–Hashmi, et al. (2016)
Aureobasidium pullulans	Pullulan	Berea sandstone core	–	–	20–25	60	69	0.4000	5.0	CFS – 28–59.9 mPa s	9	A. Elshafie et al. (2017)
Bacillus sonorensis	Polysaccharide and polyamide	Glass micromodel	38	–	–	25	–	0.0500	1.0	BP (10 g/L)	36	Bajestani et al. (2017)
Bacillus licheniformis LMG 7559	Poly γ–glutamic acid	Glass micromodel	44	20	242	–	–	0.0008	–	BP (2.5 g/L) – 29 mPa s	13[2]	Azarhava et al. (2021)
Bacillus licheniformis LMG 7559	Poly γ–glutamic acid	Glass micromodel	48	20	242	25	–	–	–	BP (5 g/L) – 29 mPa s	15[2]	Azarhava et al. (2020)
Athelia sp.	Glucan	Core (120–1193 mD)	21–24	–	1050	85	–	0.5000	1.0	BP (1 g/L) – 900 mPa s	14–18	Xia et al. (2018)
Sphingomonas sp.	Diutan gum[1]	Artificial core	23	–	6	85	–	1.0000	1.0	BP – 19 mPa s	16	K. Liang et al. (2019)
Sphingomonas sp. ATCC 53159	Diutan gum[1]	Sand (1757 mD)	44	–	274	90		0.5000	–	BP	21	Y. Li et al. (2017)
Sphingomonas sp. ATCC 53159	Diutan gum[1]	Sand (1599 mD)	44	–	274	75		0.5000	–	BP	25	Y. Li et al. (2017)
Rhizobium viscosum CECT 908	–	Sand	33	–	81	40	1	2.0000	2.0	Culture broth – 739 mPa s	14	Couto et al. (2019)
Rhizobium viscosum CECT 908	–	Sand	34	–	167	40	1	2.0000	2.0	Culture broth – 739 mPa s	26	Couto et al. (2019)
Rhizobium viscosum CECT 908	–	Sand	35	–	496	40	1	2.0000	2.0	BP – 50 mPa s	25[2]	Gudiña et al. (2023)
Kosakonia oryzae	–	Artificial core (400 mD)	17	35	20	45	–	0.3000	0.4	BP (5 g/L) + Surfactant (1 g/L) – 39 mPa s	16	Ge et al. (2021)

All the recovery assays were performed using crude oil.

[1] Commercial biopolymer. [2] Additional oil recovery (AOR) values are the corrected values obtained after subtracting the AOR obtained in the control assays.

–: Not reported. AOR: Additional oil recovery. BP: Biopolymer. CFS: Cell–free supernatant. PV: Pore volume.

Table 1.5 – Summary of different laboratory–scale MEOR *in situ* assays performed using different biopolymer–producing microorganisms.

Microorganism	Biopolymer	Substrate (permeability)	Porosity (%)	API gravity (°)	Oil Viscosity (mPa s)	Temperature (°C)	Flow rate (mL/min)	Culture volume (PV)	Shut–in time (days)	AOR (%)	Reference
Leuconostoc mesenteroides PTCC 1059	Dextran	Fractured and non–fractured glass micromodels (6020–7797 mD)	36	33	29	37	0.008	1.0	3	0–21	Soudmand–asli et al. (2007)
Pseudomonas stutzeri XP1 [1]	Dextran	Rock core (398 mD)	21	31	6	39	0.200	0.3	15	12[2]	F. Zhao, Guo, et al. (2018)
Bacillus licheniformis DM–1 [1]	Proteoglycan	Sand (3178 mD)	23	31	110	45	2.000	0.5	7	19[2]	Fan et al. (2020)
Bacillus licheniformis TT33	–	Sand	–	–	–	50	–	0.6	20	28	Suthar et al. (2009)
Enterobacter sakazakii JD + *Bacillus subtilis* I fusant	–	Sand (908 mD)	39	–	–	45	0.500	3.0	3	25	Y. Xu & Lu (2011)
Enterobacter cloacae JD + *Geobacillus* sp. fusant	–	Sand (low permeability)	38	–	–	40	2.000	0.4	7	11	Sun et al. (2013)
Enterobacter cloacae JD + *Geobacillus* sp. fusant	–	Sand (high permeability)	43	–	–	40	2.000	0.4	7	3.5	Sun et al. (2013)
Enterobacter cloacae JD transformant	–	Artificial core	–	–	–	50	1.000	2.0	3	–	Sun et al. (2011)

All the recovery assays were performed using crude oil.

[1] Indigenous microorganism. [2] Additional oil recovery (AOR) values are the corrected values obtained after subtracting the AOR obtained in the control assays.

–: Not reported. AOR: Additional oil recovery. BP: Biopolymer. CFS: Cell–free supernatant. PV: Pore volume.

As was the case with biosurfactants, comparison between the different assays is difficult due to the variability of experimental conditions. Furthermore, the underlying mechanisms of oil recovery can greatly differ between different biopolymers. Besides this, some authors report that the time of injection can also interfere with the effectiveness of oil recovery, and thus the comparison between different studies. By injecting xanthan gum earlier, skipping the secondary recovery, more oil was produced (70% of the OOIP) in a shorter time, when compared with polymer injection during tertiary recovery (50% of the OOIP) (Ramos de Souza et al., 2022). Oil recovery with schizophyllan also proved to be faster when injected early in comparison with water flooding, requiring one less pore volume of injected solution to reach the maximum recovery rate (C. Gao, 2016).

Several mechanisms can be associated with biopolymer flooding, namely, increasing the viscosity of the displacing fluid and permeability reduction through selective plugging. All the studies presented in Table 1.4 and Table 1.5 have shown that biopolymers have the ability to increase the viscosity of water, making this the most common mechanism of oil recovery. Selective plugging is usually associated with *in situ* MEOR, with some authors even suggesting that this is the main mechanism for oil recovery in such cases (Soudmand–asli et al., 2007; Sun et al., 2011; Suthar et al., 2009; Y. Xu & Lu, 2011). For instance, in an *in situ* assay using *Leuconostoc mesenteroides* PTCC 1059, the permeability of sand–pack columns was reduced by 40% due to bacterial growth and exopolysaccharide production within the substrate pores (Soudmand–asli et al., 2007).

The impact of permeability reduction in oil recovery can be evaluated with the calculation of RRF and RF. Diutan gum, for example, had higher RF and RRF values than xanthan gum, which translated to a higher recovery rate (RF = 42.9, RRF = 12.1 and AOR = 21–25% for diutan gum, compared to RF = 21.2, RRF = 8.3 and AOR = 9–14% for xanthan gum). The same relationship was observed for HPAM, which had an RF of 6.5 and an RRF of 1.6, leading to a recovery of 5–10% of additional oil (Y. Li et al., 2017). In a different study, it was observed that in comparison to diutan gum and scleroglucan, which exhibited higher RF values, the adsorption of xanthan gum and HPAM was higher (K. Liang et al., 2019). The relationship between the higher RF and oil recovery values can be explained by the higher viscosity of diutan gum and scleroglucan. Furthermore, it was observed that a higher pressure drop occurring during the injection of the biopolymers due to their viscosity, resulted in a higher oil recovery (Joshi, Al–Wahaibi, Al–Bahry, Elshafie, Al–Bemani, Al–Hashmi, et al., 2016; K. Liang et al., 2019). The pressure drop is indicative of the sweep efficiency, as well as the adsorption of the biopolymer to the rock surface,

which causes permeability reduction and can be an underlying cause of pore clogging at the well bore region.

Since RF is indicative of fluid mobility, it can be evaluated according to the flow velocity. For example, when the linear velocity was low, the RF of schizophyllan was high, indicating that the injection of the biopolymer would increase the pressure drop. However, as the velocity increased, the RF declined until it reached a plateau, which translates to higher mobility during polymer flood (C. Gao, 2016). The same was observed with the biopolymer from *Athelia* sp. in a high permeability core, that had higher RF and RRF values at higher flow rates, suggesting the ability of the biopolymer to affect fluid mobility (Xia et al., 2018). As such, the evaluation of flow velocity can give insights into the mechanisms that lead to oil recovery when using (bio)polymers. A comparison between xanthan gum and HPAM revealed that the flow velocity in narrow channels was higher after flooding with HPAM. This indicates that while HPAM improves the mobility ratio and has a higher oil recovery (23% AOR), xanthan gum is more prone to adsorption and pore clogging, having a slightly lower oil recovery rate (21% AOR) (H. Li et al., 2022).

Moreover, RF and RRF seem to be affected by the permeability of the substrate. When the substrate permeability increases, RF increases due to the higher mobility of the fluid and RRF decreases because biopolymer adsorption is not enough to cause a significant permeability reduction since the pores are bigger (Quadri et al., 2015). Besides, in higher permeability substrates, oil recovery through biopolymer flooding is usually higher, probably because there is less pore clogging caused by the biopolymer (Quadri et al., 2015; Xia et al., 2018; L. Xu et al., 2014). The presence of fractures within the substrate can also affect the oil recovery efficiency, negatively in this case. When *L. mesenteroides* PTCC 1059 was used in fractured models, oil recovery rates decreased significantly (from 21% AOR to 0–17% AOR depending on the orientation of the fracture) due to the accumulation of cells and biopolymer inside the fracture, that do not contribute to the recovery of oil (Soudmand–asli et al., 2007).

Another parameter to consider is the viscoelasticity of the biopolymer solution. Biopolymers with a higher elastic modulus (G') usually result in a higher oil recovery (Ji et al., 2020, 2022; Y. Li et al., 2017; K. Liang et al., 2019; L. Xu et al., 2014). The viscoelastic moduli can be indicative of the biopolymer conformation under shear, which affects recovery efficiency. Xu et al. (2014) studied the viscoelastic properties of welan gum and xanthan gum as a function of strain. For welan gum solutions, G' was higher than G'' at the lower strain range, indicating that the biopolymer exists in a gel–like structure, while the reverse happened at high strain, meaning that the gel–like structure was broken. For xanthan gum, on the other hand, G'' was higher than G' over the entire strain range, which is typical of a disordered

structure. Furthermore, the dynamic modulus (G) of welan gum was higher than that of xanthan gum, implying that welan gum had stronger viscoelasticity. As expected, the oil recovery rate was higher when welan gum was used (35–36% AOR compared with 27–28% AOR obtained with xanthan gum), due to the better sweep efficiency and mobility ratio reduction that is associated with more elastic fluids (L. Xu et al., 2014).

To overcome some of the limitations associated with the application of biopolymers, several strategies are being employed in order to improve oil recovery. For example, Sun and co–workers (2011) used an *Enterobacter cloacae* strain, which produces a water–insoluble biopolymer at the optimal temperature of 30°C, and a thermophilic *Geobacillus* strain to construct an engineered strain for exopolysaccharide production at higher temperatures. The obtained transformant was able to produce up to 8.83 g/L of biopolymer in molasses medium at 54°C; and was demonstrated to contribute to the enhancement of oil recovery, although with lower performance than the parental strain (Sun et al., 2011). Later, the same team improved the engineering process to develop a strain, through protoplast fusion, with better oil recovery performance (Sun et al., 2013). Similarly, *Enterobacter sakazakii* JD was genetically recombined with *B. subtilis*, that can survive in harsh environments, by protoplast fusion (Y. Xu & Lu, 2011). The obtained fusants grew and produced biopolymer under anaerobic conditions at salinities up to 100 g/L NaCl and temperatures up to 55°C. The resulting AOR at 45°C was 25% for one of the fusants, which is comparable with other studies of biopolymer *in situ* MEOR (Table 1.5).

Additionally, the effect of combining the biopolymer from *Kosakonia oryzae* with a surfactant was evaluated by Ge et al. (2021). It was observed that the biopolymer did not significantly interfere with the IFT reduction capacity of the surfactant, and the surfactant did not cause reduction of the solution's viscosity. Furthermore, this biopolymer–surfactant system maintained its properties in high salinity conditions (up to 100 g/L NaCl, 400 mg/L Ca^{2+} or 2400 mg/L Mg^{2+}) and high temperatures (up to 60°C). Overall, the oil recovery rate achieved by this binary system was around 16% (Ge et al., 2021). Sphingan, produced by *Sphingomonas* sp. WD, was combined with a synthetic non–ionic surfactant with the objective of improving oil recovery (Ji et al., 2022). The sphingan–surfactant mixture was stable at temperatures higher than 75°C, its viscosity was higher, and it exhibited more elastic properties than the sphingan solution without surfactant. Furthermore, AOR improved by 5% when the surfactant was added to the injection liquid. As stated above, the combination of both molecules can prove beneficial for MEOR operations.

1.6.2 Biopolymer MEOR: field assays

Field trials using biopolymers or biopolymer–producing microorganisms for MEOR are often limited by the reservoir conditions. The viscosity of the crude oil, reservoir temperature, salinity and permeability must be within certain ranges (< 200 mPa s, < 120°C, < 20000 ppm and > 30 mD, respectively) to ensure the viability of MEOR operations (Firozjaii & Saghafi, 2020). Furthermore, the injection of biocides is often necessary to prevent biopolymer degradation, since, as stated above, biopolymers can be consumed by indigenous bacteria, which leads to decreased recovery rates. For example, a single well assay performed in an offshore field in the Norwegian Sea, found that, even when injecting a biocide together with the biopolymer schizophyllan, biopolymer–degrading bacteria were still present in the field after the 39–day shut–in period (Beeder et al., 2018). In this example, the biopolymer was still stable after the incubation period, but it was suggested that if shut–in time had been longer, biopolymer degradation might have been an issue. Nonetheless, several field trials have demonstrated the applicability of biopolymers in oil recovery using both *in situ* and *ex situ* strategies.

In the Bockstedt oilfield in Northern Germany, a field trial, employing one injection well and three production wells, validated the effectiveness of schizophyllan in oil recovery (Leonhardt et al., 2014). The stability of the biopolymer, produced by *S. commune*, was evaluated under reservoir conditions, and it was found to be stable at temperatures up to 135°C. The biopolymer solution was produced offsite and was mixed with biocide prior to injection. Seven months into the trial, no injectivity issues were detected, which was in line with the observed laboratory studies; there was no significant increase in microbial communities after biopolymer injection and no degradation of the biopolymer was observed, which was probably due to the addition of biocide. The preliminary results showed a predicted increase of 25% in oil recovery (Leonhardt et al., 2014). Two years after the beginning of the trial, another field trial was employed in the same area and under similar conditions. Over the course of one year, the production rate in the closest production well increased by 20% (C. Gao, 2016).

In the Fuyu oil field in China, a selective plugging strategy was employed to improve oil recovery (Nagase et al., 2002). The microbes isolated from the reservoir were found to produce a cellulous biopolymer that can effectively clog pores, using molasses as the main carbon source. Injection of the microbes with nutrients was followed by a 10–day shut–in period to allow for the cell to grow and produce the desired biopolymer. Production results show that the oil production rate increased by eight times, while the amount of water present in the outlet decreased from 99% to 75% (Nagase et al., 2002).

1.7 Aim of the thesis

In laboratory assays, biosurfactants and biopolymers were demonstrated to be potential alternatives to synthetic surfactants and polymers for application in oil recovery. As discussed in this chapter, biosurfactants display a similar or better performance than chemical surfactants, and they are more environmentally friendly. However, the main bottleneck for their widespread use is their high production costs. In the last years, due to the interest in biosurfactants for application in several fields, considerable efforts have been performed regarding the use of agro–industrial residues as substrates for their production in order to reduce their market price. Furthermore, significant advances were made in the optimization of the production process, which contributed to increasing their productivity. Finally, genetic engineering approaches allowed the modification of wild–type biosurfactant–producing strains, improving their production titers and directing the metabolic pathways to the production of biosurfactant congeners with better properties.

Biopolymers, on the other hand, have proved, in some cases, to be more stable under reservoir conditions than chemical polymers and have remarkable viscoelastic properties, besides being more environmentally friendly. Their high biodegradability, however, can pose a problem when considering oil recovery applications, requiring the use of biocides. Furthermore, the combination of biopolymers and biosurfactants has the potential to increase oil recovery even more. Although there is a lack of field trials using both biomolecules simultaneously, laboratory experiments validate their synergistic effect.

The production of biosurfactants and biopolymers *in situ* by indigenous or injected microorganisms is one of the most promising approaches for their application in oil recovery, as it is expected to be a less expensive approach when compared with the *ex situ* strategy. Although production *in situ* exhibits some limitations, laboratory and field assays demonstrated its feasibility. Consequently, the screening of new microorganisms with the ability to grow and produce biosurfactants at the oil reservoir conditions, together with a better understanding of the microbial processes that take place in the oil reservoirs, are crucial to developing this promising technology.

The aim of this thesis was to develop biotechnological processes that would promote the additional recovery of oil, focusing on the production of several biomolecules with potential application in MEOR,

specifically biosurfactants and biopolymers, and their combination to reach better recovery rates. In order to achieve this goal, this thesis was developed with four main objectives (Figure 1.8):

- Screening, based on the literature, of biomolecules (biosurfactants and biopolymers) and microorganisms that might promote the additional recovery of oil;
- Production optimization of the most interesting biomolecules for different modes of application;
- Application of these biomolecules and microorganisms in MEOR using sand–pack columns and evaluation of their mechanisms of action;
- Simulation studies for potential application of this technology in field trials.

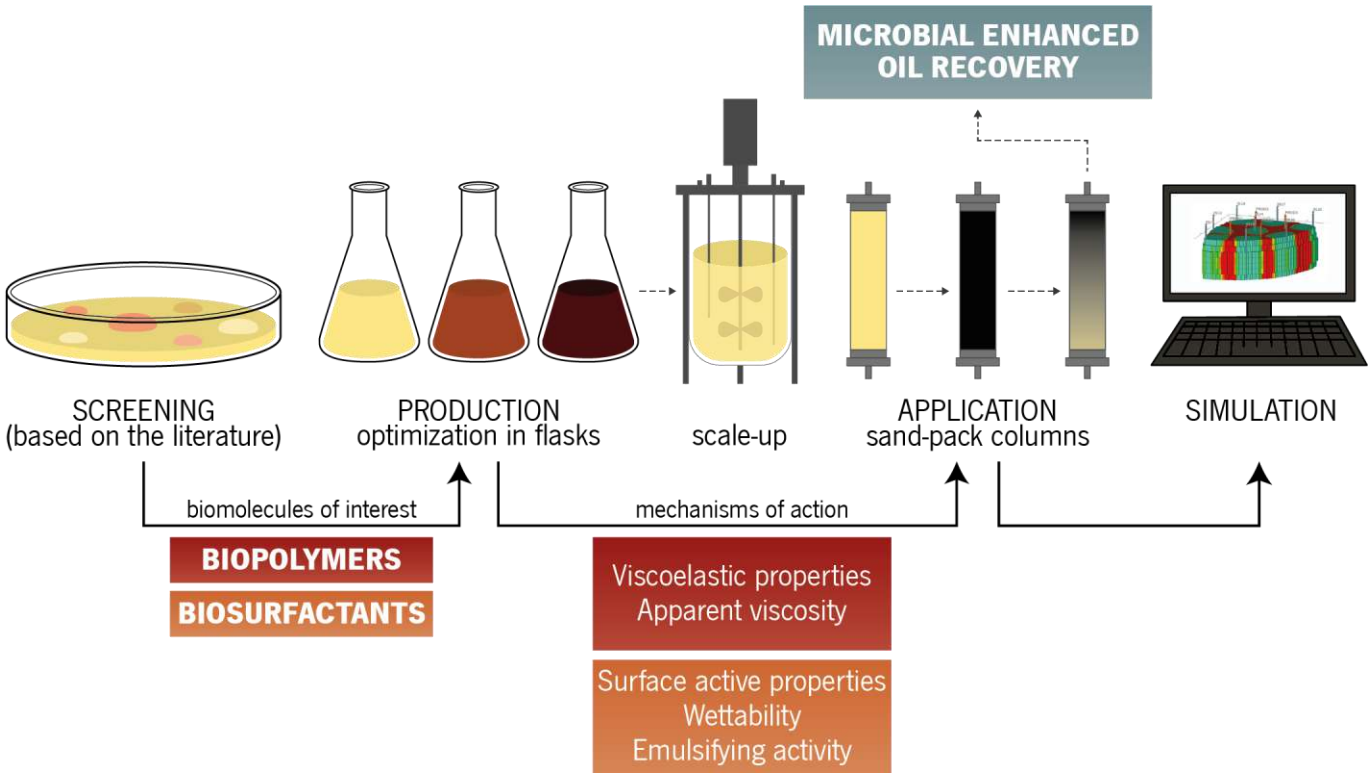

Figure 1.8 – Schematic overview of the main objectives of the thesis.

1.8 References

Aboelkhair, H., Diaz, P., & Attia, A. (2022a). Biosurfactant production using Egyptian oil fields indigenous bacteria for microbial enhanced oil recovery. *Journal of Petroleum Science and Engineering*, *208*, 109601. https://doi.org/10.1016/j.petrol.2021.109601

Aboelkhair, H., Diaz, P., & Attia, A. (2022b). Environmental comparative study of biosurfactants production and optimization using bacterial strains isolated from Egyptian oil fields. *Journal of Petroleum Science and Engineering*, *216*, 110796. https://doi.org/10.1016/j.petrol.2022.110796

Ahmadi, M. A., & Shadizadeh, S. R. (2018). Spotlight on the New Natural Surfactant Flooding in Carbonate Rock Samples in Low Salinity Condition. *Scientific Reports*, *8*(1), 1–15. https://doi.org/10.1038/s41598–018–29321–w

Akanji, L. T., Rehman, R., Onyemara, C. C., Ebel, R., & Jamal, A. (2021). A novel technique for interface analysis: Behaviour of sophorolipids biosurfactant obtained from Meyerozyma spp. MF138126 during low–salinity heavy–crude experiments. *Fuel*, *297*, 120607. https://doi.org/10.1016/j.fuel.2021.120607

Al–Ghailani, T., Al–Wahaibi, Y. M., Joshi, S. J., Al–Bahry, S. N., Elshafie, A. E., & Al–Bemani, A. S. (2021). Application of a new bio–ASP for enhancement of oil recovery: Mechanism study and core displacement test. *Fuel*, *287*, 119432. https://doi.org/10.1016/j.fuel.2020.119432

Al–Ghamdi, A., Haq, B., Al–Shehri, D., Muhammed, N. S., & Mahmoud, M. (2022). Surfactant formulation for Green Enhanced Oil Recovery. *Energy Reports*, *8*, 7800–7813. https://doi.org/10.1016/j.egyr.2022.05.293

Ali, N., Wang, F., Xu, B., Safdar, B., Ullah, A., Naveed, M., Wang, C., & Rashid, M. T. (2019). Production and application of biosurfactant produced by bacillus licheniformis Ali5 in enhanced oil recovery and motor oil removal from contaminated sand. *Molecules*, *24*(24), 4448. https://doi.org/10.3390/molecules24244448

Alvarez, V. M., Guimarães, C. R., Jurelevicius, D., de Castilho, L. V. A., de Sousa, J. S., da Mota, F. F., Freire, D. M. G., & Seldin, L. (2020). Microbial enhanced oil recovery potential of surfactin–producing Bacillus subtilis AB2.0. *Fuel*, *272*, 117730. https://doi.org/10.1016/j.fuel.2020.117730

Alvarez Yela, A. C., Tibaquirá Martínez, M. A., Rangel Piñeros, G. A., López, V. C., Villamizar, S. H., Núñez Vélez, V. L., Abraham, W. R., Vives Flórez, M. J., & González Barrios, A. F. (2016). A comparison between conventional Pseudomonas aeruginosa rhamnolipids and Escherichia coli transmembrane proteins for oil recovery enhancing. *International Biodeterioration and Biodegradation*, *112*, 59–65. https://doi.org/10.1016/j.ibiod.2016.04.033

Amani, H. (2015). Study of enhanced oil recovery by rhamnolipids in a homogeneous 2D micromodel. *Journal of Petroleum Science and Engineering*, *128*, 212–219. https://doi.org/10.1016/j.petrol.2015.02.030

Arora, P., Kshirsagar, P. R., Rana, D. P., & Dhakephalkar, P. K. (2019). Hyperthermophilic Clostridium sp. N–4 produced a glycoprotein biosurfactant that enhanced recovery of residual oil at 96 °C in lab studies. *Colloids and Surfaces B: Biointerfaces*, *182*, 110372. https://doi.org/10.1016/J.COLSURFB.2019.110372

Ashish, M. D. (Das). (2018). Application of biosurfactant produced by an adaptive strain of C.tropicalis MTCC230 in microbial enhanced oil recovery (MEOR) and removal of motor oil from contaminated sand and water. *Journal of Petroleum Science and Engineering*, *170*, 40–48. https://doi.org/10.1016/j.petrol.2018.06.034

Astuti, D. I., Purwasena, I. A., Putri, R. E., Amaniyah, M., & Sugai, Y. (2019). Screening and characterization of biosurfactant produced by Pseudoxanthomonas sp. G3 and its applicability for enhanced oil recovery. *Journal of Petroleum Exploration and Production Technology*, 1–11. https://doi.org/10.1007/s13202–019–0619–8

Azarhava, H., Bajestani, M. I., Jafari, A., Vakilchap, F., & Mousavi, S. M. (2020). Production and physicochemical characterization of bacterial poly gamma– (glutamic acid) to investigate its performance on enhanced oil recovery. *International Journal of Biological Macromolecules*, *147*, 1204–1212. https://doi.org/10.1016/j.ijbiomac.2019.10.090

Azarhava, H., Jafari, A., Vakilchap, F., & Mousavi, S. M. (2021). Stability and performance of poly γ–(glutamic acid) in the presence of sulfate ion for enhanced heavy oil recovery. *Journal of Petroleum Science and Engineering*, *196*, 107688. https://doi.org/10.1016/j.petrol.2020.107688

Bajestani, M. I., Mousavi, S. M., Jafari, A., & Shojaosadati, S. A. (2017). Biosynthesis and physicochemical characterization of a bacterial polysaccharide/polyamide blend, applied for microfluidics study in porous media. *International Journal of Biological Macromolecules*, *96*, 100–110. https://doi.org/10.1016/j.ijbiomac.2016.11.048

Beckman, J. W. (1926). Action of bacteria on mineral oil. *Industrial and Engineering Chemistry News Edition*, *4*(21), 10.

Beeder, J., Skarstad, A., Prasad, D., Todosijevic, A., Mahler, E., Fleck, C., & Lehr, F. (2018, June 8). Biopolymer injection in offshore single–well test. *Society of Petroleum Engineers – SPE Europec Featured at 80th EAGE Conference and Exhibition 2018*. https://doi.org/10.2118/190758–ms

Bera, A., Mandal, A., & Guha, B. B. (2014). Synergistic effect of surfactant and salt mixture on interfacial tension reduction between crude oil and water in enhanced oil recovery. *Journal of Chemical and Engineering Data*, *59*(1), 89–96. https://doi.org/10.1021/je400850c

Bhattacharya, M., Guchhait, S., Biswas, D., & Singh, R. (2019). Evaluation of a microbial consortium for crude oil spill bioremediation and its potential uses in enhanced oil recovery. *Biocatalysis and Agricultural Biotechnology*, *18*. https://doi.org/10.1016/j.bcab.2019.101034

Biktasheva, L., Gordeev, A., Selivanovskaya, S., & Galitskaya, P. (2022). Di- and Monorhamnolipids Produced by the Pseudomonas putida PP021 Isolate Significantly Enhance the Degree of Recovery of Heavy Oil from the Romashkino Oil Field (Tatarstan, Russia). *Processes*, *10*(4). https://doi.org/10.3390/pr10040779

Câmara, J. M. D. A., Sousa, M. A. S. B., Barros Neto, E. L., & Oliveira, M. C. A. (2019). Application of rhamnolipid biosurfactant produced by Pseudomonas aeruginosa in microbial–enhanced oil recovery (MEOR). *Journal of Petroleum Exploration and Production Technology*, 1–9. https://doi.org/10.1007/s13202–019–0633–x

Chai, L., Zhang, F., She, Y., Banat, I., & Hou, D. (2015). Impact of a Microbial–Enhanced Oil Recovery Field Trial on Microbial Communities in a Low–Temperature Heavy Oil Reservoir. *Nature Environment and Pollution Technology*, *14*(3), 455–462.

Chen, L., Zhang, G., Ge, J., Jiang, P., Tang, J., & Liu, Y. (2013). Research of the heavy oil displacement mechanism by using alkaline/surfactant flooding system. *Colloids and Surfaces A: Physicochemical and Engineering Aspects*, *434*, 63–71. https://doi.org/10.1016/j.colsurfa.2013.05.035

Correia, J., Gudiña, E. J., Lazar, Z., Janek, T., & Teixeira, J. A. (2022). Cost–effective rhamnolipid production by Burkholderia thailandensis E264 using agro–industrial residues. *Applied Microbiology and Biotechnology*, *106*(22), 7477–7489. https://doi.org/10.1007/s00253–022–12225–1

Couto, M. R., Gudiña, E. J., Ferreira, D., Teixeira, J. A., & Rodrigues, L. R. (2019). The biopolymer produced by Rhizobium viscosum CECT 908 is a promising agent for application in microbial enhanced oil recovery. *New Biotechnology*, *49*, 144–150. https://doi.org/10.1016/j.nbt.2018.11.002

Cui, Q. F., Sun, S. S., Luo, Y. J., Yu, L., & Zhang, Z. Z. (2017). Comparison of in–situ and ex–situ microbial enhanced oil recovery by strain Pseudomonas aeruginosa WJ–1 in laboratory sand–pack columns. *Petroleum Science and Technology*, *35*(21), 2044–2050. https://doi.org/10.1080/10916466.2017.1380042

Cui, Q. F., Zheng, W. T., Yu, L., Xiu, J. L., Zhang, Z. Z., Luo, Y. J., & Sun, S. S. (2017). Emulsifying action of Pseudomonas aeruginosa L6–1 and its metabolite with crude oil for oil recovery enhancement. *Petroleum Science and Technology*, *35*(11), 1174–1179. https://doi.org/10.1080/10916466.2017.1315725

Daryasafar, A., Jamialahmadi, M., Moghaddam, M. B., & Moslemi, B. (2016). Using biosurfactant producing bacteria isolated from an Iranian oil field for application in microbial enhanced oil recovery. *Petroleum Science and Technology*, *34*(8), 739–746. https://doi.org/10.1080/10916466.2016.1154869

Das, A. J., & Kumar, R. (2019). Production of biosurfactant from agro–industrial waste by Bacillus safensis J2 and exploring its oil recovery efficiency and role in restoration of diesel contaminated soil. *Environmental Technology and Innovation*, *16*, 100450. https://doi.org/10.1016/j.eti.2019.100450

Datta, P., Tiwari, P., & Pandey, L. M. (2020). Oil washing proficiency of biosurfactant produced by isolated Bacillus tequilensis MK 729017 from Assam reservoir soil. *Journal of Petroleum Science and Engineering*, *195*, 107612. https://doi.org/10.1016/j.petrol.2020.107612

de Araujo, L. L. G. C., Sodré, L. G. P., Brasil, L. R., Domingos, D. F., de Oliveira, V. M., & da Cruz, G. F. (2019). Microbial enhanced oil recovery using a biosurfactant produced by Bacillus safensis isolated from mangrove microbiota – Part I biosurfactant characterization and oil displacement test. *Journal of Petroleum Science and Engineering*, *180*, 950–957. https://doi.org/10.1016/j.petrol.2019.06.031

Dong, H., Xia, W., Dong, H., She, Y., Zhu, P., Liang, K., Zhang, Z., Liang, C., Song, Z., Sun, S., & Zhang, G. (2016). Rhamnolipids Produced by Indigenous Acinetobacter junii from Petroleum Reservoir and its Potential in Enhanced Oil Recovery. *Frontiers in Microbiology*, *7*. https://doi.org/10.3389/fmicb.2016.01710

Dong, H., Zheng, A., He, Y., Wang, X., Li, Y., Yu, G., Gu, Y., Banat, I. M., Sun, S., She, Y., & Zhang, F. (2022). Optimization and characterization of biosurfactant produced by indigenous: Brevibacillus borstelensis isolated from a low permeability reservoir for application in MEOR. *RSC – Royal Society of Chemistry Advances*, *12*(4), 2036–2047. https://doi.org/10.1039/d1ra07663a

Du, C., Song, Y., Yao, Z., Su, W., Zhang, G., & Wu, X. (2019). Developments in in–situ microbial enhanced oil recovery in Shengli oilfield. *Energy Sources, Part A: Recovery, Utilization, and Environmental Effects*, 1–11. https://doi.org/10.1080/15567036.2019.1648603

El–Sheshtawy, H. S., Aiad, I., Osman, M. E., Abo–ELnasr, A. A., & Kobisy, A. S. (2015). Production of biosurfactant from Bacillus licheniformis for microbial enhanced oil recovery and inhibition the growth of sulfate reducing bacteria. *Egyptian Journal of Petroleum*, *24*(2), 155–162. https://doi.org/10.1016/j.ejpe.2015.05.005

El–Sheshtawy, H. S., Aiad, I., Osman, M. E., Abo–ELnasr, A. A., & Kobisy, A. S. (2016). Production of biosurfactants by Bacillus licheniformis and Candida albicans for application in microbial enhanced oil recovery. *Egyptian Journal of Petroleum*, *25*(3), 293–298. https://doi.org/10.1016/j.ejpe.2015.07.018

Elshafie, A. E., Joshi, S. J., Al–Wahaibi, Y. M., Al–Bemani, A. S., Al–Bahry, S. N., Al–Maqbali, D., & Banat, I. M. (2015). Sophorolipids production by Candida bombicola ATCC 22214 and its potential application in microbial enhanced oil recovery. *Frontiers in Microbiology*, *6*(NOV), 1324. https://doi.org/10.3389/fmicb.2015.01324

Elshafie, A., Joshi, S. J., Al–Wahaibi, Y. M., Al–Bahry, S. N., Al–Bemani, A. S., Al–Hashmi, A., & Al–Mandhari, M. S. (2017, April 4). Isolation and Characterization of Biopolymer Producing Omani Aureobasidium Pullulans Strains and Its Potential Applications in Microbial Enhanced Oil Recovery. *SPE Oil and Gas India Conference and Exhibition*. https://doi.org/10.2118/185326–ms

Elumalai, P., Parthipan, P., Narenkumar, J., Anandakumar, B., Madhavan, J., Oh, B. T., & Rajasekar, A. (2019). Role of thermophilic bacteria (Bacillus and Geobacillus) on crude oil degradation and biocorrosion in oil reservoir environment. *3 Biotech*, *9*(3), 1–11. https://doi.org/10.1007/s13205–019–1604–0

Fan, Y., Wang, J., Gao, C., Zhang, Y., & Du, W. (2020). A novel exopolysaccharide–producing and long–chain n–alkane degrading bacterium Bacillus licheniformis strain DM–1 with potential application for in–situ enhanced oil recovery. *Scientific Reports*, *10*(1), 8519. https://doi.org/10.1038/s41598–020–65432–z

Fernandes, P. L., Rodrigues, E. M., Paiva, F. R., Ayupe, B. A. L., McInerney, M. J., & Tótola, M. R. (2016). Biosurfactant, solvents and polymer production by Bacillus subtilis RI4914 and their application for enhanced oil recovery. *Fuel*, *180*, 551–557. https://doi.org/10.1016/j.fuel.2016.04.080

Firozjaii, A. M., & Saghafi, H. R. (2020). Review on chemical enhanced oil recovery using polymer flooding: Fundamentals, experimental and numerical simulation. In *Petroleum* (Vol. 6, Issue 2, pp. 115–122). Elsevier. https://doi.org/10.1016/j.petlm.2019.09.003

Fulazzaky, M. A., & Astuti, D. I. (2015). Laboratory simulation of microbial enhanced oil recovery using Geobacillus toebii R–32639 isolated from the Handil reservoir. *RSC Advances*, *5*(5), 3908–3916. https://doi.org/10.1039/c4ra14065f

Gao, C. (2015). Potential of Welan gum to enhance oil recovery. *Journal of Petroleum Exploration and Production Technology*, *5*(2), 197–200. https://doi.org/10.1007/s13202–014–0135–9

Gao, C. (2016). Application of a novel biopolymer to enhance oil recovery. *Journal of Petroleum Exploration and Production Technology*, *6*(4), 749–753. https://doi.org/10.1007/s13202–015–0213–7

Gao, P., Li, G., Li, Y., Li, Y., Tian, H., Wang, Y., Zhou, J., & Ma, T. (2016). An exogenous surfactant–producing Bacillus subtilis facilitates indigenous microbial enhanced oil recovery. *Frontiers in Microbiology*, *7*(FEB), 186. https://doi.org/10.3389/fmicb.2016.00186

Ge, M. R., Miao, S. J., Liu, J. F., Gang, H. Z., Yang, S. Z., & Mu, B. Z. (2021). Laboratory studies on a novel salt–tolerant and alkali–free flooding system composed of a biopolymer and a bio–based surfactant for oil recovery. *Journal of Petroleum Science and Engineering*, *196*, 107736. https://doi.org/10.1016/j.petrol.2020.107736

Gudiña, E. J., Couto, M. R., Silva, S. P., Coelho, E., Coimbra, M. A., Teixeira, J. A., & Rodrigues, L. R. (2023). Sustainable Exopolysaccharide Production by Rhizobium viscosum CECT908 Using Corn Steep Liquor and Sugarcane Molasses as Sole Substrates. *Polymers*, *15*(1), 20. https://doi.org/10.3390/polym15010020

Gudiña, E. J., Pereira, J. F. B., Costa, R., Coutinho, J. A. P., Teixeira, J. A., & Rodrigues, L. R. (2013). Biosurfactant–producing and oil–degrading Bacillus subtilis strains enhance oil recovery in laboratory sand–pack columns. *Journal of Hazardous Materials*, *261*, 106–113. https://doi.org/10.1016/j.jhazmat.2013.06.071

Gudiña, E. J., Pereira, J. F. B., Costa, R., Evtuguin, D. V., Coutinho, J. A. P., Teixeira, J. A., & Rodrigues, L. R. (2015). Novel bioemulsifier produced by a Paenibacillus strain isolated from crude oil. *Microbial Cell Factories*, *14*(1), 1–11. https://doi.org/10.1186/s12934–015–0197–5

Gudiña, E. J., Pereira, J. F. B., Rodrigues, L. R., Coutinho, J. A. P., & Teixeira, J. A. (2012). Isolation and study of microorganisms from oil samples for application in Microbial Enhanced Oil Recovery. *International Biodeterioration and Biodegradation*, *68*, 56–64. https://doi.org/10.1016/j.ibiod.2012.01.001

Gudiña, E. J., Teixeira, J. A., & Rodrigues, L. R. (2015). Microbial enhanced oil recovery. In U. C. Sharma, S. Sivakumar, & R. Prasad (Eds.), *Energy Science and Technology Vol. 3: Oil and Natural Gas* (1st ed., pp. 149–177). Studium Press LLC.

Guimarães, C. R., Pasqualino, I. P., de Sousa, J. S., Nogueira, F. C. S., Seldin, L., de Castilho, L. V. A., & Freire, D. M. G. (2021). Bacillus velezensis H2O–1 surfactin efficiently maintains its interfacial properties in extreme conditions found in post–salt and pre–salt oil reservoirs. *Colloids and Surfaces B: Biointerfaces*, *208*, 112072. https://doi.org/10.1016/j.colsurfb.2021.112072

Hadia, N. J., Ottenheim, C., Li, S., Hua, N. Q., Stubbs, L. P., & Lau, H. C. (2019). Experimental investigation of biosurfactant mixtures of surfactin produced by Bacillus Subtilis for EOR application. *Fuel*, *251*, 789–799. https://doi.org/10.1016/j.fuel.2019.03.111

Hajibagheri, F., Lashkarbolooki, M., Ayatollahi, S., & Hashemi, A. (2017). The synergic effects of anionic and cationic chemical surfactants, and bacterial solution on wettability alteration of carbonate rock: An experimental investigation. *Colloids and Surfaces A: Physicochemical and Engineering Aspects*, *513*, 422–429. https://doi.org/10.1016/j.colsurfa.2016.11.010

Haloi, S., Saikia, M. D., Gogoi, S. B., Mohan, R., & Medhi, T. (2021). Aggregation and static adsorption behaviour of Achromobacter sp. TMB1 produced rhamnolipids on sandstone core in relation to microbial enhanced oil recovery. *Journal of Petroleum Science and Engineering*, *205*, 108831. https://doi.org/10.1016/j.petrol.2021.108831

Haloi, S., Sarmah, S., Gogoi, S. B., & Medhi, T. (2020). Characterization of Pseudomonas sp. TMB2 produced rhamnolipids for ex–situ microbial enhanced oil recovery. *3 Biotech*, *10*(3), 1–17.

https://doi.org/10.1007/s13205-020-2094-9

Hongyan, H., Weiyao, Z., Zhiyong, S., & Ming, Y. (2017). Mechanisms of oil displacement by Geobacillus stearothermophilus producing bio-emulsifier for MEOR. *Petroleum Science and Technology*, *35*(17), 1791–1798. https://doi.org/10.1080/10916466.2017.1320675

Hoseini-Moghadam, S. M. A., Ghiasimehr, B., Torkaman, M., & Mirmarghabi, P. (2021). The role of temperature and porous media morphology on the performance of anionic and cationic surfactants for enhanced heavy oil recovery. *Journal of Molecular Liquids*, *339*, 116051. https://doi.org/10.1016/j.molliq.2021.116051

Hu, F., Cai, W., Lin, J., Wang, W., & Li, S. (2021). Genetic engineering of the precursor supply pathway for the overproduction of the nC14-surfactin isoform with promising MEOR applications. *Microbial Cell Factories*, *20*(1), 1–14. https://doi.org/10.1186/s12934-021-01585-4

Ibrahim, H. M. M. (2018). Characterization of biosurfactants produced by novel strains of Ochrobactrum anthropi HM-1 and Citrobacter freundii HM-2 from used engine oil-contaminated soil. *Egyptian Journal of Petroleum*, *27*(1), 21–29. https://doi.org/10.1016/j.ejpe.2016.12.005

IEA. (2022). *International Energy Agency: Oil Market Report. June 2022*. https://www.iea.org/reports/oil-market-report-june-2022

Jang, H. Y., Zhang, K., Chon, B. H., & Choi, H. J. (2015). Enhanced oil recovery performance and viscosity characteristics of polysaccharide xanthan gum solution. *Journal of Industrial and Engineering Chemistry*, *21*, 741–745. https://doi.org/10.1016/j.jiec.2014.04.005

Jha, S. S., Joshi, S. J., & Geetha, S. J. (2016). Lipopeptide production by Bacillus subtilis R1 and its possible applications. *Brazilian Journal of Microbiology*, *47*(4), 955–964. https://doi.org/10.1016/j.bjm.2016.07.006

Ji, S., Li, H., Wang, G. H., Lu, T., Ma, W., Wang, J., Zhu, H., & Xu, H. (2020). Rheological behaviors of a novel exopolysaccharide produced by Sphingomonas WG and the potential application in enhanced oil recovery. *International Journal of Biological Macromolecules*, *162*, 1816–1824. https://doi.org/10.1016/j.ijbiomac.2020.08.114

Ji, S., Wei, F., Li, B., Li, P., Li, H., Li, S., Wang, J., Zhu, H., & Xu, H. (2022). Synergistic effects of microbial polysaccharide mixing with polymer and nonionic surfactant on rheological behavior and enhanced oil recovery. *Journal of Petroleum Science and Engineering*, *208*, 109746. https://doi.org/10.1016/j.petrol.2021.109746

Joshi, S. J., Al-Wahaibi, Y. M., Al-Bahry, S., Elshafie, A., Al-Bemani, A. S., Al-Bahri, A., & Al-Mandhari, M. S. (2016). Production, characterization, and application of bacillus licheniformis W16 biosurfactant in enhancing oil recovery. *Frontiers in Microbiology*, *7*(NOV), 1853. https://doi.org/10.3389/fmicb.2016.01853

Joshi, S. J., Al-Wahaibi, Y. M., Al-Bahry, S., Elshafie, A., Al-Bemani, A. S., Al-Hashmi, A., Samuel, P., Sassi, M., Al-Farsi, H., & Al-Mandhari, M. S. (2016, March 21). Production and Application of Schizophyllan in Microbial Enhanced Heavy Oil Recovery. *Society of Petroleum Engineers - SPE EOR Conference at Oil and Gas West Asia 2016*. https://doi.org/10.2118/179775-ms

Karimi, M., Mahmoodi, M., Niazi, A., Al-Wahaibi, Y., & Ayatollahi, S. (2012). Investigating wettability alteration during MEOR process, a micro/macro scale analysis. *Colloids and Surfaces B: Biointerfaces*, *95*, 129–136. https://doi.org/10.1016/j.colsurfb.2012.02.035

Ke, C. Y., Lu, G. M., Li, Y. Bin, Sun, W. J., Zhang, Q. Z., & Zhang, X. L. (2018). A pilot study on large–scale microbial enhanced oil recovery (MEOR) in Baolige Oilfield. *International Biodeterioration and Biodegradation*, *127*, 247–253. https://doi.org/10.1016/j.ibiod.2017.12.009

Ke, C. Y., Lu, G. M., Wei, Y. L., Sun, W. J., Hui, J. F., Zheng, X. Y., Zhang, Q. Z., & Zhang, X. L. (2019). Biodegradation of crude oil by Chelatococcus daeguensis HB–4 and its potential for microbial enhanced oil recovery (MEOR)in heavy oil reservoirs. *Bioresource Technology*, *287*. https://doi.org/10.1016/j.biortech.2019.121442

Ke, C. Y., Sun, W. J., Li, Y. Bin, Lu, G. M., Zhang, Q. Z., & Zhang, X. L. (2018). Microbial enhanced oil recovery in Baolige Oilfield using an indigenous facultative anaerobic strain Luteimonas huabeiensis sp. nov. *Journal of Petroleum Science and Engineering*, *167*, 160–167. https://doi.org/10.1016/j.petrol.2018.04.015

Khademolhosseini, R., Jafari, A., Mousavi, S. M., Hajfarajollah, H., Noghabi, K. A., & Manteghian, M. (2019). Physicochemical characterization and optimization of glycolipid biosurfactant production by a native strain of Pseudomonas aeruginosa HAK01 and its performance evaluation for the MEOR process. *Royal Society of Chemistry – RSC Advances*, *9*(14), 7932–7947. https://doi.org/10.1039/C8RA10087J

Kumar, S., & Mandal, A. (2016). Studies on interfacial behavior and wettability change phenomena by ionic and nonionic surfactants in presence of alkalis and salt for enhanced oil recovery. *Applied Surface Science*, *372*, 42–51. https://doi.org/10.1016/j.apsusc.2016.03.024

Lan, G., Fan, Q., Liu, Y., Liu, Y., Liu, Y., Yin, X., & Luo, M. (2015). Effects of the addition of waste cooking oil on heavy crude oil biodegradation and microbial enhanced oil recovery using Pseudomonas sp. SWP– 4. *Biochemical Engineering Journal*, *103*, 219–226. https://doi.org/10.1016/j.bej.2015.08.004

Lapasin, R., & Pricl, S. (1999). Rheology of Industrial Polysaccharides: Theory and Applications. In *Rheology of Industrial Polysaccharides: Theory and Applications*. Aspen Publishers. https://doi.org/10.1007/978–1–4615–2185–3

Lee, K. S., Kwon, T.–H., Park, T., & Jeong, M. S. (2020). Microbiology and Microbial Products for Enhanced Oil Recovery. In *Theory and Practice in Microbial Enhanced Oil Recovery* (pp. 27–65). Gulf Professional Publishing. https://doi.org/10.1016/b978–0–12–819983–1.00002–8

Leonhardt, B., Ernst, B., Reimann, S., Steigerwald, A., & Lehr, F. (2014). Field testing the Polysaccharide schizophyllan: Results of the first year. *Society of Petroleum Engineers – SPE DOE Improved Oil Recovery Symposium Proceedings*, *1*, 57–72. https://doi.org/10.2118/169032–ms

Li, H., Zhu, W., Niu, H., Gao, Y., Chen, Z., Song, Z., & Kong, D. (2022). 2–D porous flow field reveals different EOR mechanisms between the biopolymer and chemical polymer. *Journal of Petroleum Science and Engineering*, *210*, 110084. https://doi.org/10.1016/j.petrol.2021.110084

Li, L., Chen, J., Jin, X., Wang, Z., Wu, Y., & Dai, C. (2021). Novel polyhydroxy anionic surfactants with excellent water–solid interfacial wettability control capability for enhanced oil recovery. *Journal of Molecular Liquids*, *343*, 116973. https://doi.org/10.1016/j.molliq.2021.116973

Li, Y., Xu, L., Gong, H., Ding, B., Dong, M., & Li, Y. (2017). A Microbial Exopolysaccharide Produced by Sphingomonas Species for Enhanced Heavy Oil Recovery at High Temperature and High Salinity. *Energy and Fuels*, *31*(4), 3960–3969. https://doi.org/10.1021/acs.energyfuels.6b02923

Li, Z., Lin, J., Wang, W., Huang, H., Yu, D., & Li, S. (2022). Effect of Rhamnolipid Amidation on Biosurfactant Adsorption Loss and Oil–Washing Efficiency. *Langmuir*, *38*(8), 2435–2444. https://doi.org/10.1021/acs.langmuir.1c02551

Liang, K., Han, P., Chen, Q., Su, X., & Feng, Y. (2019). Comparative Study on Enhancing Oil Recovery under High Temperature and High Salinity: Polysaccharides Versus Synthetic Polymer. *ACS Omega*, *4*(6), 10620–10628. https://doi.org/10.1021/acsomega.9b00717

Liang, X., Shi, R., Radosevich, M., Zhao, F., Zhang, Y., Han, S., & Zhang, Y. (2017). Anaerobic lipopeptide biosurfactant production by an engineered bacterial strain for in situ microbial enhanced oil recovery. *Royal Society of Chemistry – RSC Advances*, *7*(33), 20667–20676. https://doi.org/10.1039/c7ra02453c

Liu, Qi, Niu, J., Yu, Y., Wang, C., Lu, S., Zhang, S., Lv, J., & Peng, B. (2021). Production, characterization and application of biosurfactant produced by Bacillus licheniformis L20 for microbial enhanced oil recovery. *Journal of Cleaner Production*, *307*, 127193. https://doi.org/10.1016/j.jclepro.2021.127193

Liu, Qiang, Lin, J., Wang, W., Huang, H., & Li, S. (2015). Production of surfactin isoforms by Bacillus subtilis BS–37 and its applicability to enhanced oil recovery under laboratory conditions. *Biochemical Engineering Journal*, *93*, 31–37. https://doi.org/10.1016/j.bej.2014.08.023

Mahmoud, T., Samak, N. A., Abdelhamid, M. M., Aboulrous, A. A., & Xing, J. (2021). Modification Wettability and Interfacial Tension of Heavy Crude Oil by Green Bio–surfactant Based on Bacillus licheniformis and Rhodococcus erythropolis Strains under Reservoir Conditions: Microbial Enhanced Oil Recovery. *Energy and Fuels*, *35*(2), 1648–1663. https://doi.org/10.1021/acs.energyfuels.0c03781

Muhammed, N. S., Haq, M. B., Al–Shehri, D., Rahaman, M. M., Keshavarz, A., & Zakir Hossain, S. M. (2020). Comparative study of green and synthetic polymers for enhanced oil recovery. In *Polymers* (Vol. 12, Issue 10, pp. 1–32). MDPI AG. https://doi.org/10.3390/polym12102429

Nagase, K., Zhang, S. T., Asami, H., Yazawa, N., Fujiwara, K., Enomoto, H., Hong, C. X., & Liang, C. X. (2002, April 13). A Successful Field Test of Microbial EOR Process in Fuyu Oilfield, China. *Society of Petroleum Engineers – SPE DOE Improved Oil Recovery Symposium*. https://doi.org/10.2118/75238–ms

Nasiri, M. A., & Biria, D. (2020). Extraction of the indigenous crude oil dissolved biosurfactants and their potential in enhanced oil recovery. *Colloids and Surfaces A: Physicochemical and Engineering Aspects*, *603*, 125216. https://doi.org/10.1016/j.colsurfa.2020.125216

Negin, C., Ali, S., & Xie, Q. (2017). Most common surfactants employed in chemical enhanced oil recovery. In *Petroleum* (Vol. 3, Issue 2, pp. 197–211). Elsevier. https://doi.org/10.1016/j.petlm.2016.11.007

Nikolova, C., & Gutierrez, T. (2020). Use of Microorganisms in the Recovery of Oil From Recalcitrant Oil Reservoirs: Current State of Knowledge, Technological Advances and Future Perspectives. In *Frontiers in Microbiology* (Vol. 10, p. 2996). Frontiers Media S.A. https://doi.org/10.3389/fmicb.2019.02996

Niu, J., Liu, Q., Lv, J., & Peng, B. (2020). Review on microbial enhanced oil recovery: Mechanisms, modeling and field trials. In *Journal of Petroleum Science and Engineering* (Vol. 192, p. 107350). Elsevier. https://doi.org/10.1016/j.petrol.2020.107350

Okoro, E. E., Efajemue, E. A., Sanni, S. E., Olabode, O. A., Orodu, O. D., & Ojo, T. (2022). Application of thermotolerant petroleum microbes at reservoir conditions for enhanced oil recovery. *Petroleum*. https://doi.org/10.1016/j.petlm.2022.01.008

Onaizi, S. A., Alsulaimani, M., Al–Sakkaf, M. K., Bahadi, S. A., Mahmoud, M., & Alshami, A. (2021). Crude oil/water nanoemulsions stabilized by biosurfactant: Stability and pH–Switchability. *Journal of Petroleum Science and Engineering*, *198*, 108173. https://doi.org/10.1016/j.petrol.2020.108173

Paul, I., Mandal, T., & Mandal, D. D. (2022). Assessment of bacterial biosurfactant production and application in Enhanced Oil Recovery (EOR)—A green approach. *Environmental Technology and Innovation*, *28*, 102733. https://doi.org/10.1016/j.eti.2022.102733

Pereira, J. F. B., Gudiña, E. J., Costa, R., Vitorino, R., Teixeira, J. A., Coutinho, J. A. P., & Rodrigues, L. R. (2013). Optimization and characterization of biosurfactant production by Bacillus subtilis isolates towards microbial enhanced oil recovery applications. *Fuel*, *111*, 259–268. https://doi.org/10.1016/j.fuel.2013.04.040

Pinho de Aguiar, K. L. N., Palermo, L. C. M., & Mansur, C. R. E. (2021). Polymer viscosifier systems with potential application for enhanced oil recovery: A review. *Oil and Gas Science and Technology*, *76*(1), 65. https://doi.org/10.2516/ogst/2021044

Pu, W., Shen, C., Wei, B., Yang, Y., & Li, Y. (2018). A comprehensive review of polysaccharide biopolymers for enhanced oil recovery (EOR) from flask to field. *Journal of Industrial and Engineering Chemistry*, *61*, 1–11. https://doi.org/10.1016/J.JIEC.2017.12.034

Purwasena, I. A., Astuti, D. I., Syukron, M., Amaniyah, M., & Sugai, Y. (2019). Stability test of biosurfactant produced by Bacillus licheniformis DS1 using experimental design and its application for MEOR. *Journal of Petroleum Science and Engineering*, *183*, 106383. https://doi.org/10.1016/j.petrol.2019.106383

Qi, Y.–B., Zheng, C.–G., Lv, C.–Y., Lun, Z.–M., & Ma, T. (2018). Compatibility between weak gel and microorganisms in weak gel–assisted microbial enhanced oil recovery. *Journal of Bioscience and Bioengineering*, *126*(2), 235–240. https://doi.org/10.1016/j.jbiosc.2018.02.011

Quadri, S. M. R., Jiran, L., Shoaib, M., Hashmet, M. R., Al Sumaiti, A. M., & Alhassan, S. M. (2015, November 9). Application of biopolymer to improve oil recovery in high temperature high salinity carbonate reservoirs. *Society of Petroleum Engineers – SPE Abu Dhabi International Petroleum Exhibition and Conference 2015*. https://doi.org/10.2118/177915–ms

Ramos de Souza, E., Rodrigues, P. D., Sampaio, I. C. F., Bacic, E., Crugeira, P. J. L., Vasconcelos, A. C., dos Santos Silva, M., dos Santos, J. N., Quintella, C. M., Pinheiro, A. L. B., & Almeida, P. F. de. (2022). Xanthan gum produced by Xanthomonas campestris using produced water and crude glycerin as an environmentally friendlier agent to enhance oil recovery. *Fuel*, *310*, 122421. https://doi.org/10.1016/j.fuel.2021.122421

Rellegadla, S., Jain, S., & Agrawal, A. (2019). Oil reservoir simulating bioreactors: tools for understanding petroleum microbiology. In *Applied Microbiology and Biotechnology*. Springer. https://doi.org/10.1007/s00253–019–10311–5

Rellegadla, S., Prajapat, G., & Agrawal, A. (2017). Polymers for enhanced oil recovery: fundamentals and selection criteria. In *Applied Microbiology and Biotechnology* (Vol. 101, Issue 11, pp. 4387–4402). Springer Berlin Heidelberg. https://doi.org/10.1007/s00253–017–8307–4

Roelants, S. L. K. W., Van Renterghem, L., Maes, K., Everaert, B., Redant, E., Vanlerberghe, B., Demaeseneire, S. L., & Soetaert, W. (2019). Microbial Biosurfactants: From Lab to Market. In *Microbial Biosurfactants and their Environmental and Industrial Applications* (pp. 341–363). CRC Press. https://doi.org/10.1201/b21950-13

Safdel, M., Anbaz, M. A., Daryasafar, A., & Jamialahmadi, M. (2017). Microbial enhanced oil recovery, a critical review on worldwide implemented field trials in different countries. In *Renewable and Sustainable Energy Reviews* (Vol. 74, pp. 159–172). Pergamon. https://doi.org/10.1016/j.rser.2017.02.045

Saikia, R. R., Deka, S., Deka, M., & Sarma, H. (2012). Optimization of environmental factors for improved production of rhamnolipid biosurfactant by Pseudomonas aeruginosa RS29 on glycerol. *Journal of Basic Microbiology*, *52*(4), 446–457. https://doi.org/10.1002/jobm.201100228

Sakthipriya, N., Kumar, G., Agrawal, A., Doble, M., & Sangwai, J. S. (2021). Impact of Biosurfactants, Surfactin, and Rhamnolipid Produced fromBacillus subtilisandPseudomonas aeruginosa, on the Enhanced Recovery of Crude Oil and Its Comparison with Commercial Surfactants. *Energy and Fuels*, *35*(12), 9883–9893. https://doi.org/10.1021/acs.energyfuels.1c00679

Saravanan, A., Kumar, P. S., Vardhan, K. H., Jeevanantham, S., Karishma, S. B., Yaashikaa, P. R., & Vellaichamy, P. (2020). A review on systematic approach for microbial enhanced oil recovery technologies: Opportunities and challenges. In *Journal of Cleaner Production* (Vol. 258, p. 120777). Elsevier Ltd. https://doi.org/10.1016/j.jclepro.2020.120777

Sari, C. N., Hertadi, R., Harahap, A. F. P., Ramadhan, M. Y. A., & Gozan, M. (2020). Process optimization of palm oil mill effluent–based biosurfactant of Halomonas meridiana BK–AB4 originated from bledug kuwu mud volcano in central java for microbial enhanced oil recovery. *Processes*, *8*(6), 716. https://doi.org/10.3390/PR8060716

Sarma, H., Bustamante, K. L. T., & Prasad, M. N. V. (2019). Biosurfactants for oil recovery from refinery sludge: Magnetic nanoparticles assisted purification. In *Industrial and Municipal Sludge: Emerging Concerns and Scope for Resource Recovery* (pp. 107–132). Butterworth-Heinemann. https://doi.org/10.1016/B978-0-12-815907-1.00006-4

Sharma, N., Lavania, M., Kukreti, V., & Lal, B. (2020). Instigation of indigenous thermophilic bacterial consortia for enhanced oil recovery from high temperature oil reservoirs. *PLoS ONE*, *15*(5), e0229889. https://doi.org/10.1371/journal.pone.0229889

Sharma, R., Singh, J., & Verma, N. (2018a). Optimization of rhamnolipid production from Pseudomonas aeruginosa PBS towards application for microbial enhanced oil recovery. *3 Biotech*, *8*(1), 20. https://doi.org/10.1007/s13205-017-1022-0

Sharma, R., Singh, J., & Verma, N. (2018b). Production, characterization and environmental applications of biosurfactants from Bacillus amyloliquefaciens and Bacillus subtilis. *Biocatalysis and Agricultural Biotechnology*, *16*, 132–139. https://doi.org/10.1016/j.bcab.2018.07.028

Sheng, J. J. (2014). A comprehensive review of alkaline–surfactant–polymer (ASP) flooding. In *Asia-Pacific Journal of Chemical Engineering* (Vol. 9, Issue 4, pp. 471–489). John Wiley & Sons, Ltd. https://doi.org/10.1002/apj.1824

Shreve, G. S., & Makula, R. (2019). Characterization of a new rhamnolipid biosurfactant complex from pseudomonas isolate DYNA270. *Biomolecules*, *9*(12), 885. https://doi.org/10.3390/biom9120885

Song, Z., Zhu, W., Sun, G., & Blanckaert, K. (2015). Dynamic investigation of nutrient consumption and injection strategy in microbial enhanced oil recovery (MEOR) by means of large–scale experiments. *Applied Microbiology and Biotechnology*, *99*(15), 6551–6561. https://doi.org/10.1007/s00253–015–6586–1

Soudmand–asli, A., Ayatollahi, S. S., Mohabatkar, H., Zareie, M., & Shariatpanahi, S. F. (2007). The in situ microbial enhanced oil recovery in fractured porous media. *Journal of Petroleum Science and Engineering*, *58*(1–2), 161–172. https://doi.org/10.1016/j.petrol.2006.12.004

Sun, S., Luo, Y., Cao, S., Li, W., Zhang, Z., Jiang, L., Dong, H., Yu, L., & Wu, W. M. (2013). Construction and evaluation of an exopolysaccharide–producing engineered bacterial strain by protoplast fusion for microbial enhanced oil recovery. *Bioresource Technology*, *144*, 44–49. https://doi.org/10.1016/j.biortech.2013.06.098

Sun, S., Zhang, Z., Luo, Y., Zhong, W., Xiao, M., Yi, W., Yu, L., & Fu, P. (2011). Exopolysaccharide production by a genetically engineered Enterobacter cloacae strain for microbial enhanced oil recovery. *Bioresource Technology*, *102*(10), 6153–6158. https://doi.org/10.1016/j.biortech.2011.03.005

Suthar, H., Hingurao, K., Desai, A., & Nerurkar, A. (2009). Selective plugging strategy based microbial enhanced oil recovery using Bacillus licheniformis TT33. *Journal of Microbiology and Biotechnology*, *19*(10), 1230–1237. https://doi.org/10.4014/jmb.0904.04043

Tackie–Otoo, B. N., Ayoub Mohammed, M. A., Yekeen, N., & Negash, B. M. (2020). Alternative chemical agents for alkalis, surfactants and polymers for enhanced oil recovery: Research trend and prospects. In *Journal of Petroleum Science and Engineering* (Vol. 187, p. 106828). Elsevier. https://doi.org/10.1016/j.petrol.2019.106828

Tao, W., Lin, J., Wang, W., Huang, H., & Li, S. (2020). Biodegradation of aliphatic and polycyclic aromatic hydrocarbons by the thermophilic bioemulsifier–producing Aeribacillus pallidus strain SL–1. *Ecotoxicology and Environmental Safety*, *189*, 109994. https://doi.org/10.1016/j.ecoenv.2019.109994

Varjani, S., & Upasani, V. N. (2016). Core Flood study for enhanced oil recovery through ex–situ bioaugmentation with thermo– and halo–tolerant rhamnolipid produced by Pseudomonas aeruginosa NCIM 5514. *Bioresource Technology*, *220*, 175–182. https://doi.org/10.1016/j.biortech.2016.08.060

Veerabhadrappa, S. K., Trivedi, J. J., & Kuru, E. (2013). Visual confirmation of the elasticity dependence of unstable secondary polymer floods. *Industrial and Engineering Chemistry Research*, *52*(18), 6234–6241. https://doi.org/10.1021/ie303241b

Wang, C., Liu, P., Wang, Y., Yuan, Z., & Xu, Z. (2018). Experimental Study of Key Effect Factors and Simulation on Oil Displacement Efficiency for a Novel Modified Polymer BD–HMHEC. *Scientific Reports*, *8*(1), 1–9. https://doi.org/10.1038/s41598–018–22259–z

Wang, X. T., Liu, B., Li, X. Z., Lin, W., Li, D. A., Dong, H., & Wang, L. (2022). Biosurfactants produced by novel facultative–halophilic Bacillus sp. XT–2 with biodegradation of long chain n–alkane and the application for enhancing waxy oil recovery. *Energy*, *240*, 122802. https://doi.org/10.1016/j.energy.2021.122802

Wang, X., Yang, Y., & Xi, W. (2016). Microbial enhanced oil recovery of oil–water transitional zone in thin–shallow extra heavy oil reservoirs: A case study of Chunfeng Oilfield in western margin of

Junggar Basin, NW China. *Petroleum Exploration and Development*, *43*(4), 689–694. https://doi.org/10.1016/S1876-3804(16)30080-5

Wu, B., Xiu, J., Yu, L., Huang, L., Yi, L., & Ma, Y. (2022). Biosurfactant production by Bacillus subtilis SL and its potential for enhanced oil recovery in low permeability reservoirs. *Scientific Reports*, *12*(1), 1–10. https://doi.org/10.1038/s41598-022-12025-7

Xia, W., Dong, X., Zhang, Y., & Ma, T. (2018). Biopolymer from marine Athelia and its application on heavy oil recovery in heterogeneous reservoir. *Carbohydrate Polymers*, *195*, 53–62. https://doi.org/10.1016/j.carbpol.2018.04.061

Xia, W., Shen, W., Yu, L., Zheng, C., Yu, W., & Tang, Y. (2016). Conversion of petroleum to methane by the indigenous methanogenic consortia for oil recovery in heavy oil reservoir. *Applied Energy*, *171*, 646–655. https://doi.org/10.1016/j.apenergy.2016.03.059

Xia, W., Tong, L., Jin, T., Hu, C., Zhang, L., Shi, L., Zhang, J., Yu, W., Wang, F., & Ma, T. (2021). N,S-Heterocycles biodegradation and biosurfactantproduction under CO2/N2 conditions by Pseudomonas and its application on heavy oil recovery. *Chemical Engineering Journal*, *413*, 128771. https://doi.org/10.1016/j.cej.2021.128771

Xingbiao, W., Yanfen, X., Sanqing, Y., Zhiyong, H., & Yanhe, M. (2015). Influences of microbial community structures and diversity changes by nutrients injection in Shengli oilfield, China. *Journal of Petroleum Science and Engineering*, *133*, 421–430. https://doi.org/10.1016/j.petrol.2015.06.020

Xu, L., Xu, G., Yu, L., Gong, H., Dong, M., & Li, Y. (2014). The displacement efficiency and rheology of welan gum for enhanced heavy oil recovery. *Polymers for Advanced Technologies*, *25*(10), 1122–1129. https://doi.org/10.1002/pat.3364

Xu, Y., & Lu, M. (2011). Microbially enhanced oil recovery at simulated reservoir conditions by use of engineered bacteria. *Journal of Petroleum Science and Engineering*, *78*(2), 233–238. https://doi.org/10.1016/j.petrol.2011.06.005

Xue, L., Liu, P., & Zhang, Y. (2023). Status and Prospect of Improved Oil Recovery Technology of High Water Cut Reservoirs. *Water (Switzerland)*, *15*(7), 1342. https://doi.org/10.3390/w15071342

Yun, W., Chang, S., Cogswell, D. A., Eichmann, S. L., Gizzatov, A., Thomas, G., Al-Hazza, N., Abdel-Fattah, A., & Wang, W. (2020). Toward Reservoir-on-a-Chip: Rapid Performance Evaluation of Enhanced Oil Recovery Surfactants for Carbonate Reservoirs Using a Calcite-Coated Micromodel. *Scientific Reports*, *10*(1), 1–12. https://doi.org/10.1038/s41598-020-57485-x

Zhang, J., Gao, H., & Xue, Q. (2020). Potential applications of microbial enhanced oil recovery to heavy oil. In *Critical Reviews in Biotechnology* (Vol. 40, Issue 4, pp. 459–474). Taylor and Francis Ltd. https://doi.org/10.1080/07388551.2020.1739618

Zhao, F., Guo, C., Cui, Q., Hao, Q., Xiu, J., Han, S., & Zhang, Y. (2018). Exopolysaccharide production by an indigenous isolate Pseudomonas stutzeri XP1 and its application potential in enhanced oil recovery. *Carbohydrate Polymers*, *199*(11), 375–381. https://doi.org/10.1016/j.carbpol.2018.07.038

Zhao, F., Li, P., Guo, C., Shi, R. J., & Zhang, Y. (2018). Bioaugmentation of oil reservoir indigenous Pseudomonas aeruginosa to enhance oil recovery through in-situ biosurfactant production without air injection. *Bioresource Technology*, *251*, 295–302. https://doi.org/10.1016/j.biortech.2017.12.057

Zhao, F., Shi, R., Cui, Q., Han, S., Dong, H., & Zhang, Y. (2017). Biosurfactant production under diverse conditions by two kinds of biosurfactant–producing bacteria for microbial enhanced oil recovery. *Journal of Petroleum Science and Engineering*, *157*, 124–130. https://doi.org/10.1016/j.petrol.2017.07.022

Zhao, F., Zhu, H., Cui, Q., Wang, B., Su, H., & Zhang, Y. (2021). Anaerobic production of surfactin by a new Bacillus subtilis isolate and the in situ emulsification and viscosity reduction effect towards enhanced oil recovery applications. *Journal of Petroleum Science and Engineering*, *201*, 108508. https://doi.org/10.1016/j.petrol.2021.108508

Zhao, J., Dai, C., Ding, Q., Du, M., Feng, H., Wei, Z., Chen, A., & Zhao, M. (2015). The structure effect on the surface and interfacial properties of zwitterionic sulfobetaine surfactants for enhanced oil recovery. *Royal Society of Chemistry – RSC Advances*, *5*(18), 13993–14001. https://doi.org/10.1039/c4ra16235h

Zulkifli, N. N., Mahmood, S. M., Akbari, S., Manap, A. A. A., Kechut, N. I., & Elrais, K. A. (2019). Evaluation of new surfactants for enhanced oil recovery applications in high–temperature reservoirs. *Journal of Petroleum Exploration and Production Technology*, *10*(2), 283–296. https://doi.org/10.1007/s13202–019–0713–y

CHAPTER 2.

Screening of biopolymer–producing microorganisms with potential application in Microbial Enhanced Oil Recovery

Abstract

Biopolymers constitute a promising alternative to chemical polymers in several industrial applications, including microbial enhanced oil recovery (MEOR). Microbial polysaccharides, in particular, have important characteristics, like being water–soluble and behaving like a viscous hydrogel when in solution, that make them interesting targets for MEOR applications. Here, several microorganisms were studied to evaluate their biopolymer production ability, according to the amount of crude biopolymer produced and the viscosity of the culture broth. Among the different microorganisms studied (*Aureobasidium pullulans* CCY 27–1–94, *Bacillus subtilis* strains isolated from a Brazilian oilfield, *Leuconostoc mesenteroides* A4 and *Zymomonas mobilis* ATCC 29191), *A. pullulans* and *L. mesenteroides* were selected for further work. The first due to the amount of biopolymer produced and the fact that it had already been used in MEOR studies, and the second due to its fast production of around 12 g/L of biopolymer and the viscosity achieved in the culture broth.

2.1 Introduction

Polymers are the basis of most materials used in modern society. These macromolecules consist of monomers, mainly composed of carbon, hydrogen, oxygen, nitrogen and sulfur atoms, arranged in a repeating structure. Polymers can originate from natural systems (plants, animals or microorganisms) or be artificially produced (mainly from petroleum) (Shrivastava, 2018). Microbial biopolymers are a heterogenous group of macromolecules that include polynucleotides, polypeptides and polysaccharides (Lee et al., 2020; Verma et al., 2020). The wide array of biological functions for which they are responsible is reflected in their wide range of rheological behaviors, varying from viscous fluids to bioplastics. This, and the fact that they represent an environmentally friendly source, makes them interesting alternatives to synthetic polymers in several industrial applications. In fact, their applications span different industrial sectors, including food, cosmetics, toiletries, paints, textiles, chemicals, oil recovery, pharmaceuticals and biomedical products (Verma et al., 2020).

The most interesting biopolymers used in oil recovery are exopolysaccharide (EPS) biopolymers since they exist outside of the cell, facilitating their recovery, and form viscous hydrogels in solution. Several microorganisms can produce such biopolymers, including *Aureobasidium pullulans* (pullulan), *Leuconostoc mesenteroides* (dextran), *Zymomonas mobilis* (levan) and some species of *Bacillus* (levan) (Lee et al., 2020). Besides EPS, some polypeptides, like poly–γ–glutamic acid (γ–PGA) have also been evaluated in oil recovery applications (Azarhava et al., 2020, 2021; Fan et al., 2020; Suthar et al., 2009).

Pullulan is usually produced by the yeast–like fungus *A. pullulans* from different carbon sources, such as sucrose, glucose, fructose, maltose, mannose, and even agricultural waste (Lee et al., 2020; Wani et al., 2021). This biopolymer, which is composed of repetitions of monomers of three glucose molecules, is highly biodegradable and resistant to heat. It forms a viscous fluid in solution, but contains no elasticity (Verma et al., 2020). Furthermore, pullulan can form biofilms that are water–soluble, biodegradable and impermeable to oxygen (Cheng et al., 2011b).

Dextran denotes a diverse family of microbial neutral EPS. It is commercially produced by *L. mesenteroides* in media containing sucrose, although it can also be produced by other microorganisms (Lee et al., 2020; Verma et al., 2020). This is a glucosidic biopolymer whose structure varies according to the producing microorganism. Its molecular weight, for example, ranges from 106–109 g/mol, depending on the chain length of the biopolymer (Lee et al., 2020; Rehm, 2010). Like other polysaccharides, dextran is water soluble and has a viscosity that changes with concentration, temperature and molecular weight (Rehm, 2010). Furthermore, dextran produced by *L. mesenteroides*

exhibits a shear thinning behavior, typical of biopolymers, and the properties of a weak gel (Castro–Rodríguez et al., 2019).

Levan is a homopolysaccharide of fructofuranose molecules that can be produced by several microbial species, including *Bacillus* spp. and *Zymomonas* spp. (Lee et al., 2020; Verma et al., 2020). Among these, *Z. mobilis* is proposed as a potential candidate for large–scale production of levan (Ernandes & Garcia–Cruz, 2011). This biopolymer is highly soluble in water and oil and has a very low viscosity. Like dextran and other polysaccharides, its molecular weight depends on the microorganism used for its production. However, the molecular weight of levan is usually on the high end when it is produced in a sucrose medium (Ernandes & Garcia–Cruz, 2011).

In this work, several microbial strains belonging to species previously described as biopolymer producers, including *A. pullulans*, *L. mesenteroides*, *Z. mobilis* and *Bacillus subtilis*, were screened for biopolymer production. The screening process was done by precipitation of the biopolymer with ethanol and determination of its dry weight or measurement of the apparent viscosity in the culture broth.

2.2 Materials and methods

2.2.1 Strains and culture conditions

Based on the literature, several microbial strains belonging to species described as biopolymer producers were selected to evaluate their potential for application in MEOR. These microorganisms were grown using different culture media and conditions, as previously reported in the literature (Table 2.1). *A. pullulans* CCY 27–1–94 and *Z. mobilis* ATCC 29191 were obtained from the culture collection of the Centre of Biological Engineering, whereas *L. mesenteroides* A4 and *B. subtilis* isolates belonged to the collection of biosurfactant–producing microorganisms from our research group.

The strains were maintained in Luria–Bertani (LB) medium (or deMan, Rogosa, Sharpe (MRS) medium in the case of *L. mesenteroides* A4), supplemented with 20% (v/v) of glycerol at –80°C. Pre–cultures were prepared by inoculating 20 mL of medium with 100 µL from a frozen stock, and were incubated overnight at the appropriate temperature (Table 2.1).

Table 2.1 – Description of the culture media and growth conditions for the microorganisms used in biopolymer production assays.

Microorganism	Expected biopolymer	Culture medium	Culture medium composition	Operational conditions	Reference
***Aureobasidium pullulans* CCY 27–1–94**	Pullulan	Ap1	Sucrose 50 g/L; Yeast Extract 0.4 g/L; K_2HPO_4 5 g/L; $(NH_4)_2SO_4$ 0.6 g/L; $MgSO_4 \cdot 7H_2O$ 0.4 g/L; NaCl 1 g/L; pH 6.5	150 rpm 30°C	Prasongsuk et al. (2007)
		Ap2	Glucose 20 g/L; Yeast Extract 0.4 g/L; K_2HPO_4 5 g/L; $(NH_4)_2SO_4$ 0.6 g/L; $MgSO_4 \cdot 7H_2O$ 0.4 g/L; NaCl 1 g/L; pH 6.2	150 rpm 30°C	Elshafie et al. (2017)
		Ap3	Sucrose 75 g/L; Yeast Extract 3 g/L; K_2HPO_4 5 g/L; $(NH_4)_2SO_4$ 5 g/L; $MgSO_4 \cdot 7H_2O$ 0.2 g/L; NaCl 1 g/L; pH 5.0	150 rpm 30°C	Cheng et al. (2011a)
***Bacillus subtilis* (PX191, PX551, PX552, PX571 and PX572)**	Levan	Bs1	Sucrose 160 g/L; Yeast Extract 10 g/L; K_2HPO_4 3 g/L; KH_2PO_4 1 g/L; $MgSO_4 \cdot 7H_2O$ 0.5 g/L; pH 7.0	150 rpm 37°C	Liu et al. (2009)
***Leuconostoc mesenteroides* A4**	Dextran	Lm1	Sucrose 50 g/L; Tryptone 5 g/L; Soya peptone 5 g/L; Meat extract 5 g/L; Yeast extract 2.5 g/L; Ascorbic acid 0.5 g/L; Di–sodium–glycerophosphate 19 g/L; $MgSO_4 \cdot 7H_2O$ 0.25 g/L; pH 6.9	180 rpm or static 30°C	Han et al. (2014)
		Lm2	Sucrose 150 g/L; Peptone 10 g/L; Yeast Extract 5 g/L; K_2HPO_4 2 g/L; $MgSO_4$ 0.2 g/L; $CaCl_2$ 0.02 g/L; NaCl 0.01 g/L; $FeSO_4$ 0.01 g/L; $MnSO_4$ 0.01 g/L; pH 7.0	180 rpm or 120 rpm 30°C	Han et al. (2014)
		Lm3 and Lm4	Sucrose 100 g/L (Lm3) or 200 g/L (Lm4); Peptone 10 g/L; Yeast Extract 5 g/L; Meat Extract 5 g/L; K_2HPO_4 2 g/L; Diammonium citrate 2 g/L; Sodium acetate 5 g/L; $MgSO_4 \cdot 7H_2O$ 0.1 g/L; $MnSO_4 \cdot H_2O$ 0.05 g/L; pH 7.0	150 rpm or static 30°C	Castro–Rodríguez et al. (2019)
***Zymomonas mobilis* ATCC 29191**	Levan	Zm1	Sucrose 200 g/L; Yeast Extract 5 g/L; KH_2PO_4 1 g/L; $(NH_4)_2SO_4$ 1g/L; $MgSO_4 \cdot 7H_2O$ 0.5 g/L; pH 7.0	150 rpm 30°C	Ernandes & Garcia–Cruz (2011)

Biopolymer production by the different microorganisms was evaluated in flasks which were inoculated with 1% (v/v) of the pre–culture and incubated at the designated temperature and agitation speed in an orbital shaker (Table 2.1). Samples were taken at different time intervals to determine biopolymer production, as described in the following section.

2.2.2 Biopolymer recovery and quantification

Each of the collected samples was first centrifuged (9400 x *g*, 20 min) to remove the cells. The biopolymer was then precipitated by adding two volumes of ethanol (99%, v/v) to the cell–free supernatant (CFS) and incubating the mixture at –20°C for 24h. Afterwards, the samples were centrifuged (9400 x *g*, 20 min, 4°C), the supernatant was discarded, the pellet containing the biopolymer was resuspended in 2 mL of demineralized water and the biopolymer was dried at 60°C for 24h. The amount of crude biopolymer produced was determined as dry weight and expressed as g/L culture.

2.2.3 Apparent viscosity measurements

The production of biopolymer by *L. mesenteroides* A4 was also followed by measuring the apparent viscosity of the CFS using a hybrid rheometer (Discovery HR1, TA Instruments, USA). Measurements were performed at 40°C using a cone–plate geometry (diameter 60 mm; angle 2.006°; gap 0.064 mm) at different shear rates (0.1 – 300 s^{-1}) through three successive flow ramps (0.1 → 300 s^{-1}; 300 → 0.1 s^{-1}; 0.1 → 300 s^{-1}). The values presented correspond to a shear rate of 1.4 s^{-1}.

2.3 Results

The ability of certain microbial strains to produce biopolymer was screened based on the amount of crude biopolymer produced and the apparent viscosity of the culture broth (Figure 2.1 – 2.3). Some cultures, as was the case of *Z. mobilis* ATCC 29191, did not exhibit a visual increase in viscosity and it was assumed that they did not produce biopolymer in the conditions tested. The same happened with the *B. subtilis* isolates, even though the amount of product recovered through ethanol precipitation reached 38.0 g/L after 120h (Figure 2.2). This may happen because other compounds/metabolites, besides biopolymers, precipitate in the presence of ethanol.

The cultures of *A. pullulans* CCY 27–1–94 produced the lowest amount of crude biopolymer (6.7 g/L after 72h) (Figure 2.1); nonetheless, this biopolymer had already been studied for MEOR applications (Elshafie et al., 2017) and so it was selected to perform further assays. The apparent viscosity of the biopolymer produced by this strain was measured in the following chapter. *L. mesenteroides* A4 produced 12.4 g of crude biopolymer/L in static conditions after only 48h of growth in the Lm4 medium, while producing around 3 times less biopolymer at 180 rpm. The first condition was thus selected for further assays. Furthermore, since the highest viscosity values for *L. mesenteroides* A4 were achieved using the Lm1 medium (Figure 2.3), this medium was also selected for further optimization.

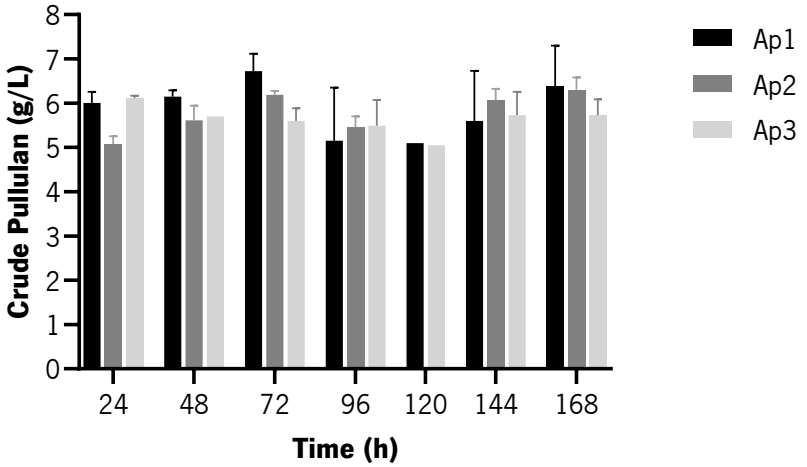

Figure 2.1 – Crude pullulan (g/L) produced over time by *Aureobasidium pullulans* CCY 27–1–94 grown in Ap1, Ap2 and Ap3 media (200 mL) in 500 mL flasks at 30°C and 150 rpm.

Results correspond to the average ± standard deviation of two measurements.

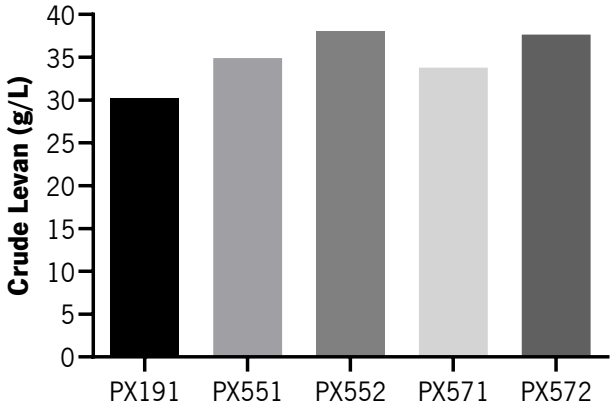

Figure 2.2 – Crude levan (g/L) produced after 120h by different *Bacillus subtilis* isolates (PX191, PX551, PX552, PX571 and PX572) grown in Bs1 medium (200 mL) in 500 mL flasks at 37°C and 150 rpm.

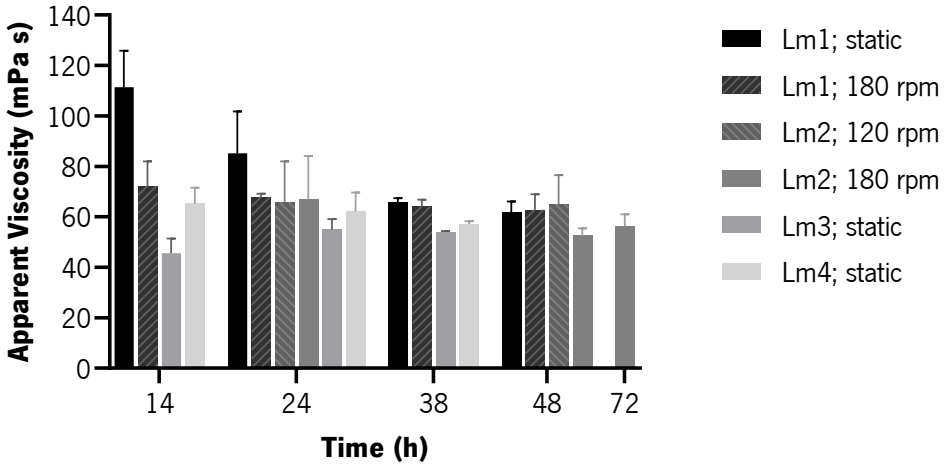

Figure 2.3 – Apparent viscosity (mPa s) values over time of culture broth samples of *Leuconostoc mesenteroides* A4 grown in different culture media (20 mL) in 100 mL flasks at 30°C and different agitation speeds.

Results correspond to the average ± standard deviation of one sample measured through three successive flow ramps at 40°C and shear rate 1.4 s^{-1}.

Four other *Bacillus*–like isolates (P#01, P#02, P#03 and P#04) were studied for biosurfactant production. During those assays, it was observed that some of them were also able to produce biopolymer since the viscosity of the culture medium increased over time. These results will be presented and discussed in detail in a further chapter (Chapter 6).

2.4 Discussion

The microorganisms herein studied have shown specific nutritional requirements in order to produce biopolymer. *Z. mobilis* ATCC 29191 did not produce significant results due to the low culture medium viscosity observed. This microorganism can produce levan and ethanol simultaneously through alternative metabolic pathways. The medium composition upon fermentation can redirect the metabolism of *Z. mobilis* toward the bioproduct of interest, leading to increased or decreased levan production (Santos Ferreira et al., 2022). High sucrose concentrations are commonly used for the production of levan by this microorganism and other components like nitrogen, sulfate and magnesium have been reported as essential nutrients (de Oliveira et al., 2007; Ernandes & Garcia–Cruz, 2011). Using the Zm1 medium and under similar operational conditions, Ernandes & Garcia–Cruz (2011) reported levan titers of 63 g/L after 24h of growth, while Santos Ferreira et al. (2022) reported a titer of 13 g/L. However, in the latter study, the viscosity of levan solutions was close to 17 mPa s, which does not translate to a visual increase

in the viscosity of the broth. As such, the *Z. mobilis* strain evaluated in this work may have produced biopolymer even though the viscosity did not increase. Nevertheless, higher viscosities are preferred for biopolymers used in MEOR.

In the case of *B. subtilis* isolates, a low culture broth viscosity was also observed. According to previous studies, sucrose concentration is the main factor that affects levan production by *Bacillus* spp., but culture conditions like pH, temperature and agitation speed also contribute to its production. In a medium containing 200 g/L of sucrose, a *B. subtilis* strain isolated from natto reached a maximum concentration of 49.4 g levan/L, with a lower titer being obtained when less sucrose was used (Shih et al., 2005). With the Bs1 culture medium containing 160 g/L of sucrose, *Paenibacillus polymyxa* ESJ–3 produced 22.8 g/L of levan (Liu et al., 2009). The values of potential levan production by *B. subtilis* isolates obtained here fall within this range. Furthermore, two types of levan can be produced by *Bacillus* spp., a high molecular weight levan and a low–molecular weight one (Nakapong et al., 2013; Shih et al., 2005). Both exhibit low viscosities in solution, but low–molecular weight levan has a lower intrinsic viscosity (Arvidson et al., 2006). Thus, even though ethanol precipitation resulted in around 38 g/L of precipitate, it is thought that this biopolymer may have a low molecular weight due to the low viscosity observed.

Regarding pullulan production by *A. pullulans* CCY 27–1–94, different carbon and nitrogen sources appear to generate different results depending on the strain used. Prasongsuk et al. (2007) evaluated pullulan production in different strains using glucose or sucrose as carbon source and $(NH_4)_2SO_4$, $NaNO_3$ or peptone as nitrogen source. Sucrose seemed to generate the best results in all strains, while the preferred nitrogen source was either peptone or $(NH_4)_2SO_4$. The highest amount of pullulan produced in Ap1 was 25.2 g/L (Prasongsuk et al., 2007), while the titer obtained in this study with a similar medium was 6.7 g/L. In the other media tested, the maximum amount of crude pullulan obtained was also lower than what is reported in the literature (6.3 g/L compared to 12.7 g/L in the literature with the medium Ap2, and 6.1 g/L compared to 20.7 g/L in the literature with the medium Ap3) (Cheng et al., 2011a; Elshafie et al., 2017). The differences observed may be due to the strain used here, that displays a lower ability to produce biopolymer.

The best results in terms of produced biopolymer (12.4 g/L) and culture broth viscosity (up to 111 mPa s) were obtained with *L. mesenteroides* A4. Other studies using the same media, however, reported productions between 20 and 30 g/L (Castro–Rodríguez et al., 2019; Han et al., 2014), which are higher than those obtained here. Those studies evaluated dextran production by *L. mesenteroides* using an

agitation speed of 180 rpm (Castro–Rodríguez et al., 2019; Han et al., 2014), but some works reported interesting results when this bacterium was grown under static conditions (Siddiqui et al., 2014; Xing et al., 2018). In our case, the best results were obtained under such conditions. Furthermore, it was observed that this strain produces a pellicle in the surface of the culture medium when grown under static conditions, which can explain some of the variations observed in the viscosity measurements between duplicates, since the culture medium is less homogenous when compared with assays performed under shaking conditions. This property has been previously observed, and the pellicle can contain the water–insoluble dextran produced by the bacteria (Padmanabhan et al., 2003). Additionally, previous works have demonstrated the potential of *L. mesenteroides* in *in situ* MEOR (Soudmand–asli et al., 2007).

Overall, two of the studied microorganisms (*A. pullulans* CCY 27–1–94 and *L. mesenteroides* A4) have shown promising features to be used in biopolymer based MEOR, with a focus in the *ex situ* approach. Thus, these were selected for further studies.

2.5 References

Arvidson, S. A., Rinehart, B. T., & Gadala–Maria, F. (2006). Concentration regimes of solutions of levan polysaccharide from Bacillus sp. *Carbohydrate Polymers*, *65*(2), 144–149. https://doi.org/10.1016/j.carbpol.2005.12.039

Azarhava, H., Bajestani, M. I., Jafari, A., Vakilchap, F., & Mousavi, S. M. (2020). Production and physicochemical characterization of bacterial poly gamma– (glutamic acid) to investigate its performance on enhanced oil recovery. *International Journal of Biological Macromolecules*, *147*, 1204–1212. https://doi.org/10.1016/j.ijbiomac.2019.10.090

Azarhava, H., Jafari, A., Vakilchap, F., & Mousavi, S. M. (2021). Stability and performance of poly γ–(glutamic acid) in the presence of sulfate ion for enhanced heavy oil recovery. *Journal of Petroleum Science and Engineering*, *196*, 107688. https://doi.org/10.1016/j.petrol.2020.107688

Castro–Rodríguez, D., Hernández–Sánchez, H., & Yáñez–Fernández, J. (2019). Structural characterization and rheological properties of dextran produced by native strains isolated of Agave salmiana. *Food Hydrocolloids*, *90*, 1–8. https://doi.org/10.1016/j.foodhyd.2018.11.052

Cheng, K. C., Demirci, A., & Catchmark, J. M. (2011a). Evaluation of medium composition and fermentation parameters on pullulan production by Aureobasidium pullulans. *Food Science and Technology International*, *17*(2), 99–109. https://doi.org/10.1177/1082013210368719

Cheng, K. C., Demirci, A., & Catchmark, J. M. (2011b). Pullulan: Biosynthesis, production, and applications. In *Applied Microbiology and Biotechnology* (Vol. 92, Issue 1, pp. 29–44). https://doi.org/10.1007/s00253–011–3477–y

de Oliveira, M. R., da Silva, R. S. S. F., Buzato, J. B., & Celligoi, M. A. P. C. (2007). Study of levan production by Zymomonas mobilis using regional low–cost carbohydrate sources. *Biochemical*

Engineering Journal, *37*(2), 177–183. https://doi.org/10.1016/j.bej.2007.04.009

Elshafie, A., Joshi, S. J., Al-Wahaibi, Y. M., Al-Bahry, S. N., Al-Bemani, A. S., Al-Hashmi, A., & Al-Mandhari, M. S. (2017, April 4). Isolation and Characterization of Biopolymer Producing Omani Aureobasidium Pullulans Strains and Its Potential Applications in Microbial Enhanced Oil Recovery. *SPE Oil and Gas India Conference and Exhibition*. https://doi.org/10.2118/185326-ms

Ernandes, F. M. P. G., & Garcia-Cruz, C. H. (2011). Nutritional requirements of Zymomonas mobilis CCT 4494 for levan production. *Brazilian Archives of Biology and Technology*, *54*(3), 589–600. https://doi.org/10.1590/S1516-89132011000300021

Fan, Y., Wang, J., Gao, C., Zhang, Y., & Du, W. (2020). A novel exopolysaccharide-producing and long-chain n-alkane degrading bacterium Bacillus licheniformis strain DM-1 with potential application for in-situ enhanced oil recovery. *Scientific Reports*, *10*(1), 8519. https://doi.org/10.1038/s41598-020-65432-z

Han, J., Hang, F., Guo, B., Liu, Z., You, C., & Wu, Z. (2014). Dextran synthesized by Leuconostoc mesenteroides BD1710 in tomato juice supplemented with sucrose. *Carbohydrate Polymers*, *112*, 556–562. https://doi.org/10.1016/j.carbpol.2014.06.035

Lee, K. S., Kwon, T.-H., Park, T., & Jeong, M. S. (2020). Microbiology and Microbial Products for Enhanced Oil Recovery. In *Theory and Practice in Microbial Enhanced Oil Recovery* (pp. 27–65). Gulf Professional Publishing. https://doi.org/10.1016/b978-0-12-819983-1.00002-8

Liu, J., Luo, J., Ye, H., Sun, Y., Lu, Z., & Zeng, X. (2009). Production, characterization and antioxidant activities in vitro of exopolysaccharides from endophytic bacterium Paenibacillus polymyxa EJS-3. *Carbohydrate Polymers*, *78*(2), 275–281. https://doi.org/10.1016/j.carbpol.2009.03.046

Nakapong, S., Pichyangkura, R., Ito, K., Iizuka, M., & Pongsawasdi, P. (2013). High expression level of levansucrase from Bacillus licheniformis RN-01 and synthesis of levan nanoparticles. *International Journal of Biological Macromolecules*, *54*(1), 30–36. https://doi.org/10.1016/j.ijbiomac.2012.11.017

Padmanabhan, P. A., Kim, D. S., Pak, D., & Sim, S. J. (2003). Rheology and gelation of water-insoluble dextran from Leuconostoc mesenteroides NRRL B-523. *Carbohydrate Polymers*, *53*(4), 459–468. https://doi.org/10.1016/S0144-8617(03)00140-1

Prasongsuk, S., Berhow, M. A., Dunlap, C. A., Weisleder, D., Leathers, T. D., Eveleigh, D. E., & Punnapayak, H. (2007). Pullulan production by tropical isolates of Aureobasidium pullulans. *Journal of Industrial Microbiology and Biotechnology*, *34*(1), 55–61. https://doi.org/10.1007/s10295-006-0163-7

Rehm, B. H. A. (2010). Bacterial polymers: Biosynthesis, modifications and applications. In *Nature Reviews Microbiology* (Vol. 8, Issue 8, pp. 578–592). Nature Publishing Group. https://doi.org/10.1038/nrmicro2354

Santos Ferreira, J. de A., Sampaio, I. C. F., da Cruz Hora, C. E., Torres Lima Matos, J. B., de Almeida, P. F., & Chinalia, F. A. (2022). Culturing strategy for producing levan by upcycling oil produced water effluent as base medium for Zymomonas mobilis. *Process Biochemistry*, *115*, 49–56. https://doi.org/10.1016/j.procbio.2022.02.001

Shih, I. L., Yu, Y. T., Shieh, C. J., & Hsieh, C. Y. (2005). Selective production and characterization of levan by Bacillus subtilis (Natto) Takahashi. *Journal of Agricultural and Food Chemistry*, *53*(21), 8211–8215. https://doi.org/10.1021/jf058084o

Shrivastava, A. (2018). Introduction to Plastics Engineering. In *Introduction to Plastics Engineering* (pp.

1–16). Elsevier. https://doi.org/10.1016/b978–0–323–39500–7.00001–0

Siddiqui, N. N., Aman, A., Silipo, A., Qader, S. A. U., & Molinaro, A. (2014). Structural analysis and characterization of dextran produced by wild and mutant strains of Leuconostoc mesenteroides. *Carbohydrate Polymers*, *99*, 331–338. https://doi.org/10.1016/j.carbpol.2013.08.004

Soudmand–asli, A., Ayatollahi, S. S., Mohabatkar, H., Zareie, M., & Shariatpanahi, S. F. (2007). The in situ microbial enhanced oil recovery in fractured porous media. *Journal of Petroleum Science and Engineering*, *58*(1–2), 161–172. https://doi.org/10.1016/j.petrol.2006.12.004

Suthar, H., Hingurao, K., Desai, A., & Nerurkar, A. (2009). Selective plugging strategy based microbial enhanced oil recovery using Bacillus licheniformis TT33. *Journal of Microbiology and Biotechnology*, *19*(10), 1230–1237. https://doi.org/10.4014/jmb.0904.04043

Verma, M. L., Kumar, S., Jeslin, J., & Dubey, N. K. (2020). Microbial production of biopolymers with potential biotechnological applications. In *Biopolymer–Based Formulations: Biomedical and Food Applications* (pp. 105–137). Elsevier. https://doi.org/10.1016/B978–0–12–816897–4.00005–9

Wani, S. M., Mir, S. A., Khanday, F. A., & Masoodi, F. A. (2021). Advances in pullulan production from agro–based wastes by Aureobasidium pullulans and its applications. In *Innovative Food Science and Emerging Technologies* (Vol. 74, p. 102846). Elsevier. https://doi.org/10.1016/j.ifset.2021.102846

Xing, H., Du, R., Zhao, F., Han, Y., Xiao, H., & Zhou, Z. (2018). Optimization, chain conformation and characterization of exopolysaccharide isolated from Leuconostoc mesenteroides DRP105. *International Journal of Biological Macromolecules*, *112*, 1208–1216. https://doi.org/10.1016/j.ijbiomac.2018.02.068

CHAPTER 3.

Screening biopolymer and biosurfactant production for application in Microbial Enhanced Oil Recovery

Abstract

Biopolymer production by *Leuconostoc mesenteroides* A4 was optimized using various culture media and growth conditions. When grown in static conditions with a synthetic medium containing 100 g/L of sucrose, this microorganism produced 12.9 g/L of crude biopolymer with an apparent viscosity value of 326 ± 8 mPa s in just 24h. Using the agro–industrial by–products corn steep liquor (CSL) or sugarcane molasses as substitutes for certain medium components, this strain produced a biopolymer with similar viscosities as that produced in the synthetic medium. CSL was also used as a substrate for biopolymer production by *Rhizobium viscosum* CECT 908 and biosurfactant (surfactin) production by *Bacillus subtilis* strains isolated from a Brazilian oilfield. In a double–walled bioreactor, operating at constant stirring and aeration rates (250 rpm and 1.7 vvm), the viscosity of the culture medium increased to 618 ± 6 mPa s due to biopolymer production by *R. viscosum* CECT 908. Additionally, the production of surfactin by *B. subtilis* #311 increased when moving from a batch mode of operation to a fed–batch mode, lowering the minimum surface tension of the culture medium from 24.0 ± 0.1 mN/m to 22.6 ± 0.1 mN/m. In fed–batch mode, this strain produced 1.1 g/L of surfactin, which reduced the surface tension of PBS to 25.5 ± 0.1 mN/m and had a CMC of 21.5 mg/L. These results provide valuable insights into the optimization of biotechnological processes for the production of metabolites useful for application in microbial enhanced oil recovery (MEOR) using several microorganisms.

3.1 Introduction

As discussed in Chapters 1 and 2, biosurfactants and biopolymers from different microorganisms have been evaluated for their potential use in oil recovery applications. One important step in this evaluation is their production optimization in terms of growth conditions and culture media used to obtain the highest amount of product with the lowest possible production cost.

The high production cost of these biomolecules is one of the main limitations of their industrial scale application, with culture media raw materials accounting for 10–30% of those costs (Mohanty et al., 2021; Sharma et al., 2013). In order to reduce production costs, several agro–industrial wastes and by–products can be used as alternative cost–effective substrates. In this work, corn steep liquor (CSL) and sugarcane molasses were evaluated for biopolymer and biosurfactant production. CSL is the liquid by–product of the corn wet–milling industry and is used in biotechnological processes as an inexpensive source of nitrogen (Gudiña, Rodrigues, et al., 2015; Hofer et al., 2018). Besides amino acids and proteins, CSL is rich in vitamins and minerals, and contains variable amounts of carbohydrates (as detailed in Table 5.1, Chapter 5), meaning that it can be also used as a low–cost carbon source (Gudiña, Rodrigues, et al., 2015). Sugarcane molasses is the by–product obtained during the crystallization of sugar from liquid extracts of sugarcane, which contains around 50% of carbohydrates, as well as other important nutrients such as vitamins (Gudiña, Rodrigues, et al., 2015). These substrates have been previously used to produce biosurfactants (Chaprão et al., 2018; Gudiña et al., 2016; Gudiña, Fernandes, et al., 2015; Gudiña, Rodrigues, et al., 2015; Jha et al., 2016; Segovia et al., 2021; Soares da Silva et al., 2017, 2021) and biopolymers (Fan et al., 2020; Gudiña et al., 2023; Lee et al., 2014; Sharma et al., 2013; Sun et al., 2011, 2013; Xia et al., 2018; Xu & Lu, 2011) by different microorganisms, constituting a valuable approach for cost–effective processes that promote a circular economy.

Since oil recovery operations require large amounts of biomolecules, the scale–up process is another important step in production optimization. In this work, the production of biopolymers and biosurfactants was scaled–up from shake flasks to lab–scale stirred bioreactors. During this process, several parameters must be taken into account, like the oxygen transfer rate, shear induced by agitation, the size of seed culture and other operational parameters (temperature, pH, concentration of nutrients) (Hewitt & Nienow, 2007; Marques et al., 2010; Schmidt, 2005). The oxygen transfer rate, that is necessary for aerobic processes, is influenced by the stirring rate and the airflow input in bioreactors (Marques et al., 2010). Typically, increasing either of these parameters will result in a higher oxygen transfer rate. However, if the stirring rate is too high, it may cause mechanical stress on the cells in

suspension, decreasing the overall productivity of the process (Hewitt & Nienow, 2007; Schmidt, 2005). Additionally, the oxygen transfer rate is influenced by the liquid properties of the fluid (Garcia–Ochoa & Gomez, 2009). This is particularly important in the case of biopolymer production because the culture broth becomes more viscous as time goes by, which decreases the oxygen transfer rate by creating heterogeneous areas within the bioreactor. This also affects nutrient distribution, leading to areas of lower productivity (Garcia–Ochoa & Gomez, 2009; Hewitt & Nienow, 2007). Thus, it may become necessary to adjust the stirring rate and air flow input during the fermentation.

The size of the seed culture is another parameter that must be adjusted when scaling up. As the reactor volume is bigger than the volume used in shake flasks, the size of the inoculum (as the percentage of the culture volume) must be increased to try to prevent cell stress (Schmidt, 2005). The other parameters like temperature and pH are usually kept constant when moving from shake flasks to bioreactors but may need adjusting in some cases (Hewitt & Nienow, 2007; Marques et al., 2010; Schmidt, 2005). Moreover, the scale–up of microbial processes will greatly differ with the microorganism used and the desired product. As such, each case must be evaluated independently to obtain the best scale–up strategy.

The aim of this work was to develop cost–effective bioprocesses to produce biopolymers from *Rhizobium viscosum* CECT 908, *Aureobasidium pullulans* CCY 27–1–94 and *Leuconostoc mesenteroides* A4, as well as biosurfactants from *Bacillus subtilis* strains isolated from a Brazilian oilfield.

3.2 Materials and methods

3.2.1 Strains and culture conditions

Several microbial strains capable of producing biopolymers or biosurfactants were used in this study. The microorganisms were grown using different culture media (Table 3.1) and conditions, based on the results obtained in Chapter 2. The strains were maintained in Luria–Bertani (LB) medium (deMan, Rogosa, Sharpe (MRS) in the case of *L. mesenteroides* A4), supplemented with 20% (v/v) of glycerol at –80°C, or Rv1 medium supplemented with 15% (v/v) of glycerol in the case of *R. viscosum* CECT 908. Pre–cultures were prepared by inoculating 20 mL of medium with 100 µL from a frozen stock and were incubated overnight, or during 48h in the case of *R. viscosum* CECT 908, at the appropriate temperature.

Table 3.1 – Description of the culture media for the microorganisms used in the optimization of biomolecules production.

Microorganism	Expected bioproduct	Culture medium	Culture medium composition	Reference
***Aureobasidium pullulans* CCY 27–1–94**	Pullulan (Biopolymer)	Ap1	Sucrose 50 g/L; Yeast Extract 0.4 g/L; K_2HPO_4 5 g/L; $(NH_4)_2SO_4$ 0.6 g/L; $MgSO_4 \cdot 7H_2O$ 0.4 g/L; NaCl 1 g/L	Prasongsuk et al. (2007)
***Leuconostoc mesenteroides* A4**	Dextran (Biopolymer)	Lm1	Sucrose 50 g/L; Tryptone 5 g/L; Soya peptone 5 g/L; Meat extract 5 g/L; Yeast extract 2.5 g/L; Ascorbic acid 0.5 g/L; Di–sodium–glycerophosphate 19 g/L; $MgSO_4 \cdot 7H_2O$ 0.25 g/L	Han et al. (2014)
		Lm3 and Lm4	Sucrose 100 g/L (Lm3) or 200 g/L (Lm4); Peptone 10 g/L; Yeast Extract 5 g/L; Meat Extract 5 g/L; K_2HPO_4 2 g/L; Diammonium citrate 2 g/L; Sodium acetate 5 g/L; $MgSO_4 \cdot 7H_2O$ 0.1 g/L; $MnSO_4 \cdot H_2O$ 0.05 g/L	Castro–Rodríguez et al. (2019)
***Rhizobium viscosum* CECT 908**	– (Biopolymer)	Rv1	Glucose 25 g/L; Yeast Extract 3 g/L; K_2HPO_4 2 g/L; $MgSO_4 \cdot 7H_2O$ 0.1 g/L	Couto et al. (2019)
***Bacillus subtilis* (#191, #309, #311, #317, #551, #552, #571 and #572)**	Surfactin (Biosurfactant)	Bs2	Corn Steep Liquor (CSL) 10% (v/v)	Gudiña, Fernandes, et al. (2015)

3.2.2 Production of biomolecules in flasks

Biopolymer production by *A. pullulans* CCY 27–1–94 and *L. mesenteroides* A4 was evaluated in either 500 mL flasks with 200 mL of culture medium or 250 mL flasks with 100 mL of culture medium, respectively. Each flask was inoculated with 1% (v/v) of a pre–culture (prepared as described in the previous section) and incubated at 30°C and 150 rpm for *A. pullulans* CCY 27–1–94, and 30°C and 150 rpm or under static conditions for *L. mesenteroides* A4.

In the case of *L. mesenteroides* A4, the synthetic medium Lm4 was used as control, while CSL (kindly provided by COPAM – Companhia Portuguesa de Amidos, S. A. (Portugal)) and sugarcane molasses (kindly provided by RAR: Refinarias de Açúcar Reunidas, S.A. (Portugal)) were evaluated as alternative substrates. CSL was used at different concentrations (1–20% (v/v)) as an alternative nitrogen source (instead of peptone, yeast extract and meat extract in Lm4 medium) and sugarcane molasses (100–400 g/L) was used as an alternative carbon source (instead of sucrose).

Biosurfactant production by *B. subtilis* strains (#191, #309, #311, #317, #551, #552, #571 and #572) isolated from crude oil samples from a Brazilian oilfield (Gudiña et al., 2012) was evaluated in 250 mL flasks containing 100 mL of low–cost Bs2 medium. Each flask was inoculated with 1% (v/v) of a pre–culture (prepared as described in the previous section) and incubated at 37°C and 150 rpm.

All the media were adjusted to pH 7.0. Samples were taken at different time intervals to determine apparent viscosity (in biopolymer production assays) and surface tension (ST) (in biosurfactant production assays), as described in the following sections.

3.2.3 Production of biomolecules in bioreactor

The scale–up process for the production of the *R. viscosum* CECT 908 biopolymer was performed in a 2 L–bioreactor (Bioengineering AG, Switzerland) with 1 L of Rv1 medium or in a 3.7 L–bioreactor (RALF Advanced, Bioengineering AG, Switzerland) with 2 L of the same medium. The scale–up process for the production of the *B. subtilis* #311 biosurfactant was performed in a 3.7 L–bioreactor (RALF Advanced, Bioengineering AG, Switzerland) with 1.5 or 2 L of the Bs2 medium. Because Bs2 medium contains high amounts of precipitates, which can interfere with the bioreactor's performance, it was centrifuged (15316 x *g*, 20 min) before being introduced in the reactor vessel. Silicon anti–foaming agent (0.05% (v/v) (Sigma–Aldrich)) was added to each of the culture media to avoid the formation of foam.

A pre–culture was first prepared in Rv1 or LB medium (20 mL), grown over 48h or overnight at 30°C or 37°C and 150 rpm, for *R. viscosum* CECT 908 and *B. subtilis* #311, respectively, and used to inoculate a second pre–culture containing 100 mL of the same culture medium, which was incubated at the same conditions. Subsequently, the *B. subtilis* #311 inoculum was centrifuged (5514 x *g*, 10 min) and the cells were washed with the same volume of a phosphate–buffered saline (PBS) solution (NaCl 8.77 g/L, K_2HPO_4 0.87 g/L, KH_2PO_4 0.68 g/L; pH 7.0), and then resuspended in a minimum volume of the same buffer, which was later used to inoculate the bioreactor. The bioreactor for *R. viscosum* CECT 908 growth was directly inoculated with the second pre–culture.

The experiments were conducted under batch mode under different conditions. Biosurfactant production by *B. subtilis* #311 was also studied under fed–batch mode, where 500 mL of concentrated culture medium (40% (v/v) CSL) were added at a flow rate of 1 mL/min after 24h of growth. Samples were taken at different time points and used to determine apparent viscosity, ST, bacterial growth and substrate consumption.

3.2.4 Biopolymer recovery

Each of the collected samples was first centrifuged (9400 x *g*, 20 min) to remove the cells. The biopolymer from *A. pullulans* CCY 27–1–94 and *L. mesenteroides* A4 was then precipitated by adding two volumes of ethanol (99%, v/v) to the cell–free supernatant (CFS) and incubating the mixture at –20°C for 24h. Afterwards, the samples were centrifuged (9400 x *g*, 20 min, 4°C), the pellet containing the biopolymer was resuspended in a minimum amount of demineralized water, freeze–dried and stored at –20°C.

The biopolymer from *R. viscosum* CECT 908 was precipitated using hexadecyl–trimethylammonium bromide (CTAB), as described by Novak and co–workers (1992) and resuspended in a minimum volume of demineralized water to determine apparent viscosity.

3.2.5 Biosurfactant recovery

The collected samples were centrifuged (9400 x *g*, 20 min) to remove the cells. The biosurfactant produced by *B. subtilis* #311 was recovered through acid precipitation (Gudiña, Fernandes, et al., 2015) by adjusting the pH of the CFS to 2.0 with 18 % (v/v) HCl and incubating at 4°C overnight. Next, the samples were centrifuged (9400 x *g*, 20 min, 4°C) to recover the precipitate (crude biosurfactant), which was dissolved in a minimum amount of demineralized water and had its pH adjusted to 7.0 with 10 mM NaOH. For further purification, the aqueous biosurfactant solution was extracted with 4 volumes of a chloroform:methanol solution (2:1, v/v), by continuously stirring for 1 h; subsequently, the aqueous and the organic phases were allowed to separate, and the organic phase containing the biosurfactant was recovered and allowed to evaporate. The extraction was repeated three times before the purified biosurfactant was freeze–dried and stored at –20°C.

3.2.6 Analytical techniques

3.2.6.1 Bacterial growth determination

Bacterial growth in bioreactor was determined by cell dry weight. Samples were centrifuged (9400 x *g*, 20 min) to separate the cells, which were resuspended in a minimum volume of demineralized water and dried at 60°C for 24h. The amount of cells was determined as dry weight and expressed as g cells/L culture.

3.2.6.2 Reducing sugars determination

Reducing sugars were determined by the dinotrosalicylic acid (DNS) method (Miller, 1959).

3.2.6.3 Apparent viscosity measurements

The apparent viscosity was determined as described in Chapter 2 (2.2.3).

3.2.6.4 Surface tension measurement and critical micelle concentration (CMC)

ST of CFS and biosurfactant solutions was measured using the Ring method described elsewhere (Gudiña et al., 2016). A KRÜSS K20 Tensiometer (KRÜSS GmbH, Germany) equipped with a 1.9 cm De Noüy platinum ring was used at room temperature (25°C). Due to the fast decrease of the ST (which in some cases achieved the minimum values after 24h) in some cases it was necessary to dilute the CFS up to 100 times in order to evaluate the production of surfactin over time. All the measurements were done in triplicate.

Critical micelle concentrations (CMC) were calculated by measuring the ST of purified surfactin solutions prepared in PBS at different concentrations, as described elsewhere (Gudiña et al., 2016).

3.3 Results

3.3.1 Optimization of biopolymer production

3.3.1.1 Biopolymer production by *A. pullulans* CCY 27–1–94 and *L. mesenteroides* A4 in synthetic media

To determine the optimal conditions that generate the highest biopolymer production by *A. pullulans* CCY 27–1–94 and *L. mesenteroides* A4, various growth conditions were tested using the corresponding synthetic media (Table 3.2). *A. pullulans* CCY 27–1–94 produced less crude biopolymer (1.5 g/L) when compared to *L. mesenteroides* A4 in the different conditions tested (4.3–21.1 g/L), even though the viscosity of the biopolymer produced (58 ± 1 mPa s) was similar to that of *L mesenteroides* A4 in some of the cases (dextran production in Lm4 medium with agitation).

Table 3.2 – Quantification of the crude biopolymers produced by *Aureobasidium pullulans* CCY 27–1–94 (pullulan) and *Leuconostoc mesenteroides* A4 (dextran) in different media and growth conditions; and viscosity of solutions prepared with different concentrations of the biopolymer produced in each condition.

Biopolymer	Culture medium	Agitation speed (rpm)	Time (h)	BP produced (g/L)	BP solution (g/L)	Viscosity (at 40°C and 1.4 s^{-1}) (mPa s)
Pullulan	Ap1	150	72	1.5	20	58 ± 1
Dextran	Lm1	0	14	18.5	40	296 ± 76
			24	17.5	40	87 ± 2
		180	14	14.9	40	2422 ± 2139*
			24	16.8	40	122 ± 3*
	Lm3	0	24	12.9 ± 1.7	40	326 ± 8
			48	13.4 ± 0.6	40	218 ± 15
			72	13.0 ± 0.2	40	238 ± 16
	Lm4	0	24	21.1 ± 0.2	40	227 ± 2
			48	18.6 ± 0.6	40	116 ± 5
			72	18.1 ± 0.2	40	109 ± 3
		150	24	4.9	20	54 ± 2*
			48	4.3	20	51 ± 3*

* Viscosity values corresponding to the average ± standard deviation of one sample measured through three successive flow ramps, while other values correspond to the average of two independent samples measured in a similar way. BP: biopolymer.

Regarding *L. mesenteroides* A4, the highest viscosity values (2422 ± 2139 mPa s) were obtained using the culture medium Lm1 with agitation (Table 3.2). However, the biopolymer produced here was deemed to be unstable due to the very high variation displayed in its viscosity values. The highest production, on the other hand, was obtained with the Lm4 medium in static conditions, where it produced up to 21.1 g of crude biopolymer/L in just 24h of growth. As such, this condition was selected for further studies along with the Lm3 medium that produced 12.9 g/L of crude biopolymer with a viscosity value of 326 ± 8 mPa s. Furthermore, it was observed that longer incubation times (up to 72h) did not improve biopolymer production, even producing lower amounts of crude biopolymer with lower apparent viscosity values with the Lm4 medium. The high biopolymer production and relatively high apparent viscosity values obtained in a short fermentation time (24h) make this microorganism an attractive alternative for biopolymer production.

3.3.1.2 Production of dextran by *Leuconostoc mesenteroides* A4 using agro–industrial by–products

The culture medium that offered the best results regarding biopolymer production in the previous assays (Lm4) was used as a base medium for optimization with alternative low–cost substrates. Some of the medium components were replaced by agro–industrial waste products, namely sugarcane molasses (100–400 g/L) to substitute sucrose as a carbon source and CSL (1–20%) to substitute peptone, yeast extract and meat extract as a nitrogen source (Figure 3.1).

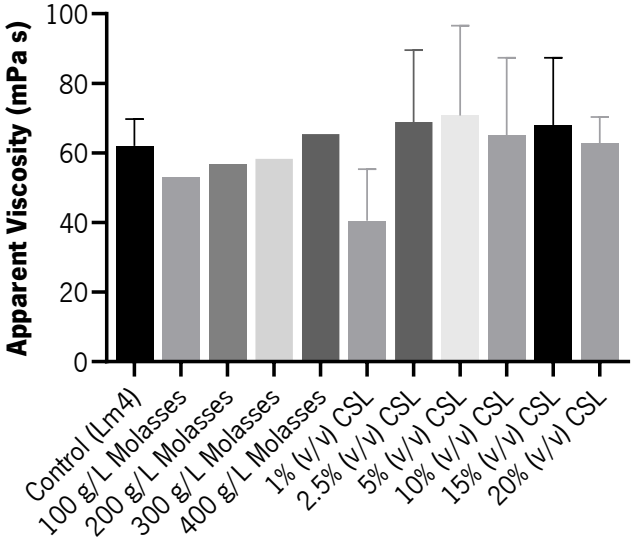

Figure 3.1 – Apparent viscosity values of culture broth samples obtained from cultures of *Leuconostoc mesenteroides* A4 grown for 24h in a modified Lm4 medium containing different concentrations of sugarcane molasses (100–200 g/L) or different concentrations of CSL (1–20% (v/v)).

Experiments were performed at 30°C and static conditions. Results correspond to the average ± standard deviation of one sample measured through three successive flow ramps at 40°C and shear rate 1.4 s^{-1}.

None of the tested media, however, resulted in a significant increase of the apparent viscosity values obtained with the standard synthetic medium Lm4 (57 mPa s measured in the cell–free supernatant).

3.3.1.3 Production of biopolymer by *R. viscosum* CECT 908 in bioreactor

The production of *R. viscosum* CECT 908 biopolymer in bioreactor was evaluated over 120h of growth at 30°C with varying agitation speeds (200 rpm, 250 rpm, increasing from 250 rpm to 400 rpm after 48h) and aeration rates (0.4, 1.3 and 1.7 vvm (volume of air per volume of cultivation broth per minute)) (Figure 3.2). Some of the tested conditions resulted in an excessive formation of foam and were stopped after 72 or 96h.

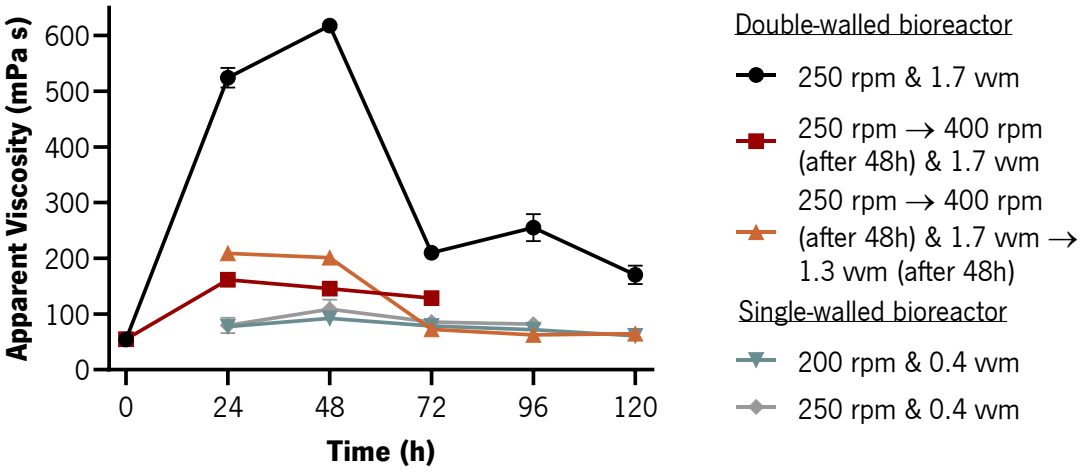

Figure 3.2 – Apparent viscosity values (mPa s) over time of *Rhizobium viscosum* CECT 908 grown in bioreactor with Rv1 medium at different operational conditions.

Results correspond to the average ± standard deviation of one or two assays measured through three successive flow ramps at 40°C and shear rate 1.4 s^{-1}.

The design of the bioreactors used, as well as their working volumes, were also different. The 2 L–bioreactor, used with 1 L of culture medium, was made up of a double–jacket vessel where cooling and heating water would flow for temperature control. The use of this bioreactor should result in a better heat distribution due to the expected viscosity in the culture medium. The 3.7 L–bioreactor (working with 2 L of medium), on the other hand, used hollow baffles within a single–walled vessel for temperature

control. However, in both cases, as the viscosity increased, temperature gradients were formed due to a deficient homogenization of the culture medium inside the bioreactor.

In all the assays, the highest viscosity values were achieved at 48h of growth, after which the viscosity started to decrease, suggesting the degradation of the biopolymer produced (Figure 3.2). The best results in terms of apparent viscosity values were obtained with the double–walled bioreactor when a constant stirring rate of 250 rpm was used (618 ± 6 mPa s). However, none of the assays resulted in viscosities as high as those obtained in assays performed in flasks using the same culture medium (739 ± 30 mPa s, as reported by Couto et al. (2019)), which suggests that these bioreactors may not be appropriate for this purpose.

3.3.2 Optimization of biosurfactant production by *B. subtilis* isolates

3.3.2.1 Evaluating the potential of *B. subtilis* isolates for biosurfactant production using corn steep liquor

The production of biosurfactant (surfactin) was evaluated with eight *B. subtilis* strains (#191, #309, #311, #317, #551, #552, #571 and #572) isolated from crude oil samples from a Brazilian oilfield that were grown in a low–cost medium (Bs2) (Table 3.3). Among the different strains, the isolates #309, #311 and #317 exhibited the lowest ST values. Accordingly, *B. subtilis* #311 was selected for further studies regarding the bioprocess optimization for surfactin production.

Table 3.3 – Surface tension values (mN/m) obtained with the different *Bacillus subtilis* isolates grown in 10% (v/v) CSL medium for 48h at 37°C and 150 rpm.

Isolate	24h			48h		
	ST (mN/m)	ST^{-1} (mN/m)	ST^{-2} (mN/m)	ST (mN/m)	ST^{-1} (mN/m)	ST^{-2} (mN/m)
#191	49.4 ± 0.5	–	–	44.1 ± 1.5	–	–
#309	26.4 ± 0.0	27.9 ± 0.1	39.2 ± 1.4	25.9 ± 0.1	27.4 ± 0.0	33.8 ± 0.3
#311	26.2 ± 0.0	27.5 ± 0.1	35.3 ± 0.4	25.9 ± 0.0	27.2 ± 0.0	33.3 ± 0.4
#317	26.3 ± 0.0	27.9 ± 0.1	39.0 ± 1.3	26.1 ± 0.1	27.7 ± 0.1	35.3 ± 0.8
#551	27.8 ± 0.1	33.9 ± 0.7	–	27.9 ± 0.1	32.4 ± 0.3	–
#552	27.6 ± 0.1	37.9 ± 2.3	–	27.6 ± 0.0	32.8 ± 0.4	–
#571	49.7 ± 0.1	–	–	47.5 ± 0.3	–	–
#572	51.6 ± 0.2	–	–	51.9 ± 0.4	–	–

ST_{0h} = 52.8 ± 0.3 mN/m. ST: surface tension of the cell–free supernatant (CFS). ST^{-1}: surface tension of the CFS diluted 10 times with demineralized water. ST^{-2}: surface tension of the CFS diluted 100 times with demineralized water. Results correspond to the average ± standard deviation of five ST measurements.

3.3.2.2 Surfactin production by *B. subtilis* #311 in bioreactor

The production of surfactin by *B. subtilis* #311 in bioreactor was conducted in batch mode at 37°C, with an agitation speed of 300 rpm and aeration rates ranging from 0.4 to 0.6 vvm (Figure 3.3). The lowest ST value obtained in bioreactor operating at 0.6 vvm (24.0 ± 0.1 mN/m without dilution and 36.7 ± 0.4 mN/m diluted 100 times) was similar to the one obtained in flasks for the same period of time (48h) (25.9 ± 0. 1 mN/m without dilution and 33.3 ± 0.4 diluted 100 times). However, the ST seemed to stabilize after only 24h of growth, indicating that the microorganism may either be consuming most of the nutrients provided within the first 24h, not leaving enough nutrients for further biosurfactant production; the ST reached the minimum possible value; or other limiting factor is present.

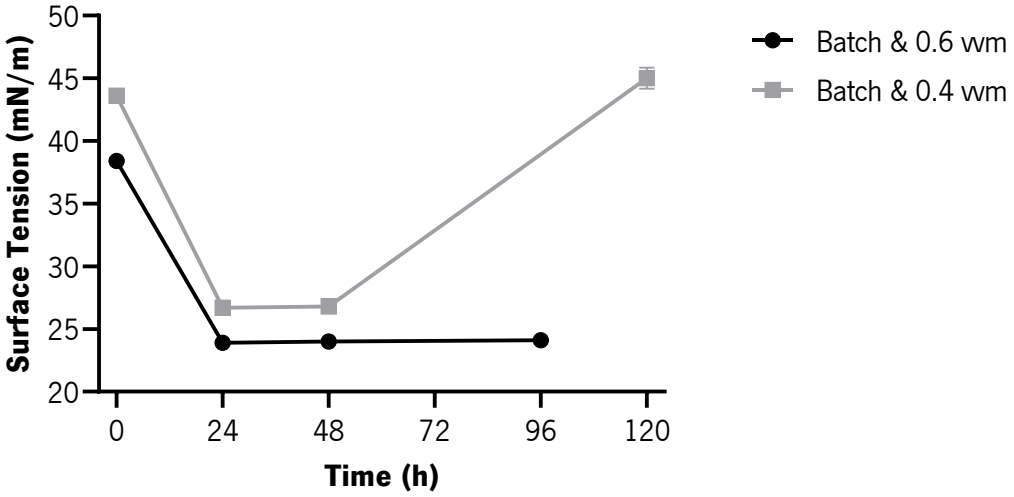

Figure 3.3 – Surface tension values (mN/m) over time of *Bacillus subtilis* #311 grown in batch mode in bioreactor with 10% (v/v) CSL medium.

To evaluate whether a fast nutrient consumption may be limiting surfactin production, two fed–batch assays were performed, where a concentrated culture medium was added to the fermentation vessel after 24h (Figure 3.4). However, the ST values did not reduce any further over the course of these fermentations. Furthermore, after 24h some sugar is still present in the fermentation medium (3.8–4.0 g of reducing sugars/L of the 8.1 g/L provided in the beginning), suggesting that it is not sugar depletion

that led to a decrease in surfactin production in batch mode. In fact, it seems like the nutrients added during fed–batch were used in part for cell growth, since there is a noticeable increase in cell dry weight by the end of the fermentation period (Figure 3.4).

The best results regarding biosurfactant production with the bioreactor operating in fed–batch mode were obtained at 0.6 vvm, with a minimum ST value of 22.6 ± 0.1 mN/m measured in the CFS (Figure 3.4). In this case, 1.1 g/L of surfactin were produced in 48h, which reduced the ST of PBS to 25.5 ± 0.1 mN/m and had a CMC of 21.5 mg/L.

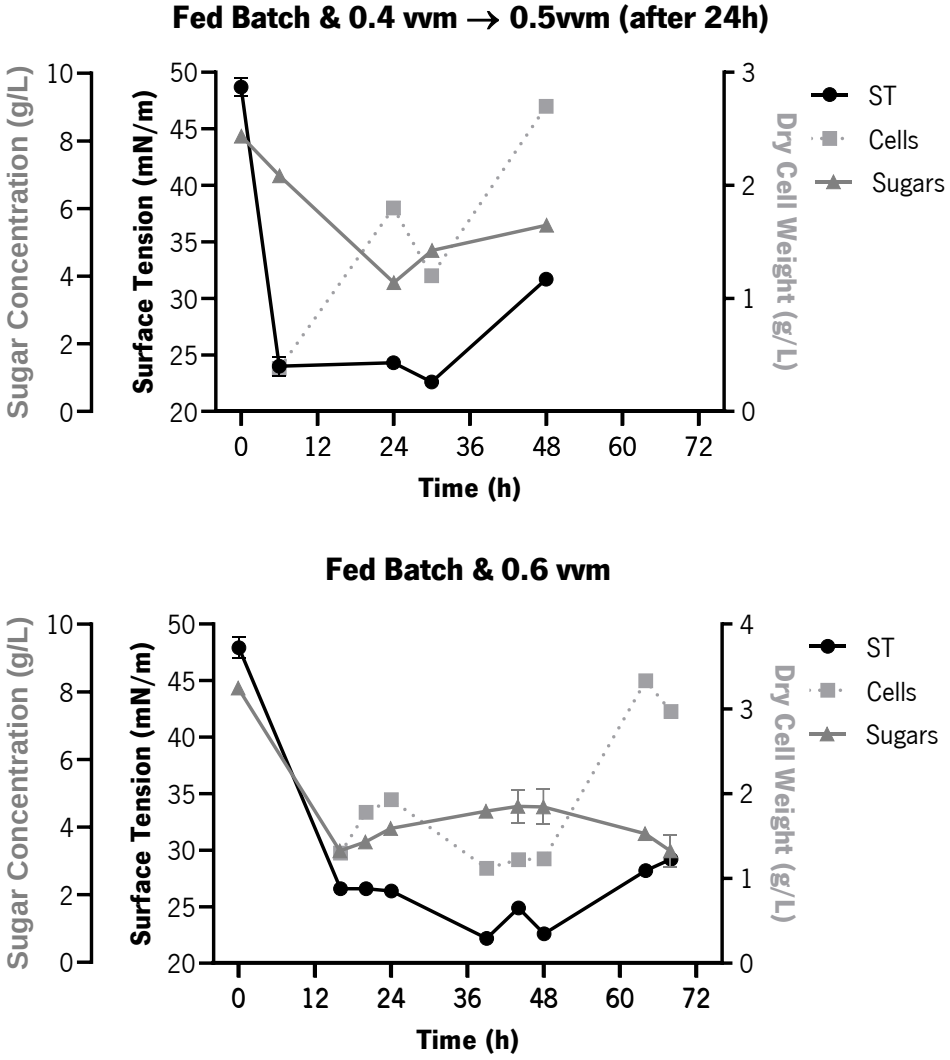

Figure 3.4 – Surface tension values (mN/m), reducing sugars concentration (g/L) and cell dry weight (g/L) over time of *Bacillus subtilis* #311 grown in fed–batch mode in bioreactor with 10% (v/v) CSL medium.

3.4 Discussion

According to the results obtained in the previous chapter (Chapter 2), the best culture media for each microorganism (*A. pullulans* CCY 27–1–94 and *L. mesenteroides* A4) were optimized for biopolymer production using different culture conditions. With *A. pullulans* CCY 27–1–94, the amount of crude biopolymer produced was only 1.5 g/L (Table 3.2), while in the literature it has been reported that this microorganism is able to produce from 12.7 to 25.2 g of biopolymer/L in similar conditions (Elshafie et al., 2017; Prasongsuk et al., 2007). Although in both cases the biopolymer was recovered using ethanol precipitation, in this work, the produced biopolymer was quantified as a freeze–dried precipitate, which might explain the different results obtained. Moreover, the fact that different strains were used may also influence the results.

Additionally, the viscosity of the biopolymer solution obtained here was lower than in previous studies. In this work, the apparent viscosity obtained for a solution containing 20 g biopolymer/L was 1.0 ± 0.3 mPa s (at shear rate of 264 s^{-1}), while in the literature, apparent viscosity values of 15.3 mPa s and 59.9 mPa s (at shear rate of 264 s^{-1}) were obtained for a 10 g/L solution and the CFS, respectively (Prasongsuk et al., 2007), or 2.1 mPa s (measured with a viscometer) for a 5 g/L solution (Cheng et al., 2011). However, the conditions at which the viscosity was measured differ between studies, namely, the temperature used here (40°C) was higher, to simulate the reservoir conditions, which results in a lower viscosity value.

Biopolymer production with *L. mesenteroides* A4 under shaking conditions ranged from 4.3 to 4.9 g/L in the Lm4 medium or 14.9 to 16.8 g/L in the Lm1 medium over 48h of growth (Table 3.2), which is lower than the titers reported in the literature under similar conditions (between 20 and 30 g/L) (Castro–Rodríguez et al., 2019; Han et al., 2014). Viscosity values in these conditions were also lower than what is reported in the literature (8.0–9.4 mPa s for solutions containing 20 g biopolymer/L compared to 10–210 mPa s for 30 g/L solutions, measured at a shear rate of 15 s^{-1} with the Lm4 medium) (Castro–Rodríguez et al., 2019). Again, the temperature at which the viscosity was measured in this work was higher than in the other studies (40°C compared to 25°C), which may influence the values obtained.

Nonetheless, when using the Lm4 medium under static conditions, *L. mesenteroides* A4 yielded a maximum of 21.1 g biopolymer/L, with a viscosity value of 227 ± 2 mPa s for a 40 g/L solution at shear rate 1.4 s^{-1} (Table 3.2). The highest viscosity, however, was achieved in the Lm3 medium. Compared to

other studies that used similar conditions, the strain studied here generated results within the same range (326 ± 8 mPa s obtained here in the Lm3 medium compared to 342 mPa s reported by Siddiqui et al. (2014)). This indicates that *L. mesenteroides* A4 may be better suited for biopolymer production under static conditions. Furthermore, the highest viscosity value obtained in this work is 2.5 times higher than the one measured using a commercial dextran (Sigma–Aldrich) solution (132 ± 1 mPa s), both of them at a concentration of 40 g/L.

On the other hand, biopolymer production by *L. mesenteroides* A4 using low–cost substrates (CSL and sugarcane molasses) did not result in a significant increase (Figure 3.1). To the best of our knowledge, no other studies were performed with *L. mesenteroides* using these substrates for biopolymer production. Nonetheless, this microorganism was previously grown in a tomato juice medium supplemented with sucrose, where it produced more biopolymer with a higher viscosity than in the synthetic medium (Han et al., 2014).

R. viscosum CECT 908 was also evaluated in this work for biopolymer production in bioreactor using a synthetic medium. Optimization was performed by adjusting either the stirring rate and/or the aeration rate, which influence oxygen transfer in the culture medium, and heat distribution, in either a single– or a double–walled stirred bioreactor. Because the culture broth is more viscous than water and the biopolymer produced is sensitive to shear stress, a double–walled system is likely to be more efficient in heat distribution (Garcia–Ochoa & Gomez, 2009; Hewitt & Nienow, 2007), as is shown by the higher viscosities obtained in this system (Figure 3.2).

Additionally, it was observed that, in the double–walled system, constant stirring and aeration rates (250 rpm and 1.7 vvm) generated better results than having them adjusted through the fermentation period (Figure 3.2). This is likely because the cells suffer more shear stress with a higher stirring rate, even though the culture medium became more viscous over time and, consequently, harder to distribute homogenously through the vessel. Furthermore, results show that the maximum viscosities in each case are achieved fairly early, at only 48h of growth, and rapidly start decreasing from that point on. Nonetheless, the apparent viscosity obtained in the best condition in bioreactor was still lower than the one obtained with flasks using the same culture medium (618 ± 6 mPa s in bioreactor compared to 739 ± 30 mPa s in flasks) (Couto et al., 2019).

Surfactin production by *B. subtilis* isolates (#191, #309, #311, #317, #551, #552, #571 and #572) using a low–cost medium containing CSL as sole ingredient was also evaluated in this work (Table 3.3). Strains #191, #571 and #572 were not capable of decreasing the ST of the culture medium,

indicating that, in these conditions, they did not produce surfactin, although they have been reported as biosurfactant producers in a previous work (Gudiña et al., 2012). The other strains all lowered the medium ST to values as low as 25.9 mN/m and the ST^{-2} to 33.3 ± 0.4 mN/m after 48h of growth. In previous studies, *B. subtilis* strains isolated from the same oil reservoir and grown in the same culture medium herein studied, decreased the ST to 30.7 ± 0.4 mN/m (Gudiña, Fernandes, et al., 2015), while in a mineral medium containing glucose as a carbon source, ST was reduced to values between 27.9 and 28.4 mN/m (Pereira et al., 2013). The ST values obtained in those studies when the culture broth was diluted 100 times (ST^{-2}) fell between 42.3 and 59.8 mN/m, which are typical values for this microorganism (Gudiña, Fernandes, et al., 2015; Pereira et al., 2013). Other agro–industrial wastes and by–products, besides CSL, have been studied as alternative substrates for surfactin production by *B. subtilis*, including cassava wastewater (de Andrade et al., 2016), rice mill processing residue (Gurjar & Sengupta, 2015), sugarcane molasses (Verma et al., 2023), date molasses (Al–Bahry et al., 2013), crude glycerol (Janek et al., 2021) and brewery waste (Nazareth et al., 2021).

The production of surfactin by the *B. subtilis* isolate that offered the best results (#311) was further validated in bioreactor (Figure 3.3 and Figure 3.4). Several strategies have been used to produce surfactin in bioreactors, mainly to overcome excessive foam formation or take advantage of it since the biosurfactant is commonly trapped in the foam (Gudiña & Teixeira, 2022). For this purpose, foam fractionation columns or bioreactors that allow foam recovery can be used and have been shown to produce considerable amounts of surfactin, even when using alternative substrates (from 239.7 mg/L to 4.5 g/L) (de Andrade et al., 2016; Nazareth et al., 2021; Santos da Silva et al., 2015). Another problem associated to surfactin production is the product inhibition beyond a certain concentration. To overcome this and sustain a longer–term biosurfactant production, a semicontinuous mode of operation can be used. A recent study has shown that surfactin yield in this mode, using molasses as a sole substrate, increased from 0.58 g biosurfactant/g substrate to 0.97 g/g and was extended up to 21 days when compared to batch mode production, even though the product concentration remained similar (13.9 g/L and 13.7 g/L, respectively) (Verma et al., 2023). The higher production achieved in comparison with the one obtained in the present work (1.1 g/L) could probably be attributed to the partial renewal of the culture broth, but also to the different methodologies used to quantify surfactin concentration, besides the different *B. subtilis* strains used.

Overall, biopolymer production by *L. mesenteroides* A4 was improved by altering its growth conditions. The best results were achieved in only 24h of growth and under static conditions. Even though

high concentrations of biopolymer were needed to obtain high viscosities, this microorganism still poses an interesting alternative for application in MEOR. Regarding the scale–up process of biopolymer production by *R. viscosum* CECT 908, some of the conditions tested showed promising results that were achieved in a short time. For *B. subtilis* #311, a fed–batch process was developed to produce surfactin in a bioreactor. However, more work will be necessary to fully optimize these processes.

3.5 References

Al–Bahry, S. N., Al–Wahaibi, Y. M., Elshafie, A. E., Al–Bemani, A. S., Joshi, S. J., Al–Makhmari, H. S., & Al–Sulaimani, H. S. (2013). Biosurfactant production by Bacillus subtilis B20 using date molasses and its possible application in enhanced oil recovery. *International Biodeterioration and Biodegradation*, *81*, 141–146. https://doi.org/10.1016/j.ibiod.2012.01.006

Castro–Rodríguez, D., Hernández–Sánchez, H., & Yáñez–Fernández, J. (2019). Structural characterization and rheological properties of dextran produced by native strains isolated of Agave salmiana. *Food Hydrocolloids*, *90*, 1–8. https://doi.org/10.1016/j.foodhyd.2018.11.052

Chaprão, M. J., da Silva, R. de C. F. S., Rufino, R. D., Luna, J. M., Santos, V. A., & Sarubbo, L. A. (2018). Production of a biosurfactant from Bacillus methylotrophicus UCP1616 for use in the bioremediation of oil–contaminated environments. *Ecotoxicology*, *27*(10), 1310–1322. https://doi.org/10.1007/s10646–018–1982–9

Cheng, K. C., Demirci, A., & Catchmark, J. M. (2011). Evaluation of medium composition and fermentation parameters on pullulan production by Aureobasidium pullulans. *Food Science and Technology International*, *17*(2), 99–109. https://doi.org/10.1177/1082013210368719

Couto, M. R., Gudiña, E. J., Ferreira, D., Teixeira, J. A., & Rodrigues, L. R. (2019). The biopolymer produced by Rhizobium viscosum CECT 908 is a promising agent for application in microbial enhanced oil recovery. *New Biotechnology*, *49*, 144–150. https://doi.org/10.1016/j.nbt.2018.11.002

de Andrade, C. J., Barros, F. F. C., de Andrade, L. M., Rocco, S. A., Luis Sforça, M., Pastore, G. M., & Jauregi, P. (2016). Ultrafiltration based purification strategies for surfactin produced by Bacillus subtilis LB5A using cassava wastewater as substrate. *Journal of Chemical Technology and Biotechnology*, *91*(12), 3018–3027. https://doi.org/10.1002/jctb.4928

Elshafie, A., Joshi, S. J., Al–Wahaibi, Y. M., Al–Bahry, S. N., Al–Bemani, A. S., Al–Hashmi, A., & Al–Mandhari, M. S. (2017, April 4). Isolation and Characterization of Biopolymer Producing Omani Aureobasidium Pullulans Strains and Its Potential Applications in Microbial Enhanced Oil Recovery. *SPE Oil and Gas India Conference and Exhibition*. https://doi.org/10.2118/185326–ms

Fan, Y., Wang, J., Gao, C., Zhang, Y., & Du, W. (2020). A novel exopolysaccharide–producing and long–chain n–alkane degrading bacterium Bacillus licheniformis strain DM–1 with potential application for in–situ enhanced oil recovery. *Scientific Reports*, *10*(1), 8519. https://doi.org/10.1038/s41598–020–65432–z

Garcia–Ochoa, F., & Gomez, E. (2009). Bioreactor scale–up and oxygen transfer rate in microbial processes: An overview. In *Biotechnology Advances* (Vol. 27, Issue 2, pp. 153–176). Elsevier. https://doi.org/10.1016/j.biotechadv.2008.10.006

Gudiña, E. J., Couto, M. R., Silva, S. P., Coelho, E., Coimbra, M. A., Teixeira, J. A., & Rodrigues, L. R. (2023). Sustainable Exopolysaccharide Production by Rhizobium viscosum CECT908 Using Corn Steep Liquor and Sugarcane Molasses as Sole Substrates. *Polymers*, *15*(1), 20. https://doi.org/10.3390/polym15010020

Gudiña, E. J., Fernandes, E. C., Rodrigues, A. I., Teixeira, J. A., & Rodrigues, L. R. (2015). Biosurfactant production by Bacillus subtilis using corn steep liquor as culture medium. *Frontiers in Microbiology*, *6*(FEB). https://doi.org/10.3389/fmicb.2015.00059

Gudiña, E. J., Pereira, J. F. B., Rodrigues, L. R., Coutinho, J. A. P., & Teixeira, J. A. (2012). Isolation and study of microorganisms from oil samples for application in Microbial Enhanced Oil Recovery. *International Biodeterioration and Biodegradation*, *68*, 56–64. https://doi.org/10.1016/j.ibiod.2012.01.001

Gudiña, E. J., Rodrigues, A. I., Alves, E., Domingues, M. R., Teixeira, J. A., & Rodrigues, L. R. (2015). Bioconversion of agro–industrial by–products in rhamnolipids toward applications in enhanced oil recovery and bioremediation. *Bioresource Technology*, *177*, 87–93. https://doi.org/10.1016/j.biortech.2014.11.069

Gudiña, E. J., Rodrigues, A. I., de Freitas, V., Azevedo, Z., Teixeira, J. A., & Rodrigues, L. R. (2016). Valorization of agro–industrial wastes towards the production of rhamnolipids. *Bioresource Technology*, *212*, 144–150. https://doi.org/10.1016/j.biortech.2016.04.027

Gudiña, E. J., & Teixeira, J. A. (2022). Bacillus licheniformis: The unexplored alternative for the anaerobic production of lipopeptide biosurfactants? In *Biotechnology Advances* (Vol. 60, p. 108013). Elsevier. https://doi.org/10.1016/j.biotechadv.2022.108013

Gurjar, J., & Sengupta, B. (2015). Production of surfactin from rice mill polishing residue by submerged fermentation using Bacillus subtilis MTCC 2423. *Bioresource Technology*, *189*, 243–249. https://doi.org/10.1016/j.biortech.2015.04.013

Han, J., Hang, F., Guo, B., Liu, Z., You, C., & Wu, Z. (2014). Dextran synthesized by Leuconostoc mesenteroides BD1710 in tomato juice supplemented with sucrose. *Carbohydrate Polymers*, *112*, 556–562. https://doi.org/10.1016/j.carbpol.2014.06.035

Hewitt, C. J., & Nienow, A. W. (2007). The Scale–Up of Microbial Batch and Fed–Batch Fermentation Processes. In *Advances in Applied Microbiology* (Vol. 62, pp. 105–135). Academic Press. https://doi.org/10.1016/S0065–2164(07)62005–X

Hofer, A., Hauer, S., Kroll, P., Fricke, J., & Herwig, C. (2018). In–depth characterization of the raw material corn steep liquor and its bioavailability in bioprocesses of Penicillium chrysogenum. *Process Biochemistry*, *70*, 20–28. https://doi.org/10.1016/j.procbio.2018.04.008

Janek, T., Gudiña, E. J., Połomska, X., Biniarz, P., Jama, D., Rodrigues, L. R., Rymowicz, W., & Lazar, Z. (2021). Sustainable surfactin production by bacillus subtilis using crude glycerol from different wastes. *Molecules*, *26*(12), 3488. https://doi.org/10.3390/molecules26123488

Jha, S. S., Joshi, S. J., & Geetha, S. J. (2016). Lipopeptide production by Bacillus subtilis R1 and its possible applications. *Brazilian Journal of Microbiology*, *47*(4), 955–964. https://doi.org/10.1016/j.bjm.2016.07.006

Lee, N. R., Lee, S. M., Cho, K. S., Jeong, S. Y., Hwang, D. Y., Kim, D. S., Hong, C. O., & Son, H. J. (2014). Improved production of poly–γ–glutamic acid by Bacillus subtilis D7 isolated from Doenjang, a Korean traditional fermented food, and its antioxidant activity. *Applied Biochemistry and Biotechnology*, *173*(4), 918–932. https://doi.org/10.1007/s12010–014–0908–0

Marques, M. P. C., Cabral, J. M. S., & Fernandes, P. (2010). Bioprocess scale–up: Quest for the

parameters to be used as criterion to move from microreactors to lab–scale. In *Journal of Chemical Technology and Biotechnology* (Vol. 85, Issue 9, pp. 1184–1198). John Wiley & Sons, Ltd. https://doi.org/10.1002/jctb.2387

Miller, G. L. (1959). Use of Dinitrosalicylic Acid Reagent for Determination of Reducing Sugar. *Analytical Chemistry*, *31*(3), 426–428. https://doi.org/10.1021/ac60147a030

Mohanty, S. S., Koul, Y., Varjani, S., Pandey, A., Ngo, H. H., Chang, J. S., Wong, J. W. C., & Bui, X. T. (2021). A critical review on various feedstocks as sustainable substrates for biosurfactants production: a way towards cleaner production. In *Microbial Cell Factories* (Vol. 20, Issue 1, pp. 1–13). BioMed Central. https://doi.org/10.1186/s12934–021–01613–3

Nazareth, T. C., Zanutto, C. P., Maass, D., Ulson De Souza, A. A., & Ulson De Souza, S. M. D. A. G. (2021). Impact of oxygen supply on surfactin biosynthesis using brewery waste as substrate. *Journal of Environmental Chemical Engineering*, *9*(4), 105372. https://doi.org/10.1016/j.jece.2021.105372

Novak, J. S., Tanenbaum, S. W., & Nakas, J. P. (1992). Heteropolysaccharide formation by Arthrobacter viscosus grown on xylose and xylose oligosaccharides. *Applied and Environmental Microbiology*, *58*(11), 3501–3507.

Pereira, J. F. B., Gudiña, E. J., Costa, R., Vitorino, R., Teixeira, J. A., Coutinho, J. A. P., & Rodrigues, L. R. (2013). Optimization and characterization of biosurfactant production by Bacillus subtilis isolates towards microbial enhanced oil recovery applications. *Fuel*, *111*, 259–268. https://doi.org/10.1016/j.fuel.2013.04.040

Prasongsuk, S., Berhow, M. A., Dunlap, C. A., Weisleder, D., Leathers, T. D., Eveleigh, D. E., & Punnapayak, H. (2007). Pullulan production by tropical isolates of Aureobasidium pullulans. *Journal of Industrial Microbiology and Biotechnology*, *34*(1), 55–61. https://doi.org/10.1007/s10295–006–0163–7

Santos da Silva, M. T., Soares, C. M. F., Lima, A. S., & Santana, C. C. (2015). Integral production and concentration of surfactin from Bacillus sp. ITP–001 by semi–batch foam fractionation. *Biochemical Engineering Journal*, *104*, 91–97. https://doi.org/10.1016/j.bej.2015.04.010

Schmidt, F. R. (2005). Optimization and scale up of industrial fermentation processes. In *Applied Microbiology and Biotechnology* (Vol. 68, Issue 4, pp. 425–435). Springer Verlag. https://doi.org/10.1007/s00253–005–0003–0

Segovia, V., Reyes, A., Rivera, G., Vázquez, P., Velazquez, G., Paz–González, A., & Hernández–Gama, R. (2021). Production of rhamnolipids by the Thermoanaerobacter sp. CM–CNRG TB177 strain isolated from an oil well in Mexico. *Applied Microbiology and Biotechnology*, *105*(14–15), 5833–5844. https://doi.org/10.1007/s00253–021–11468–8

Sharma, N., Prasad, G. S., & Choudhury, A. R. (2013). Utilization of corn steep liquor for biosynthesis of pullulan, an important exopolysaccharide. *Carbohydrate Polymers*, *93*(1), 95–101. https://doi.org/10.1016/j.carbpol.2012.06.059

Siddiqui, N. N., Aman, A., Silipo, A., Qader, S. A. U., & Molinaro, A. (2014). Structural analysis and characterization of dextran produced by wild and mutant strains of Leuconostoc mesenteroides. *Carbohydrate Polymers*, *99*, 331–338. https://doi.org/10.1016/j.carbpol.2013.08.004

Soares da Silva, R. de C. F., Almeida, D. G., Meira, H. M., Silva, E. J., Farias, C. B. B., Rufino, R. D., Luna, J. M., & Sarubbo, L. A. (2017). Production and characterization of a new biosurfactant from Pseudomonas cepacia grown in low–cost fermentative medium and its application in the oil industry. *Biocatalysis and Agricultural Biotechnology*, *12*, 206–215.

https://doi.org/10.1016/j.bcab.2017.09.004

Soares da Silva, R. de C. F., Luna, J. M., Rufino, R. D., & Sarubbo, L. A. (2021). Ecotoxicity of the formulated biosurfactant from Pseudomonas cepacia CCT 6659 and application in the bioremediation of terrestrial and aquatic environments impacted by oil spills. *Process Safety and Environmental Protection*, *154*, 338–347. https://doi.org/10.1016/j.psep.2021.08.038

Sun, S., Luo, Y., Cao, S., Li, W., Zhang, Z., Jiang, L., Dong, H., Yu, L., & Wu, W. M. (2013). Construction and evaluation of an exopolysaccharide–producing engineered bacterial strain by protoplast fusion for microbial enhanced oil recovery. *Bioresource Technology*, *144*, 44–49. https://doi.org/10.1016/j.biortech.2013.06.098

Sun, S., Zhang, Z., Luo, Y., Zhong, W., Xiao, M., Yi, W., Yu, L., & Fu, P. (2011). Exopolysaccharide production by a genetically engineered Enterobacter cloacae strain for microbial enhanced oil recovery. *Bioresource Technology*, *102*(10), 6153–6158. https://doi.org/10.1016/j.biortech.2011.03.005

Verma, R., Sharma, S., Kundu, L. M., Maiti, S. K., & Pandey, L. M. (2023). Enhanced production of biosurfactant by Bacillus subtilis RSL2 in semicontinuous bioreactor utilizing molasses as a sole substrate. *Journal of Biotechnology*, *362*, 24–35. https://doi.org/10.1016/j.jbiotec.2022.12.007

Xia, W., Dong, X., Zhang, Y., & Ma, T. (2018). Biopolymer from marine Athelia and its application on heavy oil recovery in heterogeneous reservoir. *Carbohydrate Polymers*, *195*, 53–62. https://doi.org/10.1016/j.carbpol.2018.04.061

Xu, Y., & Lu, M. (2011). Microbially enhanced oil recovery at simulated reservoir conditions by use of engineered bacteria. *Journal of Petroleum Science and Engineering*, *78*(2), 233–238. https://doi.org/10.1016/j.petrol.2011.06.005

CHAPTER 4.

Application of biomolecules for Microbial Enhanced Oil Recovery

Abstract

Biopolymer flooding is a promising strategy in Microbial Enhanced Oil Recovery (MEOR) applications, where different types of biopolymers can be explored for their viscosifying potential. In this work, three types of biopolymers (commercial xanthan gum and the biopolymers produced by *Rhizobium viscosum* CECT 908 and *Leuconostoc mesenteroides* A4) were evaluated for their potential application in MEOR regarding their rheological properties and oil recovery efficiency in sand–pack column assays. They all displayed the ability to increase water viscosity, having a shear–thinning or pseudoplastic behavior that is desirable in MEOR. Furthermore, the biopolymer from *R. viscosum* CECT 908 demonstrated remarkable viscoelastic properties, exhibiting a weak gel conformation. Besides, this biopolymer was able to withstand high temperatures and salinities, being able to maintain up to 55% of its viscosity when submitted to harsh conditions.

Sand–pack column assays confirmed the ability of these biopolymers to recover two different oils efficiently. With the lighter oil obtained from the Potiguar oilfield, recovery rates increased by 8.4%, 12.2% and 5.4% when commercial xanthan gum and the biopolymers produced by *R. viscosum* CECT 908 and *L. mesenteroides* A4, respectively, were used. Using a heavier oil, recovery rates reached up to 25.8% and 21.5% with the biopolymers produced by *R. viscosum* CECT 908 and *L. mesenteroides* A4, respectively. Furthermore, the combination of biopolymers and rhamnolipids in oil recovery showed that there may be a positive synergistic effect between the two biomolecules that should be further explored. Overall, the biomolecules studied here proved to be interesting candidates for application in MEOR.

4.1 Introduction

For several years, biosurfactants and biopolymers have been used in the oil industry as agents for Microbial Enhanced Oil Recovery (MEOR) applications. Biosurfactants improve oil recovery by reducing the capillary forces, and thus reducing the interfacial tension (IFT) of the rock–oil–water interfaces, shifting the rock wettability towards a more water wet state (Negin et al., 2017), besides emulsifying the oil that is trapped in the reservoir pores (Dong et al., 2022; Hoseini–Moghadam et al., 2021; Onaizi et al., 2021). Among the biosurfactants tested for MEOR applications, rhamnolipids (RLs) have been widely studied. More specifically, the RLs from *Pseudomonas aeruginosa* have shown some interesting results in retrieving light crude oils, being able to form stable emulsions (Onaizi et al., 2021) as well as reduce the IFT (Khademolhosseini et al., 2019).

Conversely, biopolymers can increase the viscosity of the displacing fluid, creating a more uniform displacement front and thus improving sweep efficiency (Rellegadla et al., 2017). Furthermore, biopolymers can contribute to oil recovery by selective plugging of high permeability zones. Dextran, for example, which is produced by *Leuconostoc mesenteroides* among other microorganisms, can be used as a selective plugging agent (Lee et al., 2020), while pullulan, produced by *Aureobasidium pullulans* has shown better effects in increasing water viscosity (Elshafie et al., 2017). The biopolymer produced by *Rhizobium viscosum* CECT 908, recently studied in our laboratory, has also shown positive results in oil recovery applications. This biopolymer can recover up to 14 – 26% of additional oil in sand–pack column assays while increasing the viscosity of the culture broth up to 10500 mPa s (Couto et al., 2019; Gudiña et al., 2023).

To predict the effectiveness of a certain biopolymer in MEOR, it is essential to evaluate its rheological properties. Biopolymers usually exhibit a shear thinning behavior, decreasing their viscosity with increasing shear rate due to a structural rearrangement of the molecules in the direction of the flow (Ianniruberto, 2015; Lapasin & Pricl, 1999). The viscoelasticity of biopolymer solutions also affects their ability to recover oil. In rheology, it is considered that most materials exhibit a combination of rheological behaviors that can be accommodated between the ideal Newtonian liquid (viscous) and Hookean solid (elastic). When stress is applied over time, viscous liquids deform at a constant rate and maintain the deformed state when the external force is removed. In contrast, elastic solids are instantly deformed with stress and regain their initial configuration without it (Papanicolaou & Zaoutsos, 2010). Most biopolymers exhibit a viscoelastic behavior, being able to regain part of their original molecular configuration when shear stress stops being applied, thus recovering their viscosity (Papanicolaou & Zaoutsos, 2010; Roeder,

2013). These properties are useful in oil recovery since the higher flow rates at the well–bore region cause the viscosity of the biopolymer to decrease, improving fluid injection. In contrast, the lower shear rate inside the well increases the biopolymer viscosity, thus improving sweep efficiency (Gudiña, Teixeira, et al., 2015). Furthermore, the prevalence of elastic over viscous behavior is usually favored in biopolymer flooding. Biopolymer solutions with a higher elasticity create a more stable flow front inside the reservoir pores, which can more effectively displace the residual oil (Veerabhadrappa et al., 2013).

Additionally, biosurfactants and biopolymers can be used simultaneously in MEOR. For example, several works studied the compatibility of (bio)surfactants and (bio)polymers and concluded that neither affected the properties of the other; hence, the (bio)surfactants did not cause reduction of the solution viscosity, and the (bio)polymers did not interfere with the surface tension (ST) and/or IFT reduction capacity of the (bio)surfactants (Ge et al., 2021; Qi et al., 2018). Furthermore, it was found that the oil recovery rates increased when using the binary systems, in comparison with the individual treatments. This work evaluated the combination of the RLs from *P. aeruginosa* PX112 and biopolymers from *R. viscosum* CECT 908 or commercial xanthan gum for MEOR applications. The ability of the biopolymers from *L. mesenteroides* A4 to recover oil was also evaluated.

As discussed in previous chapters (Chapter 1 and Chapter 2), these biomolecules have several advantages over their chemical counterparts, including their biodegradability and stability under reservoir conditions. Thus, studying the stability of these biomolecules in such conditions becomes essential. In this work, stability studies under different temperature and salinity conditions were also performed with the biopolymer from *R. viscosum* CECT 908.

This work aimed to determine the applicability of several biomolecules in MEOR by studying their rheological properties and oil recovery ability using different oils and treatment approaches.

4.2 Materials and methods

4.2.1 Rhamnolipid production

P. aeruginosa PX112 was used for RL production. The strain was maintained in Luria Bertani (LB) medium, supplemented with 20% (v/v) of glycerol at –80°C. Pre–cultures were prepared by inoculating 20 mL of a low–cost medium (CSLM: 10% (v/v) corn steep liquor (CSL) and 10% (w/v) sugarcane molasses; pH 7.0) with 100 µL from a frozen stock and were incubated overnight, at 37°C

and 200 rpm. RL production was performed in 500 mL flasks with 250 mL of the same medium, which were inoculated with 1% (v/v) of the pre–culture and incubated at 37°C and 200 rpm for 144h.

The RLs produced were recovered through adsorption chromatography using the polystyrene resin Amberlite® XAD®–2 (Sigma–Aldrich), as described in (Gudiña & Rodrigues, 2019). In brief, a 125 mL glass column was filled with Amberlite XAD–2 and equilibrated with two volumes of 0.1 M potassium phosphate buffer (pH 6.1). Subsequently, 150 mL of cell–free supernatant (CFS) (centrifuged at 15316 x *g* for 20 min) were diluted with one volume of demineralized water, adjusted to pH 6.1 and introduced into the column. The column was washed with two volumes of demineralized water to remove the non–adsorbed compounds, followed by 300 mL of methanol to elute the RLs. After evaporation of the solvent, the recovered RLs were dissolved in a minimum amount of demineralized water and freeze–dried. The products obtained were weighed and stored at –20°C.

4.2.2 Biopolymer production

R. viscosum CECT 908 was used for biopolymer production. The strain was maintained in a synthetic medium (Rv1: 25 g/L glucose, 3 g/L yeast extract, 2 g/L K_2HPO_4 and 0.1 g/L $MgSO_4 \cdot 7H_2O$; pH 7.0) supplemented with 15% (v/v) of glycerol, at –80°C. Pre–cultures were prepared by inoculating 20 mL of Rv1 medium with 100 µL from a frozen stock and were incubated at 30°C and 150 rpm over 48h. Biopolymer production was performed in 500 mL flasks containing 200 mL of a low–cost medium (Rv2: 60 g/L sugarcane molasses and 1% (v/v) CSL; pH 7.0 (Gudiña et al., 2023)), which were inoculated with 1% (v/v) of the pre–culture and incubated at 30°C and 150 rpm for 72h. The biopolymer was then precipitated from the CFS using hexadecyl–trimethylammonium bromide (CTAB) and purified, as described by Novak et al. (1992). The purified biopolymer was freeze–dried and stored at –20°C.

Biopolymer production by *L. mesenteroides* A4 was performed in 250 mL flasks with 100 mL of culture medium (Lm3 or Lm4: 100 g/L or 200 g/L sucrose, 10 g/L peptone, 5 g/L yeast extract, 5 g/L meat extract, 2 g/L K_2HPO_4, 2 g/L diammonium citrate, 5 g/L sodium acetate, 0.1 g/L $MgSO_4 \cdot 7H_2O$ and 0.05 g/L $MnSO_4 \cdot H_2O$; pH 7.0). The strain was maintained in MRS medium, supplemented with 20% (v/v) of glycerol at –80°C. Pre–cultures were prepared by inoculating 20 mL of medium with 100 µL from a frozen stock and were incubated overnight at 30°C and 150 rpm. Each flask was inoculated with 1% (v/v) of a pre–culture and incubated at 30°C and under static conditions for 24h. After centrifuging the cultures, the biopolymer was precipitated by adding two volumes of ethanol (99%, v/v) to the CFS and incubating the mixture at –20°C for 24h. Afterwards, the samples were centrifuged (9400

x *g*, 20 min, 4°C), the pellet containing the biopolymer was resuspended in a minimum amount of demineralized water, freeze–dried and stored at –20°C.

4.2.3 Rheological properties and stability

The rheological properties of the biopolymer solutions (either the biopolymer from *L. mesenteroides* A4, the biopolymer from *R. viscosum* CECT 908 or commercial xanthan gum (Sigma Aldrich)) were determined using a hybrid rheometer (Discovery HR1, TA Instruments, USA) with a cone–plate geometry (diameter 60 mm; angle 2.006°; gap 0.064 mm).

Steady flow properties of the biopolymers were measured under rate control mode at shear rates from 10^{-4} to 10^{3} s^{-1}. Dynamic viscoelastic properties were measured in two steps: first, an oscillatory strain sweep (from 0.02 to 100%) was performed at a constant frequency (1 Hz) to determine the deformation of the biopolymer in the linear viscoelastic range; then, oscillatory frequency sweeps (from 0.01 to 10 Hz) were performed at a constant strain within the linear viscoelastic range. These studies were carried out at 25°C.

Apparent viscosity measurements were performed at 40°C at different shear rates (0.1 – 300 s^{-1}) through three successive flow ramps (0.1 ⟶ 300 s^{-1}; 300 ⟶ 0.1 s^{-1}; 0.1 ⟶ 300 s^{-1}), as described in Chapter 2 (2.2.3). The values presented correspond to a shear rate of 1.4 s^{-1}.

To study the stability of the *R. viscosum* CECT 908 biopolymer when subjected to different temperatures, the apparent viscosity of a biopolymer solution (2.7 g/L) was measured at temperatures ranging from 20 to 80°C. The effect of salinity on the apparent viscosity of the biopolymer solution was evaluated by adding NaCl at different concentrations (10 – 150 g/L); in this case, the samples were allowed to stabilize for 24h before measuring their apparent viscosity as described above.

4.2.4 Surface tension measurement

ST of RL and biopolymer solutions was measured as described in Chapter 3 (3.2.6.4).

4.2.5 Oil recovery assays using sand–pack columns

The performance of xanthan gum, *L. mesenteroides* A4 biopolymer and *R. viscosum* CECT 908 biopolymer, with or without RLs, in oil recovery was studied using sand–pack columns, as described by

Gudiña et al. (2013). The assays were performed using crude oil from the Potiguar oilfield in Brazil (apparent viscosity at 40°C ($\eta_{40°C}$) of 110 mPa s at 1.4 s^{-1}) or a heavy crude oil mixture ($\eta_{40°C}$ = 247 mPa s at 1.4 s^{-1}) that was obtained by mixing different proportions of Mukhaizna and CLB crude oils. The oils were provided by PARTEX oil and gas, and their apparent viscosities were measured using a hybrid rheometer (DiscoveryhR1, TA Instruments, USA) equipped with a cone plate geometry (diameter 60 mm; angle 2.006°; gap 0.064 mm) at 40°C.

To perform these assays, vertically oriented acrylic columns with a volume of 280 mL were used at 40°C and a constant flow rate of 2 mL/min. The columns, provided with a sieve and cap fixed at the bottom, were tightly packed with dry sand (previously sifted with a 0.45 mm sieve). After packing the sand, top sieves and caps (with holes for the insertion of inlet and outlet tubes), provided with rubber 'O' rings to hermetically seal the columns, were fixed.

The columns were first flooded with demineralized water. The pore volume (PV in mL) was determined by measuring the volume of water required to saturate each column and the porosity (%) was calculated by dividing the PV by the total volume of the column. Crude oil was injected into the columns, and the original oil in place (OOIP in mL) was calculated as the volume of oil retained by the columns. The initial oil saturation (S_{oi}, %) was calculated as follows:

$$S_{oi} = \frac{OOIP}{PV} \times 100 \quad (5.1)$$

Subsequently, the columns were incubated at 40°C for 24h and then flooded again with demineralized water to remove the excess oil; this step continued until oil was no longer observed in the effluent. The amount of oil recovered (oil recovered after water flooding (S_{orwf} in mL) was determined volumetrically, and the residual oil saturation (S_{or}, %) was calculated as follows:

$$S_{or} = \frac{OOIP - S_{orwf}}{OOIP} \times 100 \quad (5.2)$$

Subsequently, 100 or 200 mL of different biomolecule solutions (crude biopolymer or CFS from *L. mesenteroides* A4, xanthan gum, and purified biopolymer or culture broth from *R. viscosum* CECT 908, with or without RLs from *P. aeruginosa* PX112) prepared in demineralized water were injected into the columns, followed by the injection of demineralized water to make up 400 mL of injected fluid.

Alternatively, 1 PV of commercial RLs (RL–90, Sigma Aldrich) or the CFS from *P. aeruginosa* PX112 were injected into the columns and incubated for 48h. Next, 200 mL of a xanthan gum solution

($\eta_{40°C}$ = 99 ± 6 mPa s at 1.4 s^{-1}; prepared at 1 g/L) were injected into the columns, followed by 200 mL of demineralized water.

Control assays were performed under the same conditions by injecting 400 mL of demineralized water into the columns. The volume of oil recovered (oil recovered after biomolecule flooding (S_{orbf}, mL)) was measured, and the additional oil recovery (AOR, %) was calculated as follows:

$$AOR = \frac{S_{orbf}}{OOIP - S_{orwf}} \times 100 \quad (5.3)$$

4.3 Results

4.3.1 Rheological properties of the biopolymers

R. viscosum CECT 908 produced 3.7 g/L of biopolymer when grown in a low–cost medium (Rv2), achieving an apparent viscosity of 3833 ± 100 mPa s in the CFS (measured at 40°C and a shear rate of 1.4 s^{-1}). *L. mesenteroides* A4 produced 12.9 ± 1.7 or 21.1 ± 0.2 g/L of biopolymer when grown in the synthetic media Lm3 or Lm4, respectively (Chapter 3).

The flow properties of solutions prepared with those biopolymers and commercial xanthan gum at different concentrations under shear were characterized at 25°C (Figure 4.1). The three biopolymers are characterized by a non–Newtonian flow and a shear–thinning behavior. Accordingly, the shear stress of the solutions increases with increasing shear rate while the apparent viscosity decreases. Nonetheless, some of the concentrations tested display a characteristic Newtonian plateau at low shear rates, as observed by the constant viscosity and linear shear stress obtained in the shear rate range between 10^{-3} to around 10^{-1} s^{-1} (Figure 4.1). Furthermore, all the biopolymer solutions exhibit an initial yield stress, showing no deformation up to a certain level of strain stress, after which they start to flow. This value is depicted as the first shear stress point obtained in the steady flow curves and is higher at higher biopolymer concentrations (Figure 4.1 – Top). As expected, the viscosity of the biopolymer solutions also displays a strong correlation with concentration, with higher viscosities being obtained with the more concentrated solutions (Figure 4.1 – Bottom).

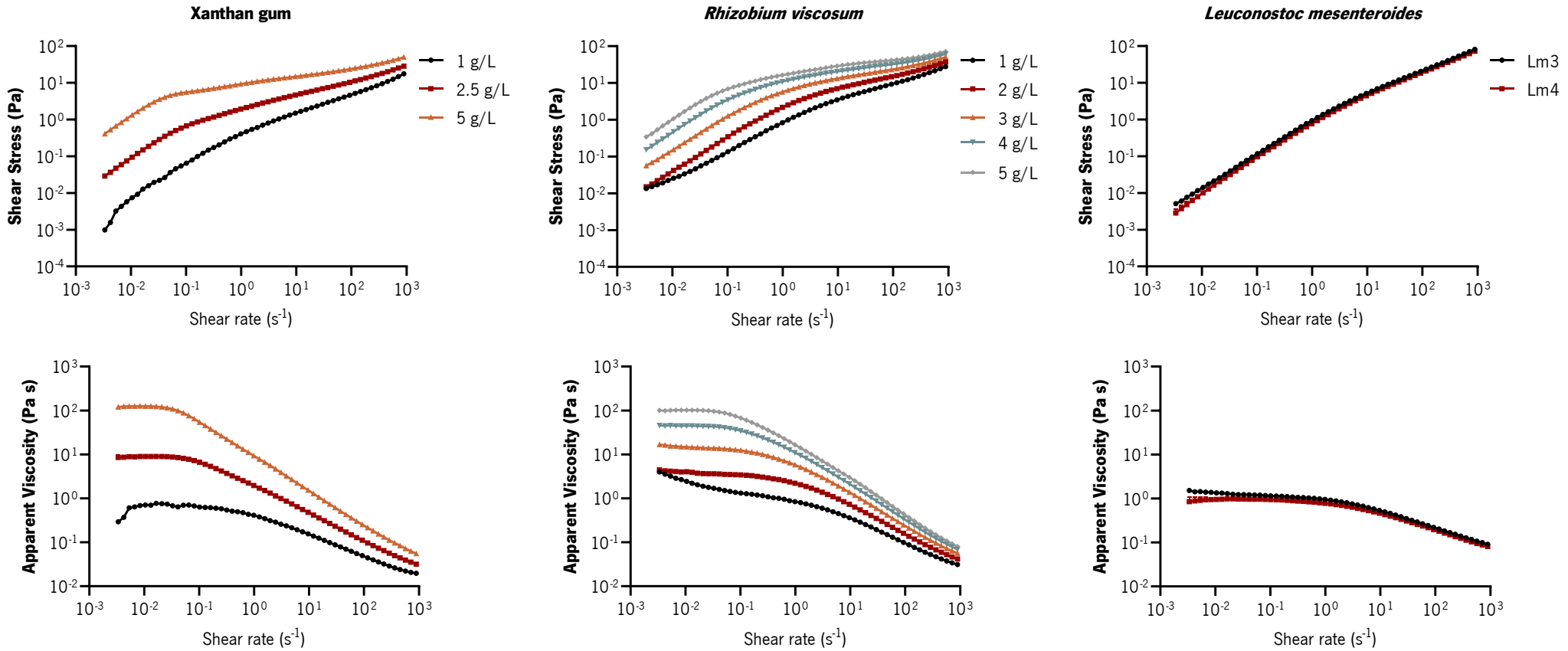

Figure 4.1 – Steady flow curves for the solutions of biopolymer produced by *Rhizobium viscosum* CECT 908 in Rv2 medium (1 – 5 g/L), *Leuconostoc mesenteroides* A4 in Lm3 or Lm4 media (60 g/L) and commercial xanthan gum (1 – 5 g/L). Top: shear stress (Pa) as a function of shear rate (s^{-1}). Bottom: apparent viscosity (Pa) as a function of shear rate (s^{-1}).

The dynamic viscoelastic moduli of the biopolymer solutions are displayed in Figure 4.2, where the storage (or elastic) modulus (G') represents the elastic properties of the biomolecules in solution, and the loss (or viscous) modulus (G'') represents the viscous properties (Lapasin & Pricl, 1999). In the oscillatory strain sweep, for both xanthan gum and the biopolymer from *R. viscosum* CECT 908, the elastic component occurs in solution in a higher proportion than the viscous component over the entire strain range. The opposite happens with the biopolymer from *L. mesenteroides* A4, where the viscous component is more prevalent (Figure 4.2). At high strain values, G' starts decreasing in all solutions. However, for *L. mesenteroides* A4 biopolymer, that inflection point occurs sooner, indicating that it cannot withstand the same degree of strain as the other biopolymers. Furthermore, at higher concentrations, the viscoelastic moduli of xanthan gum and *R. viscosum* CECT 908 biopolymer solutions are also higher, indicating a more prominent viscoelasticity (Figure 4.2).

In the frequency sweep test, similar patterns are observed between the viscoelastic moduli of the biopolymer solutions (Figure 4.2): the elastic component is generally dominating in xanthan gum and *R. viscosum* CECT 908 biopolymer solutions, indicating that gel–like structures might be formed in solution; while the viscous component is the dominating factor in *L. mesenteroides* A4 biopolymer solutions over the entire frequency range, implying that their behavior is more similar to a viscous fluid.

Regarding the biopolymer from *L. mesenteroides* A4, no differences were observed in the viscoelastic properties between the two production media tested. This suggests that a biopolymer with similar rheological properties might be produced in both. For xanthan gum and *R. viscosum* CECT 908 biopolymer solutions, there was a crossover (in the frequency sweep tests) between G' and G'', which happens sooner at higher concentrations. This indicates that as the concentration of biopolymer increased, the more likely it was for them to form gel–like entangled networks in solution (Figure 4.2) (Liang et al., 2019).

4.3.1.1 Stability of the biopolymer produced by *Rhizobium viscosum* CECT 908 using a low–cost medium

To determine the temperature and salinity range at which the biopolymer from *R. viscosum* CECT 908 remains stable, the viscosity of the biopolymer in aqueous solution was measured at different temperatures ranging from 20 to 80°C (Figure 4.3) and with different concentrations of NaCl (10, 50, 100 and 150 g/L) added to the solution (Figure 4.4).

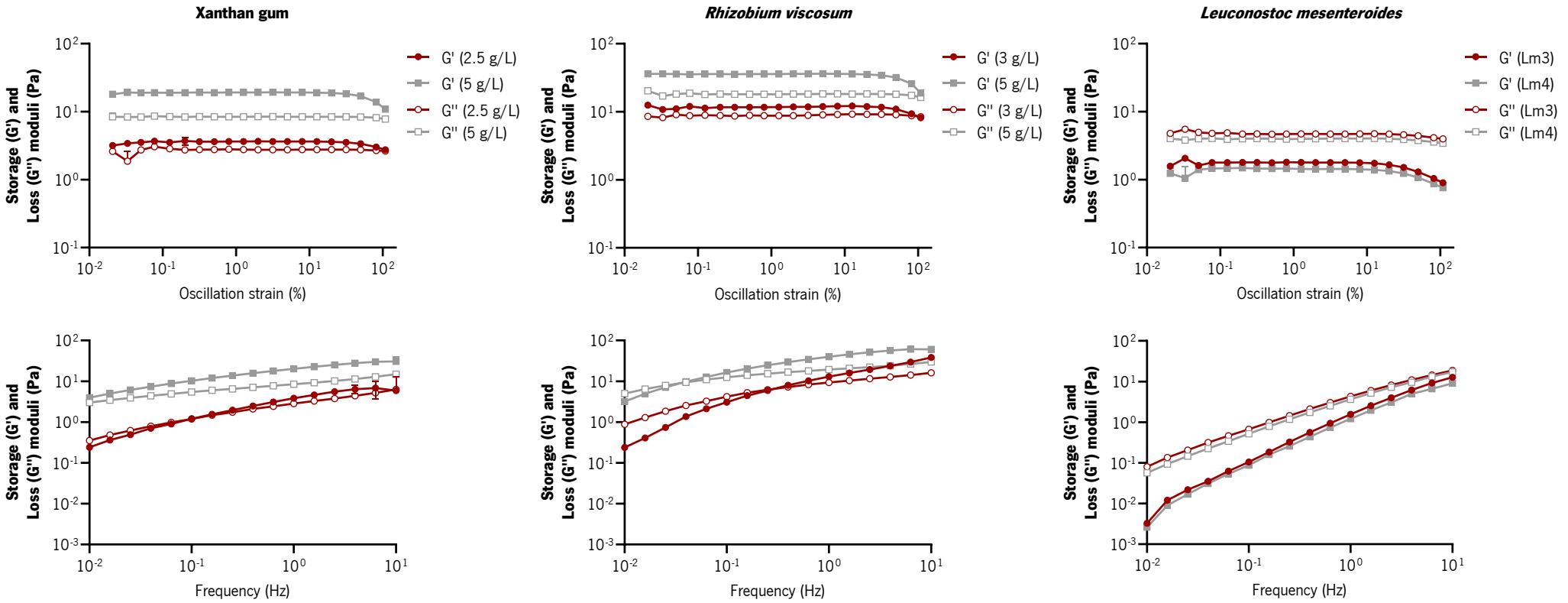

Figure 4.2 – Dynamic viscoelastic properties of the solutions of biopolymer produced by *Rhizobium viscosum* CECT 908 in Rv2 medium (3 – 5 g/L), *Leuconostoc mesenteroides* A4 in Lm3 or Lm4 media (60 g/L) and commercial xanthan gum (2.5 – 5 g/L). Top: storage modulus (G') and loss modulus (G'') as a function of strain at a constant frequency (1 Hz). Bottom: G' and G'' as a function of frequency (Hz), at a constant strain (1% for xanthan gum and *R. viscosum* CECT 908; 5% for *L. mesenteroides* A4).

As the temperature increased, the apparent viscosity of the biopolymer decreased (Figure 4.3). However, the biopolymer remained stable even at the highest temperature tested (80°C). The apparent viscosity was also reduced in the presence of NaCl; however, despite this reduction, the biopolymer remained stable at NaCl concentrations as high as 150 g/L (Figure 4.4).

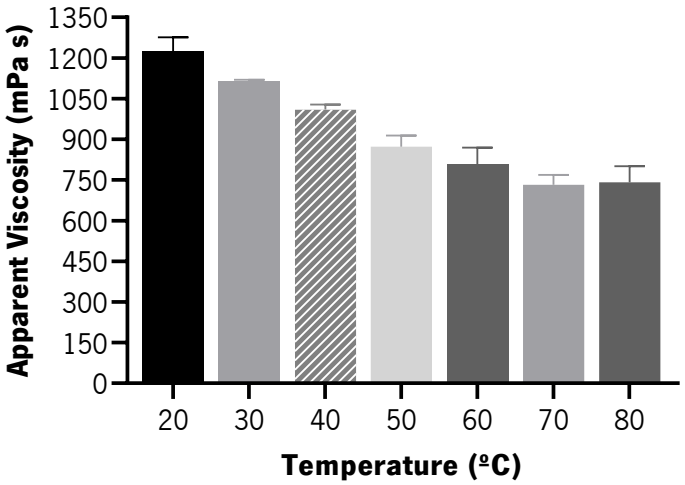

Figure 4.3 – Apparent viscosity values (mPa s) of aqueous solutions of the purified biopolymer (2.7 g/L) produced by *Rhizobium viscosum* CECT 908 grown in Rv2 medium, measured at different temperatures. Results represent the average ± standard deviation of one sample measured through three successive flow ramps at 40°C and shear rate 1.4 s^{-1}.

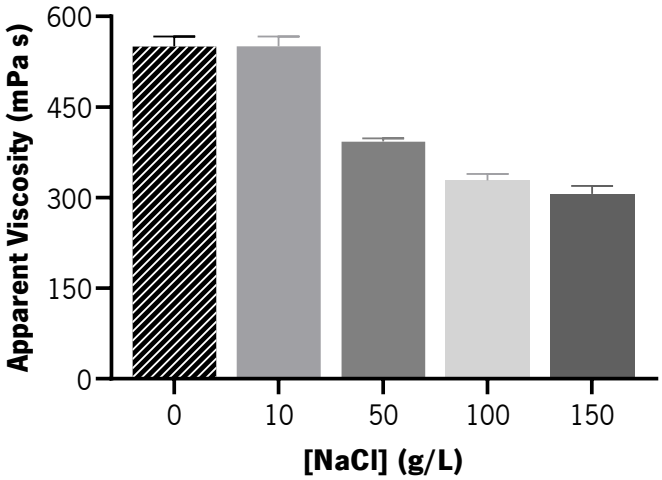

Figure 4.4 – Apparent viscosity values (mPa s) of aqueous solutions of the purified biopolymer (2 g/L) produced by *Rhizobium viscosum* CECT 908 grown in Rv2 medium with the addition of different NaCl concentrations.

Results represent the average ± standard deviation of one sample measured through three successive flow ramps at 40°C and shear rate 1.4 s^{-1}.

4.3.1.2 Effect of rhamnolipids on the viscosity of the biopolymer produced by *Rhizobium viscosum* CECT 908

The effect of combining two biomolecules with different mechanisms of action in oil recovery was studied using sand–pack columns. Before performing those experiments, to determine the most appropriate concentration of RLs to add to the biopolymer solution, several mixtures were evaluated in terms of surface activity and apparent viscosity (Table 4.1). The resulting combination should have a low ST, due to the addition of a surface–active compound, while maintaining a viscosity value similar to that of the biopolymer solution.

Table 4.1 – Surface tension (mN/m) and apparent viscosity (mPa s) values of solutions containing biopolymer (BP) produced by *Rhizobium viscosum* CECT 908 in Rv2 medium (purified BP (1 g/L) and the diluted culture broth) and purified rhamnolipids (RL) (25 and 100 mg/L) produced by *Pseudomonas aeruginosa* PX112 in Pa1 medium.

Solution	Surface tension (mN/m)	Viscosity (mPa s)
1 g/L *R. viscosum* BP	63.8 ± 7.0	246 ± 30
1 g/L *R. viscosum* BP + 25 mg/L *P. aeruginosa* RL	33.3 ± 1.2	238 ± 3
1 g/L *R. viscosum* BP + 100 mg/L *P. aeruginosa* RL	30.4 ± 3.6	244 ± 53
R. viscosum broth	55.5 ± 0.8	266 ± 3
R. viscosum broth + 100 mg/L *P. aeruginosa* RL	32.2 ± 0.4	265 ± 5

Apparent viscosity values presented correspond to a shear rate of 1.4 s^{-1}, measured at 40°C. Results represent the average ± standard deviation of one sample measured through three consecutive flow ramps (apparent viscosity) or measured five times (surface tension).

The presence of RLs did not seem to affect the viscosity of the biopolymer solution (Table 4.1). The ST of the solution containing 100 mg/L of RLs was slightly lower than that of 25 mg/L of RLs. Furthermore, RLs are more effective in reducing the ST of the purified biopolymer solution (30.4 ± 3.6 mN/m) when compared with the *R. viscosum* CECT 908 culture broth (32.2 ± 0.4 mN/m). According to these results, 100 mg/L was selected as the concentration of RLs to be added to the biopolymer solutions to conduct oil recovery assays.

4.3.2 Oil recovery assays using biopolymers

The performance of the biopolymer produced by *R. viscosum* CECT 908 in a low–cost medium in MEOR was evaluated using sand–pack columns through an *ex situ* approach. Using a heavy oil mixture ($\eta_{40°C}$ = 247 mPa s at 1.4 s^{-1}), the purified biopolymer, at different concentrations and viscosity values, was able to recover 14.3% or 25.8% more oil than the control (Table 4.2). Higher recoveries were achieved using biopolymer solutions with lower apparent viscosity values, which can be due to the formation of a more stable oil displacement front. With the culture broth, recovery rates were 4% lower than those obtained with the biopolymer solution with a similar apparent viscosity value (Table 4.2), probably due to other compounds produced by *R. viscosum* in the culture broth that contribute negatively to oil recovery. The differences observed in the recovery rates could also be attributed to the variability between assays, in which case it could be said that the purification step may not be necessary since the culture broth can still achieve significant oil recovery rates.

Table 4.2 – Results obtained in *ex situ* MEOR sand–pack column assays with a heavy oil mixture ($\eta_{40°C}$ = 247 mPa s at 1.4 s^{-1}) using the crude biopolymer (BP) produced by *Leuconostoc mesenteroides* A4 in Lm3 and Lm4 media, and the BP produced by *Rhizobium viscosum* CECT 908 in Rv2 medium (diluted culture broth or purified BP).

Oil recovery parameters	Treatment				
	Leuconostoc mesenteroides		*Rhizobium viscosum*		
	Crude BP (Lm3)	Crude BP (Lm4)	Purified BP		Culture broth
$\eta_{40°C}$ (mPa s)	67 ± 1	156 ± 7	164 ± 23	246 ± 30	266 ± 3
PV (mL)	95.0	85.0	85.0	86.3 ± 4.8	90.0 ± 0.0
Porosity (%)	33.9	30.4	30.4	30.8 ± 1.7	32.1 ± 0.0
OOIP (mL)	84.0	78.0	80.0	78.0 ± 3.2	76.3 ± 2.5
S_{oi} (%)	88.4	91.8	94.1	90.7 ± 6.5	84.7 ± 2.7
S_{orwf} (mL)	45.0	40.0	45.0	50.0 ± 0.0	52.5 ± 3.5
S_{or} (%)	46.4	48.7	43.8	35.8 ± 2.6	31.2 ± 2.4
S_{orbf} (mL)	11.7	11.4	12.0	6.4 ± 1.2	4.5 ± 0.2
AOR (%)	21.5	21.5	25.8	14.3 ± 3.2	10.2 ± 0.1

The AOR value is the corrected value obtained after subtracting the additional oil recovery from the control assays. The results for the last two assays represent the average of two independent experiments ± standard deviation.

The performance of the biopolymers produced by *L. mesenteroides* A4 in MEOR was also evaluated using the same crude oil. When produced in Lm3 or Lm4 media, the biopolymer from *L. mesenteroides*

A4 recovered 21.5% more oil than the control, showing that it could be an effective agent for application in oil recovery (Table 4.2). These values were close to those obtained with the biopolymer from *R. viscosum* CECT 908 at a similar viscosity (164 ± 23 mPa s; 25.8% AOR). Furthermore, the same recovery rates were obtained using *L. mesenteroides* A4 biopolymer solutions with low (67 ± 1 mPa s) and high (156 ± 7 mPa s) viscosities, meaning that lower amounts of biopolymer could be used to achieve the same results.

When using a lighter oil ($\eta_{40°C}$ = 110 mPa s at 1.4 s^{-1}), the biopolymer from *L. mesenteroides* A4 recovered 5.4% more oil than the control (Table 4.3). There was no difference between the oil recovery obtained with the CFS or the crude biopolymer, indicating that the purification step might not be necessary to achieve the best results. Between the two oils, better results were observed with the heavy oil mixture, indicating that this biopolymer could be more effective in recovering heavy oils.

Table 4.3 – Results obtained in *ex situ* MEOR sand–pack column assays with the oil from the Potiguar oilfield ($\eta_{40°C}$ = 110 mPa s at 1.4 s^{-1}) using xanthan gum (1 g/L), the biopolymer produced by *Leuconostoc mesenteroides* A4 in Lm3 medium (crude biopolymer and cell–free supernatant (CFS)) and the biopolymer from *Rhizobium viscosum* CECT 908 in Rv2 medium (diluted culture broth or purified biopolymer).

Oil recovery parameters	Treatment				
	Xanthan gum (1 g/L)	*Leuconostoc mesenteroides*		*Rhizobium viscosum*	
		Crude BP	CFS	Purified BP	Culture broth
$\eta_{40°C}$ (mPa s)	106 ± 9	115 ± 4	62 ± 3	134 ± 6	109 ± 1
PV (mL)	89.0 ± 1.4	97.5 ± 3.5	97.5 ± 3.5	98.0 ± 0.0	105.0 ± 0.0
Porosity (%)	31.8 ± 0.5	34.8 ± 1.3	34.8 ± 1.3	35.0 ± 0.0	37.5 ± 0.0
OOIP (mL)	80.1 ± 1.1	85.6 ± 4.1	88.5 ± 7.4	75.5 ± 0.2	86.5 ± 2.1
S_{oi} (%)	90.0 ± 2.6	87.8 ± 1	90.9 ± 10.9	77.0 ± 0.2	82.4 ± 2.0
S_{orwf} (mL)	45.0 ± 0.0	50.0 ± 0.0	50.0 ± 0.0	45.0 ± 0.0	57.5 ± 3.5
S_{or} (%)	43.8 ± 0.7	41.5 ± 2.8	43.3 ± 4.8	40.4 ± 0.2	33.6 ± 2.5
S_{orbf} (mL)	5.5 ± 0.8	4.5 ± 0.1	4.8 ± 0.2	5.9 ± 1.3	4.2 ± 0.1
AOR (%)	8.4 ± 2.7	5.4 ± 1.2	5.4 ± 3.0	12.2 ± 4.3	7.1 ± 0.5

The AOR value is the corrected value obtained after subtracting the additional oil recovery from the control assays. The results represent the average of two independent experiments ± standard deviation.

The best recovery rates with the oil from the Potiguar oilfield were obtained with the biopolymer from *R. viscosum* CECT 908. Recovery rates with the purified biopolymer and the culture broth are 12.2% and 7.1% higher when compared with the control, respectively (Table 4.3). Regarding xanthan gum, it performed better than the biopolymer from *L. mesenteroides* A4, but worse than the purified biopolymer

from *R. viscosum* CECT 908 (Table 4.3). This shows the potential of the *R. viscosum* CECT 908 biopolymer for MEOR application.

4.3.3 Oil recovery assays using combinations of biopolymers and biosurfactants

The combination of biosurfactants and biopolymers for application in MEOR was also evaluated in this work using two injection strategies through an *ex situ* approach. The first consisted of injecting 1 PV of RLs solution, which was incubated for 48h inside the column, followed by injecting 2 PV of a xanthan gum solution (Table 4.4). By first incubating the column with the biosurfactant, the aim was to reduce the oil's IFT and shift the wettability of the sand to a more water–wet state to facilitate oil recovery through biopolymer flooding.

Table 4.4 – Results obtained in *ex situ* MEOR sand–pack column assays with the oil from the Potiguar oilfield ($\eta_{40°C}$ = 110 mPa s at 1.4 s^{-1}) using commercial rhamnolipids (RL–90) and the cell–free supernatant (CFS) from *Pseudomonas aeruginosa* PX112 grown in CSLM medium, incubated for 48h and followed by xanthan gum (1 g/L) injection.

Oil recovery parameters	Treatment	
	RL–90 (2 g/L)	*Pseudomonas aeruginosa* CFS in CSLM medium
$\eta_{40°C}$ (mPa s)	95 ± 2	99 ± 6
ST (mN/m)	29.9 ± 0.1	29.9 ± 0.1
PV (mL)	95.0 ± 4.2	91.0 ± 1.4
Porosity (%)	33.9 ± 1.5	32.5 ± 0.5
OOIP (mL)	75.0 ± 4.5	72.6 ± 2.0
S_{oi} (%)	78.9 ± 1.2	79.8 ± 0.9
S_{orwf} (mL)	42.5 ± 3.5	40.0 ± 0.0
S_{or} (%)	43.3 ± 1.3	44.9 ± 1.5
S_{orbf} (mL)	6.6 ± 0.8	5.4 ± 1.8
AOR (%)	13.1 ± 2.0	9.1 ± 4.4

The AOR value is the corrected value obtained after subtracting the additional oil recovery from the control assays. The results represent the average of two independent experiments ± standard deviation.

However, in these conditions, the RLs from *P. aeruginosa* PX112 do not have a significant effect in oil recovery and only xanthan gum was responsible for the increase in the recovery rates (9.1% AOR obtained in the assay using RLs and xanthan gum, compared with 8.4% AOR when only xanthan gum was injected) (Table 4.3 and Table 4.4). On the other hand, when the commercial RLs were used, the recovery

rate increased around 5% more than in the assay using only xanthan gum, despite the ST values of both RLs solutions being the same (29.9 mN/m) (Table 4.4).

Because other studies in the literature where both biomolecules were evaluated together usually inject them at the same time (Al–Ghailani et al., 2021; Fernandes et al., 2016; Ge et al., 2021; Ji et al., 2022; Qi et al., 2018), the second approach consisted on the injection of different solutions containing the two biomolecules (Table 4.5). Results show that, in the conditions tested, the combination of these biomolecules (*R. viscosum* CECT 908 biopolymer and *P. aeruginosa* PX112 RLs) improves the oil recovery process when using the heavier oil mixture (Table 4.2 and Table 4.5), thus being an interesting approach to develop further. With the crude oil from the Potiguar oilfield, however, the combinations of both biomolecules did not increase the oil recovery rates (6.8% AOR with both biomolecules compared with 7.1% AOR with the culture broth from *R. viscosum* CECT 908) (Table 4.3 and Table 4.5).

Table 4.5 – Results obtained in *ex situ* MEOR sand–pack column assays with a heavy oil mixture ($\eta_{40°C}$ = 247 mPa s at 1.4 s^{-1}) or the oil from the Potiguar oilfield ($\eta_{40°C}$ = 110 mPa s at 1.4 s^{-1}) using a solution containing both the purified biopolymer (BP) or the diluted culture broth from *Rhizobium viscosum* CECT 908 and the purified RLs from *Pseudomonas aeruginosa* PX112 (100 mg/L).

	Treatment		
	Heavy oil mixture		Potiguar oil
Oil recovery parameters	*Rhizobium viscosum* BP + *Pseudomonas aeruginosa* RL (100 mg/L)	*Rhizobium viscosum* broth + *Pseudomonas aeruginosa* RL (100 mg/L)	*Rhizobium viscosum* broth + *Pseudomonas aeruginosa* RL (100 mg/L)
$\eta_{40°C}$ (mPa s)	244 ± 53	265 ± 5	107 ± 4
ST (mN/m)	30.4 ± 3.6	32.2 ± 0.4	33.9 ± 1.1
PV (mL)	92.5 ± 6.5	85.0	102.5 ± 3.5
Porosity (%)	33.0 ± 2.3	30.4	36.6 ± 1.3
OOIP (mL)	73.1 ± 5.5	73.0	83.7 ± 3.7
S_{oi} (%)	79.3 ± 7.3	85.9	81.6 ± 0.8
S_{orwf} (mL)	48.8 ± 2.5	50.0	52.5 ± 3.5
S_{or} (%)	33.2 ± 1.7	31.5	37.3 ± 1.4
S_{orbf} (mL)	7.0 ± 1.3	6.3	4.4 ± 0.1
AOR (%)	20.2 ± 3.8	18.9	6.8 ± 0.1

The AOR value is the corrected value obtained after subtracting the additional oil recovery from the control assays. The results represent the average of two independent experiments ± standard deviation.

Other sand–pack column assays using the RLs from *Burkholderia thailandensis* E264 and the biomolecules produced by a *Bacillus velezensis* isolate were performed and are presented in Chapter 5 and Chapter 6, respectively.

4.4 Discussion

Three different biopolymers (commercial xanthan gum and the biopolymers produced by *R. viscosum* CECT 908 and *L. mesenteroides* A4) were evaluated in this study regarding their rheological properties and their ability to recover oil in sand–pack column assays. These displayed a shear–thinning or pseudoplastic behavior as viscosity decreased and shear stress increased, with increasing shear rate (Figure 4.1). Furthermore, as expected, in the case of xanthan gum and the biopolymer produced by *R. viscosum* CECT 908, the viscosity of solutions increased with increasing biopolymer concentrations. Usually, this effect is attributed to the increased interactions of the molecules in the solution that form aggregates and, consequently, increase molecular weight (Sofia & Djamel, 2016). Although a higher viscosity is generally better for oil recovery, a biopolymer concentration and/or molecular weight that is too high can increase the pressure at the wellbore region, causing injectivity problems (Firozjaii & Saghafi, 2020). In this regard, the biopolymer from *R. viscosum* CECT 908 presented higher viscosities in solution when compared with xanthan gum, potentially making it a better alternative for MEOR. The higher viscosities of this biopolymer have been attributed to its extended conformation and high acetylation degree (Gudiña et al., 2023).

In xanthan gum and *R. viscosum* CECT 908 biopolymer solutions, G' was higher than G'' in the strain oscillatory tests, which can be attributed to the rigid conformation of the biopolymer in solution (Figure 4.2). This conformation is responsible for a lower mobility inside the reservoir, in contrast with the high mobility of water, that is crucial in order to displace the oil efficiently (Sofia & Djamel, 2016). Nonetheless, the plots resulting from the frequency sweep tests show a crossover point between the two moduli in the tested frequency range. The crossover point becomes less evident, happening at increasingly lower frequencies, as the biopolymer concentration increases. This means that the elastic behavior could prevail from a specific biopolymer concentration while the biopolymer flows at either low or high velocities. Thus, a more stable flow front could be maintained for a longer injection time, improving the overall oil recovery (Liang et al., 2019).

Some studies report similar results for the rheological behavior of xanthan gum solutions, attributing the prevalence of the elastic modulus to its rigid double helix conformation (Y. Li et al., 2017; Sofia & Djamel, 2016). On the other hand, some studies showed a prevalence of G'' over G' in the frequency sweep tests performed with xanthan gum solutions, a typical behavior in disordered structures (Liang et al., 2019; Xu et al., 2014). These studies, however, generally use lower concentrations of biopolymer (1–3 g/L) and/or perform the assays at higher temperatures and salinities, which could explain the differences observed.

In general, the dynamic moduli of the biopolymer from *R. viscosum* CECT 908 were higher than those of xanthan gum, hence it has a stronger viscoelasticity. This, combined with the higher viscosities of the biopolymer solution, translates to a better oil recovery efficiency (12.2% AOR for the purified biopolymer from *R. viscosum* CECT 908, compared with 8.4% AOR for the xanthan gum solution) (Table 4.3) (Ji et al., 2020, 2022; Y. Li et al., 2017; Liang et al., 2019; Xu et al., 2014).

The oil recovery efficiency of the biopolymer from *R. viscosum* CECT 908 has been previously studied, yielding recovery rates between 14 and 27% (Couto et al., 2019; Gudiña et al., 2023). These values are slightly higher than the ones obtained here, nonetheless, a similar trend was observed: the oil recovery rate was higher with the heavier oil (Table 4.2 and Table 4.3). This could be due to a lower mobility ratio between the oil and water/biopolymer phases, which increases the sweep efficiency and results in a more uniform oil displacement front (Rellegadla et al., 2017). Furthermore, this biopolymer seems more effective in oil recovery in the purified form, probably because other components in the culture broth could interfere with the recovery process. As for xanthan gum, the AOR values obtained here are lower than the recovery rates obtained in similar works (9–28% AOR) (Gudiña et al., 2023; Jang et al., 2015; Ji et al., 2020; H. Li et al., 2022; Y. Li et al., 2017; Liang et al., 2019; Ramos de Souza et al., 2022; Xu et al., 2014). However, the conditions used greatly vary between different studies, making it difficult to compare results.

In *L. mesenteroides* A4 biopolymer solutions, the viscous component (G'') was prevalent over the elastic one (G') (Figure 4.2). Again, this behavior is indicative of disordered structures that typically result in low oil recovery rates (Liang et al., 2019; Xu et al., 2014). Nonetheless, the recovery rates obtained with this biopolymer in sand–pack column assays using a heavy oil mixture ($\eta_{40°C}$ = 247 mPa s at 1.4 s^{-1}) were similar to those obtained with the biopolymer from *R. viscosum* CECT 908 (21.5% AOR compared with 25.8% AOR, respectively) (Table 4.2). Moreover, the different viscosities obtained with each of the culture media used to produce this biopolymer (67 ± 1 mPa s with the Lm3 medium and

156 ± 7 mPa s with the Lm4 medium) did not account for any differences in the recovery rates obtained. Hence, a cheaper medium (Lm3), that uses half the amount of sucrose, could produce a biopolymer with similar rheological properties (Figure 4.1 and Figure 4.2) and oil recovery efficiency (Table 4.2). As with the biopolymer from *R. viscosum* CECT 908, recovery rates were lower when using a lighter oil ($\eta_{40°C}$ = 110 mPa s at 1.4 s^{-1}) (5.4% AOR). Again, this could be attributed to a more favorable mobility ratio between the two phases when the heavier oil mixture is used. Furthermore, the same amount of oil was recovered when either the CFS or the crude biopolymer were used, hence a purification step would not be deemed necessary in such cases. In a previous study, *L. mesenteroides* was evaluated for oil recovery through an *in situ* approach, yielding recovery rates up to 21% AOR depending on the morphology of the substrate (Soudmand–asli et al., 2007). These results suggest that *L. mesenteroides* A4 could also be an interesting candidate for *in situ* MEOR. Soudmand–asli et al. (2007) reported that the primary mechanism of oil recovery was selective plugging, also associated with biopolymer production, although in this case, the production is *in situ*.

The stability of the biopolymer at different temperatures and salinities is also an important factor to consider and must be evaluated under specific reservoir conditions. At high temperatures and salt concentrations, the biopolymer solutions usually experience a reduction in viscosity due to the transition from the ordered to the disordered molecular state (Muhammed et al., 2020). This reduction in viscosity was observed with the biopolymer from *R. viscosum* CECT 908 (produced in a low–cost medium) at temperatures up to 80°C (27% viscosity reduction) and NaCl concentrations up to 150 g/L (44% viscosity reduction). Nonetheless, the biopolymer remained stable under these conditions.

In a previous work, the stability of this biopolymer (produced in a synthetic medium) was tested by subjecting the cell–free supernatant to different temperatures over the course of 2h and to different NaCl concentrations (Couto et al., 2019). It was shown that incubation at 80°C did not affect the viscosity of the biopolymer, but the viscosity decreased around 20% at higher temperatures. Furthermore, NaCl did not affect the performance of the biopolymer at concentrations up to 200 g/L. This shows that the biopolymer from *R. viscosum* CECT 908 could be an interesting candidate for MEOR as it can withstand various reservoir conditions.

The combination of biopolymers and biosurfactants in oil recovery was also evaluated in this study. The two biomolecules have different mechanisms of action that promote oil recovery, with biopolymers increasing the viscosity of the injected water and contributing to selective plugging (Lee et al., 2020; Rellegadla et al., 2017) and biosurfactants decreasing the IFT of the oil–water–rock system, emulsifying

the trapped oil and shifting the wettability of the substrate towards a more water–wet state (Dong et al., 2022; Hoseini–Moghadam et al., 2021; Negin et al., 2017; Onaizi et al., 2021). By first injecting the RLs from *P. aeruginosa* (commercial RLs or RLs from *P. aeruginosa* PX112 produced in CSLM medium) into the sand–pack column, it was expected that these would facilitate oil recovery through biopolymer flooding, since the oil would not adhere as strongly to the substrate. However, only when the commercial RLs were used did the recovery rate increase compared to the assay using the biopolymer alone (13.1% AOR and 8.4% AOR, respectively) (Table 4.3 and Table 4.4). It is estimated that the CFS from *P. aeruginosa* PX112 contained around 3.2 g of RLs/L (Gudiña, Rodrigues, et al., 2015), hence the concentration of RLs in the injected solution did not seem to have an effect here. Nonetheless, by using the CFS, other components may interfere with the RLs effectiveness in recovering the oil that is trapped in the column, which could explain the results obtained.

Additional oil recovery assays were performed by injecting a treatment solution with both the RL from *P. aeruginosa* PX112, produced in CSLM medium, and the biopolymer from *R. viscosum* CECT 908, produced in a low–cost medium. Here, it became important to evaluate the effect of each biomolecule on the viscosity and the ST of the solution. It was found that the presence of RLs did not significantly decrease the viscosity of the biopolymer solution, and the biopolymer did not have a considerable effect on ST reduction (Table 4.1). These results are in line with other studies that evaluated the combination of different (bio)polymers with (bio)surfactants (Ge et al., 2021; Qi et al., 2018).

With this MEOR approach, oil recovery rates increased by 5.9% and 8.7% compared to the assays performed with the purified biopolymer and the culture broth, respectively (Table 4.5). Other studies displayed similar oil recovery improvement when combining the two types of (bio)molecules (Al–Ghailani et al., 2021; Ji et al., 2022; Qi et al., 2018). For example, the combination of a weak gel and the biosurfactant from *Bacillus* sp. W5 increased the oil recovery rate 8.9% compared to the treatment with the biosurfactant alone (Qi et al., 2018). Ji et al. (2022) also combined two (bio)molecules to study their synergistic effect in oil recovery: the biopolymer sphingan, produced by *Sphingomonas* sp. WD, and a synthetic non–ionic surfactant. The authors achieved a 5% AOR increase when both molecules were used together, thus demonstrating the potential of their combination in MEOR operations (Ji et al., 2022). Nevertheless, when using a lighter oil (from the Potiguar oilfield), there was no improvement in the oil recovery rates with this approach (Table 4.5).

In conclusion, the biomolecules studied have proven to be interesting candidates for MEOR applications. The biopolymer produced by *L. mesenteroides* A4 has shown promising results, achieving

AORs as high as those obtained with the biopolymer from *R. viscosum* CECT 908 when using a heavy oil mixture. However, the low viscosity values obtained with this biopolymer indicate that a high amount of product is needed for MEOR application. Furthermore, when using a lighter oil, the biopolymer from *R. viscosum* CECT 908 also showed better results than the biopolymers studied. In this sense, *R. viscosum* CECT 908 still poses the most viable alternative. Moreover, this biopolymer displayed good viscoelastic properties and was stable at different temperatures and salinities commonly found in oil reservoirs, making it even more attractive for MEOR applications. Additionally, the results obtained when using RLs and biopolymers suggest a synergistic effect between the two types of biomolecules that could result in improved oil recovery with minimal infrastructure alterations, especially when working with heavy oils.

4.5 References

Al–Ghailani, T., Al–Wahaibi, Y. M., Joshi, S. J., Al–Bahry, S. N., Elshafie, A. E., & Al–Bemani, A. S. (2021). Application of a new bio–ASP for enhancement of oil recovery: Mechanism study and core displacement test. *Fuel*, *287*, 119432. https://doi.org/10.1016/j.fuel.2020.119432

Couto, M. R., Gudiña, E. J., Ferreira, D., Teixeira, J. A., & Rodrigues, L. R. (2019). The biopolymer produced by Rhizobium viscosum CECT 908 is a promising agent for application in microbial enhanced oil recovery. *New Biotechnology*, *49*, 144–150. https://doi.org/10.1016/j.nbt.2018.11.002

Dong, H., Zheng, A., He, Y., Wang, X., Li, Y., Yu, G., Gu, Y., Banat, I. M., Sun, S., She, Y., & Zhang, F. (2022). Optimization and characterization of biosurfactant produced by indigenous: Brevibacillus borstelensis isolated from a low permeability reservoir for application in MEOR. *RSC – Royal Society of Chemistry Advances*, *12*(4), 2036–2047. https://doi.org/10.1039/d1ra07663a

Elshafie, A., Joshi, S. J., Al–Wahaibi, Y. M., Al–Bahry, S. N., Al–Bemani, A. S., Al–Hashmi, A., & Al–Mandhari, M. S. (2017, April 4). Isolation and Characterization of Biopolymer Producing Omani Aureobasidium Pullulans Strains and Its Potential Applications in Microbial Enhanced Oil Recovery. *SPE Oil and Gas India Conference and Exhibition*. https://doi.org/10.2118/185326–ms

Fernandes, P. L., Rodrigues, E. M., Paiva, F. R., Ayupe, B. A. L., McInerney, M. J., & Tótola, M. R. (2016). Biosurfactant, solvents and polymer production by Bacillus subtilis RI4914 and their application for enhanced oil recovery. *Fuel*, *180*, 551–557. https://doi.org/10.1016/j.fuel.2016.04.080

Firozjaii, A. M., & Saghafi, H. R. (2020). Review on chemical enhanced oil recovery using polymer flooding: Fundamentals, experimental and numerical simulation. In *Petroleum* (Vol. 6, Issue 2, pp. 115–122). Elsevier. https://doi.org/10.1016/j.petlm.2019.09.003

Ge, M. R., Miao, S. J., Liu, J. F., Gang, H. Z., Yang, S. Z., & Mu, B. Z. (2021). Laboratory studies on a novel salt–tolerant and alkali–free flooding system composed of a biopolymer and a bio–based surfactant for oil recovery. *Journal of Petroleum Science and Engineering*, *196*, 107736. https://doi.org/10.1016/j.petrol.2020.107736

Gudiña, E. J., Couto, M. R., Silva, S. P., Coelho, E., Coimbra, M. A., Teixeira, J. A., & Rodrigues, L. R. (2023). Sustainable Exopolysaccharide Production by Rhizobium viscosum CECT908 Using Corn

Steep Liquor and Sugarcane Molasses as Sole Substrates. *Polymers*, *15*(1), 20. https://doi.org/10.3390/polym15010020

Gudiña, E. J., Pereira, J. F. B., Costa, R., Coutinho, J. A. P., Teixeira, J. A., & Rodrigues, L. R. (2013). Biosurfactant–producing and oil–degrading Bacillus subtilis strains enhance oil recovery in laboratory sand–pack columns. *Journal of Hazardous Materials*, *261*, 106–113. https://doi.org/10.1016/j.jhazmat.2013.06.071

Gudiña, E. J., Rodrigues, A. I., Alves, E., Domingues, M. R., Teixeira, J. A., & Rodrigues, L. R. (2015). Bioconversion of agro–industrial by–products in rhamnolipids toward applications in enhanced oil recovery and bioremediation. *Bioresource Technology*, *177*, 87–93. https://doi.org/10.1016/j.biortech.2014.11.069

Gudiña, E. J., & Rodrigues, L. R. (2019). Microbial Surfactants: Alternative to Vegetable Oil Surfactants. *Methods in Molecular Biology*, *1995*, 383–393. https://doi.org/10.1007/978–1–4939–9484–7_22

Gudiña, E. J., Teixeira, J. A., & Rodrigues, L. R. (2015). Microbial enhanced oil recovery. In U. C. Sharma, S. Sivakumar, & R. Prasad (Eds.), *Energy Science and Technology Vol. 3: Oil and Natural Gas* (1st ed., pp. 149–177). Studium Press LLC.

Hoseini–Moghadam, S. M. A., Ghiasimehr, B., Torkaman, M., & Mirmarghabi, P. (2021). The role of temperature and porous media morphology on the performance of anionic and cationic surfactants for enhanced heavy oil recovery. *Journal of Molecular Liquids*, *339*, 116051. https://doi.org/10.1016/j.molliq.2021.116051

Ianniruberto, G. (2015). Introduction on Polymer Rheology. In *Reference Module in Chemistry, Molecular Sciences and Chemical Engineering*. Elsevier. https://doi.org/10.1016/b978–0–12–409547–2.11228–4

Jang, H. Y., Zhang, K., Chon, B. H., & Choi, H. J. (2015). Enhanced oil recovery performance and viscosity characteristics of polysaccharide xanthan gum solution. *Journal of Industrial and Engineering Chemistry*, *21*, 741–745. https://doi.org/10.1016/j.jiec.2014.04.005

Ji, S., Li, H., Wang, G. H., Lu, T., Ma, W., Wang, J., Zhu, H., & Xu, H. (2020). Rheological behaviors of a novel exopolysaccharide produced by Sphingomonas WG and the potential application in enhanced oil recovery. *International Journal of Biological Macromolecules*, *162*, 1816–1824. https://doi.org/10.1016/j.ijbiomac.2020.08.114

Ji, S., Wei, F., Li, B., Li, P., Li, H., Li, S., Wang, J., Zhu, H., & Xu, H. (2022). Synergistic effects of microbial polysaccharide mixing with polymer and nonionic surfactant on rheological behavior and enhanced oil recovery. *Journal of Petroleum Science and Engineering*, *208*, 109746. https://doi.org/10.1016/j.petrol.2021.109746

Khademolhosseini, R., Jafari, A., Mousavi, S. M., Hajfarajollah, H., Noghabi, K. A., & Manteghian, M. (2019). Physicochemical characterization and optimization of glycolipid biosurfactant production by a native strain of Pseudomonas aeruginosa HAK01 and its performance evaluation for the MEOR process. *Royal Society of Chemistry – RSC Advances*, *9*(14), 7932–7947. https://doi.org/10.1039/C8RA10087J

Lapasin, R., & Pricl, S. (1999). Rheology of Industrial Polysaccharides: Theory and Applications. In *Rheology of Industrial Polysaccharides: Theory and Applications*. Aspen Publishers. https://doi.org/10.1007/978–1–4615–2185–3

Lee, K. S., Kwon, T.–H., Park, T., & Jeong, M. S. (2020). Microbiology and Microbial Products for

Enhanced Oil Recovery. In *Theory and Practice in Microbial Enhanced Oil Recovery* (pp. 27–65). Gulf Professional Publishing. https://doi.org/10.1016/b978-0-12-819983-1.00002-8

Li, H., Zhu, W., Niu, H., Gao, Y., Chen, Z., Song, Z., & Kong, D. (2022). 2-D porous flow field reveals different EOR mechanisms between the biopolymer and chemical polymer. *Journal of Petroleum Science and Engineering*, *210*, 110084. https://doi.org/10.1016/j.petrol.2021.110084

Li, Y., Xu, L., Gong, H., Ding, B., Dong, M., & Li, Y. (2017). A Microbial Exopolysaccharide Produced by Sphingomonas Species for Enhanced Heavy Oil Recovery at High Temperature and High Salinity. *Energy and Fuels*, *31*(4), 3960–3969. https://doi.org/10.1021/acs.energyfuels.6b02923

Liang, K., Han, P., Chen, Q., Su, X., & Feng, Y. (2019). Comparative Study on Enhancing Oil Recovery under High Temperature and High Salinity: Polysaccharides Versus Synthetic Polymer. *ACS Omega*, *4*(6), 10620–10628. https://doi.org/10.1021/acsomega.9b00717

Muhammed, N. S., Haq, M. B., Al-Shehri, D., Rahaman, M. M., Keshavarz, A., & Zakir Hossain, S. M. (2020). Comparative study of green and synthetic polymers for enhanced oil recovery. In *Polymers* (Vol. 12, Issue 10, pp. 1–32). MDPI AG. https://doi.org/10.3390/polym12102429

Negin, C., Ali, S., & Xie, Q. (2017). Most common surfactants employed in chemical enhanced oil recovery. In *Petroleum* (Vol. 3, Issue 2, pp. 197–211). Elsevier. https://doi.org/10.1016/j.petlm.2016.11.007

Novak, J. S., Tanenbaum, S. W., & Nakas, J. P. (1992). Heteropolysaccharide formation by Arthrobacter viscosus grown on xylose and xylose oligosaccharides. *Applied and Environmental Microbiology*, *58*(11), 3501–3507.

Onaizi, S. A., Alsulaimani, M., Al-Sakkaf, M. K., Bahadi, S. A., Mahmoud, M., & Alshami, A. (2021). Crude oil/water nanoemulsions stabilized by biosurfactant: Stability and pH-Switchability. *Journal of Petroleum Science and Engineering*, *198*, 108173. https://doi.org/10.1016/j.petrol.2020.108173

Papanicolaou, G. C., & Zaoutsos, S. P. (2010). Viscoelastic constitutive modeling of creep and stress relaxation in polymers and polymer matrix composites. In *Creep and Fatigue in Polymer Matrix Composites* (pp. 3–47). Elsevier Ltd. https://doi.org/10.1533/9780857090430.1.3

Qi, Y.-B., Zheng, C.-G., Lv, C.-Y., Lun, Z.-M., & Ma, T. (2018). Compatibility between weak gel and microorganisms in weak gel-assisted microbial enhanced oil recovery. *Journal of Bioscience and Bioengineering*, *126*(2), 235–240. https://doi.org/10.1016/j.jbiosc.2018.02.011

Ramos de Souza, E., Rodrigues, P. D., Sampaio, I. C. F., Bacic, E., Crugeira, P. J. L., Vasconcelos, A. C., dos Santos Silva, M., dos Santos, J. N., Quintella, C. M., Pinheiro, A. L. B., & Almeida, P. F. de. (2022). Xanthan gum produced by Xanthomonas campestris using produced water and crude glycerin as an environmentally friendlier agent to enhance oil recovery. *Fuel*, *310*, 122421. https://doi.org/10.1016/j.fuel.2021.122421

Rellegadla, S., Prajapat, G., & Agrawal, A. (2017). Polymers for enhanced oil recovery: fundamentals and selection criteria. In *Applied Microbiology and Biotechnology* (Vol. 101, Issue 11, pp. 4387–4402). Springer Berlin Heidelberg. https://doi.org/10.1007/s00253-017-8307-4

Roeder, R. K. (2013). Mechanical Characterization of Biomaterials. In *Characterization of Biomaterials* (pp. 49–104). Elsevier Inc. https://doi.org/10.1016/B978-0-12-415800-9.00003-6

Sofia, G. B., & Djamel, A. (2016). A Rheological Study of Xanthan Polymer for Enhanced Oil Recovery. *Journal of Macromolecular Science, Part B: Physics*, *55*(8), 793–809. https://doi.org/10.1080/00222348.2016.1207544

Soudmand–asli, A., Ayatollahi, S. S., Mohabatkar, H., Zareie, M., & Shariatpanahi, S. F. (2007). The in situ microbial enhanced oil recovery in fractured porous media. *Journal of Petroleum Science and Engineering*, *58*(1–2), 161–172. https://doi.org/10.1016/j.petrol.2006.12.004

Veerabhadrappa, S. K., Trivedi, J. J., & Kuru, E. (2013). Visual confirmation of the elasticity dependence of unstable secondary polymer floods. *Industrial and Engineering Chemistry Research*, *52*(18), 6234–6241. https://doi.org/10.1021/ie303241b

Xu, L., Xu, G., Yu, L., Gong, H., Dong, M., & Li, Y. (2014). The displacement efficiency and rheology of welan gum for enhanced heavy oil recovery. *Polymers for Advanced Technologies*, *25*(10), 1122–1129. https://doi.org/10.1002/pat.3364

CHAPTER 5.

Cost–effective rhamnolipid production by *Burkholderia thailandensis* E264 using agro–industrial residues

This chapter is based on the following paper:

Correia, J., Gudiña, E.J., Lazar, Z., Janek, T. & Teixeira, J.A. (2022). Cost–effective rhamnolipid production by *Burkholderia thailandensis* E264 using agro–industrial residues. Appl Microbiol Biotechnol, 106, 7477–7489. https://doi.org/10.1007/s00253–022–12225–1

Abstract

The agro–industrial by–products corn steep liquor (CSL) and olive mill wastewater (OMW) were evaluated as low–cost substrates for rhamnolipid production by *Burkholderia thailandensis* E264. In a culture medium containing CSL (7.5% (v/v)) as sole substrate, *B. thailandensis* E264 produced 175 mg rhamnolipid/L, which is about 1.3 times the amount produced in the standard medium, which contains glycerol, peptone and meat extract. When the CSL medium was supplemented with OMW (10% (v/v)), rhamnolipid production further increased up to 253 mg/L in flasks and 269 mg/L in bioreactor. Rhamnolipids produced in CSL+OMW medium reduced the surface tension up to 27.1 mN/m, with a critical micelle concentration of 51 mg/L, better than the values obtained with the standard medium (28.9 mN/m and 58 mg/L, respectively). However, rhamnolipids produced in CSL+OMW medium displayed a weak emulsifying activity, as well as a lower potential for wettability alteration, when compared to those produced in the other media. Whereas di–rhamnolipid congeners represented between 90 and 95% of rhamnolipids produced by *B. thailandensis* E264 in CSL and the standard medium, the relative abundance of mono–rhamnolipids increased up to 55% in the culture medium containing OMW. The difference in the rhamnolipid congeners produced in each medium explains their different surface–active properties. To the best of our knowledge, this is the first report of rhamnolipid production by *B. thailandensis* using a culture medium containing agro–industrial by–products as sole ingredients. Furthermore, rhamnolipids produced in the different media recovered around 60% of crude oil from contaminated sand, demonstrating its potential application in the petroleum industry and bioremediation.

5.1 Introduction

Biosurfactants are amphiphilic surface–active compounds produced by various microorganisms, comprised of hydrophobic and hydrophilic moieties, that contribute to the reduction of surface and interfacial tensions. Their structure also promotes emulsification and demulsification, wetting, spreading, foaming and solubilization of immiscible compounds (Gudiña & Teixeira, 2022; Varjani et al., 2021). These biomolecules are attracting increasing interest over their chemical counterparts due to their advantages (lower toxicity and higher biodegradability) and potential applications in bioremediation, pharmaceuticals, cosmetics, agriculture, food and petroleum industries, among others (Gudiña & Teixeira, 2022; Jahan et al., 2020).

Rhamnolipids are among the most widely studied biosurfactants. They are composed of one or two rhamnose molecules, linked to one to three β–hydroxy fatty acids, either saturated or unsaturated, with a chain length of 8 to 16 carbon atoms (Varjani et al., 2021). In addition to their surface–activity and emulsifying properties, rhamnolipids exhibit antimicrobial and antifungal activity (Ndlovu et al., 2017; Rodrigues et al., 2021). However, their main producer, *Pseudomonas aeruginosa*, is an opportunistic human pathogen, raising concerns regarding the safety of the rhamnolipids it produces and limiting their application in several fields (Toribio et al., 2010). Furthermore, the high operational costs associated to their production restricts their industrial–scale applications (Jahan et al., 2020). Several attempts to reduce the production costs of rhamnolipids have been conducted and include the use of low–cost agro–industrial wastes and by–products as substrates (Gudiña, Rodrigues, et al., 2015; Gudiña et al., 2016; Varjani et al., 2021).

To overcome these concerns, alternative rhamnolipid–producing microorganisms are being studied. For example, *Lysinibacillus sphaericus* IITR51 and *Planococcus* spp. produce rhamnolipids with antimicrobial properties (V. K. Gaur et al., 2019, 2020). *Enterobacter cloacae* BAGM01 has been reported to produce rhamnolipids that are stable at high temperatures (up to 121°C) and salinities (35 g NaCl/L), using different carbon sources, including diesel and sunflower oil (Curiel–Maciel et al., 2021). *Thermoanaerobacter* sp. CM–CNRG TB177 is also able to produce rhamnolipids using alternative carbon sources like molasses (Segovia et al., 2021). *Paraburkholderia* sp. C3 produces rhamnolipids that demonstrated to be useful in bioremediation applications using the biodiesel by–product glycerol as carbon source (Cao et al., 2021).

Burkholderia thailandensis E264 is another non–pathogenic rhamnolipid producer, that has been widely studied in the past years. This microorganism produces mainly di–rhamnolipids with longer β–

hydroxy fatty acid chains (C14, C16) when compared to *P. aeruginosa* (mainly C10) (Dubeau et al., 2009). Two identical gene clusters, containing the genes *rhlA*, *rhlB* and *rhlC*, are present in the genome of *B. thailandensis*, and both of them contribute to rhamnolipids biosynthesis (Dubeau et al., 2009). On the contrary, in *P. aeruginosa*, only a single copy of those genes exists, and the genes *rhlA* and *rhlB* are present in one operon, whereas the gene *rhlC* is present in a different location in the genome (Toribio et al., 2010). However, due to the low rhamnolipid yields of *B. thailandensis* comparing to *P. aeruginosa*, it is important to develop new strategies to improve their yield in a way that is cost–effective.

In this work, corn steep liquor (CSL) was evaluated as substrate for rhamnolipid production by *B. thailandensis* E264. Olive mill wastewater (OMW) is another interesting substrate that has been used as an inexpensive source of long–chain fatty acids for rhamnolipid production by *P. aeruginosa* (Gudiña et al., 2016). OMW is a liquid residue generated during the extraction of olive oil. It contains long–chain fatty acids, carbohydrates, phenolic compounds, organic acids, tannins, pectins and minerals (Dermeche et al., 2013). Due to its low biodegradability, OMW is difficult to process and an environmentally hazardous residue. About 30 million m^3 of OMW are produced in the Mediterranean countries per year; consequently, the valorization of this residue is a crucial aspect for reaching circular economy within the olive oil sector (Dermeche et al., 2013; Hamimed et al., 2021).

The aim of this work was to optimize rhamnolipid production by *B. thailandensis* E264 using CSL and OMW as low–cost substrates, characterize the rhamnolipids produced, and study their applicability in microbial enhanced oil recovery (MEOR) and bioremediation.

5.2 Materials and methods

5.2.1 Strain and culture conditions

B. thailandensis E264 (ATCC 700388) was used in this study. The strain was maintained in Luria–Bertani (LB) medium, supplemented with 20% (v/v) of glycerol at −80°C. Pre–cultures were prepared by inoculating 20 mL of standard (S) medium (glycerol 40 g/L, peptone 5 g/L, meat extract 3 g/L, pH 7.0) with 100 µL from a frozen stock, and were incubated overnight at 30°C and 180 rpm.

5.2.2 Rhamnolipid production in flasks

Rhamnolipid production by *B. thailandensis* E264 was evaluated in 500 mL flasks, containing 150 mL of the different culture media. Each flask was inoculated with 1.5 mL of a pre–culture and incubated at 30°C and 180 rpm for different time intervals (between 96 and 240h). S medium was used as control, as it has been previously used for rhamnolipid production by *B. thailandensis* (Dubeau et al., 2009; Elshikh et al., 2017; Funston et al., 2016, 2017). CSL (kindly provided by COPAM – Companhia Portuguesa de Amidos, S. A. (Portugal)) and OMW (obtained from an olive oil mill located in the north of Portugal) were evaluated as alternative substrates. Both substrates were characterized in our previous works (Gudiña, Rodrigues, et al., 2015; Gudiña et al., 2016), and their composition is provided in Table 5.1.

Table 5.1 – Characterization of corn steep liquor (CSL) and olive mill wastewater (OMW) used in this work.

Parameter	Value	Reference
CSL		
Total carbohydrates (g/L) (Phenol–sulfuric)	75.0 ± 2.0	(Gudiña, Rodrigues, et al., 2015)
Total proteins (g/L) (Lowry)	5.0 ± 0.2	(Gudiña, Rodrigues, et al., 2015)
Glucose (g/L) (HPLC)	20.8 ± 3.5	This study
Fructose (g/L) (HPLC)	20.9 ± 3.1	This study
Lactic acid (g/L) (HPLC)	128.1 ± 1.0	This study
OMW		
Total phenols (g/L) (Folin–Ciocalteu)	2.6 ± 0.1	(Gudiña et al., 2016)
Total carbohydrates (g/L) (Phenol–sulfuric)	21.2 ± 1.3	(Gudiña et al., 2016)
Total proteins (g/L) (Lowry)	0.45 ± 0.1	(Gudiña et al., 2016)
Glucose (g/L) (HPLC)	3.4 ± 0.1	This study
Fructose (g/L) (HPLC)	9.4 ± 0.1	This study
Lipids (g/L) (Soxtec)	4.8 ± 0.3	(Gudiña et al., 2016)
Palmitic acid (C16) (mg/L) (GC)	513.0 ± 32.0	(Gudiña et al., 2016)
Stearic acid (C18) (mg/L) (GC)	129.0 ± 12.0	(Gudiña et al., 2016)
Oleic acid (C18:1) (mg/L) (GC)	3387.0 ± 89.0	(Gudiña et al., 2016)
Linoleic acid (C18:2) (mg/L) (GC)	284.0 ± 21.0	(Gudiña et al., 2016)

CSL was diluted with demineralized water at different concentrations (5–20% (v/v)) and used as culture medium, either alone or supplemented with OMW (5–25% (v/v)). All the media were adjusted to

pH 7.0. Samples were taken at different time intervals to determine bacterial growth, rhamnolipid production and substrates consumption, as described in the following sections. All experiments were performed in triplicate.

5.2.3 Optimizing a glycerol and CSL–based medium for rhamnolipid production

To optimize rhamnolipid production, a central composite rotational design (CCRD) was performed using the Statistica 12.0 software for two independent variables: CSL (X_1) and glycerol (X_2) concentrations. Each variable was evaluated in five levels (Table 5.2) over 11 runs that were simulated by the statistical software, where 3 of those were repetitions at the central point. The independent response analyzed was surface tension reduction after 120h of growth at 30°C and 180 rpm, calculated as the difference between the surface tension of demineralized water (approximately 70 mN/m) and the surface tension (ST) measured on the cell–free supernatants, as described in a following section. The results were subjected to an analysis of variance (ANOVA).

Table 5.2 – Experimental level and ranges for the independent variables used in the CCRD.

Independent variable	Code	Experimental design level				
		–1.41	–1	0	+1	+1.41
CSL (% (v/v))	X_1	5.95	6.70	8.50	10.30	11.05
Glycerol (mL/L)	X_2	1.99	3.90	8.50	13.10	15.00

5.2.4 Rhamnolipid production in bioreactor

The scale–up process was performed in a 3.7 L–bioreactor (RALF Advanced, Bioengineering AG, Switzerland) with 2 L of the culture medium containing CSL (7.5% (v/v)) and OMW (10% (v/v)). Because this medium contains high amounts of precipitates, which can interfere with the bioreactor's performance, it was centrifuged (15316 x g, 20 min) before being introduced in the reactor vessel. Two mL of silicon anti–foaming agent (Sigma–Aldrich) were added to the culture medium to avoid the formation of foam.

A pre–culture of *B. thailandensis* E264 was first prepared in S medium (20 mL), grown overnight at 30°C and 150 rpm, and used to inoculate a second pre–culture, containing 100 mL of the same culture medium used in the bioreactor, which was incubated for 48h at 30°C and 150 rpm. Subsequently, the inoculum was centrifuged (5514 x g, 10 min) and the cells were resuspended in 5 mL of a phosphate–buffered saline (PBS) solution, which were used to inoculate the bioreactor.

The experiments were conducted under batch mode over 78h at 30°C. Optimization of the culture conditions was performed in the different media (S, CSL and CSL+OMW) by evaluating various stirring rates (250–350 rpm) and air flows (constant air flow at 0.3–0.4 vvm (volume of air per unit volume per minute) or an alternating air flow cycle that shifted from no airflow over 50 s to 0.3 vvm for another 50 s). After optimization, stirring rate and air flow were kept constant at 350 rpm and 0.3 vvm, respectively. Samples were taken at different time points and used to determine bacterial growth, substrates consumption and rhamnolipid production. Experiments were performed in duplicate.

5.2.5 Rhamnolipid recovery

Rhamnolipids produced by *B. thailandensis* E264 were recovered through adsorption chromatography using the polystyrene resin Amberlite® XAD®–2 (Sigma–Aldrich). A 125 mL column was filled with Amberlite XAD–2 and equilibrated with two volumes of 0.1 M potassium phosphate buffer (pH 6.1). Subsequently, 100 mL of cell–free supernatant (centrifuged at 15316 x g for 20 min) were adjusted to pH 6.1 and introduced into the column, which was then washed with four volumes of demineralized water to remove the non–adsorbed compounds. The column was further washed with 300 mL of solutions with increasing concentrations of methanol (25, 50 and 75% (v/v)), followed by 200 mL of pure methanol. The presence of rhamnolipids in the eluents was assessed by thin–layer chromatography (TLC) (data not shown), according to Rodrigues and co–workers (2017). After evaporation of the solvents, the recovered rhamnolipids were dissolved in 20 mL of demineralized water and freeze–dried. The products obtained were weighed and stored at –20°C. The amount of rhamnolipids produced was determined gravimetrically.

5.2.6 Analytical techniques

5.2.6.1 Bacterial growth determination

Bacterial growth was determined through the plate count technique. Samples (1 mL) were taken at different time points of fermentation and were serially diluted with NaCl–Tween buffer (9 g/L of NaCl and 100 mg/L of Tween 80); 100 µL of each dilution was plated on a LB agar plate and incubated at 30°C for 48h. The number of colony forming units (CFU) at each dilution was counted and the average expressed as CFU/mL.

5.2.6.2 Substrates consumption determination

Substrates consumption was evaluated by high–performance liquid chromatography (HPLC) using an Aminex HPX–87H (300 × 7.8 mm, Bio–Rad, USA) column coupled to a refractive index detector (RI–2031 Plus, JASCO) and an ultraviolet (UV) detector (K–2501, Knauer). Samples collected at different time points of fermentation were centrifuged (2450 x *g*,15 min) to remove the cells, and the supernatants were filtered and analyzed. H_2SO_4 (5 mM) was used as mobile phase at a flow rate of 0.6 mL/min, and the column was maintained at 60°C. The concentrations of glucose, fructose and lactic acid were calculated according to calibration curves prepared using pure compounds.

5.2.6.3 Surface tension measurement and critical micelle concentration

Surface tension (ST) and critical micelle concentrations (CMC) were determined as described in Chapter 3 (3.2.6.4), with solutions prepared in 10 mM Tris–HCl buffer (pH 7.4).

5.2.6.4 Emulsifying activity

Emulsifying activity (E_{24}) of rhamnolipid solutions was determined against n–hexadecane, as described elsewhere (Gudiña et al., 2016). All emulsification indexes were determined in duplicate.

5.2.6.5 Contact angle measurement

To evaluate the ability of the produced rhamnolipids to alter surface wettability, contact angles were measured between a water/rhamnolipid solution droplet and an oil–coated glass surface at room temperature using an automatic optical contact angle measuring system (OCA 20, DataPhysics). Clean microscope glass slides were aged in crude oil from the Potiguar oilfield in Brazil (kindly provided by PARTEX oil and gas) at 50°C for 7 days. After ageing, the glass slides were left at room temperature to dry the oil and wiped with a clean paper towel to remove excess free oil from the surface. Contact angles were then measured through the sessile drop method by placing a drop of rhamnolipid solution at different concentrations (2 x CMC and 5 x CMC) or the cell–free supernatant on the oil–coated glass slide. Measurements were taken 0, 2 and 5 minutes after the drop contacted the surface. Demineralized water was used as control and the results from the *B. thailandensis* E264 rhamnolipids were compared to a solution of commercial rhamnolipids (RL–90, Sigma–Aldrich, 90% of purity).

5.2.7 Rhamnolipid characterization

5.2.7.1 Fourier transform infrared spectroscopy

The rhamnolipid mixtures previously obtained were characterized through Fourier transform infrared spectroscopy (FTIR). FTIR spectra were recorded using the IRSpirit FTIR spectrometer (Shimadzu, Kyoto, Japan) at room temperature (25°C). The main functional groups of rhamnolipids were observed between 400 and 4000 wavenumbers (cm^{-1}) at a resolution of 2 cm^{-1}.

5.2.7.2 Identification of rhamnolipid congeners

Individual rhamnolipid congeners present in the different rhamnolipid mixtures were identified by electrospray ionization (ESI) mass spectrometry (MS) using a Compact™ Mass Spectrometer (Bruker Daltonics, Bremen, Germany) in negative electrospray ionization mode. The instrument parameters were as follows: electrospray voltage: –5 kV; scan range: 50–3000 m/z; drying gas: nitrogen; flow rate: 4.0 L/min; temperature: 200°C. For MS spectra analysis, a Bruker Compass Data Analysis 4.2 software was used.

5.2.7.3 Gas chromatography–mass spectrometry

The different rhamnolipid mixtures (1 mg) were refluxed in 2 N HCl (0.5 mL) for 2h. The 3–hydroxy fatty acids (3–OH–FAs) were extracted three times with hexane (10 mL). Next, the free 3–OH–FAs were derivatized using 2.5% sulfuric acid in methanol and resulting 3–hydroxy fatty acid methyl esters (3–OH–FAMEs) were analyzed by gas chromatography–mass spectrometry (GC–MS) (Shimadzu, Kyoto, Japan) using a Zebron ZB–FAME capillary column (30 m × 0.25 mm × 0.20 µm). Split injection mode was used for injecting the sample (1 µL at 250°C) using helium (1 mL/min). All the experiments were performed in triplicate.

5.2.8 Oil recovery assays

5.2.8.1 Oil recovery in sand–pack columns

Oil recovery assays in sand–pack columns were performed as described in Chapter 4 (4.2.5). The assays were performed using Light Arabian crude oil (apparent viscosity at 40°C ($\eta_{40°C}$) of 8 mPa

s at 1.4 s^{-1}), crude oil from the Potiguar oilfield in Brazil ($\eta_{40°C}$ = 110 mPa s at 1.4 s^{-1}) or a crude oil mixture ($\eta_{40°C}$ = 247 mPa s at 1.4 s^{-1}).

In columns containing Arabian Light crude oil, 1 pore volume (PV) of the cell–free supernatant (CFS) in CSL medium was injected into the columns and incubated for 24h or 48h, followed by the injection of 400 mL of demineralized water. Control assays were performed under the same conditions by injecting 1 PV + 400 mL of demineralized water into the columns.

In columns containing the oil mixture, 1 PV of CFS in CSL medium was injected into the columns and incubated for 24h. Next, 200 mL of CFS from *R. viscosum* CECT 908 in Rv2 medium (as described in Chapter 4) ($\eta_{40°C}$ = 263 ± 3 mPa s at 1.4 s^{-1}) were injected into the columns to test the synergistic effect between biosurfactants and biopolymers, followed by 200 mL of demineralized water. Control assays were performed under the same conditions by injecting 1 PV of demineralized water + 200 mL of CFS from *R. viscosum* CECT 908 + 200 mL of demineralized water or 1 PV + 400 mL of demineralized water into the columns.

In columns containing Potiguar oil, 1 PV of RL–90 or CFS in CSL or CSL+OMW media were injected into the columns and incubated for 24h or 48h. Next, 200 mL of a xanthan gum (Sigma Aldrich) solution prepared at 1 g/L ($\eta_{40°C}$ = 99 ± 6 mPa s at 1.4 s^{-1}) were injected into the columns, followed by 200 mL of demineralized water.

5.2.8.2 Recovering oil from artificially contaminated sand

Bioremediation assays were performed using artificially contaminated sand, containing 10% (w/w) of crude oil from the Potiguar oilfield in Brazil ($\eta_{40°C}$ = 110 mPa s at 1.4 s^{-1}, and a density of 910 g/L). To prepare the artificially contaminated sand, 40 g of dry sand were mixed with 4 g of crude oil in 100 mL flasks and allowed to age for 5 days at 50°C. Afterwards, 40 mL of CFS samples from cultures of *B. thailandensis* E264 performed in different culture media (S, CSL and CSL+OMW) were added to each flask. Control assays were performed using 40 mL of the corresponding uninoculated culture medium. The flasks were incubated at 150 rpm and 50°C for 24h. After the incubation period, the oil removed from the sand was recovered from the liquid surface and its volume was measured. In order to compare the performance of rhamnolipids produced by *B. thailandensis* E264 in the different culture media with RL–90, they were dissolved in the uninoculated culture media (S, CSL and CSL+OMW) at a concentration

of 200 mg/L, and oil recovery assays were performed as described above. All the experiments were carried out in triplicate.

5.3 Results

5.3.1 Rhamnolipid production by *B. thailandensis* E264 in flasks

Rhamnolipid production by *B. thailandensis* E264 was first evaluated using the standard (S) medium (Figure 5.1). The rhamnolipids produced reduced the culture medium ST to 32.1 ± 1.4 mN/m after 96h of growth. During this time, only about 25% of the total amount of glycerol provided (40 g/L) was consumed by *B. thailandensis* E264 to produce 139 ± 64 mg/L of rhamnolipids.

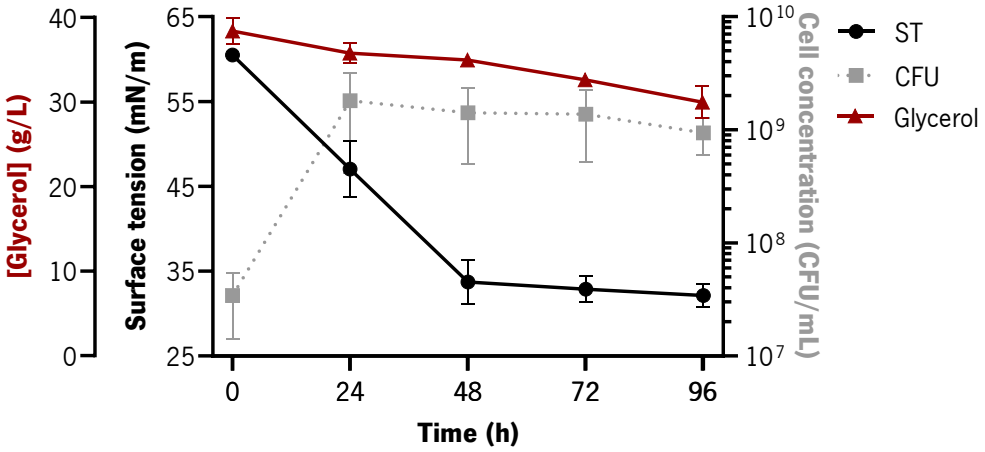

Figure 5.1 – Surface tension values (mN/m), glycerol concentration (g/L) and bacterial growth (CFU/mL) over time of *Burkholderia thailandensis* E264 grown in standard (S) medium in flasks at 30°C and 180 rpm.

Aiming to reduce the production costs, rhamnolipid production by *B. thailandensis* E264 was evaluated using several low–cost media containing agro–industrial residues as sole ingredients (Table 5.3). CSL was evaluated as a sole substrate for rhamnolipid production at different concentrations (5–20% (v/v)). The best results were obtained with a culture medium containing 7.5% (v/v) CSL, achieving ST values around 30 mN/m after 72h of growth (Table 5.3 and Figure 5.2). Subsequently, the effect of supplementing the CSL medium with different concentrations of OMW (5–25% (v/v)) was studied. The lowest ST values (around 27.4 mN/m) were obtained with the medium containing 7.5% (v/v) CSL and 10% (v/v) OMW as sole substrates after 72–96h of growth (Table 5.3). Evolution of ST, bacterial growth

and substrates consumption with this culture medium is illustrated in Figure 5.2. For the other culture media presented in Table 5.3, no significant ST reductions were achieved even after 240h of growth when compared with those observed at 96h (data not shown). Consequently, they were not considered for rhamnolipid production.

Table 5.3 – Surface tension values (mN/m) obtained with *Burkholderia thailandensis* E264 grown in CSL (5–20% (v/v)) and CSL supplemented with OMW (5–25% (v/v)) at 30°C and 180 rpm.

Culture medium	Surface Tension (mN/m)				
	0h	24h	48h	72h	96h
5% CSL	50.2 ± 0.4	44.8 ± 1.2	36.2 ± 3.5	35.6 ± 1.2	38.2 ± 2.0
7.5% CSL	48.6 ± 0.6	47.2 ± 1.9	33.0 ± 1.7	30.3 ± 0.9	32.1 ± 0.9
10% CSL	48.3 ± 0.5	48.4 ± 0.5	37.6 ± 4.5	32.8 ± 1.3	32.5 ± 1.2
12.5% CSL	47.9 ± 0.8	47.1 ± 1.1	48.7 ± 1.8	46.3 ± 5.5	37.5 ± 0.8
15% CSL	47.5 ± 0.7	–	49.6 ± 0.7	50.0 ± 0.6	–
20% CSL	46.1 ± 0.3	–	48.6 ± 0.8	49.5 ± 0.7	–
7.5% CSL + 5% OMW	41.0 ± 0.5	–	37.4 ± 0.9	28.2 ± 0.4	27.7 ± 0.2
7.5% CSL + 10% OMW	41.8 ± 0.6	43.3 ± 0.2	29.8 ± 0.9	27.4 ± 0.4	27.5 ± 0.2
7.5% CSL + 15% OMW	39.7 ± 0.4	–	43.3 ± 0.3	42.5 ± 0.2	42.1 ± 0.2
7.5% CSL + 20% OMW	40.1 ± 0.4	–	42.6 ± 0.2	42.2 ± 0.2	41.5 ± 0.1
7.5% CSL + 25% OMW	40.2 ± 0.4	–	42.0 ± 0.3	41.8 ± 0.2	41.3 ± 0.3
Control (S medium)	60.5 ± 0.8	47.0 ± 3.3	33.7 ± 2.6	32.9 ± 1.6	32.1 ± 1.4

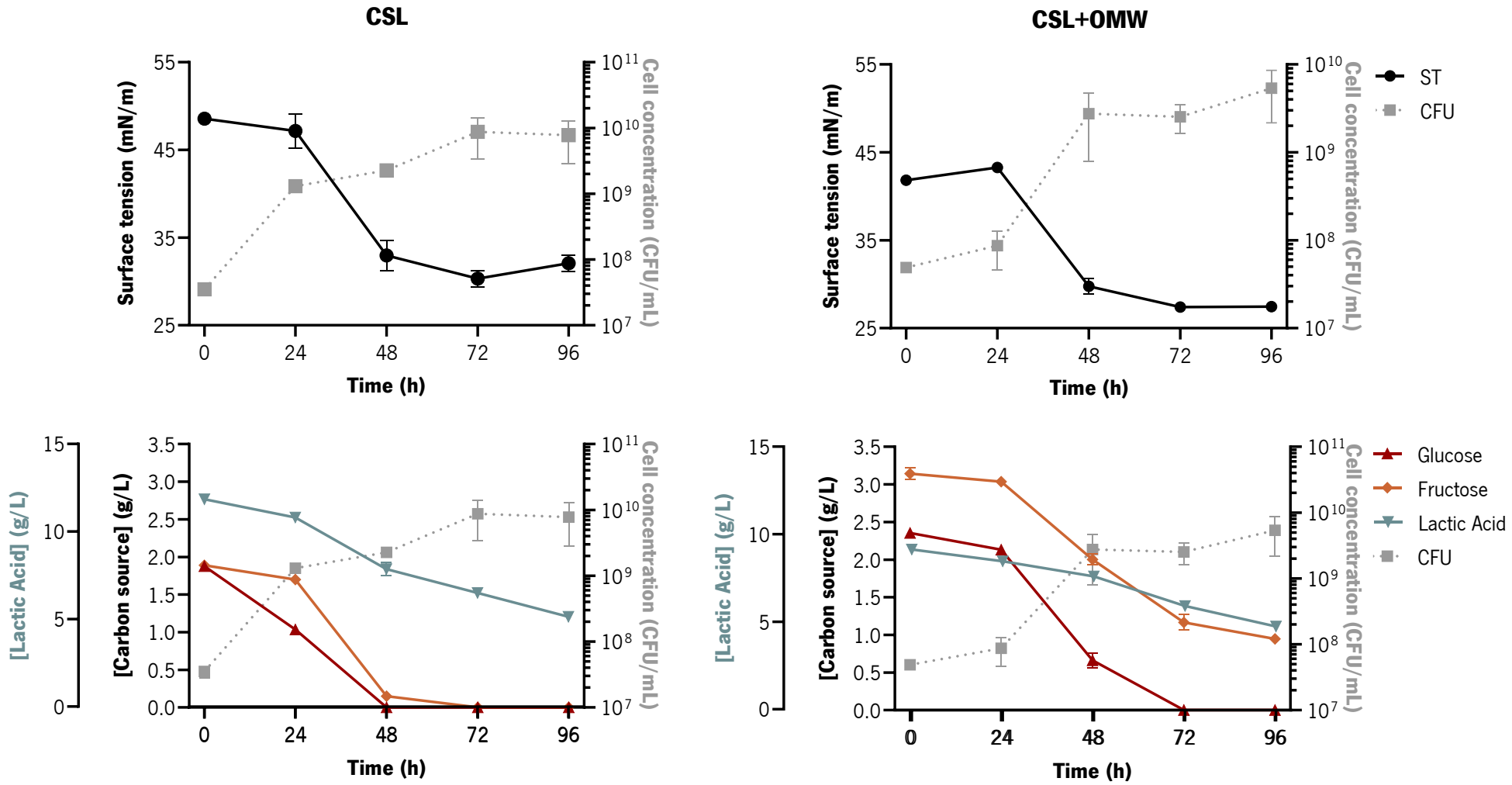

Figure 5.2 – Top: surface tension values (mN/m) and bacterial growth (CFU/mL); Bottom: carbon source and lactic acid concentrations (g/L), and bacterial growth (CFU/mL) over time of *Burkholderia thailandensis* E264 grown in flasks in CSL and CSL+OMW media at 30°C and 180 rpm.

HPLC analysis showed that in the CSL medium (7.5% (v/v) CSL), glucose (1.9 g/L) and fructose (1.9 g/L) were fully consumed within the first 48h of growth. In the CSL+OMW medium (7.5% (v/v) CSL + 10% (v/v) OMW), which contains a higher concentration of both sugars (2.4 g glucose/L, 3.2 g fructose/L), fructose was not completely exhausted, even after 96h. Moreover, 4.9 and 6.8 g/L of lactic acid present in CSL+OMW and CSL media, respectively, were consumed, that might be used as an additional carbon source (Figure 5.2). The low–cost media also allowed a higher bacterial growth than the standard medium, although in the CSL+OMW medium there was almost no growth during the first 24h, probably due to the presence of inhibitory compounds in OMW, such as phenolic compounds (Gudiña et al., 2016) (Table 5.1 and Figure 5.2).

The amount of rhamnolipids produced in the CSL medium after 72h of growth was 175 ± 3 mg/L, which is about 1.3 times the amount obtained in the standard medium. By supplementing the CSL medium with OMW, rhamnolipid production further increased up to 253 ± 46 mg/L in 96h. To the best of our knowledge, this is the first report of rhamnolipid production by *B. thailandensis* using a culture medium containing agro–industrial by–products as sole ingredients.

5.3.2 Optimization of rhamnolipid production in CSL medium supplemented with glycerol

In previous assays (Section 5.3.1), it was observed that the carbon sources in CSL medium were fully consumed by *B. thailandensis* E264 within 48h of growth. In order to maximize rhamnolipid production using this by–product, several concentrations of glycerol were added to increase the carbon source content of the medium. An experimental CCRD was used to determine the optimum quantities of each component that should be added to the medium to increase rhamnolipid production (Table 5.2). The results for ST reduction measured for the CFS diluted 2.5 times (Table 5.4) were subjected to a regression analysis, where a first–order regression model was obtained:

$$ST\ reduction = 37.667 - 5.070X_1 \quad (5.4)$$

The model had an R^2 of 0.86219, indicating that there is a good agreement between the values of ST reduction observed and the ones predicted by the model (Table 5.4).

Table 5.4 – Experimental CCRD matrix with the independent variables and surface tension (ST) reduction response, observed (measured in the cell–free supernatant diluted 2.5 times) and predicted by the first–order regression model.

Experiment	Coded variable		Response variable: ST reduction (mN/m)	
	X_1	X_2	Observed	Predicted
1	–1	–1	37.500	39.169
2	–1	+1	39.000	38.495
3	+1	–1	21.800	25.830
4	+1	+1	29.700	31.556
5	–1.41	0	38.500	38.407
6	+1.41	0	27.500	24.068
7	0	–1.41	37.800	34.501
8	0	+1.41	38.300	38.074
9	0	0	37.100	37.667
10	0	0	37.900	37.667
11	0	0	38.000	37.667

The significance of the model was checked by ANOVA (Table 5.5). It was shown that only the linear term for CSL concentration (X_1) was significant at the 95% confidence level, having a *p*–value < 0.05. Furthermore, this term was shown to have a negative effect on the model (Equation 5.4), meaning that at high concentrations it negatively impacts rhamnolipid production. Figure 5.3 represents the 3D plot of the model in an estimated response over the different glycerol and CSL concentrations. The figure reveals that ST reduction improves with CSL concentrations up to 8% (v/v), approximately, but rapidly decreases with higher CSL concentrations. This is in accordance with the results obtained in this study, where CSL concentrations between 12.5 and 20% (v/v) resulted in high ST values (46.3–50.0 mN/m at 72h) (Table 5.3).

Table 5.5 – Analysis of variance (ANOVA) for the surface tension reduction.

Factor	Sum of squares	Degree of freedom	Mean squares	F value	*p*–value
$\mathbf{X_1}$	205.602	1	205.602	22.381	0.005
$\mathbf{X_1^2}$	58.354	1	58.354	6.352	0.053
$\mathbf{X_2}$	12.769	1	12.769	1.390	0.291
$\mathbf{X_2^2}$	2.685	1	2.685	0.292	0.612
$\mathbf{X_1\ X_2}$	10.240	1	10.240	1.115	0.339
Error	45.932	5	9.186		
Total SS	333.302	10			

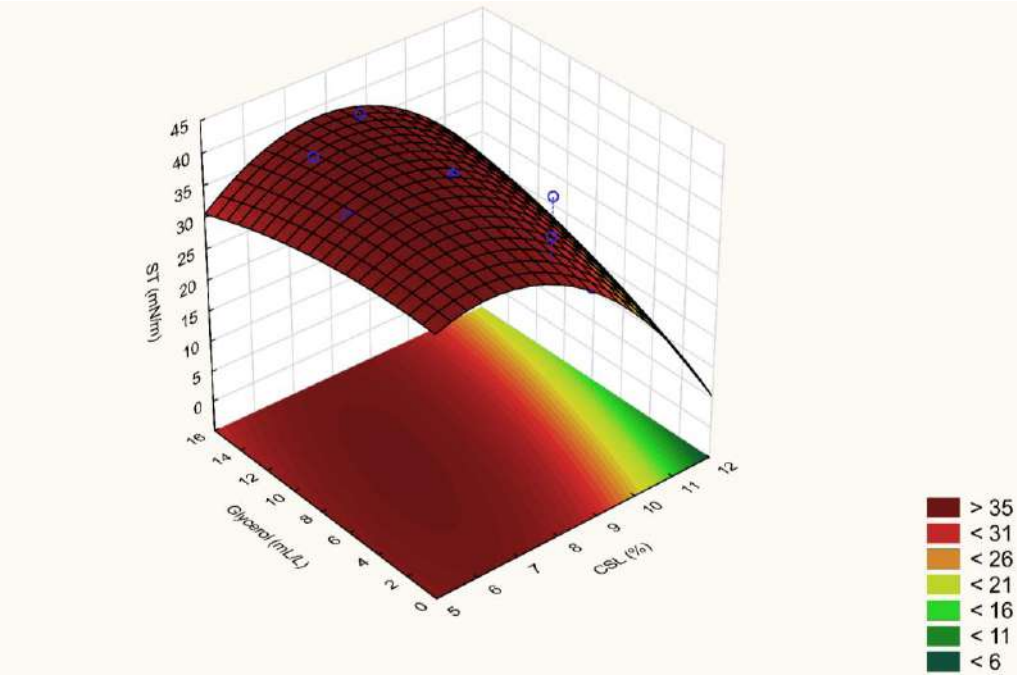

Figure 5.3 – Response surface plot showing the interactive effect of glycerol (mL/L) and CSL (% (v/v)) concentrations on surface tension reduction.

From this analysis, the optimum medium composition is: 7.081% (v/v) CSL and 8.508 (mL/L) glycerol. Using this medium, *B. thailandensis* E264 produced 315 mg/L of rhamnolipid that reduced the ST of water up to 29.3 ± 0.2 mN/m over 120h of growth. The amount of rhamnolipids produced using this culture medium was higher than using the CSL and the CSL+OMW media. However, this medium was not selected for further studies, as it will be explained in Section 5.3.5.

5.3.3 Rhamnolipid production by *B. thailandensis* E264 in bioreactor

Rhamnolipid production in bioreactor was evaluated with the different culture media previously assayed in flask assays at various operating conditions (Figure 5.4), which allowed to establish the optimum agitation and aeration rates. According to the results obtained here and in flask assays, the low–cost medium CSL+OMW was selected for further evaluation using the growth conditions that yielded the best results (350 rpm and 0.3 vvm) (Figure 5.5). Besides using different operational conditions, the inoculation method in this experiment was also different than in the other assays. Here, the second pre–culture was inoculated with the full amount of cells from the first pre–culture, thus, the bioreactor was inoculated with more cells than in the other cases.

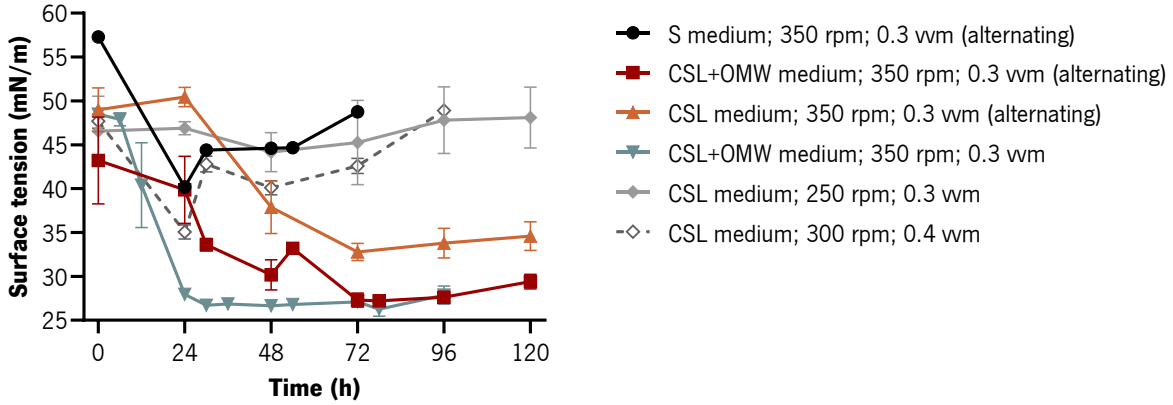

Figure 5.4 – Surface tension values (mN/m) over time of *Burkholderia thailandensis* E264 grown in bioreactor with S, CSL and CSL+OMW media at different operational conditions.

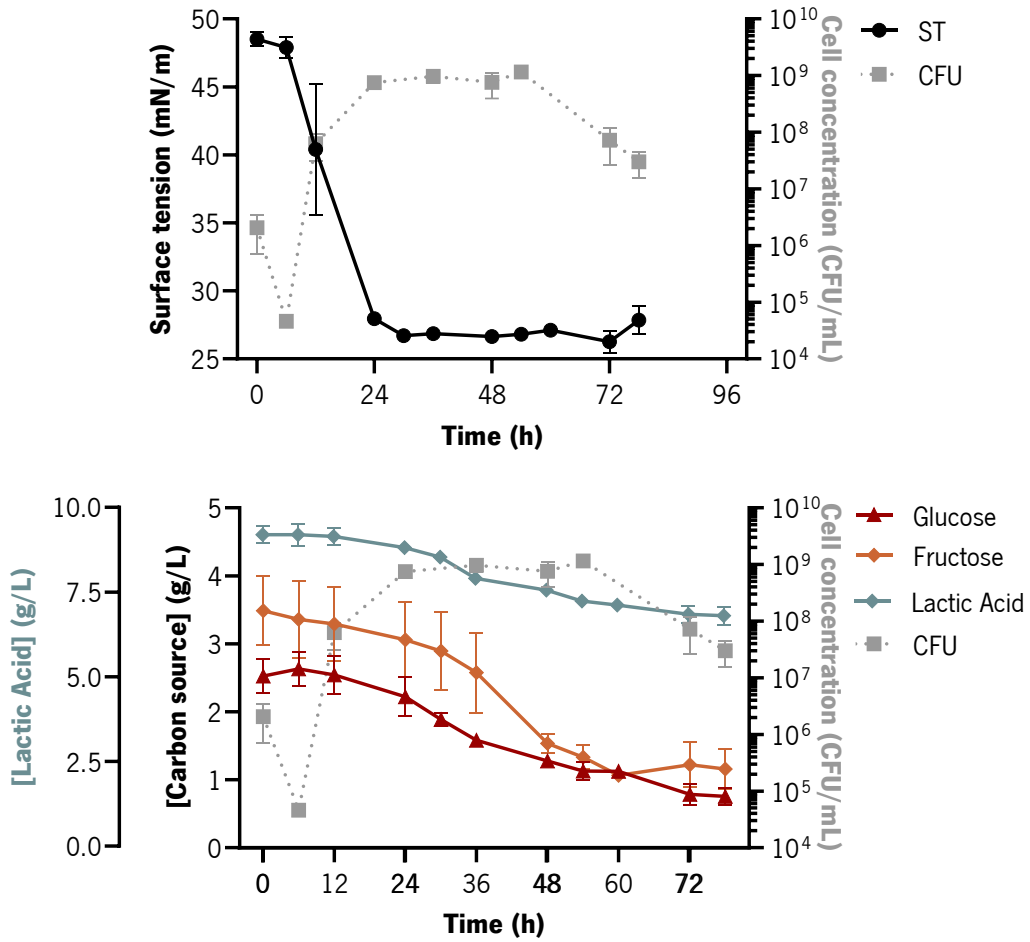

Figure 5.5 – Top: surface tension values (mN/m) and bacterial growth (CFU/mL). Bottom: carbon source and lactic acid concentrations (g/L), and bacterial growth (CFU/mL) over time of *Burkholderia thailandensis* E264 grown in bioreactor with CSL+OMW medium at 30°C, 350 rpm and 0.3 vvm.

As it can be seen in Figure 5.5, the ST decreased faster when compared with flask assays, being the lowest ST value (26.3 ± 0.8 mN/m), achieved after 72h of growth. The highest rhamnolipid production (269 ± 95 mg/L) was achieved after 54h, which results in a better productivity when compared to flask assays, where the highest production was achieved after 96h. Glucose and fructose consumption displayed similar profiles in flask and bioreactor assays, although in the last case, about 1 g glucose/L remained in the culture medium after 78h of growth. The amount of lactic acid consumed in bioreactor (2.3 g/L) was also lower than in flasks (4.9 g/L) (Figure 5.2 and Figure 5.5). Bacterial growth displayed a different behavior than the one observed in flasks. An abrupt decline in the number of cells was observed during the first hours of growth, which may be due to the mechanical stress applied to the cells in the bioreactor. In fact, in order to achieve good results regarding bacterial growth and rhamnolipid production, it was necessary to increase the size of the inoculum used for the bioreactor five times when compared with flask assays, as described in the Materials and Methods section (5.2.4). Bacterial growth was slightly lower in bioreactor (1.2×10^9 CFU/mL, compared to 5.4×10^9 CFU/mL in flask), and a decline phase was observed after 54h (Figure 5.2 and Figure 5.5).

5.3.4 Rhamnolipid chemical characterization

FTIR analysis of the products obtained in S, CSL and CSL+OMW media (Figure 5.6) displayed similar functional groups to those reported for glycolipids in previous works (Borah et al., 2015; V. K. Gaur et al., 2020; Sen et al., 2020; Xu et al., 2020). The asymmetric and symmetric stretching of methylene (–CH) were detected at 2923 cm^{-1} and 2853 cm^{-1}, respectively, for rhamnolipids produced in S and CSL media, and at 2920 cm^{-1} and 2851 cm^{-1} for the CSL+OMW medium. The characteristic band of carbonyl groups (–C=O) was found at 1724 cm^{-1} and 1657 cm^{-1} for S medium, 1714 cm^{-1} and 1650 cm^{-1} for CSL, and 1714 cm^{-1} and 1658 cm^{-1} for CSL+OMW, confirming the presence of ester compounds. The carboxylic acid plane bending (–COH–) was detected at 1454 cm^{-1} and 1397 cm^{-1} for S medium, 1453 cm^{-1} and 1400 cm^{-1} for CSL, and 1445 cm^{-1} for CSL+OMW. The stretching band observed at 1040 cm^{-1}, 1052 cm^{-1} and 1065 cm^{-1} for S, CSL and CSL+OMW media, respectively, corresponded to the –C–O– bonds between the carbon atoms and the hydroxyl groups present in the rhamnose rings. Finally, the peaks detected at 704 cm^{-1}, 705 cm^{-1} and 698 cm^{-1} for S, CSL and CSL+OMW media related to the CH_2 rocking in the lipid structure (Figure 5.6).

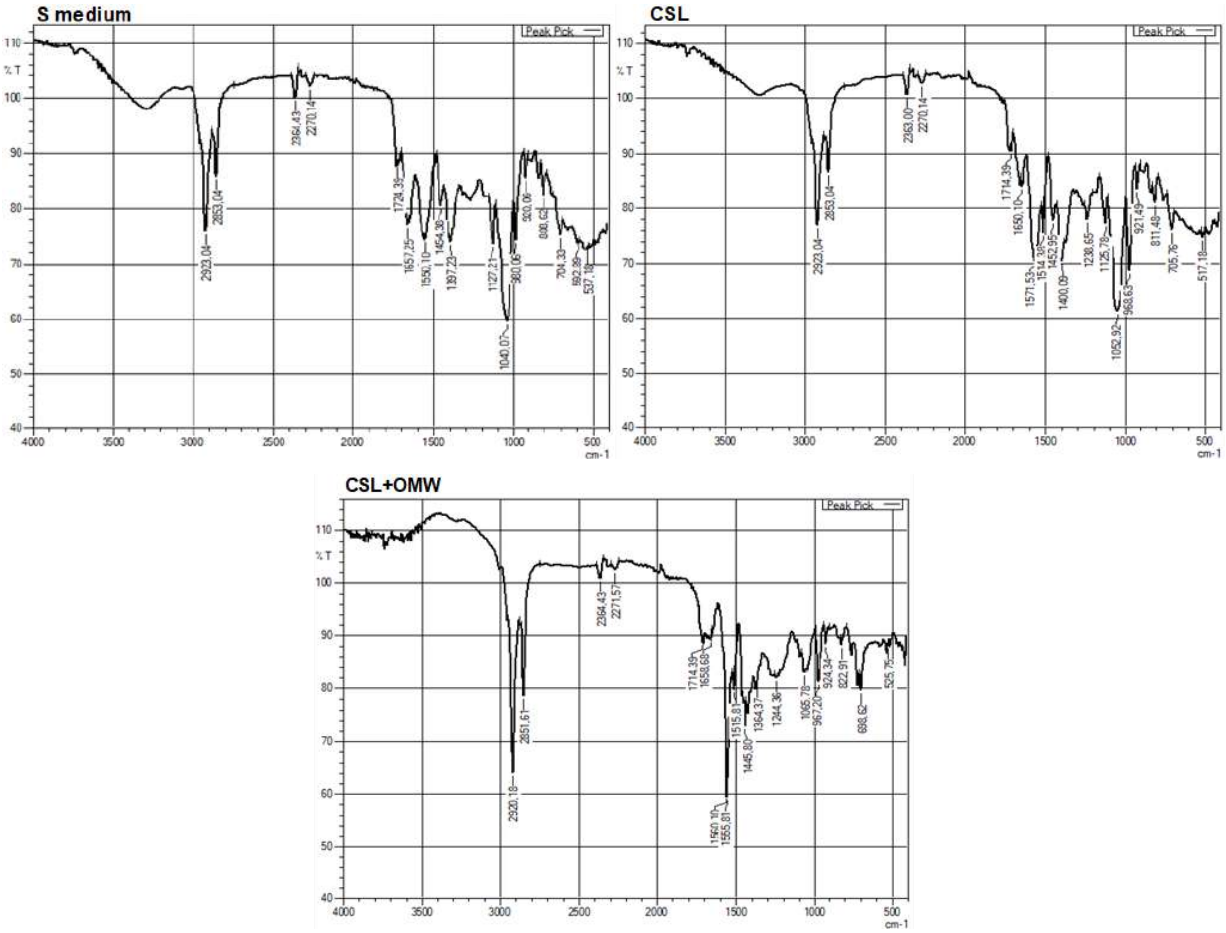

Figure 5.6 – FTIR spectra of rhamnolipids produced by *Burkholderia thailandensis* E264 in standard, CSL and CSL+OMW media.

Subsequently, the rhamnolipid congeners produced by *B. thailandensis* E264 in the different media were characterized by ESI–MS operating in negative electrospray ionization mode. The same congeners were identified in all the media, but they were present in different relative abundances (Table 5.6). The most abundant congener in S and CSL media was the di–rhamnolipid Rha–Rha–C_{14}–C_{14} (62–64%), followed by Rha–Rha–C_{12}–C_{14}/C_{14}–C_{12} (18–22%). The hydrophilic–lipophilic balance (HLB) of these rhamnolipids ranges between 10.5 and 10.9 (calculated according to the Griffin's method (Griffin, 1955), which characterizes them as oil/water emulsifiers. The supplementation of the CSL medium with OMW resulted in a substantial increase in the relative abundance of the mono–rhamnolipids Rha–C_{12}–C_{12} and Rha– C_{12}–C_{14}/C_{14}–C_{12} (Table 5.6). In fact, the relative abundance of mono–rhamnolipids increased from 5–10% in S and CSL media to 56% in the culture medium supplemented with OMW.

The mono–rhamnolipids Rha–C_{12}–C_{12}, Rha–C_{14}–C_{14} and Rha–C_{12}–C_{14}/C_{14}–C_{12} have HLB values that range from 8.3 to 9.1, being characterized as wetting and spreading agents. Because they have lower HLB values than di–rhamnolipids, they are also more hydrophobic, displaying more wetting properties than the latter.

Table 5.6 – Rhamnolipid congeners produced by *Burkholderia thailandensis* E264 and their relative abundance in the different culture media.

Rhamnolipid congeners	Pseudomolecular ion (*m/z*)	Relative abundance (%)		
		S medium	CSL	CSL+OMW
Mono–rhamnolipids (total)		*5.35*	*9.81*	*55.82*
Rha–C_{12}–C_{12}	559.38	0.76	1.66	24.74
Rha–C_{12}–C_{14}/C_{14}–C_{12}	587.41	1.86	2.92	29.79
Rha–C_{14}–C_{14}	615.45	2.73	5.23	1.29
Di–rhamnolipids (total)		*94.64*	*90.19*	*44.18*
Rha–Rha–C_{12}–C_{12}	705.44	4.95	5.9	2.27
Rha–Rha–C_{12}–C_{14}/C_{14}–C_{12}	733.47	22.63	18.04	15.62
Rha–Rha–C_{14}–C_{14}	761.50	64.09	62.60	24.59
Rha–Rha–C_{14}–C_{16}/ C_{16}–C_{14}	789.53	2.97	3.65	1.7

The analysis of the fatty acid chains present in the produced rhamnolipids identified mainly tetradecanoic acid, followed by dodecanoic acid (Table 5.7). The fatty acids identified, and their abundance, are in line with the observed rhamnolipid congeners.

Table 5.7 – The composition of 3–OH–FAMEs of rhamnolipids determined by GC–MS. The results represent the mean ± standard deviation of the analysis performed in triplicate.

3–OH–FAMEs	Relative abundance (%)		
	S medium	CSL	CSL+OMW
3–OH–dodecanoic	18.00 ± 0.21	18.04 ± 0.14	49.74 ± 0.14
3–OH–tetradecanoic	80.55 ± 0.12	80.14 ± 0.25	49.41 ± 0.17
3–OH–hexadecanoic	1.45 ± 0.09	1.82 ± 0.11	0.85 ± 0.03

5.3.5 Critical micelle concentration of rhamnolipids produced by *B. thailandensis* E264

The rhamnolipids produced in the S medium had a CMC of 58 mg/L and reduced the ST of Tris–HCl buffer from 72.0 ± 0.2 mN/m up to 28.9 ± 0.4 mN/m (Table 5.8 and Figure 5.7). In CSL medium, the CMC of the rhamnolipids produced was 108 mg/L, meaning that they were less efficient when

compared with those produced in S medium, even though their minimum ST values were similar (Table 5.8). The rhamnolipids produced in CSL+OMW medium were the most surface active, with a CMC of 51 mg/L and a minimum ST value of 27.1 ± 0.1 mN/m. Regarding the rhamnolipids produced in bioreactor using this culture medium, the CMC (48 mg/L) and the minimum ST value (27.1 ± 0.1 mN/m) were similar to those obtained in flask (Table 5.8 and Figure 5.7). Furthermore, rhamnolipid production in bioreactor was more efficient, since a similar amount of rhamnolipids, with similar surface–active properties, was produced in less time (54h instead of 96h in flask). In the optimized CSL+Glycerol medium, the CMC of the produced rhamnolipids (156 mg/L) was higher than for any of the other media, even though *B. thailandensis* E264 seemed to produce more rhamnolipids with similar surface activity to the CSL+OMW medium (ST of 27.5 ± 0.1 mN/m and 27.1 ± 0.1 mN/m, respectively) (Table 5.8 and Figure 5.7). This indicates that the rhamnolipids recovered from this medium may not be as pure as the ones recovered from the other media, or that they have a different congener distribution.

Table 5.8 – Rhamnolipid (RL) titers obtained with *Burkholderia thailandensis* E264 in standard (S), CSL, CSL+Glycerol and CSL+OMW (both in flask and bioreactor) media; Critical micelle concentration (CMC) and minimum surface tension values (ST_{min}) of rhamnolipid solutions prepared in 10 mM Tris–HCl buffer (pH 7.4).

Culture medium	RL titer (mg/L)	CMC (mg/L)	ST_{min} (mN/m)
S	139 ± 64	58	28.9 ± 0.4
CSL	175 ± 3	108	29.6 ± 0.4
CSL+Glycerol	315	156	27.5 ± 0.1
CSL+OMW (flask)	253 ± 46	51	27.1 ± 0.1
CSL+OMW (bioreactor)	269 ± 95	48	27.1 ± 0.1

5.3.6 Emulsification activity of the rhamnolipids produced by *B. thailandensis* E264

Aqueous solutions of purified rhamnolipids produced in S medium were able to stabilize emulsions with *n*–hexadecane at concentrations as low as 100 mg/L, with an E_{24} of 51 ± 4%, which increased up to 56–58% as the rhamnolipid concentration increased (Table 5.9). To note that, since the same volume of rhamnolipid solution and *n*–hexadecane was used to perform these studies, emulsifying indexes above 50% denote the complete emulsification of the oil phase.

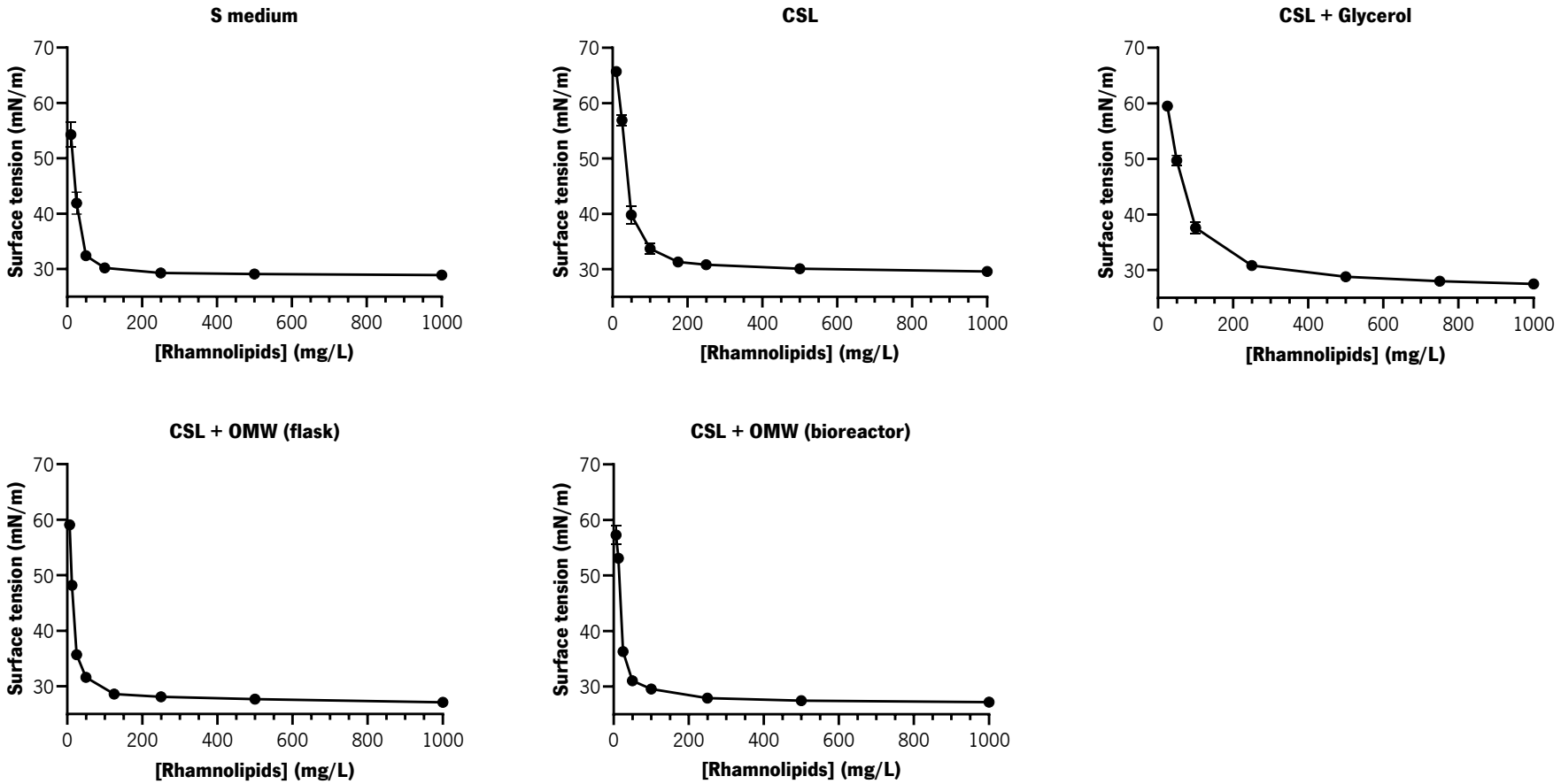

Figure 5.7 – Surface tension values (mN/m) of rhamnolipids produced by *Burkholderia thailandensis* E264 in standard, CSL, CSL+Glycerol and CSL+OMW media (both in flask and bioreactor), dissolved in 10 mM Tris–HCl buffer (pH 7.4) at different concentrations.

Regarding rhamnolipids produced in CSL medium, the emulsifying activity was similar to the one obtained in S medium with the highest rhamnolipid concentrations tested, although a weaker activity was obtained at 100 mg/L (Table 5.9). For rhamnolipids produced in CSL+OMW medium, the E_{24} was below 20% for all the concentrations tested (Table 5.9). These results can be explained by the structural differences of rhamnolipids produced in the different culture media. The mono–rhamnolipids produced mainly in CSL+OMW medium fall within the range of wetting and spreading agents in the HLB scale, while di–rhamnolipids, present in higher relative abundance in S and CSL media, are considered better emulsifying agents (Baccile et al., 2021).

Table 5.9 – Emulsification indexes (E_{24}) obtained with purified rhamnolipids produced by *Burkholderia thailandensis* E264 in standard (S), CSL and CSL+OMW media at different concentrations.

RL concentration (mg/L)	E_{24} (%)		
	S	CSL	CSL+OMW
500	56.0 ± 0.0	61.3 ± 1.8	17.4 ± 0.1
250	58.0 ± 2.8	63.3 ± 1.1	13.3 ± 0.4
100	51.1 ± 4.4	22.9 ± 2.9	4.4 ± 0.1

5.3.7 Effect of rhamnolipids produced by *B. thailandensis* E264 on the contact angle of water in an oil surface

To evaluate the effect of rhamnolipids on wettability alteration, contact angles were measured in an oil–coated glass surface. The rhamnolipids produced by *B. thailandensis* E264 reduced the contact angle of water in oil, altering the wettability of the surface from a neutral–wet state (75° < contact angle (θ) < 105°) to a water–wet state (0° < θ < 75°) during contact (Table 5.10 and Figure 5.8) (Cui, Sun, et al., 2017). As the droplets contacted the surface, contact angles were similar to those of water in all cases studied, confirming that the surface was neutral–wet in the beginning. Over a small period of time, most of the rhamnolipid solutions and CFS decreased the contact angle, thus altering the wettability of the surface to a more water–wet state, which is an underlying mechanism in MEOR applications. This was not observed for the rhamnolipids produced in S and CSL+OMW media at 2 x CMC, where the contact angle remained above the hydrophilic wetting state (75.3 ± 7.7° and 83.9 ± 1.5°, respectively) (Cui, Zheng, et al., 2017).

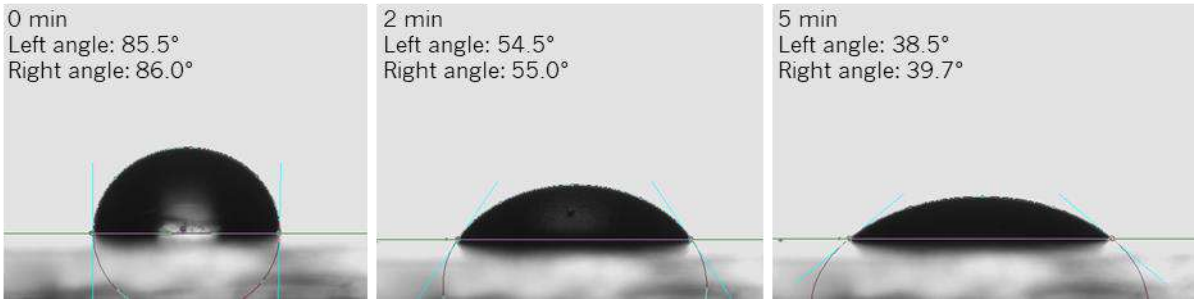

Figure 5.8 – Example of the decreasing contact angle of the rhamnolipids (5 x CMC) produced by *Burkholderia thailandensis* E264 in CSL medium on an oil–coated glass surface, showing a wettability alteration from oil/neutral–wet (at 0 min) to water–wet (at 5 min).

Table 5.10 – Contact angle (°) measurements on an oil–coated glass surface for cell–free supernatants obtained from cultures of *Burkholderia thailandensis* E264 grown in different culture media (S, CSL and CSL+OMW), rhamnolipid solutions (2 x critical micelle concentration (CMC) and 5 x CMC) and commercial rhamnolipids (RL–90 at 3 g/L, 2 x CMC and 5 x CMC).

Sample	RL concentration	Contact angles (°)		
		0 min	2 min	5 min
S (Broth)	–	86.5 ± 1.3	61.5 ± 3.0	45.6 ± 3.7
CSL (Broth)	–	75.5 ± 2.0	64.2 ± 0.8	54.1 ± 1.7
CSL+OMW (Broth)	–	75.8 ± 1.5	68.3 ± 0.9	62.0 ± 0.2
Commercial RL	3 g/L	54.3 ± 2.2	42.0 ± 0.5	38.1 ± 0.6
Control (Water)	–	91.9 ± 3.3	81.7 ± 2.8	82.0 ± 0.2
S	2 x CMC	95.7 ± 6.5	85.7 ± 3.2	75.3 ± 7.7
	5 x CMC	94.4 ± 1.6	58.8 ± 2.3	40.7 ± 0.8
CSL	2 x CMC	93.2 ± 0.5	68.0 ± 1.8	51.4 ± 2.6
	5 x CMC	87.0 ± 3.0	54.9 ± 1.0	40.1 ± 1.3
CSL+OMW	2 x CMC	96.6 ± 1.9	92.2 ± 1.5	83.9 ± 1.5
	5 x CMC	99.1 ± 0.8	82.5 ± 1.2	68.1 ± 1.6
RL–90	2 x CMC	88.2 ± 5.0	71.2 ± 2.8	62.9 ± 0.8
	5 x CMC	79.0 ± 4.0	53.9 ± 1.0	45.2 ± 0.7
Control (TrisHCl buffer)	–	89.8 ± 9.4	79.4 ± 0.8	79.7 ± 2.3

Furthermore, results show a correlation between lower ST values and a stronger wettability alteration, seen by the lower contact angles. However, this trend was not observed for the rhamnolipids produced in CSL+OMW medium, where contact angles are higher than with other media, even though the ST values are lower. When using the purified solutions, rhamnolipids from *B. thailandensis* E264 in S and CSL media had a stronger effect on wettability than the commercial rhamnolipids produced by *P. aeruginosa*.

5.3.8 Oil recovery assays

5.3.8.1 Evaluating the performance of the produced rhamnolipids in oil recovery assays using sand–pack columns

The potential application of rhamnolipids produced by *B. thailandensis* E264 in MEOR was studied using sand–pack columns with an *ex situ* approach. Using a light oil (Light Arabian crude oil, $\eta_{40°C}$ = 8 mPa s at 1.4 s^{-1}), oil recovery rates with the CFS obtained with *B. thailandensis* E264 in CSL medium increased by 6–7% when compared with the control (Table 5.11). Different incubation times for the CFS (24h and 48h), however, did not seem to impact oil recovery rates.

Table 5.11 – Results obtained in MEOR sand–pack column assays performed with the Light Arabian crude oil ($\eta_{40°C}$ = 8 mPa s at 1.4 s^{-1}) using the cell–free supernatant obtained with *Burkholderia. thailandensis* E264 in CSL medium, incubated for 24h or 48h.

Oil recovery parameters	Treatment	
	B. thailandensis E264 CFS in CSL medium	
	Incubated 24h	Incubated 48h
PV (mL)	90.0	90.0
Porosity (%)	32.1	32.1
OOIP (mL)	70.0	70.0
S_{oi} (%)	77.8	77.8
S_{orwf} (mL)	40.0	40.0
S_{or} (%)	42.9	42.9
S_{orbf} (mL)	5.2	5.0
AOR (%)	6.9	6.3

The AOR value is the corrected value obtained after subtracting the additional oil recovery obtained in the control assays.

The effect of using both rhamnolipids and a biopolymer in MEOR applications was also evaluated using a heavy crude oil mixture ($\eta_{40°C}$ = 247 mPa s at 1.4 s^{-1}) (Table 5.12). As discussed in Chapter 4, by first incubating the column with the CFS from *B. thailandensis* E264, the aim was to promote the oil recovery mechanisms of the rhamnolipids to facilitate the subsequent oil recovery during polymer flooding. In these conditions, the rhamnolipids from *B. thailandensis* E264 increased additional oil recovery rates by 6.1% in relation to the control (corresponding to the biopolymer from *R. viscosum* CECT 908) (Table 5.12 and Table 4.2, Chapter 4). Nonetheless, the effect of the rhamnolipid was not as high

as expected. It was hypothesized that the viscosity of the oil used might be too high for the rhamnolipids to show a more significant effect in oil recovery.

Table 5.12 – Results obtained in MEOR sand–pack column assays performed with the heavy crude oil mixture ($\eta_{40°C}$ = 247 mPa s at 1.4 s^{-1}) using the cell–free supernatant obtained with *Burkholderia thailandensis* E264 in CSL medium, followed by the culture broth obtained with *Rhizobium* viscosum CECT 908 in Rv2 medium.

Oil recovery parameters	Treatment	
	R. viscosum broth in Rv2 medium	*B. thailandensis* E264 CFS in CSL medium (incubated 24h)
$\eta_{40°C}$ (mPa s)	266 ± 3	263 ± 3
PV (mL)	90.0 ± 0.0	90.0 ± 0.0
Porosity (%)	32.1 ± 0.0	32.1 ± 0.0
OOIP (mL)	76.3 ± 2.5	75.2 ± 0.8
S_{oi} (%)	84.7 ± 2.7	83.6 ± 0.9
S_{orwf} (mL)	52.5 ± 3.5	52.5 ± 3.5
S_{or} (%)	31.2 ± 2.4	30.2 ± 3.9
S_{orbf} (mL)	4.5 ± 0.2	5.6 ± 0.0
AOR (%)	10.2 ± 0.1	16.3 ± 2.9

The AOR value is the corrected value obtained after subtracting the additional oil recovery obtained in the control assays. The results represent the average of two independent experiments ± standard deviation.

The effect of using both biomolecules in oil recovery was then tested using a lighter oil (Potiguar oil, $\eta_{40°C}$ = 110 mPa s at 1.4 s^{-1}) (Table 5.13 and Table 5.14). However, results show that, in these conditions, the rhamnolipids did not have a significant effect in oil recovery and only xanthan gum is responsible for the increase in the recovery rates. In fact, when using the CFS produced in CSL+OMW medium, the recovery rate decreases approximately 4% when compared to the control using only xanthan gum. The same happens when using the commercial rhamnolipids at a concentration of 250 mg/L and incubated for 24h (Table 5.13). Only when the commercial rhamnolipids are used at a higher concentration (2 g/L and incubated 48h) does the recovery rate increase around 5% more than the control using xanthan gum (Table 5.14; Table 4.3 and Table 4.4, Chapter 4). This indicates that the rhamnolipids may contribute to oil recovery when a higher concentration of product is used in the injection stream.

Table 5.13 – Results obtained in MEOR sand–pack column assays performed with the crude oil from the Potiguar oilfield ($\eta_{40°C}$ = 110 mPa s at 1.4 s^{-1}) using commercial rhamnolipids (RL–90, 250 mg/L) and the cell–free supernatant (CFS) obtained with *Burkholderia thailandensis* E264 in CSL and CSL+OMW media, incubated for 24h and followed by xanthan gum (1 g/L) injection.

Oil recovery parameters	Treatment			
	Xanthan gum	RL–90 (250 mg/L)	*B. thailandensis* E264 CFS in CSL medium	*B. thailandensis* E264 CFS in CSL+OMW medium
$\eta_{40°C}$ (mPa s)	106 ± 9	95 ± 7	97 ± 4	101 ± 1
PV (mL)	89 ± 1.4	91.0 ± 1.4	90.0 ± 0.0	87 ± 4.2
Porosity (%)	31.8 ± 0.5	32.5 ± 0.5	32.1 ± 0.0	31.1 ± 1.5
OOIP (mL)	80.1 ± 1.1	79.7 ± 4.7	81.8 ± 6	78.4 ± 3.0
S_{oi} (%)	90.0 ± 2.6	87.6 ± 6.5	90.8 ± 6.7	90.1 ± 0.9
S_{orwf} (mL)	45.0 ± 0.0	37.5 ± 3.5	45.0 ± 0.0	42.5 ± 3.5
S_{or} (%)	43.8 ± 0.7	52.7 ± 7.2	44.8 ± 4.1	45.8 ± 2.4
S_{orbf} (mL)	5.5 ± 0.8	5.2 ± 0.5	5.7 ± 0.8	4.3 ± 0.1
AOR (%)	8.4 ± 2.7	5.1 ± 1.2	7.2 ± 0.4	4.8 ± 0.6

The AOR value is the corrected value obtained after subtracting the additional oil recovery obtained in the control assays. The results represent the average of two independent experiments ± standard deviation.

Table 5.14 – Results obtained in MEOR sand–pack column assays performed with the crude oil from the Potiguar oilfield ($\eta_{40°C}$ = 110 mPa s at 1.4 s^{-1}) using commercial rhamnolipids (RL–90, 2 g/L) and the cell–free supernatant (CFS) obtained with *Burkholderia thailandensis* E264 in CSL and CSL+OMW media, incubated for 48h and followed by xanthan gum (1 g/L) injection.

Oil recovery parameters	Treatment			
	Xanthan gum	RL–90 (2 g/L)	*B. thailandensis* E264 CFS in CSL medium	*B. thailandensis* E264 CFS in CSL+OMW medium
$\eta_{40°C}$ (mPa s)	106 ± 9	95 ± 2	95 ± 3	99 ± 1
PV (mL)	89 ± 1.4	95.0 ± 4.2	90.0 ± 0.0	90.0 ± 0.0
Porosity (%)	31.8 ± 0.5	33.9 ± 1.5	32.1 ± 0.0	32.1 ± 0.0
OOIP (mL)	80.1 ± 1.1	75.0 ± 4.5	79.3 ± 1.8	76.8 ± 1.7
S_{oi} (%)	90.0 ± 2.6	78.9 ± 1.2	88.1 ± 2.0	85.3 ± 1.9
S_{orwf} (mL)	45.0 ± 0.0	42.5 ± 3.5	40.0 ± 0.0	40.0 ± 0.0
S_{or} (%)	43.8 ± 0.7	43.3 ± 1.3	49.5 ± 1.1	47.9 ± 1.2
S_{orbf} (mL)	5.5 ± 0.8	6.6 ± 0.8	5.9 ± 1.4	4.5 ± 0.6
AOR (%)	8.4 ± 2.7	13.1 ± 2.0	7.8 ± 2.9	4.9 ± 2.3

The AOR value is the corrected value obtained after subtracting the additional oil recovery obtained in the control assays. The results represent the average of two independent experiments ± standard deviation.

5.3.8.2 Recovering oil from artificially contaminated sand

To further study the performance of rhamnolipids produced by *B. thailandensis* E264 in MEOR and bioremediation, their ability to recover heavy crude oil ($\eta_{40°C}$ = 110 mPa s at 1.4 s^{-1}) from artificially contaminated sand was studied. This methodology has been widely used in bioremediation studies, as it does not require specific equipment such as sand–pack columns or core flooding systems, commonly used in MEOR studies, and is less time consuming (Bezza & Chirwa, 2015; Chaprão et al., 2018; S. Gaur et al., 2022; Gudiña, Fernandes, et al., 2015; Gudiña, Rodrigues, et al., 2015; Rufino et al., 2013; Soares da Silva et al., 2017; Teixeira Souza et al., 2018). Even though it fails to reproduce the complex reservoir properties, like porosity, permeability, pressure and injection flow rates, it can still provide useful insights into possible MEOR and bioremediation applications (Ciurko et al., 2022; Datta et al., 2020; Rellegadla et al., 2019).

Table 5.15 – Results obtained in oil recovery assays performed with the cell–free supernatant (CFS) from cultures of *Burkholderia thailandensis* E264 grown in standard (S), CSL and CSL+OMW media, and commercial rhamnolipids (RL–90) dissolved in the same uninoculated culture media at a concentration of 200 mg/L.

Treatment		ST (mN/m)	Oil recovery (%)
CFS	S	32.1 ± 1.4	61.4 ± 6.8
	CSL	30.3 ± 0.9	62.9 ± 12.5
	CSL+OMW	27.5 ± 0.2	60.7 ± 4.7
RL–90	S	30.0 ± 0.6	49.7 ± 2.6
	CSL	29.8 ± 0.3	50.6 ± 3.1
	CSL+OMW	29.5 ± 0.4	51.6 ± 2.8
Control	S	60.5 ± 0.8	9.1 ± 2.4
	CSL	48.6 ± 0.6	10.0 ± 2.0
	CSL+OMW	41.8 ± 0.6	11.3 ± 1.5

Control assays were performed using the uninoculated culture media.

The CFS obtained from the different culture media studied (S, CSL and CSL+OMW) were able to recover about 60% of the crude oil present in the samples, whereas in the control assays, the corresponding uninoculated culture media recovered around 10% of crude oil (Table 5.15). In order to compare the performance of rhamnolipids produced by *B. thailandensis* E264 in the different culture media with commercial rhamnolipids (RL–90), oil recovery assays were performed using those

rhamnolipids dissolved in the same uninoculated culture media at a concentration of 200 mg/L (similar to the rhamnolipid concentration present in the CFS of *B. thailandensis* E264 (Table 5.8)). The commercial rhamnolipids herein studied were characterized in our previous work as a mixture of two congeners: Rha–C_{10}–C_{10} (relative abundance 68%; HLB value 10.1), and Rha–Rha–C_{10}–C_{10}, (relative abundance 32%; HLB value 12.3) (Gudiña et al., 2016). Oil recoveries around 50% were obtained in all the cases (Table 5.15). According to the results obtained, it can be concluded that rhamnolipids produced by *B. thailandensis* E264 displayed a good performance in oil recovery.

5.4 Discussion

In flask assays using S medium, which contains glycerol, peptone and meat extract, *B. thailandensis* E264 produced 139 mg rhamnolipids/L. Contrary to previous studies, that reported an extended stationary phase (216–264h), associated to a continuous rhamnolipid production in *B. thailandensis* E264 (Funston et al., 2016; Irorere et al., 2018), in our case, the highest rhamnolipid production was achieved after 96h of growth; after that, the ST of the culture medium increased, probably due to the degradation of the rhamnolipids previously produced (Figure 5.1). Similarly to the results herein obtained, Funston and co–workers (2017) also reported that only 50% of the glycerol provided in the culture medium (40 g/L) was consumed by *B. thailandensis* E264 after 264h of growth (Funston et al., 2017).

CSL and OMW proved to be good substrates for rhamnolipid production by *B. thailandensis* E264, achieving titers between 1.3 and 1.8 times higher than with the standard medium. The best results were obtained using a culture medium containing CSL (7.5% (v/v)) and OMW (10% (v/v)). The inductive effect of OMW on rhamnolipid production herein observed was previously reported for *P. aeruginosa*, and it was attributed to the presence of long chain fatty acids (mainly oleic, palmitic, linoleic and stearic acids) in this substrate, which can be used for rhamnolipid biosynthesis through the β–oxidation pathway, in addition to those provided by the fatty acid *de novo* synthesis (FAS II) (Gudiña et al., 2016). In *B. thailandensis*, it was suggested that the main supplier of lipid precursors for rhamnolipid biosynthesis is FAS II, although the β–oxidation pathway also contributes with a small percentage (less than 3%) (Irorere et al., 2018). Consequently, further studies are necessary to elucidate the effect of exogenous fatty acids on rhamnolipid production by *B. thailandensis*.

The higher rhamnolipid titer obtained in the CSL+OMW medium could also be explained by the effect of the different carbon sources in rhamnolipid production. In *B. thailandensis* E264 and *Burkholderia glumae* AU6208, rhamnolipid production significantly increased when the carbon source was changed from glycerol to canola oil (Costa et al., 2011; Dubeau et al., 2009). The authors suggested that rhamnolipid production in water–soluble carbon sources, such as glycerol, is generally lower than in water–immiscible substrates, such as vegetable oils (Costa et al., 2011). That can be explained because rhamnolipids reduce the IFT between water and water–immiscible substrates, making them more readily available for uptake by the microorganism.

Rhamnolipid production by *B. thailandensis* E264 using the low–cost medium (CSL+OMW) was further validated in bioreactor (Figure 5.5). To the best of our knowledge, only a previous study evaluated rhamnolipid production by *B. thailandensis* E264 using an alternative carbon source (used cooking oil) in bioreactor, producing 2.2 g rhamnolipid/L over 120h in a 10 L–bioreactor (Kourmentza et al., 2018). However, the minimum ST values obtained in that work (around 38 mN/m) were considerably higher than the ones herein presented (26.3 mN/m), and the methodologies used to purify the rhamnolipids produced were also different (as it will be discussed later), which does not allow to compare the results obtained in both works.

The chemical characterization revealed that *B. thailandensis* E264 produced mainly di–rhamnolipids when grown in S and CSL media (Rha–Rha–C_{14}–C_{14}: 62–64%; Rha–Rha–C_{12}–C_{14}/C_{14}–C_{12}: 18–22%) (Table 5.6). These results are in accordance with those obtained in previous studies, where the di–rhamnolipid Rha–Rha–C_{14}–C_{14} was the main congener produced by *B. thailandensis* E264 using glycerol as carbon source (between 40 and 82% of total rhamnolipid congeners) (Díaz De Rienzo et al., 2016; Dubeau et al., 2009; Elshikh et al., 2017; Funston et al., 2017; Irorere et al., 2018). However, when the CSL medium was supplemented with OMW, the relative abundance of mono–rhamnolipids increased from 10% up to 56% (Table 5.6). These results suggest that the addition of fatty acids to the culture medium results in the production of higher amounts of mono–rhamnolipids. A similar trend was observed by Irorere et al. (2018) growing *B. thailandensis* E264 in a mineral medium containing as carbon source glycerol (6% mono–rhamnolipids) or heptadecanoic acid (23% mono–rhamnolipids), although the effect of oleic acid was less evident (9% mono–rhamnolipids) (Irorere et al., 2018). Likewise, when growing *B. thailandensis* E264 in a medium containing olive mill pomace (OMP, another residue from the olive oil industry) as carbon source, only mono–rhamnolipids were produced, mainly Rha–C_{14}–C_{14} (Chebbi et al., 2021). In *B. glumae* AU6208, the relative abundance of mono–rhamnolipids was 2%

when grown in glycerol, and 23% with canola oil (Costa et al., 2011). The authors suggested that glycerol favors di–rhamnolipid production because its carbon atoms are more readily incorporated into rhamnose. An increase in the relative proportion of mono–rhamnolipids (from 53% to 70%) was also reported for *P. aeruginosa* #112 when a culture medium containing CSL + sugarcane molasses was supplemented with OMW (Gudiña et al., 2016).

The surface–active properties of rhamnolipids are determined by their chemical structure (size of their hydrophilic head, length of the hydrophobic chains and presence of unsaturated bonds), which also affects their solubility in either aqueous or oil phases (Jahan et al., 2020). Mono–rhamnolipids, because they only have one rhamnose molecule, are more hydrophobic than di–rhamnolipids with fatty acid chains of the same length, and they usually exhibit lower CMC values and are able to reduce the ST more efficiently than di–rhamnolipids (Costa et al., 2011; Gudiña, Rodrigues, et al., 2015; Rodrigues et al., 2017). Accordingly, the differences observed in the surface activity of the rhamnolipids produced in the different culture media (Table 5.6, Table 5.8 and Figure 5.7) can be explained by their different congener distribution.

Rhamnolipids produced by *B. thailandensis* E264 in the different culture media herein studied displayed lower CMC values (48–108 mg/L) (Table 5.8 and Figure 5.7) when compared with those reported for the same strain in similar media in previous studies (125–225 mg/L) (Díaz De Rienzo et al., 2016; Dubeau et al., 2009; Elshikh et al., 2017). The low CMC values obtained in our study, paired with ST reductions down to 26 mN/m, indicate that these rhamnolipids have a greater degree of purity than in other cases. This can be due to the different methodologies used to recover them. In previous works, rhamnolipids produced by *B. thailandensis* were recovered through solvent (ethyl acetate) extraction, followed by a solid–phase (silica column) purification (Chebbi et al., 2021; Díaz De Rienzo et al., 2016; Dubeau et al., 2009; Funston et al., 2016, 2017; Irorere et al., 2018; Kourmentza et al., 2018). In our case, rhamnolipid extraction and purification were performed using a methodology commonly used to recover the rhamnolipids produced by *P. aeruginosa*, and the impurities present in the culture medium were removed using increasing concentrations of methanol, allowing the recovery of a product with a higher degree of purity. On the other hand, rhamnolipids produced in the CSL+Glycerol medium (obtained through CCRD) had a CMC value of 156 mg/L, even though 315 mg of rhamnolipids/L were produced. The carbon sources used in this case may play a part in the higher CMC value, given that, as stated above, glycerol favors di–rhamnolipid production (Costa et al., 2011). However, no chemical

characterization was performed for the rhamnolipids produced in this medium, so the high CMC value obtained could instead be attributed to a lower degree of purity of the extracted product.

Besides CSL and OMW, other low–cost substrates have been studied as carbon sources for rhamnolipid production by *B. thailandensis*, such as non–fermented grape marcs (a winery residue) (Chebbi et al., 2021) and used cooking oil (Kourmentza et al., 2018), with production titers of 1.07 and 2.20 g rhamnolipid/L, respectively. However, the rhamnolipids produced in those media exhibited higher CMC (500 and 225 mg/L) and minimum ST values (34.6 and 37.7 mN/m) than the ones achieved in this work. OMP was also evaluated as a low–cost substrate for rhamnolipid production by *B. thailandensis* E264 (Chebbi et al., 2021). After thermal and acid pre–treatments, OMP (2% (w/v)) was used as carbon source, yielding 270 mg rhamnolipid/L. However, as in the previous examples, those rhamnolipids exhibited a higher CMC (500 mg/L) and lower surface activity (reduced the ST of water up to 38 mN/m) when compared with the ones obtained in the present work.

Rhamnolipids produced by *B. thailandensis* E264 in S and CSL media exhibited an excellent emulsifying activity (Table 5.9). To the best of our knowledge, the emulsifying activity of purified rhamnolipids produced by *B. thailandensis* was not previously reported, and only in some cases it was studied in the rhamnolipid–containing CFS. However, the emulsifying activity was determined for the purified rhamnolipids produced by *B. glumae* AU6208 in glycerol–containing medium, where the distribution of rhamnolipid congeners was similar to the ones obtained for *B. thailandensis* E264 in S and CSL media (Costa et al., 2011). Similarly to the results herein presented, those rhamnolipids exhibited a good emulsification potential, displaying E_{24} values ranging from 44% with hexadecane to 100% with canola and motor oil.

Furthermore, the rhamnolipids produced in S and CSL media have shown to be good wetting agents, since they are able to decrease the contact angle between water and an oil–coated surface down to approximately 40° (when a solution of 5 x CMC is used) after just 5 minutes of contact time (Table 5.10). The rhamnolipids produced in the CSL+OMW medium decreased the contact angle to 62° when the culture broth was used (Table 5.10). Even though this value is still within the hydrophilic wetting state, according to the rhamnolipids congener distribution and surface activity, it would be expected that these rhamnolipids displayed a better wetting activity, predicted by their HLB value, than those produced in the other media. In another study, for example, mono–rhamnolipids produced by *P. aeruginosa* altered the wettability of a calcite surface wetted in oil at concentrations as low as 25 ppm, while di–rhamnolipids only achieved the same result at 50 ppm (Rocha et al., 2020). However, factors like the chemical

composition of the measurement surface, the properties of the oil and the molecular charge of the hydrophilic heads of the biosurfactants can affect the wettability alteration potential of a biosurfactant molecule (Mohammed & Babadagli, 2015), which can explain the results obtained with the rhamnolipids produced in the CSL+OMW medium.

In sand–pack column oil recovery assays, the CFS from *B. thailandensis* E264 grown in CSL medium recovered up to 7% of residual light oil (Table 5.11) and 6% additional heavy crude oil when injected in combination with a biopolymer (Table 5.12). Other rhamnolipid–producing microorganisms recovered between 2.5 and 56.2% of oil in similar assays (Alvarez Yela et al., 2016; Astuti et al., 2019; Câmara et al., 2019; Cui, Sun, et al., 2017; Ibrahim, 2018; Sharma et al., 2018). However, the results are not comparable due to the heterogeneity of experimental conditions and rhamnolipid properties.

In oil recovery assays from contaminated sand, the CFS from cultures of *B. thailandensis* E264 in S, CSL and CSL+OMW media recovered between 60 and 63% of heavy crude oil. The different methodologies used (sand–pack columns and flask assays) can influence the recovery rates obtained, namely when considering the amount of oil that is absorbed into the sand and area of contact between the oil and biosurfactant solution.

Although rhamnolipids produced in CSL+OMW medium displayed different congener distribution and different HLB values when compared with those produced in the other media (S and CSL), all of them proved to be effective in oil recovery from contaminated sands. Regarding the commercial rhamnolipids, they allowed the recovery of approximately 50% of crude oil (Table 5.15), slightly lower than rhamnolipids produced by *B. thailandensis* E264. Although commercial rhamnolipids, which were produced by *P. aeruginosa*, contained a high percentage of mono–rhamnolipids (even higher than those produced by *B. thailandensis* E264 in CSL+OMW medium), their HLB values were similar to those produced in S and CSL media, due to their shorter fatty acid chains (C_{10}).

Biosurfactants produced by different microorganisms (*Bacillus methylotrophicus*, *Bacillus subtilis*, *Bacillus tequilensis*, *Candida lipolytica*, *Pseudomonas cepacia*, *Wickerhamomyces anomalus*) recovered between 20% and 80% of crude oil or motor oil in oil recovery assays from contaminated sand (Bezza & Chirwa, 2015; Chaprão et al., 2018; Ciurko et al., 2022; Datta et al., 2020; S. Gaur et al., 2022; Gudiña, Fernandes, et al., 2015; Rufino et al., 2013; Soares da Silva et al., 2017; Teixeira Souza et al., 2018). In a recent study, the cell–free supernatants of cultures of *B. subtilis* #309 performed in low cost media (sunflower and rapeseed cake), containing between 1.2 and 1.4 g surfactin/L, recovered between 14% and 22% of motor oil from artificially contaminated sand after 24 h of treatment, increasing up to 30–

33% after 168h (Ciurko et al., 2022). Purified surfactin (200 mg/L) produced by *B. tequilensis* MK 729017 and commercial rhamnolipids (RL–90, Sigma–Aldrich, 90% of purity, 200 mg/L) recovered 80% of crude oil ($\eta_{30\ °C}$= 13.6 mPa s) from artificially contaminated sand after 48h of treatment, slightly lower than the recoveries obtained with the chemical surfactants SDS (2350 mg/L, 86%) and CTAB (335 mg/L, 88%) (Datta et al., 2020). Detergent formulations containing commercial rhamnolipids (RL–90, Sigma–Aldrich, 90% of purity, 200 mg/L) recovered 91% of waste engine oil from contaminated sand after 3h of treatment, while those containing purified rhamnolipids produced by *P. aeruginosa* gi (200 mg/L) allowed recoveries around 82% (S. Gaur et al., 2022). The cell–free supernatants of cultures of *P. cepacia* CCT6659 recovered 84% of motor oil from contaminated marine stones, whereas the recovery obtained with the purified biosurfactants produced by the same microorganism (3000 mg/L, 5 × CMC) was 72% (Soares da Silva et al., 2021).

Compared with these reports, the results herein obtained proved to be satisfactory. Furthermore, in this study, a heavy crude oil ($\eta_{40\ °C}$ = 110 mPa s at 1.4 s^{-1}) was used, which is more difficult to recover due to its viscosity. Moreover, the biosurfactants were used without purification, as cell–free supernatants, which would significantly reduce the production costs associated with their application. Consequently, the results obtained are promising for the application of the rhamnolipids produced by *B. thailandensis* in bioremediation or MEOR, which, to the best of our knowledge, was not previously studied.

In conclusion, low–cost culture media, containing as sole ingredients agro–industrial residues (CSL and OMW), were developed for rhamnolipid production by *B. thailandensis* E264. These media allowed the production of higher amounts of rhamnolipids (175–269 mg/L) when compared with the standard medium (139 mg/L). Rhamnolipids produced in the low–cost media reduced the surface tension up to 27 mN/m (CMC 51 mg/L). These results were further validated in bioreactor. Besides reducing the rhamnolipid production costs, these results can allow the development of strategies for the valorization of environmentally hazardous residues and promote the circular economy. Furthermore, the results obtained in the oil recovery assays, where these rhamnolipids (cell–free supernatants) recovered more than 60% of crude oil from contaminated sands, open the possibility for its application in MEOR and bioremediation.

5.5 References

Alvarez Yela, A. C., Tibaquirá Martínez, M. A., Rangel Piñeros, G. A., López, V. C., Villamizar, S. H., Núñez Vélez, V. L., Abraham, W. R., Vives Flórez, M. J., & González Barrios, A. F. (2016). A comparison between conventional Pseudomonas aeruginosa rhamnolipids and Escherichia coli transmembrane proteins for oil recovery enhancing. *International Biodeterioration and Biodegradation*, *112*, 59–65. https://doi.org/10.1016/j.ibiod.2016.04.033

Astuti, D. I., Purwasena, I. A., Putri, R. E., Amaniyah, M., & Sugai, Y. (2019). Screening and characterization of biosurfactant produced by Pseudoxanthomonas sp. G3 and its applicability for enhanced oil recovery. *Journal of Petroleum Exploration and Production Technology*, 1–11. https://doi.org/10.1007/s13202–019–0619–8

Baccile, N., Seyrig, C., Poirier, A., Alonso–De Castro, S., Roelants, S. L. K. W., & Abel, S. (2021). Self–assembly, interfacial properties, interactions with macromolecules and molecular modelling and simulation of microbial bio–based amphiphiles (biosurfactants). A tutorial review. In *Green Chemistry* (Vol. 23, Issue 11, pp. 3842–3944). The Royal Society of Chemistry. https://doi.org/10.1039/d1gc00097g

Bezza, F. A., & Chirwa, E. M. N. (2015). Production and applications of lipopeptide biosurfactant for bioremediation and oil recovery by Bacillus subtilis CN2. *Biochemical Engineering Journal*, *101*, 168–178. https://doi.org/10.1016/j.bej.2015.05.007

Borah, S. N., Goswami, D., Lahkar, J., Sarma, H. K., Khan, M. R., & Deka, S. (2015). Rhamnolipid produced by Pseudomonas aeruginosa SS14 causes complete suppression of wilt by Fusarium oxysporum f. sp. pisi in Pisum sativum. *BioControl*, *60*(3), 375–385. https://doi.org/10.1007/s10526–014–9645–0

Câmara, J. M. D. A., Sousa, M. A. S. B., Barros Neto, E. L., & Oliveira, M. C. A. (2019). Application of rhamnolipid biosurfactant produced by Pseudomonas aeruginosa in microbial–enhanced oil recovery (MEOR). *Journal of Petroleum Exploration and Production Technology*, 1–9. https://doi.org/10.1007/s13202–019–0633–x

Cao, J., Wang, W., Zhao, Z., Liu, X., & Li, Q. X. (2021). Genome, metabolic pathways and characteristics of cometabolism of dibenzothiophene and the biodiesel byproduct glycerol in Paraburkholderia sp. C3. *Bioresource Technology*, *326*, 124699. https://doi.org/10.1016/j.biortech.2021.124699

Chaprão, M. J., da Silva, R. de C. F. S., Rufino, R. D., Luna, J. M., Santos, V. A., & Sarubbo, L. A. (2018). Production of a biosurfactant from Bacillus methylotrophicus UCP1616 for use in the bioremediation of oil–contaminated environments. *Ecotoxicology*, *27*(10), 1310–1322. https://doi.org/10.1007/s10646–018–1982–9

Chebbi, A., Tazzari, M., Rizzi, C., Gomez Tovar, F. H., Villa, S., Sbaffoni, S., Vaccari, M., & Franzetti, A. (2021). Burkholderia thailandensis E264 as a promising safe rhamnolipids' producer towards a sustainable valorization of grape marcs and olive mill pomace. *Applied Microbiology and Biotechnology*, *105*(9), 3825–3842. https://doi.org/10.1007/s00253–021–11292–0

Ciurko, D., Czyżnikowska, Ż., Kancelista, A., Łaba, W., & Janek, T. (2022). Sustainable Production of Biosurfactant from Agro–Industrial Oil Wastes by Bacillus subtilis and Its Potential Application as Antioxidant and ACE Inhibitor. *International Journal of Molecular Sciences*, *23*(18), 10824. https://doi.org/10.3390/ijms231810824

Costa, S. G. V. A. O., Déziel, E., & Lépine, F. (2011). Characterization of rhamnolipid production by Burkholderia glumae. *Letters in Applied Microbiology*, *53*(6), 620–627.

https://doi.org/10.1111/j.1472–765X.2011.03154.x

Cui, Q. F., Sun, S. S., Luo, Y. J., Yu, L., & Zhang, Z. Z. (2017). Comparison of in–situ and ex–situ microbial enhanced oil recovery by strain Pseudomonas aeruginosa WJ–1 in laboratory sand–pack columns. *Petroleum Science and Technology*, *35*(21), 2044–2050. https://doi.org/10.1080/10916466.2017.1380042

Cui, Q. F., Zheng, W. T., Yu, L., Xiu, J. L., Zhang, Z. Z., Luo, Y. J., & Sun, S. S. (2017). Emulsifying action of Pseudomonas aeruginosa L6–1 and its metabolite with crude oil for oil recovery enhancement. *Petroleum Science and Technology*, *35*(11), 1174–1179. https://doi.org/10.1080/10916466.2017.1315725

Curiel–Maciel, N. F., Martínez–Morales, F., Licea–Navarro, A. F., Bertrand, B., Aguilar–Guadarrama, A. B., Rosas–Galván, N. S., Morales–Guzmán, D., Rivera–Gómez, N., Gutiérrez–Ríos, R. M., & Trejo–Hernández, M. R. (2021). Characterization of Enterobacter cloacae BAGM01 Producing a Thermostable and Alkaline–Tolerant Rhamnolipid Biosurfactant from the Gulf of Mexico. *Marine Biotechnology*, *23*(1), 106–126. https://doi.org/10.1007/s10126–020–10006–3

Datta, P., Tiwari, P., & Pandey, L. M. (2020). Oil washing proficiency of biosurfactant produced by isolated Bacillus tequilensis MK 729017 from Assam reservoir soil. *Journal of Petroleum Science and Engineering*, *195*, 107612. https://doi.org/10.1016/j.petrol.2020.107612

Dermeche, S., Nadour, M., Larroche, C., Moulti–Mati, F., & Michaud, P. (2013). Olive mill wastes: Biochemical characterizations and valorization strategies. In *Process Biochemistry* (Vol. 48, Issue 10, pp. 1532–1552). Elsevier. https://doi.org/10.1016/j.procbio.2013.07.010

Díaz De Rienzo, M. A., Kamalanathan, I. D., & Martin, P. J. (2016). Comparative study of the production of rhamnolipid biosurfactants by B. thailandensis E264 and P. aeruginosa ATCC 9027 using foam fractionation. *Process Biochemistry*, *51*(7), 820–827. https://doi.org/10.1016/j.procbio.2016.04.007

Dubeau, D., Déziel, E., Woods, D. E., & Lépine, F. (2009). Burkholderia thailandensis harbors two identical rhl gene clusters responsible for the biosynthesis of rhamnolipids. *BioMed Central – BMC Microbiology*, *9*, 263. https://doi.org/10.1186/1471–2180–9–263

Elshikh, M., Funston, S., Chebbi, A., Ahmed, S., Marchant, R., & Banat, I. M. (2017). Rhamnolipids from non–pathogenic Burkholderia thailandensis E264: Physicochemical characterization, antimicrobial and antibiofilm efficacy against oral hygiene related pathogens. *New Biotechnology*, *36*, 26–36. https://doi.org/10.1016/j.nbt.2016.12.009

Funston, S. J., Tsaousi, K., Rudden, M., Smyth, T. J., Stevenson, P. S., Marchant, R., & Banat, I. M. (2016). Characterising rhamnolipid production in Burkholderia thailandensis E264, a non–pathogenic producer. *Applied Microbiology and Biotechnology*, *100*(18), 7945–7956. https://doi.org/10.1007/s00253–016–7564–y

Funston, S. J., Tsaousi, K., Smyth, T. J., Twigg, M. S., Marchant, R., & Banat, I. M. (2017). Enhanced rhamnolipid production in Burkholderia thailandensis transposon knockout strains deficient in polyhydroxyalkanoate (PHA) synthesis. *Applied Microbiology and Biotechnology*, *101*(23–24), 8443–8454. https://doi.org/10.1007/s00253–017–8540–x

Gaur, S., Sahani, A., Chattopadhyay, P., Gupta, S., & Jain, A. (2022). Remediation of Waste Engine Oil Contaminated Soil using Rhamnolipid based Detergent Formulation. *Materials Today: Proceedings*, *77*(1), 31–38. https://doi.org/10.1016/j.matpr.2022.08.452

Gaur, V. K., Bajaj, A., Regar, R. K., Kamthan, M., Jha, R. R., Srivastava, J. K., & Manickam, N. (2019). Rhamnolipid from a Lysinibacillus sphaericus strain IITR51 and its potential application for

dissolution of hydrophobic pesticides. *Bioresource Technology*, *272*, 19–25. https://doi.org/10.1016/j.biortech.2018.09.144

Gaur, V. K., Tripathi, V., Gupta, P., Dhiman, N., Regar, R. K., Gautam, K., Srivastava, J. K., Patnaik, S., Patel, D. K., & Manickam, N. (2020). Rhamnolipids from Planococcus spp. and their mechanism of action against pathogenic bacteria. *Bioresource Technology*, *307*, 123206. https://doi.org/10.1016/j.biortech.2020.123206

Griffin, W. C. (1955). Calculation of HLB values of non–ionic surfactants. *Am Perfumer Essent Oil Rev*, *65*, 26–29.

Gudiña, E. J., Fernandes, E. C., Rodrigues, A. I., Teixeira, J. A., & Rodrigues, L. R. (2015). Biosurfactant production by Bacillus subtilis using corn steep liquor as culture medium. *Frontiers in Microbiology*, *6*(FEB). https://doi.org/10.3389/fmicb.2015.00059

Gudiña, E. J., Rodrigues, A. I., Alves, E., Domingues, M. R., Teixeira, J. A., & Rodrigues, L. R. (2015). Bioconversion of agro–industrial by–products in rhamnolipids toward applications in enhanced oil recovery and bioremediation. *Bioresource Technology*, *177*, 87–93. https://doi.org/10.1016/j.biortech.2014.11.069

Gudiña, E. J., Rodrigues, A. I., de Freitas, V., Azevedo, Z., Teixeira, J. A., & Rodrigues, L. R. (2016). Valorization of agro–industrial wastes towards the production of rhamnolipids. *Bioresource Technology*, *212*, 144–150. https://doi.org/10.1016/j.biortech.2016.04.027

Gudiña, E. J., & Teixeira, J. A. (2022). Bacillus licheniformis: The unexplored alternative for the anaerobic production of lipopeptide biosurfactants? In *Biotechnology Advances* (Vol. 60, p. 108013). Elsevier. https://doi.org/10.1016/j.biotechadv.2022.108013

Hamimed, S., Landoulsi, A., & Chatti, A. (2021). The bright side of olive mill wastewater: valuables bioproducts after bioremediation. In *International Journal of Environmental Science and Technology* (Vol. 18, Issue 12, pp. 4053–4074). Springer. https://doi.org/10.1007/s13762–021–03145–0

Ibrahim, H. M. M. (2018). Characterization of biosurfactants produced by novel strains of Ochrobactrum anthropi HM–1 and Citrobacter freundii HM–2 from used engine oil–contaminated soil. *Egyptian Journal of Petroleum*, *27*(1), 21–29. https://doi.org/10.1016/j.ejpe.2016.12.005

Irorere, V. U., Smyth, T. J., Cobice, D., McClean, S., Marchant, R., & Banat, I. M. (2018). Fatty acid synthesis pathway provides lipid precursors for rhamnolipid biosynthesis in Burkholderia thailandensis E264. *Applied Microbiology and Biotechnology*, *102*(14), 6163–6174. https://doi.org/10.1007/s00253–018–9059–5

Jahan, R., Bodratti, A. M., Tsianou, M., & Alexandridis, P. (2020). Biosurfactants, natural alternatives to synthetic surfactants: Physicochemical properties and applications. In *Advances in Colloid and Interface Science* (Vol. 275, p. 102061). Elsevier. https://doi.org/10.1016/j.cis.2019.102061

Kourmentza, C., Costa, J., Azevedo, Z., Servin, C., Grandfils, C., De Freitas, V., & Reis, M. A. M. (2018). Burkholderia thailandensis as a microbial cell factory for the bioconversion of used cooking oil to polyhydroxyalkanoates and rhamnolipids. *Bioresource Technology*, *247*, 829–837. https://doi.org/10.1016/j.biortech.2017.09.138

Mohammed, M., & Babadagli, T. (2015). Wettability alteration: A comprehensive review of materials/methods and testing the selected ones on heavy–oil containing oil–wet systems. In *Advances in Colloid and Interface Science* (Vol. 220, pp. 54–77). Elsevier. https://doi.org/10.1016/j.cis.2015.02.006

Ndlovu, T., Rautenbach, M., Vosloo, J. A., Khan, S., & Khan, W. (2017). Characterisation and antimicrobial activity of biosurfactant extracts produced by Bacillus amyloliquefaciens and

Pseudomonas aeruginosa isolated from a wastewater treatment plant. *AMB Express*, *7*(1), 1–19. https://doi.org/10.1186/s13568–017–0363–8

Rellegadla, S., Jain, S., & Agrawal, A. (2019). Oil reservoir simulating bioreactors: tools for understanding petroleum microbiology. In *Applied Microbiology and Biotechnology*. Springer. https://doi.org/10.1007/s00253–019–10311–5

Rocha, V. A. L., de Castilho, L. V. A., de Castro, R. P. V., Teixeira, D. B., Magalhães, A. V., Gomez, J. G. C., & Freire, D. M. G. (2020). Comparison of mono–rhamnolipids and di–rhamnolipids on microbial enhanced oil recovery (MEOR) applications. *Biotechnology Progress*, *36*(4), e2981. https://doi.org/10.1002/btpr.2981

Rodrigues, A. I., Gudiña, E. J., Abrunhosa, L., Malheiro, A. R., Fernandes, R., Teixeira, J. A., & Rodrigues, L. R. (2021). Rhamnolipids inhibit aflatoxins production in Aspergillus flavus by causing structural damages in the fungal hyphae and down–regulating the expression of their biosynthetic genes. *International Journal of Food Microbiology*, *348*, 109207. https://doi.org/10.1016/j.ijfoodmicro.2021.109207

Rodrigues, A. I., Gudiña, E. J., Teixeira, J. A., & Rodrigues, L. R. (2017). Sodium chloride effect on the aggregation behaviour of rhamnolipids and their antifungal activity. *Scientific Reports*, *7*(1), 1–9. https://doi.org/10.1038/s41598–017–13424–x

Rufino, R. D., Luna, J. M., Marinho, P. H. C., Farias, C. B. B., Ferreira, S. R. M., & Sarubbo, L. A. (2013). Removal of petroleum derivative adsorbed to soil by biosurfactant Rufisan produced by Candida lipolytica. *Journal of Petroleum Science and Engineering*, *109*, 117–122. https://doi.org/10.1016/j.petrol.2013.08.014

Segovia, V., Reyes, A., Rivera, G., Vázquez, P., Velazquez, G., Paz–González, A., & Hernández–Gama, R. (2021). Production of rhamnolipids by the Thermoanaerobacter sp. CM–CNRG TB177 strain isolated from an oil well in Mexico. *Applied Microbiology and Biotechnology*, *105*(14–15), 5833–5844. https://doi.org/10.1007/s00253–021–11468–8

Sen, S., Borah, S. N., Bora, A., & Deka, S. (2020). Rhamnolipid exhibits anti–biofilm activity against the dermatophytic fungi Trichophyton rubrum and Trichophyton mentagrophytes. *Biotechnology Reports*, *27*, e00516. https://doi.org/10.1016/j.btre.2020.e00516

Sharma, R., Singh, J., & Verma, N. (2018). Optimization of rhamnolipid production from Pseudomonas aeruginosa PBS towards application for microbial enhanced oil recovery. *3 Biotech*, *8*(1), 20. https://doi.org/10.1007/s13205–017–1022–0

Soares da Silva, R. de C. F., Almeida, D. G., Meira, H. M., Silva, E. J., Farias, C. B. B., Rufino, R. D., Luna, J. M., & Sarubbo, L. A. (2017). Production and characterization of a new biosurfactant from Pseudomonas cepacia grown in low–cost fermentative medium and its application in the oil industry. *Biocatalysis and Agricultural Biotechnology*, *12*, 206–215. https://doi.org/10.1016/j.bcab.2017.09.004

Soares da Silva, R. de C. F., Luna, J. M., Rufino, R. D., & Sarubbo, L. A. (2021). Ecotoxicity of the formulated biosurfactant from Pseudomonas cepacia CCT 6659 and application in the bioremediation of terrestrial and aquatic environments impacted by oil spills. *Process Safety and Environmental Protection*, *154*, 338–347. https://doi.org/10.1016/j.psep.2021.08.038

Teixeira Souza, K. S., Gudiña, E. J., Schwan, R. F., Rodrigues, L. R., Dias, D. R., & Teixeira, J. A. (2018). Improvement of biosurfactant production by Wickerhamomyces anomalus CCMA 0358 and its potential application in bioremediation. *Journal of Hazardous Materials*, *346*, 152–158. https://doi.org/10.1016/j.jhazmat.2017.12.021

Toribio, J., Escalante, A. E., & Soberón–Chávez, G. (2010). Rhamnolipids: Production in bacteria other than Pseudomonas aeruginosa. In *European Journal of Lipid Science and Technology* (Vol. 112, Issue 10, pp. 1082–1087). John Wiley & Sons, Ltd. https://doi.org/10.1002/ejlt.200900256

Varjani, S., Rakholiya, P., Yong Ng, H., Taherzadeh, M. J., Hao Ngo, H., Chang, J. S., Wong, J. W. C., You, S., Teixeira, J. A., & Bui, X. T. (2021). Bio–based rhamnolipids production and recovery from waste streams: Status and perspectives. In *Bioresource Technology* (Vol. 319, p. 124213). Elsevier. https://doi.org/10.1016/j.biortech.2020.124213

Xu, M., Fu, X., Gao, Y., Duan, L., Xu, C., Sun, W., Li, Y., Meng, X., & Xiao, X. (2020). Characterization of a biosurfactant–producing bacteria isolated from Marine environment: Surface activity, chemical characterization and biodegradation. *Journal of Environmental Chemical Engineering*, *8*(5), 104277. https://doi.org/10.1016/j.jece.2020.104277

CHAPTER 6.

Biosurfactant and biopolymer co–production by *Bacillus velezensis* P#02 from agro–industrial wastes

Abstract

Poly–γ–glutamic acid (γ–PGA) is a promising biopolymer, generally produced by different *Bacillus* species. This biopolymer has a wide range of industrial applications, from food to medical industries, and it has been successfully utilized in bioremediation. In this work, γ–PGA production by *Bacillus velezensis* P#02 (isolated from a Brazilian oilfield) was optimized. A culture medium containing corn steep liquor (CSL) as an alternative nitrogen source, glucose and L–glutamic acid was developed, allowing the production of 9.8 g/L of γ–PGA with good viscoelastic properties. The crude biopolymer produced increased the apparent viscosity of an aqueous solution up to 4466 ± 177 mPa s after 48 hours of growth, about 33 times the value obtained in the synthetic medium (PTYG). Besides γ–PGA, this strain was able to simultaneously produce biosurfactants. In a medium containing CSL and glucose as sole substrates, *B. velezensis* P#02 produced 804 mg/L of biosurfactant, which reduced the surface tension of water up to 29.7 ± 0.2 mN/m and had a critical micelle concentration (CMC) of 51 mg/L. The addition of L–glutamic acid to the medium not only increased γ–PGA production, but also increased the amount of biosurfactant produced to 900 mg/L. The biosurfactant produced in the medium supplemented with L–glutamic acid had similar surface active properties but was better at altering the wettability of oil–coated glass surfaces. Furthermore, this microorganism grows and produces biosurfactant and γ–PGA at temperatures up to 45°C, which is favorable for *in situ* microbial enhanced oil recovery (MEOR) applications. In *ex situ* sand–pack column assays, the injection of the cell–free supernatant from cultures of *B. velezensis* P#02 supplemented with additional crude γ–PGA recovered 13.9% more oil than the control. These results demonstrate the potential application of this microorganism and the biomolecules it produces in the petroleum industry.

6.1 Introduction

Poly–γ–glutamic acid (γ–PGA) is an anionic polypeptide composed of L–/D–glutamic acid monomers, polymerized through γ–amide–linkages (Verma et al., 2020). The chemical properties of this biopolymer vary greatly according to the microorganism used for its production, the fermentation conditions and the substrates used (Parati et al., 2022). Due to this high variability, γ–PGA has a wide range of industrial applications in the food, medical, pharmaceutical, and cosmetic industries, as well as in bioremediation. Furthermore, its biodegradability, biocompatibility, non–toxicity and edibility make it an attractive biopolymer for commercial uses (Parati et al., 2022; Verma et al., 2020).

The main producers of γ–PGA include several members of *Bacillus* species, like *B. subtilis*, *B. licheniformis*, *B. amyloliquefaciens* and *B. velezensis* (Flores et al., 2020; Liu et al., 2022). They are usually divided into glutamic acid–dependent producers, which require an external source of glutamic acid to polymerize into γ–PGA, and glutamic acid–independent producers, that can convert carbon sources into glutamic acid via the tricarboxylic acid (TCA) cycle, which is subsequently used to synthetize γ–PGA (Parati et al., 2022; Sirisansaneeyakul et al., 2017). Usually, glutamic acid–dependent producers generate higher titers of γ–PGA. For instance, a final concentration of 101 g/L of γ–PGA was obtained from *B. subtilis* ZJU–7, a glutamic acid–dependent producer (Huang et al., 2011); while a glutamic–acid independent producer, *B. licheniformis* TSISR 1010, produced only 40 g/L at lower productivity (Kongklom et al., 2017). Supplementing the culture medium with glutamic acid, however, significantly increases production costs, so glutamic acid–independent producers, like some strains of *B. velezensis*, are being studied as cost–effective alternatives (Cristiano–Fajardo et al., 2019; Flores et al., 2020; Hu et al., 2023; Sirisansaneeyakul et al., 2017).

Low–cost substrates can also be used to reduce γ–PGA production costs (Nair et al., 2021). Cane molasses has been used as a substitute for the carbon source (D. Zhang et al., 2012), as well as rice straw (Tang et al., 2015), corncobs (Sun et al., 2021; Zhu et al., 2014), goose feathers (Altun, 2019) and waste paper (Scheel et al., 2019). Additionally, fishmeal wastewater has been used as an alternative nitrogen source in γ–PGA production (C. Zhang et al., 2019), and waste liquor of monosodium glutamate can be used as a low–cost source of glutamic acid (Yong et al., 2011; D. Zhang et al., 2012). However, most of these alternative substrates need an acid or alkali pre–treatment prior to their utilization and usually require supplementation with additional nutrients (Nair et al., 2021). Corn steep liquor (CSL) could be an interesting low–cost carbon and nitrogen source that does not require pre–treatment (Gudiña, Rodrigues, et al., 2015). This agro–industrial residue also contains vitamins and minerals that contribute

to cell growth and production of biomolecules by microorganisms. CSL has been successfully used to produce different microbial biopolymers (Gudiña et al., 2023; Sharma et al., 2013; Xia et al., 2018), including γ–PGA (Lee et al., 2014; J. Li et al., 2022).

Besides γ–PGA, *Bacillus* spp. are also known biosurfactant producers, producing mainly lipopeptides such as surfactin (Gudiña, Fernandes, et al., 2015; Guimarães et al., 2021; Pereira et al., 2013). Under certain conditions, these microorganisms can produce both biomolecules simultaneously (Fernandes et al., 2016). For application in Microbial Enhanced Oil Recovery (MEOR), this can constitute an advantage since the combined use of biopolymers and biosurfactants has been shown to improve recovery rates (Al–Ghailani et al., 2021; Fernandes et al., 2016; Ge et al., 2021; Ji et al., 2022; Qi et al., 2018), as previously discussed (Chapter 4). Furthermore, co–producing strains are an opportunity for *in situ* applications, that are usually easier to apply and are more cost–effective than *ex situ* approaches (Ke et al., 2018; Saravanan et al., 2020).

The aim of this work was to optimize γ–PGA and biosurfactant production in *Bacillus* strains isolated from crude oil samples using CSL as a low–cost substrate. Rheological properties of the γ–PGA produced were also evaluated, as well as the surface active properties and emulsification activity of the biosurfactant. Furthermore, sand–pack column assays were performed to determine the applicability of the produced biomolecules in MEOR.

6.2 Materials and methods

6.2.1 Strains and culture conditions

Four *Bacillus*–like strains (P#01, P#02, P#03 and P#04) isolated from crude oil samples from the Potiguar oilfield (Brazil) were used in this study. The strains were maintained in Luria–Bertani (LB) medium, supplemented with 20% (v/v) of glycerol at −80°C. Pre–cultures were prepared by inoculating 20 mL of LB medium with 100 µL from a frozen stock, and were incubated overnight at 37°C and 150 rpm.

6.2.2 Biosurfactant production

6.2.2.1 Screening biosurfactant production

Biosurfactant production by the four isolates was evaluated in 250 mL flasks, containing 100 mL of LB medium. Each flask was inoculated with 1% (v/v) of a pre–culture and incubated at 37°C and 150 rpm. Samples were taken at different time intervals to determine biosurfactant production, as described in section 6.2.6.4.

6.2.2.2 Biosurfactant recovery

Biosurfactants were recovered as described in Chapter 3 (3.2.5).

6.2.3 Biopolymer production

6.2.3.1 Screening biopolymer production

Biopolymer production by the strains P#02 and P#04 was initially evaluated in 250 mL flasks containing 100 mL of different culture media with the following composition:

- 10% (v/v) corn steep liquor (CSL) (Gudiña, Fernandes, et al., 2015);
- MSS medium: 10 g/L sucrose, 10 g/L NaCl, 5 g/L Na_2HPO_4, 2 g/L NH_4NO_3, 2 g/L KH_2PO_4 and 0.2 g/L $MgSO_4 \cdot 7H_2O$ (Gudiña et al., 2012);
- PTYG medium: 10 g/L glucose, 10 g/L NaCl, 10 g/L yeast extract, 5 g/L tryptone, 0.2 g/L $MgSO_4 \cdot 7H_2O$ and 0.02 g/L $CaCl_2 \cdot 2H_2O$;
- Medium A: 10 g/L glucose, 5 g/L peptone, 3 g/L yeast extract and 3 g/L meat extract;
- MM medium: 13.9 g/L K_2HPO_4, 10 g/L sucrose, 10 g/L NaCl, 2.7 g/L KH_2PO_4, 2 g/L yeast extract, 2 g/L NH_4NO_3, 0.05 g/L $MgSO_4 \cdot 7H_2O$ and 0.025 g/L $MnSO_4 \cdot 4H_2O$;
- ML9 medium: 10 g/L sucrose, 10 g/L yeast extract, 3 g/L K_2HPO_4, 1 g/L KH_2PO_4, 0.3 g/L $CaCl_2 \cdot 2H_2O$ and 0.2 g/L $MgSO_4 \cdot 7H_2O$.

All the media were adjusted to pH 7.0. Each flask was inoculated with 1% (v/v) of a pre–culture and incubated at 37°C and 150 rpm or under static conditions. Samples were taken at different time intervals to determine biopolymer production, as described in section 6.2.6.4. Furthermore, the samples were analyzed for biosurfactant production, as described in section 6.2.6.1.

6.2.3.2 Effect of different temperatures and agitation speeds on biopolymer production

The media described in the previous section that yielded the best results (MM and PTYG) were used to optimize biopolymer production by the isolates P#02 and P#04. Biopolymer production was evaluated in 250 mL flasks, containing 100 mL of culture medium. Each flask was inoculated with 1% (v/v) of a pre–culture and incubated at different temperatures (30, 37, 45 and 50°C) and agitation speeds (0, 30, 50, 75, 100 and 150 rpm). Samples were taken at different time intervals to determine biopolymer production, as described in section 6.2.6.4. Furthermore, the samples were analyzed for biosurfactant production, as described in section 6.2.6.1.

6.2.3.3 Effect of alternative substrates on biopolymer production

Biopolymer production by the *Bacillus* sp. isolates P#02 and P#04 was evaluated in 100 mL flasks containing 50 mL of the different culture media. Each flask was inoculated with 1% (v/v) of a pre–culture and incubated at 37°C and static conditions. PTYG medium was used as control, and CSL (kindly provided by COPAM – Companhia Portuguesa de Amidos, S. A. (Portugal)) was evaluated as an alternative substrate. CSL was diluted with demineralized water at different concentrations (1 – 10% (v/v)) and used to supplement PTYG or as a substitute of the different components of PTYG. All the media were adjusted to pH 7.0. Samples were taken at different time intervals to determine biopolymer production, as described in section 6.2.6.4. Furthermore, the samples were analyzed for biosurfactant production, as described in section 6.2.6.1.

6.2.3.4 Effect of glutamic acid on biopolymer production

The effect of glutamic acid on biopolymer production by the isolate P#02 was evaluated in 100 or 500 mL flasks with 50 or 200 mL, respectively, of different culture media with the following composition:

- A: 20 g/L L–glutamic acid, 20 g/L glucose, 10 g/L $(NH_4)_2SO_4$, 1 g/L KH_2PO_4, 1 g/L Na_2HPO_4, 0.5 g/L $MgSO_4 \cdot 7H_2O$, 0.02 g/L $MnCl_2 \cdot 4H_2O$ and 0.028 g/L $FeCl_3$ (Chettri et al., 2016);
- B: 25 g/L L–glutamic acid, 30 g/L glycerol, 25 g/L yeast extract, 1.4 g/L KH_2PO_4, 3 g/L Na_2HPO_4, 0.9 g/L $MgSO_4 \cdot 7H_2O$ and 0.05 g/L $CuSO_4 \cdot 5H_2O$ (Lee et al., 2014);

- C: 10 g/L L–glutamic acid, 90 g/L glucose, 6.8 g/L NH_4Cl, 1 g/L KH_2PO_4, 0.5 g/L $MgSO_4 \cdot 7H_2O$, 0.05 g/L $MnSO_4 \cdot H_2O$, 0.02 g/L $FeCl_3$ and 0.2 g/L $CaCl_2$ (Sun et al., 2021);
- D: 20 g/L L–glutamic acid, 80 g/L glucose, 20 g/L sodium citrate dihidrate, 8 g/L NH_4Cl, 0.5 g/L KH_2PO_4, 20 g/L $NaNO_3$, 1 g/L $MgSO_4 \cdot 7H_2O$, 0.07 g/L $MnCl_2 \cdot 4H_2O$, 0.3 g/L $FeCl_3$ and 0.3 g/L $CaCl_2$ (Y. Li et al., 2020);
- PTYG+Glut(10): 10 g/L L–glutamic acid, 10 g/L glucose, 10 g/L NaCl, 10 g/L yeast extract, 5 g/L tryptone, 0.2 g/L $MgSO_4 \cdot 7H_2O$ and 0.02 g/L $CaCl_2 \cdot 2H_2O$;
- PTYG+Glut(20): 20 g/L L–glutamic acid, 10 g/L glucose, 10 g/L NaCl, 10 g/L yeast extract, 5 g/L tryptone, 0.2 g/L $MgSO_4 \cdot 7H_2O$ and 0.02 g/L $CaCl_2 \cdot 2H_2O$;
- CSLG+Glut(10): 10 g/L L–glutamic acid, 10% (v/v) CSL and 10 g/L glucose;
- CSLG+Glut(20): 20 g/L L–glutamic acid, 10% (v/v) CSL and 10 g/L glucose.

All the media were adjusted to pH 7.0. Each flask was inoculated with 1% (v/v) of a pre–culture and incubated at 37°C and static conditions or 150 rpm. Samples were taken at different time intervals to determine biopolymer production, as described in section 6.2.6.4. Furthermore, the samples were analyzed for biosurfactant production, as described in section 6.2.6.1.

6.2.3.5 Biopolymer recovery

Each of the collected samples was first centrifuged (9400 x *g*, 20 min) to remove the cells. The biopolymer was then precipitated by adding two volumes of ethanol (99%, v/v) to 30 mL of cell–free supernatant (CFS) and incubating the mixture at –20°C for 24h. Afterwards, the samples were centrifuged (9400 x *g*, 20 min, 4°C) and the pellet containing the biopolymer was resuspended in 5 mL of demineralized water to measure the apparent viscosity, as described in section 6.2.6.4, or diluted 5 times with demineralized water to purify the biopolymer, as described by Novak et al. (1992).

6.2.4 Optimizing a synthetic medium for biosurfactant and biopolymer production

To optimize biosurfactant and biopolymer production, a Plackett–Burman experimental design (PBD) was performed using the Statistica 12.0 software for seven independent variables, comprising each component of the PTYG+Glut(10) culture medium: L–glutamic acid (X_1), glucose (X_2), yeast extract (X_3), tryptone (X_4), NaCl (X_5), $CaCl_2 \cdot 2H_2O$ (X_6) and $MgSO_4 \cdot 7H_2O$ (X_7). Each variable was evaluated in three levels (Table 6.1) over 15 runs defined by the Statistica 12.0 software, where three of those were repetitions at the central point. The independent responses analyzed were apparent viscosity and surface

tension (ST) reduction after 168h of growth at 37°C and under static conditions. The latter was calculated as the difference between the ST of demineralized water (70 mN/m) and the ST measured on the CFS diluted 10 times with demineralized water, as described in section 6.2.6.1. The results were subjected to a regression analysis.

Table 6.1 – Experimental level and ranges for the independent variables used in the Plackett–Burman design (PBD).

Independent variable	Code	Experimental design level		
		–1	0	+1
L–glutamic acid (g/L)	X_1	0	5	10
Glucose (g/L)	X_2	5	10	15
Yeast extract (g/L)	X_3	2	6	10
Tryptone (g/L)	X_4	1	3	5
NaCl (g/L)	X_5	0	5	10
$CaCl_2 \cdot 2H_2O$ (g/L)	X_6	0	0.01	0.02
$MgSO_4 \cdot 7H_2O$ (g/L)	X_7	0	0.10	0.20

Next, a central composite rotational design (CCRD) was performed using the Statistica 12.0 software for the independent variables that were significant according to the PBD: L–glutamic acid (X_1), glucose (X_2), yeast extract (X_3) and tryptone (X_4). Each variable was evaluated in five levels (Table 6.2) over 30 runs defined by the statistical software, where six of those were repetitions at the central point. NaCl concentration was kept constant in all experiments at the highest concentration tested (10 g/L), as explained in the Results section. The independent responses analyzed were the same as in PBD.

Table 6.2 – Experimental level and ranges for the independent variables used in the central composite rotational design (CCRD).

Independent variable	Code	Experimental design level				
		–2	–1	0	+1	+2
L–glutamic acid (g/L)	X_1	7.49	11.87	16.25	20.62	25.00
Glucose (g/L)	X_2	10.00	15.00	20.00	25.00	30.00
Yeast extract (g/L)	X_3	0.00	1.25	2.50	3.75	5.00
Tryptone (g/L)	X_4	2.50	4.37	6.24	8.12	9.99

6.2.5 Identification of the isolate P#02

The isolate P#02, which displayed the best results regarding biosurfactant and biopolymer production, was identified by partial 16S rDNA sequencing. The 16S rDNA gene was amplified by PCR

using the primers 27F and 1492R. The resulting consensus sequence was compared with the existing sequences in the GenBank database of the National Center for Biotechnology Information (NCBI) (http://www.ncbi.nlm.nih.gov) using the nucleotide–nucleotide blast (BLASTn) network service, to determine its phylogenetic affiliation.

6.2.6 Analytical methods

6.2.6.1 Surface tension measurement and critical micelle concentration

ST and critical micelle concentration (CMC) of the CFS and biosurfactant solutions were determined as described in Chapter 3 (3.2.6.4).

6.2.6.2 Emulsifying activity

Emulsifying activity (E_{24}) of biosurfactant solutions (prepared in phosphate–buffered saline (PBS) solution) was determined as described in Chapter 5 (5.2.6.4).

6.2.6.3 Contact angle measurement

Contact angles between a water/biosurfactant solution (at different concentrations: CMC, 2 x CMC and 5 x CMC) droplet and an oil–coated glass surface were determined as described in Chapter 5 (5.2.6.5).

6.2.6.4 Rheological properties

The rheological properties (steady flow and dynamic viscoelasticity) of the crude biopolymer were determined as described in Chapter 4 (4.2.3). The apparent viscosity was determined as described in Chapter 2 (2.2.3).

6.2.7 Biopolymer characterization

6.2.7.1 Preliminary characterization

For preliminary characterization of the biopolymer produced by the isolate P#02, the purified biopolymer was subjected to acid hydrolysis with 6 M HCl at 105°C for 8h, according to the method from Zeng et al. (2012). The hydrolysate was then neutralized with 10 M NaOH and filtered for analysis.

The purified and the hydrolyzed biopolymer were analyzed by ultra–high–performance liquid chromatography (uHPLC – Nexera X2, SHIMADZU) using a Zorbax C18 column (5 µm, 4.6 × 250 mm, Agilent) coupled to an ultraviolet (UV) detector (DAD – SPD–M20A). Operating conditions were as follows: flow rate was set at 0.4 mL/min, injection volume was 20 µL, temperature of the column was kept at 30°C and UV detection was set at 290 nm. The mobile phase consisted of acetonitrile (eluent B) and ultrapure water (eluent A) mixtures, pumped into the system in a linear gradient mode: at 0 min 10% (v/v) acetonitrile, from 30 min to 31 min 90% (v/v) acetonitrile, at 34 min 10% (v/v) acetonitrile kept for 1 min. The concentration of L–glutamic acid was calculated according to a calibration curve prepared using the pure compound.

6.2.7.2 Nuclear magnetic resonance spectroscopy

The purified biopolymer produced by the isolate P#02 was dissolved in deuterium oxide (D_2O) at 1 mg/mL and analyzed on a Bruker Ascend 600 MHz nuclear magnetic resonance (NMR) spectrometer equipped with a 5 mm probe (CPP BBO 600S3 BB–H F–D–05 Z). The acquisition parameters were as follows: recycle delay: 5 s, 256 scans; data acquisition size: 64,000.

6.2.7.3 Surface–induced dissociation (SID) – Orbitrap mass spectrometry

The purified biopolymer was characterized through surface induced dissociation (SID)–Orbitrap mass spectrometry (MS). The sample was dissolved in ultrapure water (1 mg/mL) and directly infused into an LTQ–Orbitrap–XL mass spectrometer. The instrument parameters were as follows: mass range: 200 – 4 000 m/z; FT resolution: 60,000; negative polarity. SID energy was set at 35 V.

6.2.8 Oil recovery in sand–pack columns

Oil recovery assays in sand–pack columns were performed as described in Chapter 4 (4.2.5). The assays were performed using crude oil from the Potiguar oilfield in Brazil ($\eta_{40°C}$ = 110 mPa s at 1.4 s^{-1}) through *in situ* and *ex situ* approaches.

In *ex situ* assays, 200 mL of treatment solution (P#02 crude biopolymer, CFS from cultures of P#02, or CFS from cultures of P#02 with addition of P#02 crude biopolymer to increase viscosity) were injected into the columns, followed by the injection of demineralized water to make up 400 mL of injected fluid. Alternatively, 1 pore volume (PV) of CFS from cultures of P#02 performed in synthetic (PTYG) medium was injected into the columns and incubated for 48h at 40°C. Next, 200 mL of a xanthan gum (Sigma–Aldrich) solution prepared at 1 g/L ($\eta_{40°C}$ = 99 ± 6 mPa s at 1.4 s^{-1}) were injected into the columns, followed by 200 mL of demineralized water.

In *in situ* assays, 1 PV of P#02 cell culture in CSLG medium was injected into the columns and incubated for 14 days at 40°C to allow cell growth. Next, 200 mL of a xanthan gum (Sigma–Aldrich) solution, prepared at 1 g/L, were injected into the columns, followed by 200 mL of demineralized water.

6.3 Results

6.3.1 Screening biosurfactant production by *Bacillus* sp. isolates

Four *Bacillus*–like strains (P#01, P#02, P#03 and P#04) isolated from crude oil samples from a Brazilian oilfield were tested for biosurfactant production (Table 6.3). Only two (P#02 and P#04) of the four isolates reduced the surface tension of the supernatants (LB medium) to values below 30 mN/m (28.4 ± 0.1 mN/m and 28.2 ± 0.1 mN/m after 24h, respectively), which are typical values for biosurfactant–producing strains. Besides showing a significant decrease in surface tension values, both isolates also seemed to increase the viscosity of the culture medium, suggesting that these strains produce an extracellular biopolymer, as will be discussed in the following section.

Table 6.3 – Surface tension values (mN/m) obtained with the isolates P#01, P#02, P#03 and P#04 grown in LB medium at 37°C and 150 rpm.

Isolate	ST (mN/m)			ST^{-1} (mN/m)		
	24h	48h	72h	24h	48h	72h
P#01	61.3 ± 1.6	63.1 ± 1.3	51.0 ± 0.7	–	–	–
P#02	28.4 ± 0.1	28.6 ± 0.1	28.6 ± 0.2	35.9 ± 0.7	35.9 ± 1.0	36.6 ± 0.7
P#03	64.5 ± 0.6	63.8 ± 1.1	62.0 ± 1.1	–	–	–
P#04	28.2 ± 0.1	28.6 ± 0.2	28.6 ± 0.2	35.5 ± 0.9	34.9 ± 0.5	35.5 ± 0.6

ST_{0h} = 50.0 ± 0.2 mN/m. ST^{-1}_{0h} = 65.0 ± 0.3 mN/m. ST: surface tension of the cell–free supernatant (CFS); ST^{-1}: surface tension of the CFS diluted 10 times with demineralized water.

6.3.2 Screening biopolymer production by *Bacillus* sp. isolates

In order to evaluate the co–production of biosurfactants and biopolymer, *Bacillus* sp. P#02 and P#04 were grown in different culture media under static conditions or at 150 rpm (Table 6.4). Both isolates were able to produce biosurfactants in all the culture media assayed. However, biopolymer production only occurred when they were grown in the media MM and PTYG.

Table 6.4 – Surface tension values (mN/m) of the cell–free supernatant (CFS) and apparent viscosity values (mPa s) of the crude biopolymer produced by the isolates P#02 and P#04 grown in different media at 37°C and 0 – 150 rpm for 48h.

Isolate	Culture medium	Agitation (rpm)	ST (mN/m)	ST^{-1} (mN/m)	$\eta_{40°C}$ (mPa s)
P#02	CSL	150	27.7 ± 0.0	30.5 ± 0.2	–
	MSS	150	26.6 ± 0.2	36.2 ± 0.3	–
	PTYG	0	28.3 ± 0.1	37.7 ± 2.1	136 ± 4
		150	26.3 ± 0.8	29.3 ± 1.0	53 ± 4
	Medium A	0	29.2 ± 0.6	40.6 ± 1.0	–
		150	30.1 ± 0.2	37.8 ± 0.7	–
	MM	0	28.5 ± 0.1	39.5 ± 3.0	47 ± 12
		150	27.5 ± 0.1	33.7 ± 1.0	82 ± 13
	ML9	0	28.6 ± 0.6	–	–
		150	28.1 ± 0.0	30.7 ± 0.2	–
P#04	CSL	150	28.5 ± 0.1	34.0 ± 0.7	–
	MSS	150	26.4 ± 0.2	48.8 ± 3.2	–
	PTYG	0	29.1 ± 0.2	42.0 ± 2.4	165 ± 5
		150	25.8 ± 0.3	27.8 ± 0.5	64 ± 21
	Medium A	0	29.6 ± 0.2	52.0 ± 4.0	–
		150	30.1 ± 0.1	37.6 ± 0.5	–

MM	0	28.4 ± 0.1	39.1 ± 2.5	74 ± 2
	150	27.5 ± 0.0	32.3 ± 0.6	75 ± 10
ML9	0	28.5 ± 0.3	–	–
	150	27.9 ± 0.2	29.9 ± 0.2	–

ST: surface tension of the cell–free supernatant (CFS); ST^{-1}: surface tension of the CSF diluted 10 times with demineralized water. $\eta_{40°C}$: apparent viscosity values of crude biopolymer solutions measured at 40°C and a shear rate of 1.4 s^{-1}.

6.3.3 Optimization of biopolymer production by *Bacillus* sp. isolates

6.3.3.1 Effect of different temperatures and agitation speeds on biopolymer production

To optimize the production of biopolymer by the selected isolates (P#02 and P#04), they were grown under different temperatures and agitation speeds in PTYG and MM media (Table 6.5). Both isolates were found to produce biosurfactants at temperatures up to 45°C, and although they also grow at 50°C, at this temperature biosurfactant production was not observed. Biopolymer production was favored, in both isolates, when they were grown under low agitation or static conditions, the best results being achieved with the medium PTYG.

Table 6.5 – Surface tension values (mN/m) of the cell–free supernatant (CFS) and apparent viscosity values (mPa s) of the crude biopolymer produced by the isolates P#02 and P#04 grown in different media at 30 – 50°C and 0 – 150 rpm for 48h.

Isolate	Culture medium	Temp. (˚C)	Agitation (rpm)	ST (mN/m)	ST^{-1} (mN/m)	$\eta_{40°C}$ (mPa s)
P#02	MM	30	150	27.5 ± 0.0	30.6 ± 0.2	54 [1]
		37		27.5 ± 0.1	33.7 ± 1.0	82 ± 13
		45		27.5 ± 0.2	44.2 ± 4.0	59 [1]
		50		63.9 ± 1.1	–	–
	PTYG	37	0	28.3 ± 0.1	37.7 ± 2.1	136 ± 4
			30	28.2 ± 0.0	43.8 ± 4.2	94 ± 2
			50	30.1 ± 0.2	42.6 ± 2.6	139 ± 1
			75	55.3 ± 0.4	–	65 ± 18
			100	49.9 ± 6.5	–	–
			150	26.3 ± 0.8	29.3 ± 1.0	53 ± 4
P#04	MM	30	150	27.3 ± 0.3	30.2 ± 0.1	50 [1]
		37		27.5 ± 0.0	32.3 ± 0.6	75 ± 10

	45		27.2 ± 0.1	42.1 ± 3.7	61 [1]
	50		63.9 ± 1.5	–	–
PTYG	37	0	29.1 ± 0.2	42.0 ± 2.4	165 ± 5
		30	28.2 ± 0.0	37.7 ± 2.0	119 ± 0
		50	33.8 ± 0.8	–	76 ± 13
		75	55.3 ± 0.4	–	60 ± 7
		100	54.2 ± 0.7	–	–
		150	25.8 ± 0.3	27.8 ± 0.5	64 ± 21

[1] – Biopolymer extracted from 16 mL of culture and resuspended in 5 mL of demineralized water

ST: surface tension of the CFS; ST^{-1}: surface tension of the CFS diluted 10 times with demineralized water. $\eta_{40°C}$: apparent viscosity values of crude biopolymer solutions measured at 40°C and shear rate 1.4 s^{-1}.

6.3.3.2 Effect of alternative substrates on biopolymer production

Aiming to reduce production costs, biopolymer production by *Bacillus* sp. P#02 and P#04 was evaluated using several low–cost media containing CSL as an alternative substrate. CSL was added to the PTYG medium or used to replace some of its components (Table 6.6), namely the nitrogen sources (yeast extract or tryptone) and the salts (NaCl, $CaCl_2$ and $MgSO_4$). In a medium containing CSL as the sole ingredient, tested in a previous section, there was no visual increase in the viscosity of the cultures (Table 6.4). Because of this, glucose (10 g/L) was included in all the media tested here as the main carbon source to produce biopolymer.

Regarding biosurfactant production, the best results were obtained for the isolate P#02 in the PTYG+10% CSL medium, with a ST value of 27.6 ± 0.3 mN/m (Table 6.6). In this medium, however, the apparent viscosity was lower than in the other media containing 10% CSL. This, and the fact that, with the isolate P#02, the highest viscosity value was obtained with the CSLG (10% (v/v) CSL and 10 g/L glucose) medium (2308 ± 461 mPa s), suggests that the nitrogen sources present in CSL are more favorable for biopolymer production. Furthermore, results suggest that the salts present in PTYG do not to contribute to biopolymer production, even though their presence results in a higher surface activity (or the production of higher amounts of biosurfactant) (Table 6.6).

Table 6.6 – Surface tension values (mN/m) of the cell–free supernatant (CFS) and apparent viscosity values (mPa s) of the crude biopolymer produced by the isolates P#02 and P#04 grown in different media with CSL (1 – 10% (v/v)) at 37°C and static conditions for 48h.

Isolate	Culture medium	ST (mN/m)	ST^{-1} (mN/m)	$\eta_{40°C}$ (mPa s)
P#02	PTYG+1% CSL	28.8 ± 0.1	41.1 ± 3.8	70 ± 7
	PTYG+5% CSL	28.9 ± 0.1	33.1 ± 0.6	593 ± 82
	PTYG+10% CSL	27.6 ± 0.3	31.5 ± 0.6	974 ± 327
	10% CSL+Glucose	29.2 ± 0.1	37.1 ± 2.1	2308 ± 461
	10% CSL+Glucose+Tryptone	29.6 ± 0.3	33.4 ± 0.3	1073 ± 230
	10% CSL+Glucose+Salts	29.0 ± 0.1	33.2 ± 0.7	1324 ± 287
P#04	PTYG+1% CSL	29.1 ± 0.1	41.2 ± 3.2	–
	PTYG+5% CSL	30.2 ± 0.2	35.9 ± 1.2	458 ± 101
	PTYG+10% CSL	29.2 ± 0.1	40.2 ± 2.6	1057 ± 389
	10% CSL+Glucose	30.3 ± 0.1	38.4 ± 2.0	1956 ± 455
	10% CSL+Glucose+Tryptone	29.7 ± 0.2	40.7 ± 1.9	2115 ± 430
	10% CSL+Glucose+Salts	29.7 ± 0.1	39.3 ± 2.5	3181 ± 885

–: The apparent viscosity was not measured, as it was not observed a visual increase in the viscosity of the culture medium. ST: surface tension of the CFS; ST^{-1}: surface tension of the CFS diluted 10 times with demineralized water. $\eta_{40°C}$: apparent viscosity values of biopolymer solutions measured at 40°C and a shear rate of 1.4 s^{-1}, corresponding to the first and the third flow ramps from the same measurement ± standard deviation between the two ramps.

Overall, the highest viscosity value (3181 ± 885 mPa s) was obtained with the isolate P#04 when grown in the CSLG medium supplemented with the PTYG salts (Table 6.6). The apparent viscosity of the biopolymer produced by this isolate in the different media, however, displayed a high variability in the values obtained in the different flow ramps within the same measurement. As such, the biopolymer produced by this microorganism was thought to be unstable, since it appears to suffer some structural modifications when submitted to high shear rates. Accordingly, the isolate P#02 was selected for further studies.

6.3.3.3 Effect of glutamic acid on biopolymer production

The effect of glutamic acid on biopolymer production by *Bacillus* sp. P#02 was evaluated with different culture media (Table 6.7).

Table 6.7 – Surface tension values (mN/m) of the cell–free supernatant (CFS) and apparent viscosity values (mPa s) of crude biopolymer solutions obtained with the isolate P#02 grown in different media at 37°C and 0 – 150 rpm for 48h.

Culture medium	Agitation (rpm)	ST (mN/m)	ST^{-1} (mN/m)	$\eta_{40°C}$ (mPa s)
A	0	28.9 ± 0.2	44.4 ± 3.0	55 ± 0
	150	29.0 ± 0.1	35.0 ± 0.7	–
B	0	27.6 ± 0.2	32.8 ± 1.0	73 ± 1
	150	26.6 ± 0.1	28.6 ± 0.3	–
C	150	26.9 ± 0.1	30.7 ± 0.3	–
D	150	28.6 ± 0.9	40.5 ± 2.3	–
PTYG+Glut(10)	0	27.5 ± 0.2	32.7 ± 0.5	1193 ± 17
PTYG+Glut(20)	0	28.0 ± 0.2	33.6 ± 0.5	2081*
CSLG+Glut(10)	0	28.4 ± 0.0	31.8 ± 0.2	4466 ± 177
CSLG+Glut(20)	0	27.6 ± 0.2	29.6 ± 0.1	2865 ± 220

* This value was measured through a method with only one flow ramp.

ST: surface tension of the CFS; ST^{-1}: surface tension of the CSF diluted 10 times with demineralized water. $\eta_{40°C}$: apparent viscosity values of crude biopolymer solutions measured at 40°C and shear rate 1.4 s^{-1}.

The isolate was able to produce biopolymer in five of the eight media tested, while it produced biosurfactant in all the media. The addition of glutamic acid to the media increased the apparent viscosity values by a factor of 8.8 with PTYG medium (1193 ± 17 mPa s in the medium with 10 g/L of L–glutamic acid, compared to 136 ± 4 mPa s in the medium without) and 1.9 with CSLG medium (4466 ± 177 mPa s in the medium with 10 g/L of L–glutamic acid, compared to 2308 ± 461 mPa s in the medium without) (Table 6.7). This suggests that the biopolymer produced may be composed of glutamate monomers and is likely to be poly–γ–glutamic acid (γ–PGA). Furthermore, it was observed that longer incubation times resulted in a higher biopolymer production, as the apparent viscosity values increased over time, up to 4494 ± 39 mPa s in PTYG+Glut(10) medium over 168h of growth and 6286 ± 51 mPa s in CSLG+Glut(10) over 72h.

6.3.4 Identification of the isolate P#02

The isolate P#02 was identified according to the partial sequence obtained from its 16S rDNA gene. The consensus sequence obtained was compared with other sequences described in databases, showing a 99.93% similarity with *Bacillus velezensis* strain SF334 (GenBank database accession number CP125289.1). Accordingly, the isolate P#02 was identified as a *B. velezensis* strain.

6.3.5 Optimizing a synthetic medium for biosurfactant and biopolymer production

In order to try to maximize biosurfactant and biopolymer production by *B. velezensis* P#02 in the PTYG+Glut(10) medium, a PBD was used to determine which of the medium components are significant for their production. The results for apparent viscosity and ST reduction measured for the CFS diluted 10 times (Table 6.8) were subjected to a regression analysis, where a linear regression model (Table 6.9 and Table 6.10) was obtained for each response.

Regarding apparent viscosity, only L–glutamic acid, glucose and tryptone showed a significant effect (Table 6.9) at the 90% confidence level (p–value < 0.1). Based on the regression analysis, these components had a positive effect on biopolymer production, with L–glutamic acid having the highest impact on this response. This effect had already been confirmed in previous assays (Table 6.7), where the crude biopolymer produced in PTYG medium supplemented with L–glutamic acid exhibited a higher viscosity (1193 ± 17 and 2081 mPa s for PTYG+Glut(10) and PTYG+Glut(20), respectively) than in the original synthetic medium (136 ± 4 mPa s). For the surface tension reduction response, only glucose and NaCl were shown to be significant (Table 6.10) at a confidence level of 90% (p–value < 0.1), both with a positive effect on biosurfactant production.

Table 6.8 – Plackett–Burman design (PBD) matrix with the independent variables and apparent viscosity ($\eta_{40°C}$) and ST reduction (measured in the cell–free supernatant diluted 10 times).

Experiment	Coded variable							Response variable	
	X_1	X_2	X_3	X_4	X_5	X_6	X_7	$\eta_{40°C}$ (mPa s)	ST reduction (mN/m)
1	+1	–1	+1	–1	–1	–1	+1	328	35.2
2	+1	+1	–1	+1	–1	–1	–1	1310	34.4
3	–1	+1	+1	–1	+1	–1	–1	85	36.9
4	+1	–1	+1	+1	–1	+1	–1	1129	31.3
5	+1	+1	–1	+1	+1	–1	+1	1485	39.8
6	+1	+1	+1	–1	+1	+1	–1	1543	38.0
7	–1	+1	+1	+1	–1	+1	+1	246	35.4
8	–1	–1	+1	+1	+1	–1	+1	156	35.5
9	–1	–1	–1	+1	+1	+1	–1	81	36.7
10	+1	–1	–1	–1	+1	+1	+1	541	37.2
11	–1	+1	–1	–1	–1	+1	+1	52	32.3
12	–1	–1	–1	–1	–1	–1	–1	49	31.6
13	0	0	0	0	0	0	0	199	37.2
14	0	0	0	0	0	0	0	181	37.5
15	0	0	0	0	0	0	0	222	37.6

Table 6.9 – Regression analysis of the results obtained with the PBD for the apparent viscosity.

Factor	Effect	Standard Error	*t*–value	*p*–value
Mean	584.50	68.13	8.58	1.38E–04
Intercept	–767.00	304.69	–2.52	0.0455
$\mathbf{X_1}$	944.67	136.26	6.93	0.0004
$\mathbf{X_2}$	406.33	136.26	2.98	0.0246
$\mathbf{X_3}$	–5.00	136.26	–0.04	0.9719
$\mathbf{X_4}$	301.33	136.26	2.21	0.0690
$\mathbf{X_5}$	129.67	136.26	0.95	0.3780
$\mathbf{X_6}$	30.33	136.26	0.22	0.8312
$\mathbf{X_7}$	–231.33	136.26	–1.70	0.1405

Table 6.10 – Regression analysis of the results obtained with the PBD for the ST reduction.

Factor	Effect	Standard Error	*t*–value	*p*–value
Mean	35.36	0.40	88.74	1.38E–10
Intercept	4.15	1.78	2.33	0.0587
$\mathbf{X_1}$	1.25	0.80	1.57	0.1678
$\mathbf{X_2}$	1.55	0.80	1.95	0.0997
$\mathbf{X_3}$	0.05	0.80	0.06	0.9520
$\mathbf{X_4}$	0.32	0.80	0.40	0.7048
$\mathbf{X_5}$	3.98	0.80	5.00	0.0025
$\mathbf{X_6}$	–0.42	0.80	–0.52	0.6198
$\mathbf{X_7}$	1.08	0.80	1.36	0.2229

PBD was followed by a central composite rotational design (CCRD) where the significant variables were analyzed to determine the optimum concentration of each component in the culture medium to increase the yield of biomolecules. Although yeast extract was not considered significant for either biosurfactant or biopolymer production, it was also tested in CCRD with concentrations ranging from 0 to 5 g/L (Table 6.2). NaCl was set at 10 g/L, which is a commonly used concentration for biosurfactant production in other *Bacillus* sp. strains (Pereira et al., 2013). The results for apparent viscosity and ST reduction measured for the CFS diluted 10 times are presented in Table 6.11.

Because there was a lot of variability between the 6 central point experiments (Table 6.11), especially in regard to the apparent viscosity response (2141 – 5828 mPa s), not all the experiments were performed. The analysis was considered to be non–viable and the medium composition was not altered on further assays.

Table 6.11 – Central composite rotational design (CCRD) matrix with the independent variables and apparent viscosity ($\eta_{40°C}$) and ST reduction (measured in the cell–free supernatant diluted 10 times).

Experiment	Coded variable				Response variable	
	X_1	X_2	X_3	X_4	$\eta_{40°C}$ (mPa s)	ST reduction (mN/m)
1	–1	–1	–1	–1	1185	37.6
2	1	–1	–1	–1	1336	39.9
3	–1	1	–1	–1	379	39.1
4	1	1	–1	–1	705	36.2
5	–1	–1	1	–1	755	36.5
6	1	–1	1	–1	2291	35.9
7	–1	1	1	–1	1699	37.2
8	1	1	1	–1	3677	35.8
9	–1	–1	–1	1	5314	38.8
10	1	–1	–1	1	3816	36.4
11	–1	1	–1	1	–	–
12	1	1	–1	1	–	–
13	–1	–1	1	1	–	–
14	1	–1	1	1	–	–
15	–1	1	1	1	–	–
16	1	1	1	1	–	–
17	–2	0	0	0	–	–
18	2	0	0	0	–	–
19	0	–2	0	0	–	–
20	0	2	0	0	–	–
21	0	0	–2	0	130	34.8
22	0	0	2	0	2849	36.9
23	0	0	0	–2	2252	38.4
24	0	0	0	2	4787	36.1
25	0	0	0	0	2773	38.2
26	0	0	0	0	3168	36
27	0	0	0	0	2141	37.9
28	0	0	0	0	3069	38.6
29	0	0	0	0	5544	38.1
30	0	0	0	0	5828	37

6.3.6 Characterization of the biosurfactant produced by *Bacillus velezensis* P#02

6.3.6.1 Critical micelle concentration

B. velezensis P#02 produced more biosurfactant in the CSLG medium supplemented with glutamic acid (CSLG+Glut(10)), than in the medium without it, although the CMC and the minimum surface tension values obtained were similar in both media (Table 6.12 and Figure 6.1). Production with agitation did not significantly contribute to the amount of biosurfactant produced. However, the biosurfactant obtained with the CSLG+Glut(10) medium at 180 rpm had a lower CMC and better surface activity than the one produced under static conditions (44 mg/L and 28.2 ± 0.0 mN/m compared with 52 mg/L and 29.2 ± 0.1 mN/m). On the other hand, the biosurfactant obtained with the CSLG medium at 180 rpm had a higher CMC value than the other biosurfactants, and its minimum surface tension was also higher (32.5 ± 0.6 mN/m), probably since the equipment used to analyze this biosurfactant was different than the one used for the other biosurfactants.

Table 6.12 – Biosurfactant titers obtained with *Bacillus velezensis* P#02 grown in CSLG and CSLG+Glut(10) media. Critical micelle concentration (CMC) and minimum surface tension values (ST_{min}) of biosurfactant solutions prepared in PBS.

Culture medium	Growth conditions	BS titer (mg/L)	CMC (mg/L)	ST_{min} (mN/m)
CSLG	0 rpm	804	51	29.7 ± 0.2
	180 rpm	820	58	32.5 ± 0.6
CSLG+Glut(10)	0 rpm	901	52	29.2 ± 0.1
	180 rpm	868	44	28.2 ± 0.0

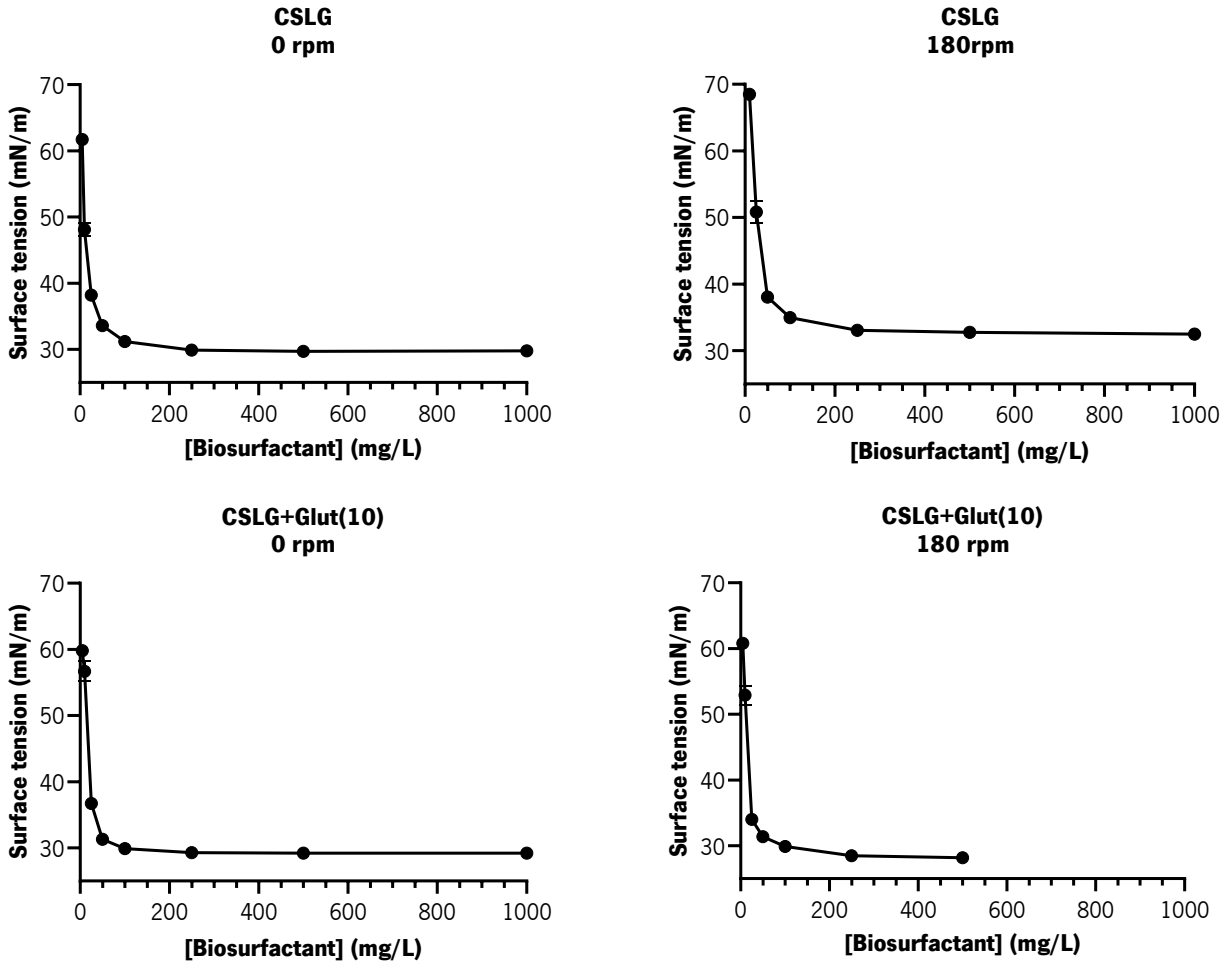

Figure 6.1 – Surface tension values (mN/m) of biosurfactants produced by *Bacillus velezensis* P#02 in CSLG and CSLG+Glut(10) media under static conditions and at 180 rpm, dissolved in PBS buffer at different concentrations.

6.3.6.2 Emulsification activity

The biosurfactants produced by *B. velezensis* P#02 in both media (CSLG and CSLG+Glut(10)) were able to stabilize emulsions with *n*–hexadecane at a concentration of 500 mg/L, with an E_{24} that ranged from 42.8 ± 1.6% to 61.3 ± 1.8% (Table 6.13). At this concentration, no significant difference was observed between the biosurfactants produced in the different media and growth conditions. At lower concentrations (250 mg/L and 100 mg/L), only the biosurfactant produced in CSLG+Glut(10) medium at 180 rpm had an E_{24} higher than 45%. The biosurfactants produced in other conditions all displayed a decrease in emulsifying activity when concentrations were lower. These results may be explained by possible structural differences of the biosurfactants produced in different media and conditions. According

to these results, the biosurfactant produced in CSLG+Glut(10) medium at 180 rpm presented the lowest CMC and ST values among the four biosurfactants studied (Table 6.12).

Table 6.13 – Emulsification indexes (E_{24}) obtained with purified biosurfactants produced by *Bacillus velezensis* P#02 in CSLG and CSLG+Glu(10) media under static conditions and at 180 rpm, at different concentrations.

BS concentration (mg/L)	E_{24} (%)			
	CSLG		CSLG+Glu(10)	
	0 rpm	180 rpm	0 rpm	180 rpm
500	58.3 ± 0.0	42.8 ± 1.6	48.8 ± 10.1	61.3 ± 1.8
250	29.2 ± 0.0	29.2 ± 5.9	27.1 ± 2.9	59.3 ± 4.6
100	10.4 ± 2.9	8.0 ± 0.0	12.3 ± 0.4	45.8 ± 5.9

Results correspond to the average ± standard deviation of 2 experiments.

6.3.6.3 Effect of the biosurfactants on the contact angle of water in an oil surface

The biosurfactants produced by *B. velezensis* P#02 were able to alter the wettability of an oil–coated surface from a neutral–wet state to a water–wet state, reducing the contact angle of water in oil from around 90° to values between 68° and 52° after five minutes of contact (Table 6.14).

Table 6.14 – Contact angle (°) measurements on an oil–coated glass surface for biosurfactant solutions (2 x CMC and 5 x CMC) produced by *Bacillus velezensis* P#02 grown in CSLG and CSLG+Glu(10) media under static conditions and at 180 rpm.

Sample	BS concentration	Contact angles (°)		
		0 min	2 min	5 min
CSLG (static)	2 x CMC	91.5 ± 2.4	77.4 ± 1.8	68.4 ± 1.8
	5 x CMC	92.8 ± 3.1	71.5 ± 3.3	61.3 ± 2.3
CSLG (180 rpm)	2 x CMC	87.6 ± 3.0	78.4 ± 1.5	68.6 ± 1.3
	5 x CMC	91.9 ± 1.6	69.8 ± 1.9	58.7 ± 1.3
CSLG+Glut(10) (static)	2 x CMC	91.9 ± 1.0	69.0 ± 1.0	59.3 ± 1.3
	5 x CMC	92.2 ± 3.9	60.1 ± 1.2	52.3 ± 1.8
CSLG+Glut(10) (180 rpm)	2 x CMC	90.3 ± 2.7	70.2 ± 2.8	61.0 ± 2.3
	5 x CMC	91.0 ± 2.1	59.0 ± 1.3	52.6 ± 1.3
Control (PBS buffer)	–	86.2 ± 1.5	81.9 ± 3.1	80.1 ± 2.7

Results correspond to the average ± standard deviation of 3 measurements.

The lowest contact angles were obtained with the biosurfactants produced in CSLG+Glut(10) medium, with a minimum around 52° at a concentration of 5 x CMC and 59–61° at 2 x CMC (Table 6.14). In both media, there was no significant difference in the contact angles obtained between the biosurfactants produced under static conditions and at 180 rpm.

6.3.7 Characterization of the biopolymer produced by *Bacillus velezensis* P#02

6.3.7.1 Preliminary characterization

A preliminary characterization of the biopolymer produced by *B. velezensis* P#02 in the medium CSLG+Glut(10) was performed using uHPLC (Figure 6.2). The aim of this analysis was to determine if the biopolymer contained L–glutamic acid monomers in its composition, which is characteristic of γ–PGA, since other preliminary assays (dinitrosalicylic acid (DNS) and phenol–sulfuric methods (data not shown)) had shown that it was not a polysaccharide biopolymer. Before characterization, the sample was hydrolyzed to break the biopolymer chain into monomers that could be detected in the uHPLC. To check whether the non–hydrolyzed biopolymer contained non–polymerized L–glutamic acid (since this substrate was added to the culture medium and could interfere with the analysis), this sample was also analyzed in the uHPLC (Figure 6.2).

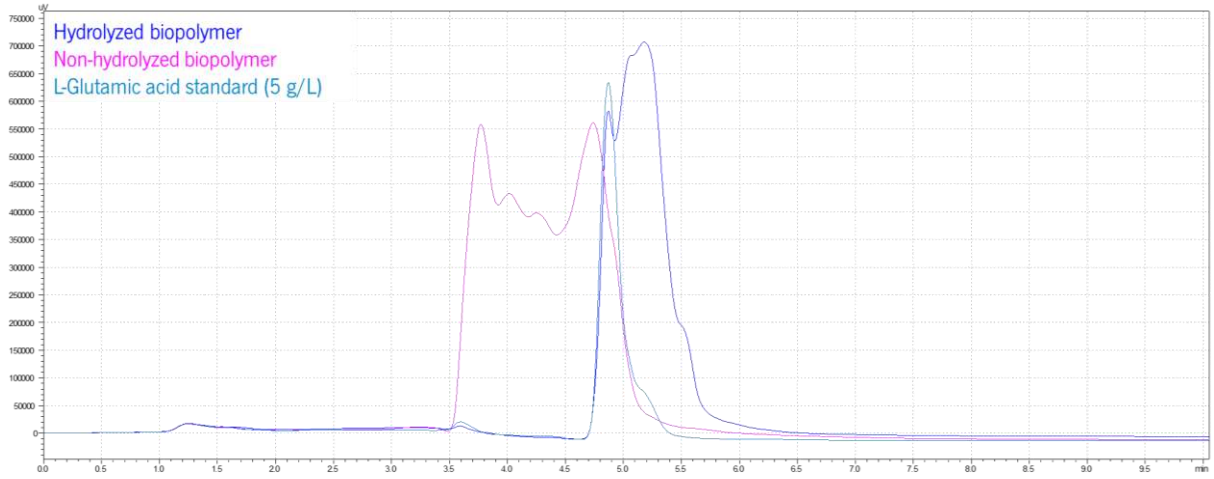

Figure 6.2 – uHPLC spectra at 290 nm for the hydrolyzed and non–hydrolyzed biopolymer from *Bacillus velezensis* P#02, and the L–glutamic acid standard (5 g/L).

The UV spectrum obtained confirmed the presence of approximately 2.9 g/L of L–glutamic acid in the hydrolyzed sample (Figure 6.2). Another peak was also observed at retention time 5.3 min, that could either be the D–isoform of glutamic acid, other compounds that can be part of the biopolymer

composition, or carbohydrate residues present in the sample. The non–hydrolyzed biopolymer sample displayed four different peaks, but none of them corresponded to L–glutamic acid as they had different retention times.

6.3.7.2 Chemical characterization

NMR analysis of the biopolymer produced by *B. velezensis* P#02 (Figure 6.3) displayed similar chemical shifts to those reported for γ–PGA in previous works (Liu et al., 2022; Samal et al., 2023): α–CH proton at around 4.10 ppm, γ–CH proton at 2.35 ppm and β–CH proton at 2.05 and 1.90 ppm. Hence, the pattern obtained was typical for PGA biopolymers, assembled through γ–amide linkages.

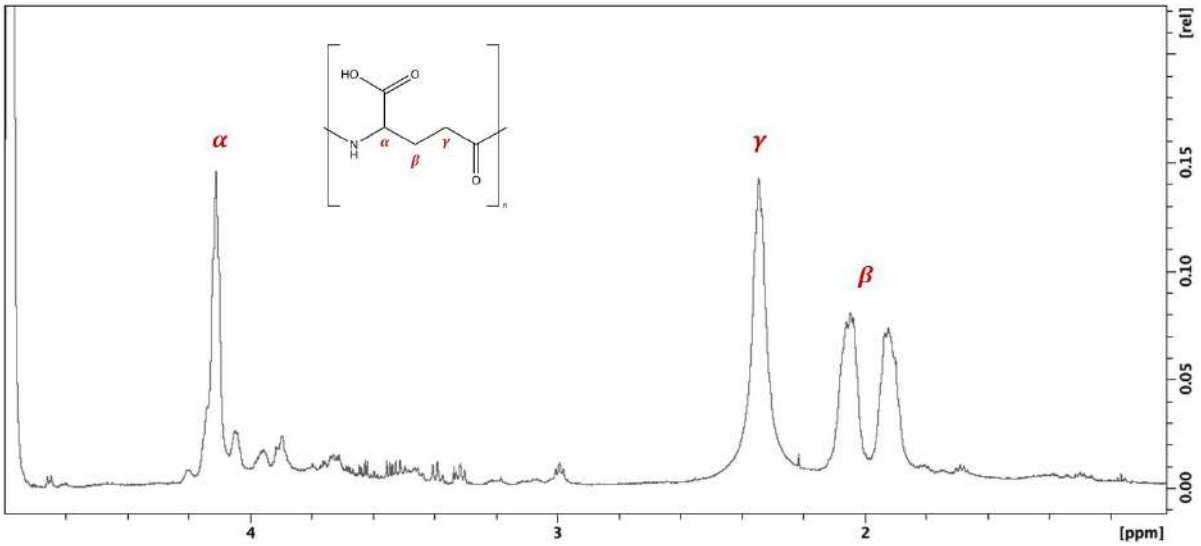

Figure 6.3 – NMR spectrum of γ–PGA produced by *Bacillus velezensis* P#02 in CSLG+Glut(10) medium.

The identification of the biopolymer was further confirmed through SID–Orbitrap MS analysis (Figure 6.4). Though complex, the typical isotopic envelope of PGA was evidenced in this sample, with their characteristic mass difference of 129.04 m/z. Due to its +2 charge, masses need to be doubled, thus resulting in 2–unit glutamic acid differences. Furthermore, the molecular weight of this biopolymer, determined through Static Light Scattering, was around 229 kDa.

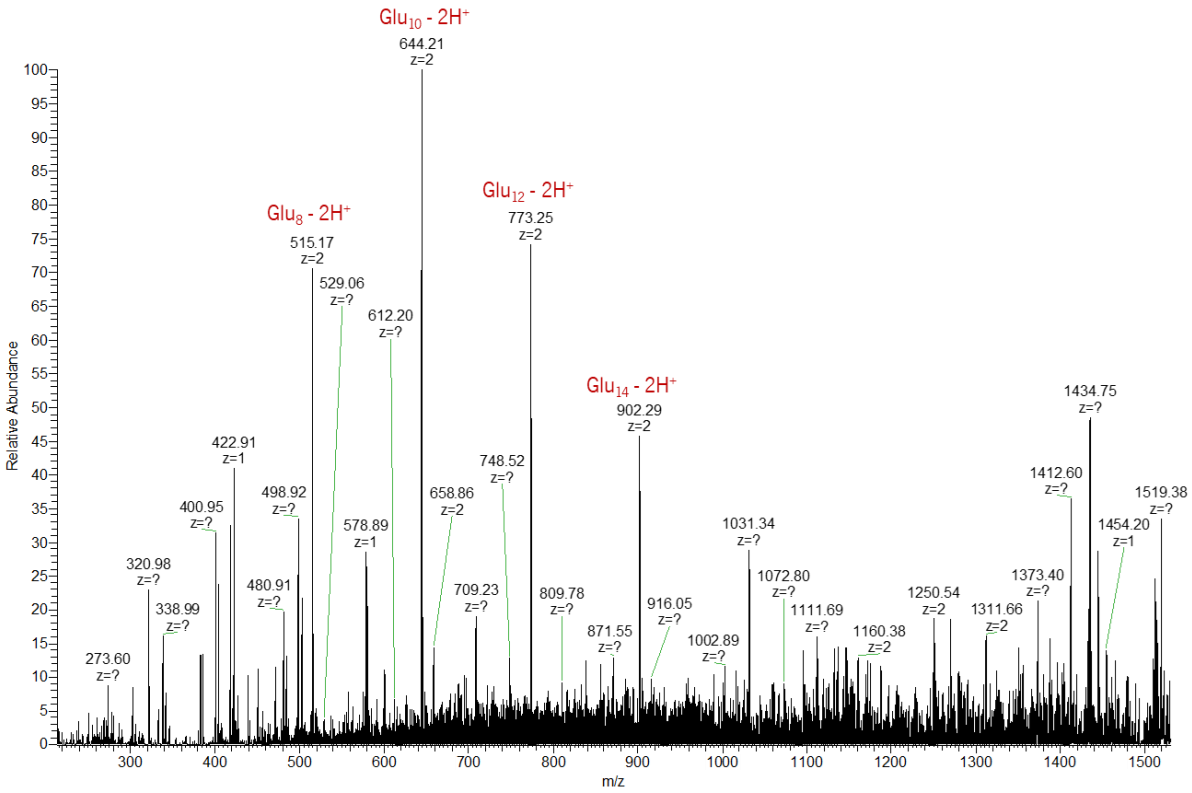

Figure 6.4 – SID–Orbitrap MS spectrum of γ–PGA produced by *Bacillus velezensis* P#02 in CSLG+Glut(10) medium.

6.3.7.3 Rheological properties

B. velezensis P#02 produced 9.8 g/L of γ–PGA when grown in CSLG+Glut(10) medium, with a maximum apparent viscosity of 3772 ± 267 mPa s in a solution containing 25 g/L of crude biopolymer. This biopolymer is characterized by a non–Newtonian flow and a shear–thinning behavior, since its apparent viscosity decreases with increasing shear rate, while the shear stress increases (Figure 6.5).

Regarding the dynamic viscoelastic properties of the γ–PGA produced by this microorganism, it is observed that the loss (or viscous) modulus (G''), which represents the viscous properties of the biopolymer in solution, is higher than the storage (or elastic) modulus (G'), representing the elastic properties (Figure 6.6). This happens both in the oscillatory strain and frequency sweep, indicating that the γ–PGA produced forms a viscous fluid in solution. At high frequencies, however, it is observed an overlap between both moduli, suggesting that a transition to a more gel–like structure may occur.

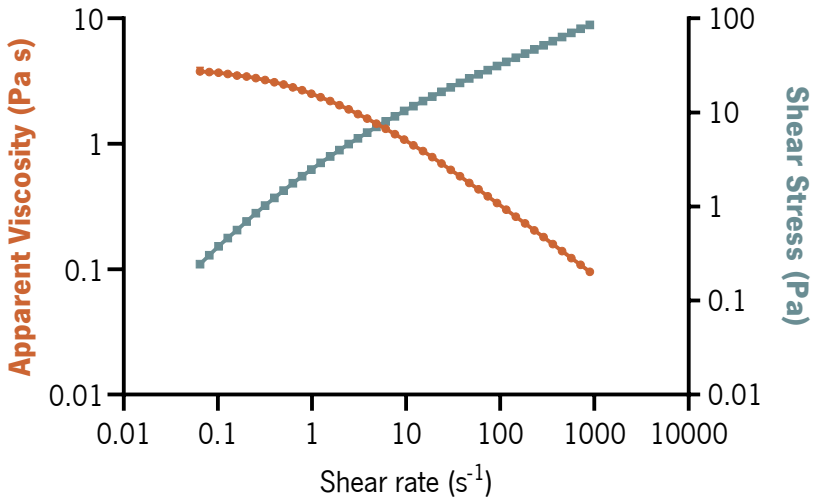

Figure 6.5 – Steady flow curves (apparent viscosity (Pa s) and shear stress (Pa) as a function of shear rate (s^{-1})) for the crude γ–PGA (25 g/L) produced by *Bacillus velezensis* P#02 in CSLG+Glut(10) medium.

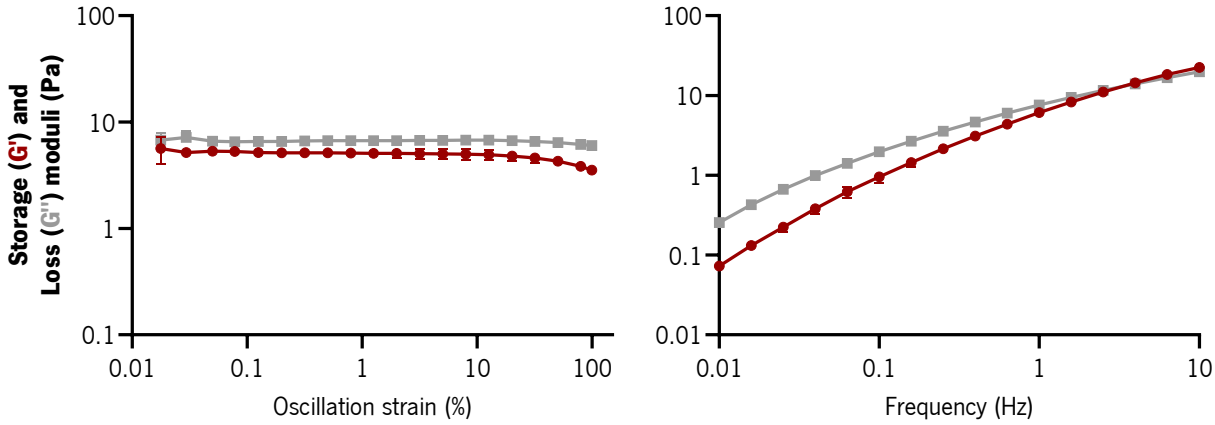

Figure 6.6 – Dynamic viscoelastic properties of the crude γ–PGA (25 g/L) produced by *Bacillus velezensis* P#02 in CSLG+Glut(10) medium. Left: storage modulus (G') and loss modulus (G'') as a function of strain, at a constant frequency (1 Hz). Right: G' and G'' as a function of frequency (Hz), at a constant strain (1%).

6.3.8 Evaluating the performance of the produced biomolecules in oil recovery assays using sand–pack columns

The potential application of the biomolecules (biosurfactant and biopolymer) produced by *B. velezensis* P#02 in microbial enhanced oil recovery (MEOR) was studied using sand–pack columns through *ex situ* and *in situ* approaches. The effect of using both biomolecules and an additional biopolymer (xanthan gum) in MEOR applications was evaluated using a heavy oil (Potiguar oil, $\eta_{40°C,\ 1.4\ s-1}$= 110

mPa s). (Table 6.15). In these conditions, only the *in situ* assay resulted in an increased oil recovery in relation to xanthan gum injection, even though it was a very small increase of 1.8%, that may be attributed to the variability between the different assays. As such, it can be concluded that xanthan gum was the only compound to produce a relevant effect in oil recovery in these assays.

Table 6.15 – Results obtained in MEOR sand–pack column assays performed with the crude oil from the Potiguar oilfield using the cell–free supernatant (CFS) obtained from cultures of *Bacillus velezensis* P#02 grown in synthetic (*ex situ* assay) and CSLG (*in situ* assay) media, followed by the injection of a xanthan gum solution (1 g/L).

Oil recovery parameters	Treatment		
	Xanthan gum	P#02 CFS in synthetic medium (*ex situ*)	P#02 culture in CSLG medium (*in situ*)
		Incubated 48h	Incubated 14 days
$\eta_{40°C}$ (mPa s)	106 ± 9	98 ± 1	100 ± 0
PV (mL)	89.0 ± 1.4	83.0 ± 1.4	93.0 ± 1.4
Porosity (%)	31.8 ± 0.5	29.6 ± 0.5	33.2 ± 0.5
OOIP (mL)	80.1 ± 1.1	79.0 ± 1.3	76.7 ± 2.4
S_{oi} (%)	90.0 ± 2.6	95.2 ± 3.2	82.5 ± 1.3
S_{orwf} (mL)	45.0 ± 0.0	38.8 ± 1.8	40.0 ± 0.0
S_{or} (%)	43.8 ± 0.7	50.9 ± 3.0	47.8 ± 1.6
S_{orbf} (mL)	5.5 ± 0.8	5.9 ± 0.8	6.4 ± 0.2
AOR (%)	8.4 ± 2.7	7.4 ± 3.0	10.2 ± 1.7

The AOR value is the corrected value obtained after subtracting the additional oil recovery obtained in the control assays. The results represent the average of two independent experiments ± standard deviation.

To test whether or not the biomolecules produced by the isolate P#02 would be effective in recovering oil without additional compounds, several assays were performed using the same oil and the CFS obtained from cultures of the isolate P#02 and/or its crude biopolymer produced in CSLG+Glu(10) medium (Table 6.16). Using the crude biopolymer solution with the lowest viscosity, oil recovery increased by 10.5% when compared to the control. Results were worse when using the CFS (6.8% more recovery than the control), which could be explained by the lower apparent viscosity of this treatment, when compared with the other assays. The best results were achieved using the CFS in combination with the crude biopolymer, with recovery increasing 13.9% when compared with the control, 7.1% when compared to the assays with just the CFS, and 3.4% when compared with the assay containing just the crude biopolymer at the lowest viscosity tested. This suggests that the biosurfactant present in the CFS has a positive effect in oil recovery and acts synergistically with the biopolymer.

Table 6.16 – Results obtained in MEOR sand–pack column assays performed with the crude oil from the Potiguar oilfield using the cell–free supernatant (CFS), crude biopolymer (BP) and CSF + crude (BP) obtained from *Bacillus velezensis* P#02 in CSLG+Glu(10) medium.

Oil recovery parameters				
	CFS	CFS+Crude BP	Crude BP	
$\eta_{40°C}$ (mPa s)	60 ± 12	157 ± 29	212 ± 10	127 ± 6
PV (mL)	96.5 ± 2.1	96.5 ± 2.1	94.0 ± 0.0	95.0 ± 1.4
Porosity (%)	34.5 ± 0.8	34.5 ± 0.8	33.6 ± 0.0	33.9 ± 0.5
OOIP (mL)	86.4 ± 1.3	84.3 ± 6.3	76.8 ± 0.9	81.3 ± 1.8
S_{oi} (%)	89.5 ± 0.6	87.3 ± 4.6	81.6 ± 1.0	85.5 ± 3.1
S_{orwf} (mL)	50.0 ± 0.0	50.0 ± 0.0	42.5 ± 3.5	45.0 ± 7.1
S_{or} (%)	42.1 ± 0.9	40.5 ± 4.4	44.6 ± 5.3	44.5 ± 9.9
S_{orbf} (mL)	5.1 ± 1.4	7.2 ± 0.4	4.8 ± 0.7	6.2 ± 0.0
AOR (%)	6.8 ± 3.4	13.9 ± 2.9	6.7 ± 0.4	10.5 ± 4.4

The AOR value is the corrected value obtained after subtracting the additional oil recovery obtained in the control assays. The results represent the average of two independent experiments ± standard deviation.

6.4 Discussion

Among the four *Bacillus* sp. isolates evaluated in this work, two of them (P#02 and P#04) were able to produce biosurfactant and biopolymer in simultaneous (Table 6.3 and Table 6.4). The production of these biomolecules, in particular the biopolymer γ–PGA, was optimized for the isolate P#02, identified as *B. velezensis*. This isolate was able to produce γ–PGA without the addition of glutamic acid to the culture medium (Table 6.7), indicating that it is a glutamic acid–independent γ–PGA producer, which is in line with previous works (Cristiano–Fajardo et al., 2019; Hu et al., 2023). Nonetheless, γ–PGA production further increased when L–glutamic acid was added to the culture medium, as indicated by the apparent viscosity increase (from 136 ± 4 mPa s in PTYG medium to 1193 ± 17 mPa s in PTYG medium supplemented with 10 g/L of L–glutamic acid) (Table 6.7). Yao and co–workers (2010) showed that *B. subtilis* NX–2 produced only a trace amount of γ–PGA in a culture medium without glutamic acid. However, the addition of L–glutamate increased its production up to 40 g/L, with 91 94% of the glutamic acid in the biopolymer having been incorporated from this source (Yao et al., 2010). Alternatively, low–cost substrates, such as waste liquor of monosodium glutamate, can also be used as an inexpensive source of glutamic acid to increase γ–PGA production (Yong et al., 2011; D. Zhang et al., 2012).

The effect of other components in the culture medium was also studied in this work and seemed to have an impact on the amount of γ–PGA produced, that was related to the apparent viscosity of crude biopolymer solutions. In the low–cost media using CSL, for example, the addition of glucose was indispensable for γ–PGA production: no increase in the apparent viscosity of the culture medium was observed in the CSL medium (Table 6.4), while a value of 2308 ± 461 mPa s was obtained in the same medium with the addition of 10 g/L of glucose (Table 6.6). Other works suggest that glucose is the most efficient carbon source to produce this biopolymer, since it enters the TCA cycle in the form of pyruvate, which is a precursor for γ–PGA (Sirisansaneeyakul et al., 2017). Higher glucose uptake rates have been shown to increase γ–PGA production, as well as promote cell growth, in *B. velezensis* 83 (Cristiano–Fajardo et al., 2019). Furthermore, the use of CSL as an alternative nitrogen source also increased γ–PGA production by the isolate P#02 (Table 6.6). Similarly, *B. subtilis* 242 showed an increase in γ–PGA production when shifting from yeast extract to CSL as nitrogen source (J. Li et al., 2022). That can be due to the presence of different vitamins and amino acids (including glutamic acid) in CSL (Hofer et al., 2018). Fishmeal wastewater (C. Zhang et al., 2019) and the wastewater from yeast molasses fermentation (Y. Li et al., 2020) are other alternative cost–effective nitrogen sources that have been shown to increase production of this biopolymer and reduce glutamic acid requirements in the fermentation medium.

The ideal conditions for biopolymer production by *B. velezensis* P#02 were static, even though, in some of the media tested, a small increase in the apparent viscosity of the culture broth was also observed when the microorganism was grown with agitation (Table 6.4). Other works, however, demonstrated that higher agitation speeds, and consequently higher oxygen transfer rates to the culture medium, resulted in increased γ–PGA production (Bajaj & Singhal, 2010; Flores et al., 2020). This effect was explained by the fact that γ–PGA production is linked to the TCA cycle, which requires the presence of oxygen to regenerate NAD^+ and other electron acceptors (Sirisansaneeyakul et al., 2017). Nonetheless, high agitation rates may disrupt the biopolymer structure, which decreases overall production and may explain the results obtained in the present work. De Cesaro and co–workers (2014) developed a different approach to increase oxygen availability in the culture medium that does not require high agitation speeds and mitigates the effect that a viscous culture broth has on oxygen transfer. The authors added polydimethylsiloxane (PDMS) as an oxygen carrier to cultures of *B. subtilis* BL53, which doubled the volumetric oxygen mass transfer coefficient and resulted in an improved γ–PGA production and productivity (de Cesaro et al., 2014).

Under these conditions, and with the CSLG+Glut(10) medium, *B. velezensis* P#02 produced 9.8 g/L of γ–PGA after 72h of growth. This value was higher than that obtained with *B. velezensis* 83, which produced up to 2.0 g/L of γ–PGA (Flores et al., 2020). Still, the amount of γ–PGA produced here was lower than the amount produced by other glutamic acid–independent producers, such as *B. subtilis* and *B. licheniformis* strains, that have reported titers between 21.4 and 39.9 g/L (Sirisansaneeyakul et al., 2017). However, the conditions used amongst the different works vary greatly, so a direct comparison of the results obtained is not straightforward.

B. velezensis P#02 was also found to produce biosurfactant, most likely a lipopeptide, under different conditions and simultaneous to γ–PGA production. In the medium with L–glutamic acid (CSLG+Glut(10)), the isolate produced 900 mg/L under static conditions, which was about 11% higher than the production in the same medium without glutamic acid (CSLG) (Table 6.12). Regarding the characteristics of the biosurfactants produced, however, there was no significant difference between the ones produced in either medium, under static conditions or with agitation (Table 6.12, Table 6.13 and Table 6.14). The biosurfactant was able to reduce the surface tension of water to values between 28.2 and 32.5 mN/m, had a CMC between 44 and 58 mg/L, and was able to form stable emulsions against *n*–hexadecane at concentrations between 100 and 500 mg/L. These values are within the typical range for biosurfactants produced by *Bacillus* spp., even though the surface tension can go as low as 20 mN/m with surfactin produced by some *B. subtillis* strains, and the CMC can start at around 16 mg/L (Chapter 1, Table 1.1). In *B. velezensis*, biosurfactants can also have a wide range of physical characteristics, depending on the specific strain that produced them and the culture conditions used. For example, *B. velezensis* H2O–1 produced 802 mg/L of surfactin, with the ability to reduce the surface tension of water to 24.8 mN/m and a critical micelle concentration of 38.7 mg/L (Guimarães et al., 2021). *B. velezensis* BSA–1, on the other hand, produced a biosurfactant with surface activity similar to the one reported here (29.0 mN/m) and was able to form stable emulsions against *n*–hexadecane with an E_{24} of 99.4% (Yin et al., 2023).

Furthermore, the biosurfactants produced by *B. velezensis* P#02 had the ability to change the wettability of an oil–coated glass surface to a more water–wet state, with better results being achieved with the biosurfactant produced in CSLG+Glut(10) medium (Table 6.14). Guimarães and co–workers (2021) also found that *B. velezensis* H2O–1 could alter the wettability of calcite that had been soaked in light and medium oils, even in high salinity conditions (Guimarães et al., 2021). This is one of the mechanisms that can aid in oil recovery, as was seen in sand–pack column assays, where the CFS from

B. velezensis P#02 grown in CSLG+Glut(10) medium recovered 6.8% of the residual oil (Table 6.16). The crude biopolymer ($\eta_{40°C} = 127 \pm 6$ mPa s at 1.4 s^{-1}) recovered 10.5% more oil than the control and, when these two treatments were used in combination, additional oil recovery rates increased to 13.9%, indicating that the biosurfactant present in the CFS and γ–PGA have a synergistic effect in oil recovery. Given the ability of *B. velezensis* P#02 to grow and produce γ–PGA and biosurfactant at temperatures up to 45°C (Table 6.5), its applicability in *in situ* MEOR was also evaluated in this work (Table 6.15). However, the results obtained were not conclusive.

Yin et al. (2023) used the CSF from *B. velezensis* BSA1, containing biosurfactant, to recover oil from sand-pack columns. The total amount of crude oil recovered was 21 times greater than the control. Furthermore, this strain was used in an *in situ* field trial and increased the daily oil production from 0.6 m^3 to 2.7 m^3, mainly due to hydrocarbon degradation (Yin et al., 2023). Using a glass micromodel, Azarhava et al. (2020) reported an AOR of 14.9% for γ–PGA produced by *B. licheniformis* LMG 7559 (Azarhava et al., 2020).

In conclusion, the co–production of γ–PGA and biosurfactant was optimized in *B. velezensis* P#02 using a low–cost medium containing CSL as an alternative nitrogen source. With this medium, and under static conditions, *B. velezensis* P#02 produced 9.8 g/L of γ–PGA with good viscoelastic properties and 900 mg/L of biosurfactant with excellent surface activity. To the best of our knowledge, this is the first work that focuses on the co–production of both biomolecules by *B. velezensis* using agro–industrial waste substrates. Furthermore, the biomolecules produced here were able to increase heavy oil recovery in *ex situ* sand–pack column assays, opening up the possibility for their application in MEOR.

6.5 References

Al-Ghailani, T., Al-Wahaibi, Y. M., Joshi, S. J., Al-Bahry, S. N., Elshafie, A. E., & Al-Bemani, A. S. (2021). Application of a new bio-ASP for enhancement of oil recovery: Mechanism study and core displacement test. *Fuel*, *287*, 119432. https://doi.org/10.1016/j.fuel.2020.119432

Altun, M. (2019). Bioproduction of γ-Poly(glutamic acid) using feather hydrolysate as a fermentation substrate. *Trakya University Journal of Natural Sciences*, *20*(1), 27–34. https://doi.org/10.23902/trkjnat.448851

Azarhava, H., Bajestani, M. I., Jafari, A., Vakilchap, F., & Mousavi, S. M. (2020). Production and physicochemical characterization of bacterial poly gamma- (glutamic acid) to investigate its performance on enhanced oil recovery. *International Journal of Biological Macromolecules*, *147*, 1204–1212. https://doi.org/10.1016/j.ijbiomac.2019.10.090

Bajaj, I. B., & Singhal, R. S. (2010). Effect of aeration and agitation on synthesis of poly(γ-glutamic acid)

in batch cultures of Bacillus licheniformis NCIM 2324. *Biotechnology and Bioprocess Engineering*, *15*(4), 635–640. https://doi.org/10.1007/s12257-009-0059-2

Chettri, R., Bhutia, M. O., & Tamang, J. P. (2016). Poly-γ-glutamic acid (PGA)-producing Bacillus species isolated from Kinema, Indian fermented soybean food. *Frontiers in Microbiology*, *7*(JUN), 971. https://doi.org/10.3389/fmicb.2016.00971

Cristiano-Fajardo, S. A., Flores, C., Flores, N., Tinoco-Valencia, R., Serrano-Carreón, L., & Galindo, E. (2019). Glucose limitation and glucose uptake rate determines metabolite production and sporulation in high cell density continuous cultures of Bacillus amyloliquefaciens 83. *Journal of Biotechnology*, *299*, 57–65. https://doi.org/10.1016/j.jbiotec.2019.04.027

de Cesaro, A., da Silva, S. B., & Ayub, M. A. Z. (2014). Effects of metabolic pathway precursors and polydimethylsiloxane (PDMS) on poly-(gamma)-glutamic acid production by Bacillus subtilis BL53. *Journal of Industrial Microbiology and Biotechnology*, *41*(9), 1375–1382. https://doi.org/10.1007/s10295-014-1477-5

Fernandes, P. L., Rodrigues, E. M., Paiva, F. R., Ayupe, B. A. L., McInerney, M. J., & Tótola, M. R. (2016). Biosurfactant, solvents and polymer production by Bacillus subtilis RI4914 and their application for enhanced oil recovery. *Fuel*, *180*, 551–557. https://doi.org/10.1016/j.fuel.2016.04.080

Flores, C., Medina-Valdez, A., Peña, C., Serrano-Carreón, L., & Galindo, E. (2020). Oxygen transfer rate determines molecular weight and production of poly(γ-glutamic acid) as well as carbon utilization by Bacillus velezensis 83. *Journal of Chemical Technology and Biotechnology*, *95*(9), 2383–2392. https://doi.org/10.1002/jctb.6420

Ge, M. R., Miao, S. J., Liu, J. F., Gang, H. Z., Yang, S. Z., & Mu, B. Z. (2021). Laboratory studies on a novel salt-tolerant and alkali-free flooding system composed of a biopolymer and a bio-based surfactant for oil recovery. *Journal of Petroleum Science and Engineering*, *196*, 107736. https://doi.org/10.1016/j.petrol.2020.107736

Gudiña, E. J., Couto, M. R., Silva, S. P., Coelho, E., Coimbra, M. A., Teixeira, J. A., & Rodrigues, L. R. (2023). Sustainable Exopolysaccharide Production by Rhizobium viscosum CECT908 Using Corn Steep Liquor and Sugarcane Molasses as Sole Substrates. *Polymers*, *15*(1), 20. https://doi.org/10.3390/polym15010020

Gudiña, E. J., Fernandes, E. C., Rodrigues, A. I., Teixeira, J. A., & Rodrigues, L. R. (2015). Biosurfactant production by Bacillus subtilis using corn steep liquor as culture medium. *Frontiers in Microbiology*, *6*(FEB). https://doi.org/10.3389/fmicb.2015.00059

Gudiña, E. J., Rodrigues, A. I., Alves, E., Domingues, M. R., Teixeira, J. A., & Rodrigues, L. R. (2015). Bioconversion of agro-industrial by-products in rhamnolipids toward applications in enhanced oil recovery and bioremediation. *Bioresource Technology*, *177*, 87–93. https://doi.org/10.1016/j.biortech.2014.11.069

Gudiña, E. J., Rodrigues, L. R., Teixeira, J. A., Pereira, J. F., Coutinho, J. A., & Soares, L. P. (2012). Biosurfactant producing microorganisms and its application to enhance oil recovery at lab scale. *Society of Petroleum Engineers - SPE EOR Conference at Oil and Gas West Asia 2012*, *1*, 363–370. https://doi.org/10.2118/154598-ms

Guimarães, C. R., Pasqualino, I. P., de Sousa, J. S., Nogueira, F. C. S., Seldin, L., de Castilho, L. V. A., & Freire, D. M. G. (2021). Bacillus velezensis H2O-1 surfactin efficiently maintains its interfacial properties in extreme conditions found in post-salt and pre-salt oil reservoirs. *Colloids and Surfaces B: Biointerfaces*, *208*, 112072. https://doi.org/10.1016/j.colsurfb.2021.112072

Hofer, A., Hauer, S., Kroll, P., Fricke, J., & Herwig, C. (2018). In-depth characterization of the raw material corn steep liquor and its bioavailability in bioprocesses of Penicillium chrysogenum. *Process Biochemistry*, *70*, 20–28. https://doi.org/10.1016/j.procbio.2018.04.008

Hu, H., Wu, C., Ge, F., Ren, Y., Li, W., & Li, J. (2023). Poly-γ-glutamic acid-producing Bacillus velezensis fermentation can improve the feed properties of soybean meal. *Food Bioscience*, *53*, 102503. https://doi.org/10.1016/j.fbio.2023.102503

Huang, J., Du, Y., Xu, G., Zhang, H., Zhu, F., Huang, L., & Xu, Z. (2011). High yield and cost-effective production of poly(γ-glutamic acid) with Bacillus subtilis. *Engineering in Life Sciences*, *11*(3), 291–297. https://doi.org/10.1002/elsc.201000133

Ji, S., Wei, F., Li, B., Li, P., Li, H., Li, S., Wang, J., Zhu, H., & Xu, H. (2022). Synergistic effects of microbial polysaccharide mixing with polymer and nonionic surfactant on rheological behavior and enhanced oil recovery. *Journal of Petroleum Science and Engineering*, *208*, 109746. https://doi.org/10.1016/j.petrol.2021.109746

Ke, C. Y., Sun, W. J., Li, Y. Bin, Lu, G. M., Zhang, Q. Z., & Zhang, X. L. (2018). Microbial enhanced oil recovery in Baolige Oilfield using an indigenous facultative anaerobic strain Luteimonas huabeiensis sp. nov. *Journal of Petroleum Science and Engineering*, *167*, 160–167. https://doi.org/10.1016/j.petrol.2018.04.015

Kongklom, N., Shi, Z., Chisti, Y., & Sirisansaneeyakul, S. (2017). Enhanced Production of Poly-γ-glutamic Acid by Bacillus licheniformis TISTR 1010 with Environmental Controls. *Applied Biochemistry and Biotechnology*, *182*(3), 990–999. https://doi.org/10.1007/s12010-016-2376-1

Lee, N. R., Lee, S. M., Cho, K. S., Jeong, S. Y., Hwang, D. Y., Kim, D. S., Hong, C. O., & Son, H. J. (2014). Improved production of poly-γ-glutamic acid by Bacillus subtilis D7 isolated from Doenjang, a Korean traditional fermented food, and its antioxidant activity. *Applied Biochemistry and Biotechnology*, *173*(4), 918–932. https://doi.org/10.1007/s12010-014-0908-0

Li, J., Chen, S., Fu, J., Xie, J., Ju, J., Yu, B., & Wang, L. (2022). Efficient molasses utilization for low-molecular-weight poly-γ-glutamic acid production using a novel Bacillus subtilis stain. *Microbial Cell Factories*, *21*(1). https://doi.org/10.1186/s12934-022-01867-5

Li, Y., Wang, J., Liu, N., Ke, L., Zhao, X., & Qi, G. (2020). Microbial synthesis of poly-γ-glutamic acid (γ-PGA) with fulvic acid powder, the waste from yeast molasses fermentation. *Biotechnology for Biofuels*, *13*(1), 1–17. https://doi.org/10.1186/s13068-020-01818-5

Liu, H., Yan, Q., Wang, Y., Li, Y., & Jiang, Z. (2022). Efficient production of poly-γ-glutamic acid by Bacillus velezensis via solid-state fermentation and its application. *Food Bioscience*, *46*, 101575. https://doi.org/10.1016/j.fbio.2022.101575

Nair, P., Navale, G. R., & Dharne, M. S. (2021). Poly-gamma-glutamic acid biopolymer: a sleeping giant with diverse applications and unique opportunities for commercialization. In *Biomass Conversion and Biorefinery* (pp. 1–19). Springer Science and Business Media Deutschland GmbH. https://doi.org/10.1007/s13399-021-01467-0

Novak, J. S., Tanenbaum, S. W., & Nakas, J. P. (1992). Heteropolysaccharide formation by Arthrobacter viscosus grown on xylose and xylose oligosaccharides. *Applied and Environmental Microbiology*, *58*(11), 3501–3507.

Parati, M., Khalil, I., Tchuenbou-Magaia, F., Adamus, G., Mendrek, B., Hill, R., & Radecka, I. (2022). Building a circular economy around poly(D/L-γ-glutamic acid)- a smart microbial biopolymer. *Biotechnology Advances*, 108049. https://doi.org/10.1016/J.BIOTECHADV.2022.108049

Pereira, J. F. B., Gudiña, E. J., Costa, R., Vitorino, R., Teixeira, J. A., Coutinho, J. A. P., & Rodrigues, L. R. (2013). Optimization and characterization of biosurfactant production by Bacillus subtilis isolates towards microbial enhanced oil recovery applications. *Fuel*, *111*, 259–268. https://doi.org/10.1016/j.fuel.2013.04.040

Qi, Y.-B., Zheng, C.-G., Lv, C.-Y., Lun, Z.-M., & Ma, T. (2018). Compatibility between weak gel and microorganisms in weak gel-assisted microbial enhanced oil recovery. *Journal of Bioscience and Bioengineering*, *126*(2), 235–240. https://doi.org/10.1016/j.jbiosc.2018.02.011

Samal, S., Banerjee, S., Dey, P., & Rangarajan, V. (2023). Production and characterization of a novel poly amino acid from a thermophilic bacterium, and preliminary testing of its coagulating potential for imminent wastewater treatment application. *International Journal of Biological Macromolecules*, 125589. https://doi.org/10.1016/J.IJBIOMAC.2023.125589

Saravanan, A., Kumar, P. S., Vardhan, K. H., Jeevanantham, S., Karishma, S. B., Yaashikaa, P. R., & Vellaichamy, P. (2020). A review on systematic approach for microbial enhanced oil recovery technologies: Opportunities and challenges. In *Journal of Cleaner Production* (Vol. 258, p. 120777). Elsevier Ltd. https://doi.org/10.1016/j.jclepro.2020.120777

Scheel, R. A., Fusi, A. D., Min, B. C., Thomas, C. M., Ramarao, B. V., & Nomura, C. T. (2019). Increased Production of the Value-Added Biopolymers Poly(R-3-Hydroxyalkanoate) and Poly(γ-Glutamic Acid) From Hydrolyzed Paper Recycling Waste Fines. *Frontiers in Bioengineering and Biotechnology*, *7*, 506748. https://doi.org/10.3389/fbioe.2019.00409

Sharma, N., Prasad, G. S., & Choudhury, A. R. (2013). Utilization of corn steep liquor for biosynthesis of pullulan, an important exopolysaccharide. *Carbohydrate Polymers*, *93*(1), 95–101. https://doi.org/10.1016/j.carbpol.2012.06.059

Sirisansaneeyakul, S., Cao, M., Kongklom, N., Chuensangjun, C., Shi, Z., & Chisti, Y. (2017). Microbial production of poly-γ-glutamic acid. In *World Journal of Microbiology and Biotechnology* (Vol. 33, Issue 9, pp. 1–8). Springer Netherlands. https://doi.org/10.1007/s11274-017-2338-y

Sun, J. D., Tang, C., Zhou, J., Wei, P., Wang, Y. J., An, W., Yan, Z. Y., & Yong, X. Y. (2021). Production of poly-γ-glutamic acid (γ-PGA) from xylose-glucose mixtures by Bacillus amyloliquefaciens C1. *3 Biotech*, *11*(2), 1–10. https://doi.org/10.1007/s13205-021-02661-7

Tang, B., Lei, P., Xu, Z., Jiang, Y., Xu, Z., Liang, J., Feng, X., & Xu, H. (2015). Highly efficient rice straw utilization for poly-(γ-glutamic acid) production by Bacillus subtilis NX-2. *Bioresource Technology*, *193*, 370–376. https://doi.org/10.1016/j.biortech.2015.05.110

Verma, M. L., Kumar, S., Jeslin, J., & Dubey, N. K. (2020). Microbial production of biopolymers with potential biotechnological applications. In *Biopolymer-Based Formulations: Biomedical and Food Applications* (pp. 105–137). Elsevier. https://doi.org/10.1016/B978-0-12-816897-4.00005-9

Xia, W., Dong, X., Zhang, Y., & Ma, T. (2018). Biopolymer from marine Athelia and its application on heavy oil recovery in heterogeneous reservoir. *Carbohydrate Polymers*, *195*, 53–62. https://doi.org/10.1016/j.carbpol.2018.04.061

Yao, J., Xu, H., Shi, N., Cao, X., Feng, X., Li, S., & Ouyang, P. (2010). Analysis of carbon metabolism and improvement of γ-polyglutamic acid production from bacillus subtilis NX-2. *Applied Biochemistry and Biotechnology*, *160*(8), 2332–2341. https://doi.org/10.1007/s12010-009-8798-2

Yin, J., Wei, X., Hu, F., Cheng, C., Zhuang, X., Song, M., Zhuang, G., Wang, F., & Ma, A. (2023). Halotolerant Bacillus velezensis sustainably enhanced oil recovery of low permeability oil reservoirs by producing biosurfactant and modulating the oil microbiome. *Chemical Engineering Journal*, *453*,

139912. https://doi.org/10.1016/j.cej.2022.139912

Yong, X., Raza, W., Yu, G., Ran, W., Shen, Q., & Yang, X. (2011). Optimization of the production of poly-γ-glutamic acid by Bacillus amyloliquefaciens C1 in solid-state fermentation using dairy manure compost and monosodium glutamate production residues as basic substrates. *Bioresource Technology*, *102*(16), 7548–7554. https://doi.org/10.1016/j.biortech.2011.05.057

Zeng, W., Chen, G., Zhang, Y., Wu, K., & Liang, Z. (2012). Studies on the UV spectrum of poly(γ-glutamic acid) based on development of a simple quantitative method. *International Journal of Biological Macromolecules*, *51*(1–2), 83–90. https://doi.org/10.1016/j.ijbiomac.2012.04.005

Zhang, C., Wu, D. J., Jia, J., & Yang, H. Q. (2019). Fishmeal Wastewater as A Low-Cost Nitrogen Source for γ-Polyglutamic Acid Production Using Bacillus subtilis. *Waste and Biomass Valorization*, *10*(4), 789–795. https://doi.org/10.1007/s12649-017-0100-1

Zhang, D., Feng, X., Zhou, Z., Zhang, Y., & Xu, H. (2012). Economical production of poly(γ-glutamic acid) using untreated cane molasses and monosodium glutamate waste liquor by Bacillus subtilis NX-2. *Bioresource Technology*, *114*, 583–588. https://doi.org/10.1016/j.biortech.2012.02.114

Zhu, F., Cai, J., Zheng, Q., Zhu, X., Cen, P., & Xu, Z. (2014). A novel approach for poly-γ-glutamic acid production using xylose and corncob fibres hydrolysate in Bacillus subtillis HB-1. *Journal of Chemical Technology and Biotechnology*, *89*(4), 616–622. https://doi.org/10.1002/jctb.4169

CHAPTER 7.

Reservoir simulation studies using biomolecules of interest for MEOR applications

Abstract

The conventional process of oil production usually results in oil recovery factors lower than 60%, leaving behind a high amount of residual oil inside the reservoir. For this reason, Enhanced Oil Recovery (EOR) is essential in extending the productive life of oil reservoirs. Among the different techniques for EOR, polymer flooding is one of the most used. As a more environmentally friendly alternative, biopolymers can be used instead of traditional chemical polymers. Furthermore, before implementing any improved oil recovery technology, it is necessary to perform the adequate simulations, to best predict the behavior of the injected chemicals in the reservoir and minimize risks and uncertainties. In this work, three biopolymers, characterized in the previous chapters, were used in MEOR simulations to determine their applicability in large scale. It was observed that higher viscosities were beneficial in terms of additional oil recovered due to improved fluid mobility and the formation of a more uniform oil displacement front. The injection of biopolymers after water flooding increased the recovery factor from 31.2% to 33.3, 39.3 and 44.1%, with γ–PGA from *Bacillus velezensis* P#02, xanthan gum and the biopolymer produced by *Rhizobium viscosum* CECT 908 (all of them at a concentration of 5 g/L), respectively. Oil production was further increased to 55.8% when the biopolymer solution from *R. viscosum* CECT 908 at 5 g/L was injected without water flooding. Additionally, the production time until the water cut reached 90% was extended by 32 years and 7 months in this scenario. This work gives valuable insights into the use of biopolymers for oil recovery, including some of the mechanisms that lead to higher production.

7.1 Introduction

The process of oil recovery usually develops over three different stages. The first stage, or primary oil recovery phase, can produce between 5 and 20% of the original oil in place (OOIP), depending on the properties of the reservoir and the crude oil (Gudiña, Pereira, et al., 2012). Secondary oil recovery, most commonly water flooding, can, in turn, recover up to 60% of the OOIP (Saravanan et al., 2020). This technique can be used until the end of life of an oil reservoir, with the employment of different strategies that aim at expanding the reservoir's life. However, in mature oilfields, around 98% of water can be produced together with crude oil before production wells are shut down. From the point when the amount of water in the production stream (water cut) exceeds 90%, the residual oil is mainly scattered throughout the reservoir, meaning that the oil production and its flow rate are significantly reduced. This happens because water flows through preferable paths, creating high permeability regions inside the reservoir. Several oilfields worldwide have entered the high water cut stage, including reservoirs in Yemen, Colombia and China (Y. Guo et al., 2019). The solution for these oilfields would be to either shut down the high water cut wells or to employ tertiary oil recovery techniques, or Enhanced Oil Recovery (EOR). These include gas injection, chemical flooding, and thermal recovery (Niu et al., 2020). This work will focus on applying alternatives to chemical EOR technologies, specifically Microbial Enhanced Oil Recovery (MEOR), in which microorganisms or their metabolites are injected into the oil wells, replacing the common chemicals used.

Before implementing an EOR or MEOR project, the reservoir needs to be assessed in terms of potential oil production, reservoir structure, geological heterogeneity, fluid flow, well patterns, well spacing, technology to be employed and economic parameters, like the state of the market (Chen et al., 2018). According to Chen et al. (2018), the oil saturation (S_{or}) at the time of evaluation should also be above 40% for a successful implementation of an EOR project. Furthermore, depending on the technology intended, there are certain reservoir properties that exclude the application of a given chemical from the beginning (Table 7.1), even though the specific values can vary between authors. Once the reservoir assessment is completed and the technology to be applied is selected, laboratory studies and reservoir simulations should be performed before moving on to pilot tests (Sayavedra et al., 2013). The simulation step is particularly important because EOR operations are costly and involve significant risk and uncertainty (Satter & Iqbal, 2016). So, it is essential to minimize the uncertainties involved with such projects by predicting the reservoir performance based on different scenarios.

Table 7.1 – Reservoir properties for chemical EOR implementation. Adapted from (Chen et al., 2018) and (Xue et al., 2023).

Properties	Surfactant flooding	Polymer flooding	Multiple compound flooding
API (°)	> 25	> 20	–
Oil viscosity (mPa s)	< 40	< 60	< 60
Reservoir permeability (mD)	> 50	> 50	> 50
Reservoir depth (m)	< 2500	< 2500	< 2500
Reservoir temperature (°C)	< 80	< 75	< 75
Reservoir lithology	Sandstone	Sandstone	Sandstone
Favorable factors	Low mineralization of reservoir water	Low temperature, fresh water and heterogeneity	Low temperature, fresh water and heterogeneity

Simulations can be done on different scales, depending on the intended purpose. For example, models that only consider one spatial dimension are commonly used to understand specific fluid displacement processes, while two–dimensional models can be used to simulate certain laboratory assays. In terms of full reservoir simulations, these are generally performed in three–dimensional models that can be classified as compositional or black–oil models. Compositional models represent the individual hydrocarbon components of the liquid and gas phases, considering the changes in their composition under dynamic reservoir conditions. Black–oil models, on the other hand, are more commonly used in reservoir simulations, and they treat the phases as single components (Satter & Iqbal, 2016). For simplicity purposes, this work will focus on the simulation of a black–oil model through the simulator software tNavigator, created by Rock Flow Dynamics. During simulation assays, different biopolymer and biosurfactant solutions (produced and evaluated throughout this thesis) will be modeled through different injection schemes.

7.2 Model description

The reservoir model used was a modified conceptual Egg model (Jansen et al., 2014), commonly used to simulate two–phase (oil–water) flows. This model is characterized by an egg shape consisting of a 60 x 60 x 7 grid with 18553 active cells (Figure 7.1). Based on the information of the target reservoir (Gudiña, Rodrigues, et al., 2012), the porosity of the model was kept constant at 25% and the permeability at 50 mD. This reservoir is a flat sandstone structure at 450 m depth with an initial pressure and temperature of 32.5 bars and 42.5°C, respectively. The parameters used are listed in Table 7.2. This model fits the screening criteria for the implementation of EOR projects (Table 7.1).

Table 7.2 – Initial reservoir model properties.

Variable	Value	Units	Reference
Reservoir properties			
Grid	60 x 60 x 7	–	(Jansen et al., 2014)
Grid–block size	8 x 8 x 4	m	(Jansen et al., 2014)
Datum depth	450	m	(Gudiña, Rodrigues, et al., 2012)
Porosity	0.25	–	(Gudiña, Rodrigues, et al., 2012)
Permeability	50	mD	(Gudiña, Rodrigues, et al., 2012)
Temperature	42.5	°C	(Gudiña, Rodrigues, et al., 2012)
Formation type	Sandstone	–	(Gudiña, Rodrigues, et al., 2012)
Rock properties			
Rock compressibility	0.0	bar	(Jansen et al., 2014)
Specific heat of rock	0.9 (at 0.0°C)	kJ/kg K	(Robertson, 1988)
Oil properties			
Oil gravity	25.0	°API	(Gudiña, Rodrigues, et al., 2012)
Oil density	910	kg/m^3	This study
Oil compressibility	1.45 x 10^{-4}	bar	(B. Guo, 2019)
Specific heat of the oil	1.8 (at 15.5°C)	kJ/kg K	(Cragoe, 1933)
	1.9 (at 40.0°C)		
	2.0 (at 60.0°C)		
Oil viscosity	2529.5 (at 15.5°C)	mPa s	This study
	39.4 (at 40.0°C)		
	20.6 (at 60.0°C)		
Water properties			
Water density	1000	kg/m^3	(B. Guo, 2019; Jansen et al., 2014)
Water compressibility	1.45 x 10^{-5}	bar	(B. Guo, 2019)
Specific heat of water	4.2	kJ/kg K	–
Water viscosity	1.0	mPa s	(Jansen et al., 2014)
Saturation region			
Endpoint oil relative permeability	0.8	–	(Jansen et al., 2014)
Endpoint water relative permeability	0.75	–	(Jansen et al., 2014)
Corey exponent for oil	4.0	–	(Jansen et al., 2014)
Corey exponent for water	3.0	–	(Jansen et al., 2014)
Residual oil saturation	0.1	–	(Jansen et al., 2014)
Connate–water saturation	0.2	–	(Jansen et al., 2014)
Initial water saturation	0.1	–	(Jansen et al., 2014)
Capillary pressure	0.0	bar	(Jansen et al., 2014)

Fluid injection and production properties			
Water/fluid injection rate (per well)	79.5	m^3/day	(Jansen et al., 2014)
Production well bottom–hole pressure	1.0 (default)	bar	tNavigator manual
Well–bore radius	0.1	m	(Jansen et al., 2014)

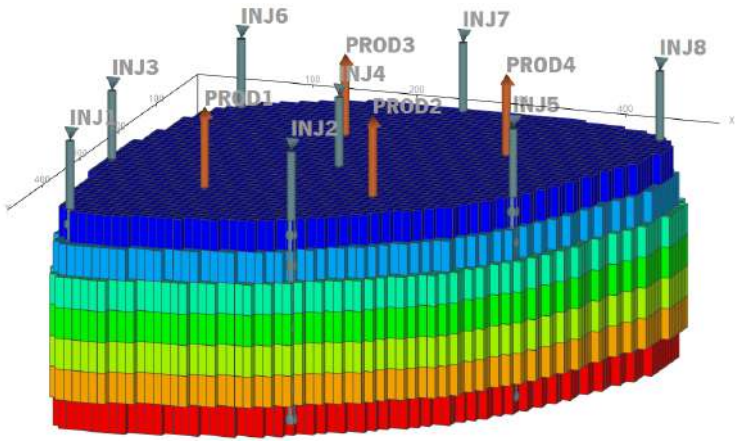

Figure 7.1 – Reservoir model depicting the position of the injector wells (blue, INJ) and the producer wells (orange, PROD).

7.3 Oil recovery simulations

7.3.1.1 Water flooding

The first step in the simulation studies was to inject water into the wells to simulate the process of water flooding. Because the target reservoir has no natural pressure support (Gudiña, Rodrigues, et al., 2012) and since the model doesn't contain gas caps (Jansen et al., 2014), primary oil recovery is not possible in this case. Hence, simulation was initiated with the secondary recovery process.

Water was injected into the wells at a rate of 79.5 m^3/day for 20 years, which is a typical production timeline for oil reservoirs. However, it was considered that, after 34 months (2.8 years) of operations, oil recovery was no longer viable through water flooding. At this point, the water production rate is rapidly increasing while the rate of oil is decreasing, meaning that water production will soon exceed oil production in absolute values (Figure 7.2, Left). Additionally, water breakthrough, the point when water started appearing in the production wells (Erivwo et al., 2019), happened after 10 months of operations. After this point, economic factors need to be evaluated before any adjustments are made to

the production scheme, since the cost of separating the oil from the water fraction starts increasing. To note that the considerations used here are theoretical, since no economic analysis was performed to determine whether the reservoir could sustain further production through water flooding. Nonetheless, since the water cut at 34 months is equal to 90% (Figure 7.2, Right) and the remaining oil saturation is 73.4%, it is considered that the reservoir has entered the high water cut stage and application of an EOR project may be recommended (Chen et al., 2018; Y. Guo et al., 2019).

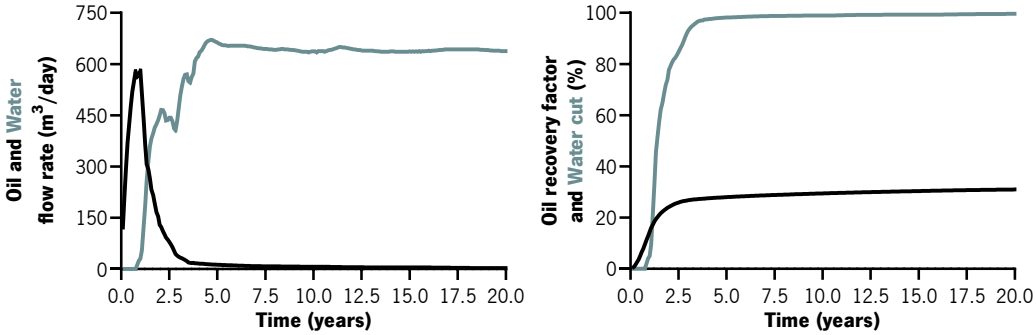

Figure 7.2 – Left: oil and water flow rate (m^3/day) through time. Right: oil recovery factor and water cut (%) through time, for water flooding simulations.

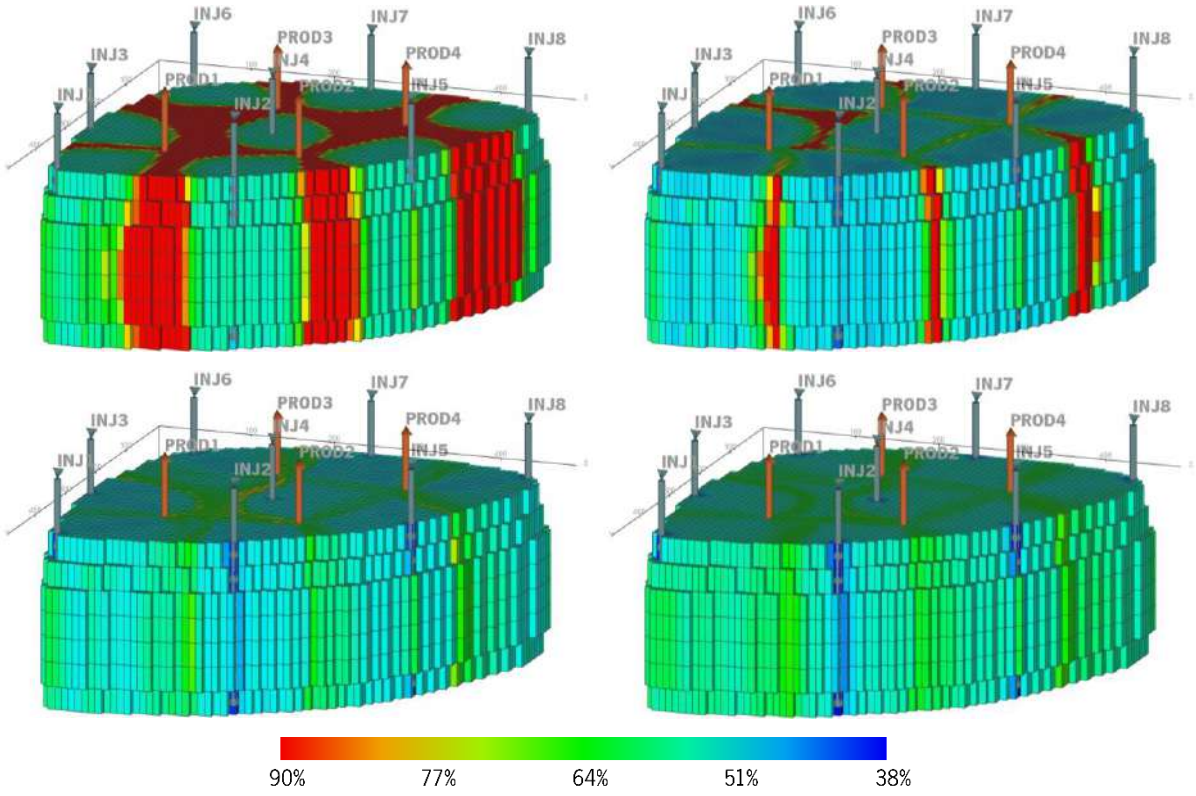

Figure 7.3 – Oil saturation within the reservoir model after 12 months (top left), 34 months (top right), 10 years (bottom left) and 20 years (bottom right) of water flooding operations.

During these first 34 months of water flooding, 2.9 x 10^5 m^3 of oil was produced, with a recovery factor (calculated as the amount of oil recovered divided by the OOIP) of 26.6% (Figure 7.2, Right). By the end of the 20 years, the amount of oil produced increased only by 15%, with a recovery factor of 31.2%. From the images of the reservoir after 12 months, 34 months, 10 years and at the end of the water flooding simulation (20 years), it is possible to see that the flooded water is spread through preferential channels and oil saturation decreases only a few percentage points (Figure 7.3). This may explain the low oil recovery obtained between the point when water cut reached 90% and the end of the simulation.

7.3.2 Water flooding followed by MEOR

The first set of MEOR operations was simulated by injecting three different biopolymer solutions (commercial xanthan gum (Sigma Aldrich), biopolymer from *Rhizobium viscosum* CECT 908 and γ–PGA from *Bacillus velezensis* P#02) at different concentrations (1.0, 2.5 and 5.0 g/L). The biopolymers were injected for 20 years after 34 months of water flooding. Their specific properties (apparent viscosity as a function of biopolymer concentration, temperature, and shear rate) were included in the model to account for the viscosity increase the biopolymers caused. The apparent viscosity values had been previously measured (Chapter 4 and Chapter 6).

All the biopolymers showed a positive effect in oil recovery after the water flooding stage (Figure 7.4). This effect was more noticeable when higher concentrations of biopolymer were used for each of the three biopolymers. The water cut fraction also decreased with the addition of biopolymers to the flooding solution, suggesting that the biopolymers push out the oil trapped outside the preferential water channels. Furthermore, it is noticeable from the graphs that biopolymer breakthrough happens later with increasing biopolymer viscosities, which, as discussed in a previous chapter, are obtained for the biopolymer produced by *R. viscosum* CECT 908. This was also the biopolymer that displayed the best results regarding oil recovered at the end of the simulation. When injected at a concentration of 5 g/L, it led to an additional oil recovery factor (AOR) of 60.1%, leaving about 55% of oil inside the reservoir (Figure 7.4 and Table 7.3).

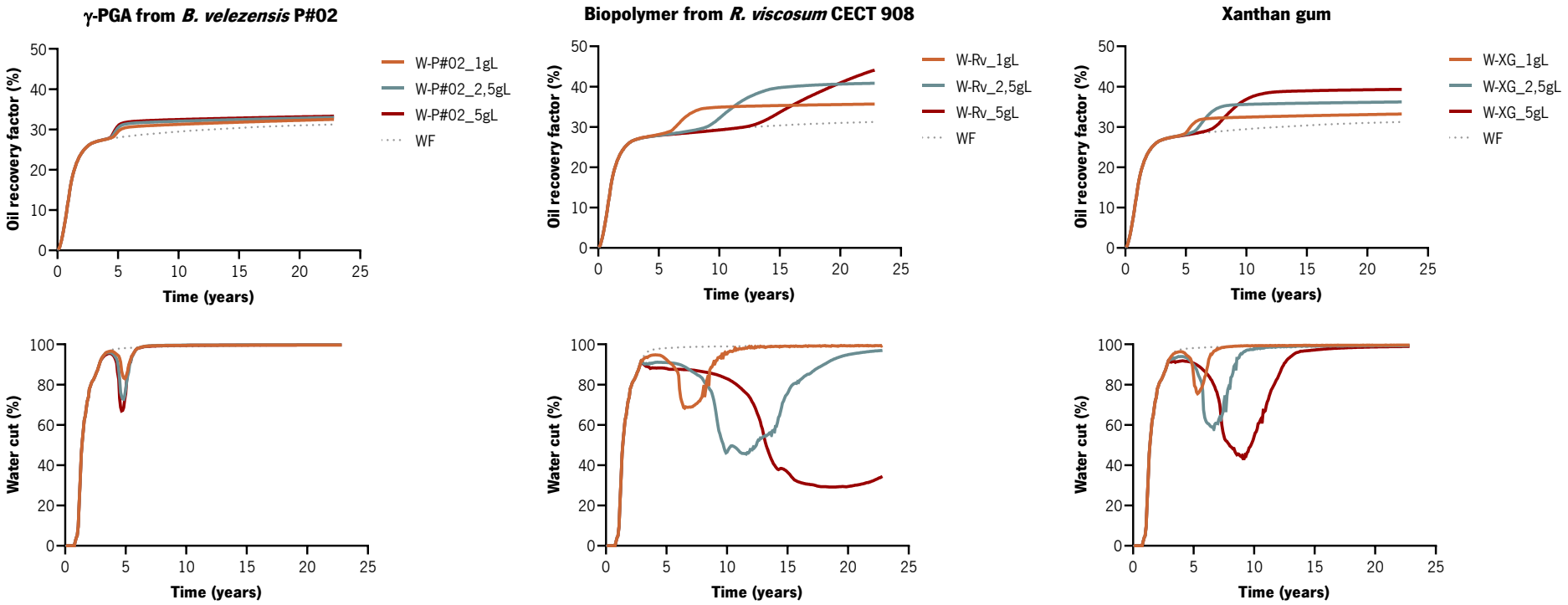

Figure 7.4 – Top: oil recovery factor (%) through time. Bottom: water cut (%) through time for water flooding (WF) or water flooding followed by biopolymer flooding simulations using xanthan gum, the biopolymer from *Rhizobium. viscosum* CECT 908 and γ–PGA from *Bacillus velezensis* P#02 at different concentrations (1.0, 2.5 and 5.0 g/L).

The pressure buildup inside the reservoir upon injection of the biopolymers was also evaluated in these simulations (Table 7.3). Higher injection pressures usually translate to higher flow rates for the injected liquid and, thus, more liquid being injected. In this scenario, it is most likely that viscous fingering, or a non–uniform oil displacement front, is occurring. As can be seen from the values in Table 7.3, the higher pressures correspond to the biopolymers with the lowest viscosity values, which explains their higher mobility.

Table 7.3 – Oil recovery parameters for water flooding (WF) or WF followed by biopolymer flooding simulations using xanthan gum, the biopolymer from *Rhizobium. viscosum* CECT 908 and γ–PGA from *Bacillus velezensis* P#02 at different concentrations (1.0, 2.5 and 5.0 g/L).

Treatment	[BP] (g/L)	BP viscosity (mPa s)	**Oil recovery parameters**					
			Average pressure (bar)	Injected volume (PV)	Total oil recovered (m^3)	S_{orbf} (m^3)	Recovery factor (%)	AOR (%)
Control (WF)	–	–	$6.6x10^2$	4.5	$3.4x10^5$	$5.0x10^4$	31.2	42.5
γ–PGA from *B. velezensis* P#02	1.0	5	$3.8x10^3$	4.5	$3.5x10^5$	$6.4x10^4$	32.5	44.3
	2.5	13	$4.6x10^3$	4.4	$3.5x10^5$	$6.9x10^4$	33.0	44.9
	5.0	24	$4.9x10^3$	3.6	$3.6x10^5$	$7.2x10^4$	33.3	45.3
BP from *R. viscosum* CECT 908	1.0	113	$5.0x10^3$	1.9	$3.8x10^5$	$9.8x10^4$	35.7	48.6
	2.5	754	$4.7x10^3$	1.3	$4.4x10^5$	$1.5x10^5$	40.8	55.6
	5.0	4803	$1.4x10^3$	1.0	$4.7x10^5$	$1.9x10^5$	44.1	60.1
Xanthan gum	1.0	64	$4.9x10^3$	2.9	$3.6x10^5$	$7.1x10^5$	33.2	45.2
	2.5	236	$5.0x10^3$	1.9	$3.9x10^5$	$1.0x10^5$	36.2	49.3
	5.0	710	$4.9x10^3$	1.5	$4.2x10^5$	$1.4x10^5$	39.3	53.5

–: not applicable. BP: biopolymer. S_{orbf}: oil recovered after biopolymer flooding. AOR: additional oil recovery. Apparent viscosity values presented correspond to a temperature of 40°C and a shear rate of 1.54 s^{-1}.

Biosurfactant flooding simulations, with the biosurfactant from *B. velezensis* P#02 and the rhamnolipids from *Burkholderia thailandensis* E264, were also attempted with no success. Hence, biosurfactant–MEOR will not be discussed in this chapter.

7.3.3 Biopolymer flooding

Considering that the performance of water flooding followed by biopolymer flooding was much better than a water flooding scenario, the injection of water was excluded from the following simulation. In this scenario, the biopolymer from *R. viscosum* CECT 908 was injected at a concentration of 5 g/L for

20 years. After this time, $6.0x10^5$ m^3 of oil had been recovered, corresponding to a recovery factor of 55.8% (Figure 7.5), which is 1.8 times higher than what was recovered in the water flooding simulation during the same period, and 1.26 times higher than injecting the biopolymer following water flooding. Furthermore, the biopolymer breakthrough happened much later in this case (after 19 years).

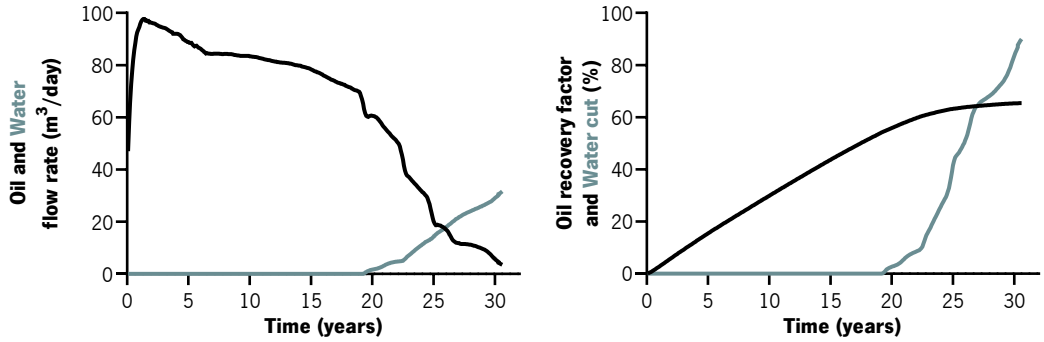

Figure 7.5 – Left: oil and water flow rate (m^3/day) through time. Right: oil recovery factor and water cut (%) through time for biopolymer flooding simulations, using the biopolymer from *Rhizobium viscosum* CECT 908 at 5 g/L.

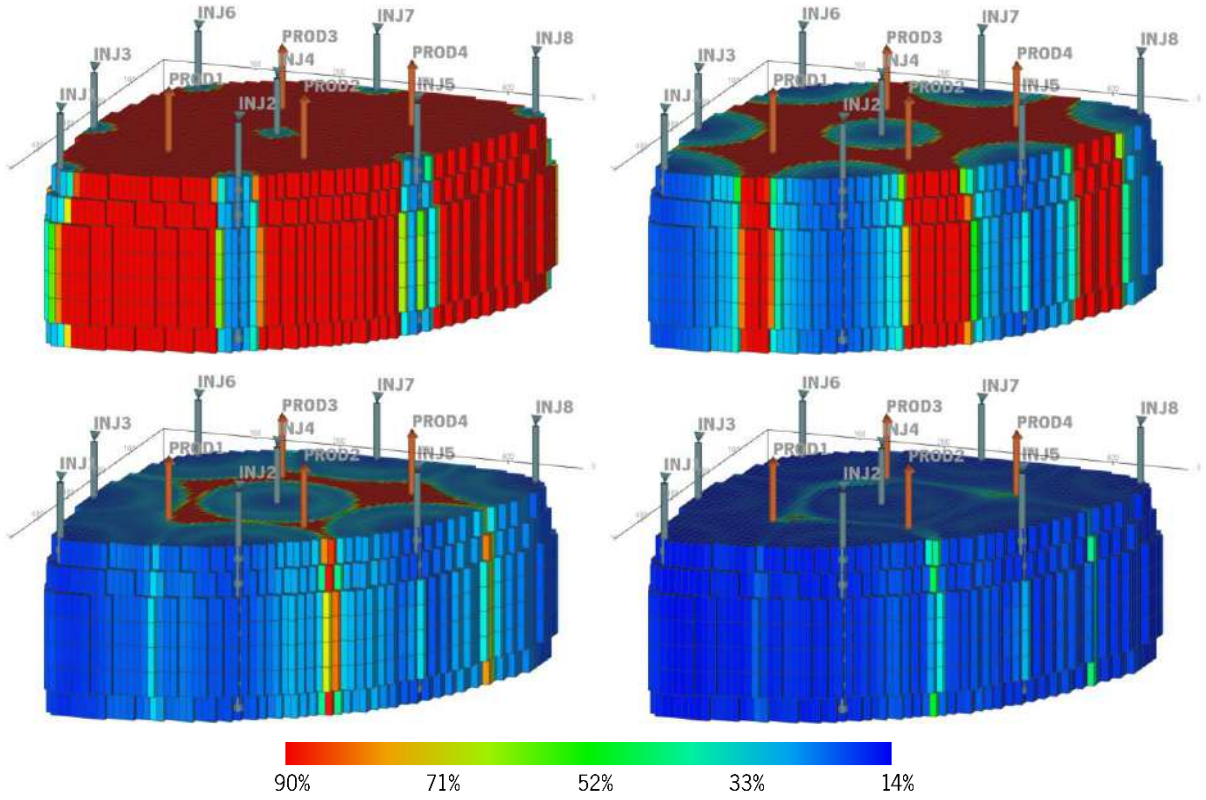

Figure 7.6 – Oil saturation within the reservoir model after 1 (top left), 10 (top right), 20 (bottom left) and 30 years (bottom right) of biopolymer flooding operations, using the biopolymer from *Rhizobium viscosum* CECT 908 at 5 g/L.

As can be seen from the reservoir images taken at different time points during the simulation, the displacement front is more uniform than in the water flooding scenario, which can explain the late breakthrough (Figure 7.6). Unlike in water flooding, the biopolymer solution flows from the injection wells forming a perfect circle.

Additionally, after 20 years of biopolymer flooding simulations, the water cut had only reached 2.7% (Figure 7.5). So, the simulation was extended for 10 years and 7 months until the water cut was at 90%. Here, the water production rate was already higher than the oil production rate, so recovery would most likely, be inefficient past this point. Nonetheless, by the end of the simulation, only 34.6% of residual oil was still present in the reservoir.

7.4 Discussion

This work provided valuable examples of possible MEOR strategies, focusing on biopolymer flooding. As discussed in previous chapters (Chapter 4 and Chapter 6), the injection of biopolymers after water flooding results in an increased oil recovery (Figure 7.4 and Table 7.3). The AOR values obtained in these simulations were lower than the ones obtained in sand–pack columns (when the values are corrected after subtracting the additional oil recovery obtained in the control assays). Nonetheless, the correlation between the different biopolymers was similar, with the biopolymer from *R. viscosum* CECT 908 leading to higher recovery rates than the other two.

The difference in the values may be due to the simulation conditions. Here, several aspects of the simulation were not considered, as the aim was to make a simple evaluation to determine the applicability of this technology on a larger scale. For example, biopolymer adsorption was not considered, so the only mechanism for oil recovery simulated was viscosity increase. Furthermore, the reservoir model used assumed that the reservoir would be homogenous. In experimental conditions, however, the sand pack is heterogeneous. A similar difference was also observed in a study that simulated oil recovery in sand–pack columns, comparing the results with those obtained under experimental conditions (Pandey et al., 2022). In water flooding, the simulation studies predicted a residual oil saturation of around 45%, while sand–pack column assays left behind 53% of OOIP. These differences could be adjusted in the model by distributing the horizontal and vertical permeability values to better fit real reservoir conditions. Moreover, the capillary number (N_{CA}) was considered null in the Egg–model used in this work. The N_{CA} is related to the injected fluids' flow velocities and increases with higher flows, leading to improved oil recovery

(Pandey et al., 2022). On the other hand, N_{CA} also increases with the viscosity of the injected fluid, which may explain the higher recovery factors obtained with biopolymers with higher apparent viscosities.

Nonetheless, comparing the simulations between water flooding and biopolymer flooding, it was possible to see that the distribution of fluids inside the porous medium differs with the viscosity of the injected fluid. The biopolymer is distributed more uniformly throughout the reservoir, leading to a more uniform oil displacement front and, ultimately, more oil recovered (Figure 7.3 and Figure 7.6) (Y. Guo et al., 2019). However, the high viscosity leads to lower flow rates, which may cause injectivity problems due to high pressure (Al–Murayri et al., 2016; Gao et al., 2014). On the other hand, lower flow rates and higher viscosity delay the injected fluid breakthrough, meaning there is no need to handle produced water for longer periods, decreasing oil processing costs (Erivwo et al., 2019). In fact, it was determined that a polymer flooding scenario, followed by water flooding, would lead to an 11% increase in oil production compared to a water flooding scenario, with a supplementary cost of 7–8 US$ per additional barrel produced (Al–Murayri et al., 2016). This, and the lower oil processing costs, make polymer an attractive alternative to conventional water flooding. Furthermore, biopolymer flooding seems to achieve a similar oil production increase, with the benefit of being more environmentally friendly.

7.5 References

Al–Murayri, M. T., Hassan, A. A., Al–Tameemi, N. M., Lara, R. G., Al–Sane, A., Suzanne, G., & Lantoine, M. (2016, December 6). Simulation of chemical EOR processes for the ratqa lower fars heavy oil field in Kuwait: Multi–scenario results and discussions. *Society of Petroleum Engineers – SPE Heavy Oil Conference and Exhibition 2016*. https://doi.org/10.2118/184086–ms

Chen, P., Balasubramanian, S., Bose, S., Alzahabi, A., & Thakur, G. (2018). An integrated workflow of IOR/EOR assessment in oil reservoirs. *Proceedings of the Annual Offshore Technology Conference*, *3*, 2285–2299. https://doi.org/10.4043/28726–ms

Cragoe, C. S. (1933). *Thermal Properties of Petroleum Products*. U.S. Government Printing Office.

Erivwo, O., Ochai, J., Agbaroji, V., & Oke, O. (2019, August 5). Considerations for mitigating early water breakthrough in horizontal wells in heavy oil reservoirs in the Niger delta – Ogini field case study. *Society of Petroleum Engineers – SPE Nigeria Annual International Conference and Exhibition 2019, NAIC 2019*. https://doi.org/10.2118/198828–MS

Gao, J., Li, Y., Li, J., Yin, D., & Wang, H. (2014). Experimental study on optimal polymer injection timing in offshore oilfields. *Proceedings of the Annual Offshore Technology Conference*, *1*, 205–210. https://doi.org/10.4043/24694–ms

Gudiña, E. J., Pereira, J. F. B., Rodrigues, L. R., Coutinho, J. A. P., & Teixeira, J. A. (2012). Isolation and study of microorganisms from oil samples for application in Microbial Enhanced Oil Recovery.

International Biodeterioration and Biodegradation, *68*, 56–64. https://doi.org/10.1016/j.ibiod.2012.01.001

Gudiña, E. J., Rodrigues, L. R., Teixeira, J. A., Pereira, J. F., Coutinho, J. A., & Soares, L. P. (2012). Biosurfactant producing microorganisms and its application to enhance oil recovery at lab scale. *Society of Petroleum Engineers – SPE EOR Conference at Oil and Gas West Asia 2012*, *1*, 363–370. https://doi.org/10.2118/154598–ms

Guo, B. (2019). Petroleum reservoir properties. In *Well Productivity Handbook* (pp. 17–51). Gulf Professional Publishing. https://doi.org/10.1016/b978–0–12–818264–2.00002–6

Guo, Y., Zhang, L., Zhu, G., Yao, J., Sun, H., Song, W., Yang, Y., & Zhao, J. (2019). A pore–scale investigation of residual oil distributions and enhanced oil recovery methods. *Energies*, *12*(19). https://doi.org/10.3390/en12193732

Jansen, J. D., Fonseca, R. M., Kahrobaei, S., Siraj, M. M., Van Essen, G. M., & Van den Hof, P. M. J. (2014). The egg model – a geological ensemble for reservoir simulation. *Geoscience Data Journal*, *1*(2), 192–195. https://doi.org/10.1002/gdj3.21

Niu, J., Liu, Q., Lv, J., & Peng, B. (2020). Review on microbial enhanced oil recovery: Mechanisms, modeling and field trials. In *Journal of Petroleum Science and Engineering* (Vol. 192, p. 107350). Elsevier. https://doi.org/10.1016/j.petrol.2020.107350

Pandey, A., Kesarwani, H., Saxena, A., Azin, R., & Sharma, S. (2022). Effect of heterogeneity and injection rates on the recovery of oil from conventional sand packs: A simulation approach. *Petroleum Research*, *8*(1), 96–102. https://doi.org/10.1016/j.ptlrs.2022.05.005

Robertson, E. C. (1988). Thermal properties of rocks. Report 88–441. In *US Department of the Interior: Geological Survey*. https://doi.org/10.3133/OFR88441

Saravanan, A., Kumar, P. S., Vardhan, K. H., Jeevanantham, S., Karishma, S. B., Yaashikaa, P. R., & Vellaichamy, P. (2020). A review on systematic approach for microbial enhanced oil recovery technologies: Opportunities and challenges. In *Journal of Cleaner Production* (Vol. 258, p. 120777). Elsevier Ltd. https://doi.org/10.1016/j.jclepro.2020.120777

Satter, A., & Iqbal, G. M. (2016). Petroleum reservoir simulation: a primer. In *Reservoir Engineering* (pp. 247–287). Gulf Professional Publishing. https://doi.org/10.1016/b978–0–12–800219–3.00015–2

Sayavedra, L., Mogollon, J. L., Boothe, M., Lokhandwala, T., & Hull, R. (2013). A discussion of different approaches for managing the timing of EOR projects. *Society of Petroleum Engineers – SPE Enhanced Oil Recovery Conference, EORC 2013: Delivering the Promise NOW!*, 906–911. https://doi.org/10.2118/165304–ms

Xue, L., Liu, P., & Zhang, Y. (2023). Status and Prospect of Improved Oil Recovery Technology of High Water Cut Reservoirs. *Water (Switzerland)*, *15*(7), 1342. https://doi.org/10.3390/w15071342

CHAPTER 8.

Conclusions and future perspectives

8.1 General conclusions

Summing up the main conclusions of this thesis, it is possible to highlight the mechanisms that can increase oil recovery in a Microbial Enhanced Oil Recovery scenario and provide remarks about the production of biopolymers and biosurfactants that aid this process.

Several of the microorganisms screened have been confirmed to produce biopolymers. By analyzing their viscoelastic properties, it was possible to evaluate which biopolymers could be used in MEOR operations. All the biopolymers studied exhibited a non–Newtonian pseudoplastic behavior, which is desirable in oil recovery applications due to the different flow rates that the biopolymer is subjected to when entering the reservoir and flowing through it. Additionally, biopolymers with higher apparent viscosities (η) were favored, as they have a better potential for oil recovery due to the lower mobility ratio of the injected fluid. This was confirmed in the sand–pack column assays, where the biopolymers that generated the best results in terms of oil recovery were the ones with higher apparent viscosities. Furthermore, it was observed that biopolymers with a more prevalent elastic modulus (G') could recover more oil, most likely due to the formation of a more uniform oil displacement front.

Overall, the biopolymer from *Rhizobium viscosum* CECT 908 generated the best results, being able to recover up to 25.8% additional heavy oil ($\eta_{40°C}$ = 247 mPa s at 1.4 s^{-1}) and 12.2% using the oil from the Potiguar oilfield ($\eta_{40°C}$ = 110 mPa s at 1.4 s^{-1}). This biopolymer displayed apparent viscosity values of 4803 mPa s when in solution at 5 g/L and exhibited a dominant elastic modulus. On the other hand, γ–PGA produced by *Bacillus velezensis* P#02 resulted in lower recovery rates (up to 10.5% when using the oil from the Potiguar oilfield), most likely related to its lower viscosifying potential (162 mPa s when in solution at 5 g/L) and the prevalence of the viscous modulus (G''). The simulation studies performed further confirmed the experimental results obtained. Additionally, the simulations demonstrated these biomolecules' applicability in large-scale reservoirs.

Through optimization of the culture medium and operational conditions, it was possible to produce simultaneously the biopolymer γ–PGA and biosurfactants by *B. velezensis* P#02 using corn steep liquor (CSL) as an alternative low-cost substrate. Rhamnolipid production by *Burkholderia thailandensis* E264 was also optimized. In this case, it was possible to produce rhamnolipids using a medium containing only agro–industrial residues and–products (CSL and olive oil mill wastewater (OMW)) as alternative substrates, both in flasks and in a laboratory–scale bioreactor.

Characterizing the biosurfactants produced allowed us to determine their underlying mechanisms for oil recovery. Besides decreasing the surface tension of aqueous solutions, the biosurfactants studied were also able to alter the wettability of oil–coated glass surfaces towards more water–wet state and form stable emulsions. With the assays performed in sand–pack columns and with oil-contaminated sands, it was concluded that all these mechanisms contribute to oil recovery. With the rhamnolipids produced by *B. thailandensis* E264 in CSL medium, for example, slightly better oil recovery was obtained than with the rhamnolipids produced in CSL+OMW medium (7.8% additional oil recovery (AOR) in the sand–pack columns and 62.9% oil recovery from contaminated sand, compared with 4.9% AOR and 60.7% oil recovery). These rhamnolipids exhibit different congener distributions, which translated to different characteristics: the ones produced in the CSL+OMW medium had better surface activity, but the ones produced in the CSL medium were able to form stable emulsions at lower concentrations and contributed more to alter the wettability of an oil–coated glass surface.

Furthermore, the research performed in this thesis revealed a clear advantage when using biopolymers and biosurfactants in oil recovery. Several injection schemes were evaluated to determine the best strategy to use these biomolecules *ex-situ*, achieving the best results when both biomolecules were injected in the same solution. Additionally, it was observed that similar recovery rates were obtained for many of the biomolecules tested when using the cell–free supernatants and the purified (or crude) biomolecules. This avoids purifying the biomolecules, making their application more accessible and cost-effective.

Considering all, the cost–effective production of biopolymers and biosurfactants using agro–industrial wastes demonstrated potential for future industrial applications. Particularly in oil recovery, these biomolecules have shown the ability to increase the recovery of different types of oils, raising the number of potential reservoirs they could be applied to. The bioprocess optimization to produce biopolymers and biosurfactants by different microorganisms also provides a basis for further development.

8.2 Future perspectives

The research efforts presented in this thesis generated a basis for future works that could be performed to further contribute to this field. Future perspectives and possible work directions are summarized below:

- This thesis focused on producing biopolymers and biosurfactants, mainly for *ex-situ* MEOR applications. However, other microbial-derived molecules, including enzymes, could also be used to improve oil recovery.
- Furthermore, optimizing the production of these biomolecules in conditions similar to reservoir conditions could allow the development of *in situ* MEOR strategies using the microorganisms as recovery agents. Applying such strategies would decrease the processing costs of the biomolecules as they would be produced inside the reservoir. Additionally, microorganisms can produce other compounds *in situ* that contribute to oil recovery, like CO_2.
- The scale–up process is another critical step to develop further before applying this technology in the field. The bioreactor design used in this thesis did not provide the best results regarding biopolymer production, since the maximum apparent viscosity was lower than the one obtained in flasks. Hence, it would be interesting to study other bioreactor configurations, such as airlift bioreactors, in which the agitation is provided by the gas injected, preventing possible physical stress and degradation of the biopolymer. Other feeding strategies could also be considered to improve the production yields of the different biomolecules.
- Finally, it is proposed that future simulation studies use the specific characteristics of a target reservoir and include economic analysis to analyze if this proposed methodology could be reliable also from an economic perspective.